



HAL
open science

Improvement of biostratigraphic and paleoenvironmental reconstruction tools based on cretaceous dinoflagellate cysts from the tethys and the atlantic

Raquel Sánchez Pellicer

► To cite this version:

Raquel Sánchez Pellicer. Improvement of biostratigraphic and paleoenvironmental reconstruction tools based on cretaceous dinoflagellate cysts from the tethys and the atlantic. Earth Sciences. Université Pierre et Marie Curie - Paris VI; Universidad de Zaragoza (Espagne), 2016. English. NNT : 2016PA066180 . tel-01691423

HAL Id: tel-01691423

<https://theses.hal.science/tel-01691423>

Submitted on 24 Jan 2018

HAL is a multi-disciplinary open access archive for the deposit and dissemination of scientific research documents, whether they are published or not. The documents may come from teaching and research institutions in France or abroad, or from public or private research centers.

L'archive ouverte pluridisciplinaire **HAL**, est destinée au dépôt et à la diffusion de documents scientifiques de niveau recherche, publiés ou non, émanant des établissements d'enseignement et de recherche français ou étrangers, des laboratoires publics ou privés.

Université Pierre et Marie Curie
Universidad de Zaragoza

Ecole doctorale Géosciences, ressources naturelles et environnement (ED 398D)

Centre de recherche sur la paléobiodiversité et les paléoenvironnements

**IMPROVEMENT OF BIOSTRATIGRAPHIC AND
PALEOENVIRONMENTAL RECONSTRUCTION TOOLS
BASED ON CRETACEOUS DINOFLAGELLATE CYSTS
FROM THE TETHYS AND THE ATLANTIC**

Par Raquel Sánchez Pellicer

Thèse de doctorat de Paléontologie

Dirigée par Loïc Villier et Javier Ferrer Plou

Présentée et soutenue publiquement le 22 Janvier 2016

Devant un jury composé de :

Prof. Baudin, François, UPMC – Paris VI (France)	Examineur
Dr. Diez Ferrer, José Bienvenido, Universidade de Vigo (España)	Rapporteur
Dr. Ferrer Plou, Javier, Universidad de Zaragoza (España)	Directeur
Dr. Masure, Edwige, UPMC – Paris VI (France)	Co-encadrant
Dr. Daniel Michoux, ISSBio – TOTAL (France)	Examineur
Prof. Molina, Eustoquio, Universidad de Zaragoza (España)	Examineur
Prof. de Vernal, Anne, UQAM (Canada)	Rapporteur
Prof. Villier, Loïc, UPMC – PARIS VI (France)	Directeur

A todos los que me han
acompañado en este viaje entre lestrigones y cíclopes,
en especial a mi familia y a Denise.

As you set out for Ithaka
hope your road is a long one,
full of adventure, full of discovery.
Laistrygonians, Cyclops,
angry Poseidon—don't be afraid of them:
you'll never find things like that on your way
as long as you keep your thoughts raised high,
as long as a rare excitement
stirs your spirit and your body.
Laistrygonians, Cyclops,
wild Poseidon—you won't encounter them
unless you bring them along inside your soul,
unless your soul sets them up in front of you.

Hope your road is a long one.
May there be many summer mornings when,
with what pleasure, what joy,
you enter harbors you're seeing for the first
time;
may you stop at Phoenician trading stations
to buy fine things,
mother of pearl and coral, amber and ebony,
sensual perfume of every kind—

as many sensual perfumes as you can;
and may you visit many Egyptian cities
to learn and go on learning from their scholars.

Keep Ithaka always in your mind.
Arriving there is what you're destined for.
But don't hurry the journey at all.
Better if it lasts for years,
so you're old by the time you reach the island,
wealthy with all you've gained on the way,
not expecting Ithaka to make you rich.

Ithaka gave you the marvelous journey.
Without her you wouldn't have set out.
She has nothing left to give you now.

And if you find her poor, Ithaka won't have
fooled you.
Wise as you will have become, so full of
experience,
you'll have understood by then what these
Ithakas mean.

REMERCIEMENTS + AGRADECIMIENTOS = REMERCIAMIENTOS

Je tiens tout d'abord à adresser mes remerciements aux membres du jury de cette thèse, à José Bienvenido Diez Ferrer et Anne de Vernal qui ont accepté d'être les rapporteurs de cette thèse ainsi qu'à François Baudin, Daniel Michoux et Eustoquio Molina qui en sont les examinateurs. Merci pour leur disponibilité et le temps qu'ils ont consacré à la lecture du manuscrit.

Esta tesis es el fruto de tres años de investigación entre el Centre de Recherche sur la Paléobiodiversité et les Paléoenvironnements, UPMC – Paris 6, y el Departamento de Ciencias de la Tierra de la Universidad de Zaragoza, merci aux responsables des deux équipes pour la confiance qu'ils m'ont accordée. También, me gustaría expresar mi gratitud a ambas escuelas doctorales por haber facilitado los trámites de una cotutela poco ordinaria.

Je remercie bien évidemment mes directeurs de thèse Loïc Villier et Javier Ferrer Plou. Merci Loïc d'avoir accepté le défi au milieu de la course, de m'avoir guidée et surtout merci de ta patience pour faire avancer ce shi, schimib, schimibi... schmilblick ! Gracias Javier por hacer siempre que las cosas fuesen fáciles.

J'exprime mes plus vifs remerciements à Edwige Masure, ma directrice officieuse, sans qui cette thèse n'aurait jamais commencé, ni vu la lumière. Merci de partager avec moi tes vastes connaissances sur les "dinos" et surtout merci de m'avoir ouvert une porte lorsque toutes les voies disparaissaient.

Je voudrais également remercier à M. Jacques Rey de m'avoir aidé à « voir » et comprendre le Basin Lusitanien depuis un bureau au 5ème et à M. Jean Dejax d'avoir partagé avec moi son art pour restaurer des lames anciennes.

Merci aussi à TOTAL d'avoir financé partiellement cette étude. À Daniel pour m'avoir guidée à travers la foule des "dinos" du Crétacé supérieur et à toute l'équipe de « bio » de m'avoir fait sentir chez moi.

No me gustaría olvidar a nadie de los que han estado cerca de mi durante estos tres años (pero seguro que no lo consigo). A Bienve, gracias por haberme hecho pensar en mis bolsillos, hace ya un montón de años... a lo tonto a lo tonto la llave me ha sido muy útil. Gracias a toda la gente de Vigo con quienes empecé a descubrir la investigación y los cafés en el cuchitril. Al disperso equipo de paleobotánicos ibéricos, gracias por los buenos ratos y las discusiones. Merci aussi à Jean Broutin et Colette de leur accueil. A tous les collègues du couloir un grand merci pour leur bonne humeur, les discussions variées et le soutien. No me olvido de la mafia et proches, gracias por soportar el pollo con patatas, disfrutar de largos cafés al sol y por acompañarme a terapia los viernes.

Y cómo no... Merci Denise ! Merci de m'avoir accueillie pendant ces années, pour tes conseils, pour les gâteaux à l'orange, pour ta générosité ... Merci pour tout!! Sans ton aide, faire cette thèse aurait été encore plus compliqué.

En estos agradecimientos no puede faltar toda mi familia, los que están y los que se han ido, gracias a todos por los ánimos y el interés. Sobre todo a mis padres y a mi hermana por su apoyo incondicional en todas y cada una de las etapas recorridas hasta llegar aquí y por habérmelo dado todo sin pedir nada a cambio.

ABSTRACT

Awareness of the vulnerability of modern society to possible changes in the global climate has stirred up the interest of the scientific community to better understand the mechanisms and feedbacks regulating the climate system. The Cretaceous period is considered a good example for the study of the Earth under “greenhouse” climate conditions and thus a good analog for future global climate evolution. Modern dinoflagellate cysts (dinocysts) are very efficient in reconstruction of oceanic fluctuations, and fossil dinocysts have great values for biostratigraphy. The thesis evaluates the performance of Cretaceous dinocyst as biostratigraphic markers, and develops an appropriate methodology, grounded on biodiversity and multivariate analysis to improve paleoenvironmental reconstructions.

In the first chapter, dinocysts are used to recognize the Upper Cretaceous and Paleocene stage boundaries in the ODP Hole 959D, drilled on the Côte d’Ivoire – Ghana transform margin. The comparison of the results with two previous evidences uncertainties in time interval delimitation. Conflicts are mostly due to low frequencies of biostratigraphic dinocyst markers.

The second chapter analyzes the dinocyst distribution along an inshore to offshore transect on the western Iberian Margin during the Albian. Contrasting the dinocyst occurrence data with the sedimentological and paleontological data allow identifying dinocyst associations with common preferences and tolerances to environmental conditions. The main factors contributing to the dinocyst distribution are the stability and predictability gradient and the nutrient availability. Paleoceanographic and paleogeographic evolution of the western Iberian margin during the Albian are clearly recorded in the spatiotemporal occurrence patterns of dinocyst associations.

The third chapter compares Aptian dinocyst distribution from two different oceanic domains, Central Atlantic and northwestern Tethyan. It is used to test the methodology and the hypothesized paleoenvironmental preferences of dinocyst issued from analysis of the Albian data. The recognized paleoenvironmental preferences and tolerances of the Aptian dinocysts precisely match those proposed for the Albian species. The distribution and evolution of Aptian dinocyst associations reflect the evolution of carbonate platforms of both the Southern Provence Basin and the western Iberian margin. The combination of dinocyst and sedimentary organic matter (SOM) allows the identification of regional and global oceanic changes, like the demise of carbonate platforms, the Oceanic Anoxic Event 1a (OAE 1a) or the regional anoxic event Fallot level.

Keywords: Dinoflagellate cysts, biostratigraphy, multivariate analysis, paleoenvironment, Cretaceous, western Iberian Margin, Southern Provence Basin

RÉSUMÉ

La prise de conscience de la vulnérabilité de la société moderne à d'éventuels changements climatiques à l'échelle globale a poussé la communauté scientifique à mieux comprendre les mécanismes de régulation et de rétroaction du système climatique. La période crétacée est considérée comme un bon exemple pour l'étude de la Terre sous climat à effet de serre, c'est un bon analogue pour l'évolution future du climat mondial. Les kystes de dinoflagellés (dinokystes) récents sont très efficaces pour reconstruire les fluctuations climatiques océaniques et les dinokystes fossilisés sont d'une grande utilité en biostratigraphie. La thèse évalue la performance des kystes crétacés comme marqueurs biostratigraphiques et développe une méthodologie appropriée, fondée sur les analyses de biodiversité et des analyses multivariées, pour améliorer les reconstructions paléoenvironnementales.

Dans le premier chapitre, les dinokystes sont utilisés pour caractériser le Crétacé supérieur – et le Paléocène du puit ODP 959D, foré sur la marge transformante de Côte d'Ivoire-Ghana. La comparaison de nos résultats avec ceux de deux études précédentes montrent des positions différentes pour les limites d'étages. Les désaccords sont la plupart du temps dus à la faible fréquence des marqueurs biostratigraphiques.

Le deuxième chapitre est dédié à la distribution des dinokystes le long d'un transect côte-large situé sur la marge ouest ibérique pendant l'Albien. La comparaison des données concernant les dinokystes avec celles de sédimentologie et de paléontologie permet d'identifier des groupes d'espèces qui ont en commun une préférence et une tolérance à certaines conditions environnementales. Les principaux facteurs contrôlant la distribution des dinokystes sont le gradient de stabilité et de prédictibilité et la disponibilité des nutriments. Les évolutions paléo-océanographiques et paléogéographiques de la marge ouest ibérique pendant l'Albien sont clairement enregistrées dans les schémas de distributions spatio-temporelles des associations de dinokystes.

Le troisième chapitre compare les répartitions des dinokystes aptiens de deux domaines océaniques différents, ceux de l'Atlantique central et du nord-ouest de la Téthys. Ce chapitre a pour objet de tester la méthodologie utilisée précédemment et les préférences paléo-environnementales des dinokystes déduites de l'analyse des données de l'Albien. Les préférences paléo-environnementales et les tolérances des dinokystes de l'Aptien correspondent précisément à celles mise en évidence pour les espèces de l'Albien. La distribution et l'histoire des associations de dinokystes de l'Aptien reflètent l'évolution des plates-formes carbonatées du Bassin Sud Provençal et de la marge ibérique occidentale. La confrontation des dinokystes et de la matière organique sédimentaire (SOM) permet l'identification des changements océaniques mondiaux et régionaux, comme la disparition des plates-formes carbonatées, l'événement anoxique océanique 1a (OAE 1a) et l'événement anoxique du niveau Fallot.

Mots-clés: kystes de dinoflagellés ; biostratigraphie ; analyse multivariée ; paléoenvironnements ; Crétacé ; Marge ibérique occidentale ; Bassin Sud-Provençal

RESUMEN

La consciencia de la vulnerabilidad de la sociedad actual a los posibles cambios del clima global ha suscitado el interés en la comunidad científica por comprender mejor los mecanismos que regulan el sistema climático. El Cretácico se considera un buen ejemplo para el estudio del clima de la Tierra con altas concentraciones de gases de efecto invernadero y por tanto, un buen análogo para la futura evolución del clima global. Los quistes de dinoflagelados (dinoquistes) actuales son herramientas útiles para la reconstrucción de las oscilaciones oceánicas recientes y los dinoquistes fósiles son de gran valor como datadores bioestratigráficos. Esta tesis evalúa la utilidad de los dinoquistes cretácicos como marcadores bioestratigráficos y desarrolla una metodología apropiada, fundada en análisis de biodiversidad y análisis multivariante, para mejorar las reconstrucciones paleoambientales.

En el primer capítulo, el estudio de dinoquistes permite establecer los límites de los pisos del Cretácico Superior y del Paleoceno en el sondeo 959D del ODP, del margen transformante de Costa de Marfil – Ghana. La comparación de los resultados aquí obtenidos con dos estudios previos de la evidencia las discrepancias en la delimitación de los pisos. Los conflictos se deben en su mayor parte a la baja frecuencia de aparición de los dinoquistes marcadores bioestratigráficos.

El segundo capítulo analiza la distribución de dinoquistes a lo largo de un transecto costa – océano en el margen Ibérico occidental durante el Albiense. La comparación de la distribución de los dinoquistes con datos sedimentológicos y paleontológicos permite identificar las asociaciones de dinoquistes que comparten preferencias y tolerancias ambientales. La disponibilidad de nutrientes y la estabilidad ambiental son identificadas como los principales factores que condicionan la distribución espacio-temporal de las asociaciones de dinoquistes.

El tercer capítulo compara la distribución de dinoquistes aptienses en dos dominios oceánicos diferentes, el Atlántico Central y el Tetis noroccidental. Este estudio evalúa la metodología y las preferencias paleoambientales propuestas a partir del estudio de los datos albienses. Las preferencias y tolerancias ambientales de los dinoquistes aptienses coinciden de forma precisa con las propuestas para las especies albienses. La distribución y evolución de las asociaciones de dinoquistes reflejan los cambios de las plataformas carbonatadas tanto de la Cuenca sud-Provenzal como del margen ibérico occidental. La combinación del estudio de dinoquistes con el estudio de la materia orgánica sedimentaria permite identificar cambios ambientales globales y regionales, como el cese de las plataformas carbonatadas, el Evento Anóxico Oceánico 1a (u OAE 1a en inglés) o el evento anóxico regional, nivel Fallot.

Palabras clave: quistes de dinoflagelados, bioestratigrafía, análisis multivariante, paleoambientes, Cretácico, margen occidental Ibérico, Cuenca Sud-Provenzal

SUMMARY

REMERCIMENTS + AGRADECIMIENTOS.....	i
ABSTRACT (En, Fr, Esp).....	iii
SUMMARY.....	1
INTRODUCTION	3
CHAPTER 1 ELUCIDATION OF THE STAGE BOUNDARIES DISCREPANCIES FROM THE ODP HOLE 959D IN THE GULF OF GUINEA	19
CHAPTER 2 SPATIO-TEMPORAL VARIABILITY OF ALBIAN COASTAL AND OCEANIC SUBTROPICAL DINOFLAGELLATE CYSTS FROM THE IBERIAN MARGIN	41
CHAPTER 3 SPATIO-TEMPORAL VARIABILITY OF APTIAN DINOFLAGELLATE CYSTS	99
GENERAL CONCLUSIONS AND PERSPECTIVES (En, Fr, Esp)	151
Bibliography	163
Figure list.....	187
Table list.....	191
PLATES	193
APPENDIX.....	205

INTRODUCTION

1. <u>Philosophical approach</u>	5
1.1. Cretaceous paleogeography, paleoceanography and paleoclimatology	6
1.2. New results and findings	9
2. <u>Dinoflagellates</u>	11
2.1. Geographical and ecological distribution of dinocysts	15
3. <u>Objectives and structure of the thesis</u>	16

1. Philosophical approach

The Cretaceous Period climate has long been described as warmer than the present days, generally ice free, with low thermal gradient and high levels of atmospheric carbon dioxide (e.g. Frakes, 1979; Barron, 1983; Lini *et al.*, 1992; Frakes *et al.*, 1992; Huber *et al.*, 1995; Wilson and Norris, 2001). The Cretaceous climate is thus considered a good example for the study of the Earth system in “greenhouse” climate conditions. Current increase in atmospheric greenhouse gases concentration has stirred up the interest on warm intervals in Earth history.

Understanding of the Earth system requires integration of information from all its spheres. The interactions among the outer Earth layers and the energy inputs from the solar system, orbital forcing, play a major role in conditioning the main Earth climatic modes (e.g. Imbrie and Imbrie, 1980). Landmass / ocean distribution (paleogeography) influences the oceanic and atmospheric latitudinal heat transfer, modeling regional climates (e.g. Barron *et al.*, 1980; Ramstein *et al.*, 1997; Fluteau *et al.*, 1999). The biological activity can buffer environmental changes, through the balance between photosynthesis and respiration processes (e.g. Charlson *et al.*, 1987; Berry, 1992; Wang and Eltahir, 2000; Riding, 2006). Because the atmosphere and the oceans are permeable units, the biological effects in the composition of the one would be coupled with changes in the other (e.g. Joos *et al.*, 1996; Baldocchi *et al.*, 1988; Carpenter *et al.*, 2012). The soils, and the type and volume of geological material subject to alteration, the transfer and the trap of material of biological origin into sediments contribute to climate regulation.

The sedimentary rocks record the information on Earth and Biosphere evolution. The study of the sedimentary record during warm periods, like the Cretaceous, will allow us to better constraints future scenarios for climate and biosphere. However, the relevance of geological information for understanding and modeling of future earth conditions depends on accuracy of reconstructed paleoenvironmental conditions and resolution of the time constraints, which is the background philosophy of my doctoral thesis.

1.1. Cretaceous paleogeography, paleoceanography and paleoclimatology

The Cretaceous was a period of major changes in the paleogeographical distribution of continental and oceanic masses and so in the paleoceanographical conditions (Fig. 1). One of the most prominent events during the Cretaceous was the opening of the South Atlantic Ocean. Although the seafloor spreading started in southernmost South Atlantic during the Valanginian, 134 Ma ago (Channell *et al.*, 1995), the final breakup (i.e., separation of continental-oceanic boundary) took place between the upper Albian and the lower Cenomanian in the Equatorial Atlantic (e.g. Nürnberg and Müller, 1991; Granot *et al.*, 2012), leading to the establishment of a shallow-water connection between the Central and South Atlantic Oceans (Förster *et al.*, 2007; Moullade and Guèrin, 1982; Moullade *et al.*, 1993). Deep water circulation started during the Upper Cretaceous (Antobreh *et al.*, 2009; Granot *et al.*, 2012; Pletsch *et al.*, 2001; Murphy and Thomas, 2013), probably during the Campanian (Friedrich and Erbacher, 2006).

The Cretaceous continental spreading and long-term sea level rise favored the widespread development of shallow seas (Steuber, 2002; Haq, 2014). Extensive carbonate platform developed (Fig. 2) in shallow environments in the Atlantic, Tethys

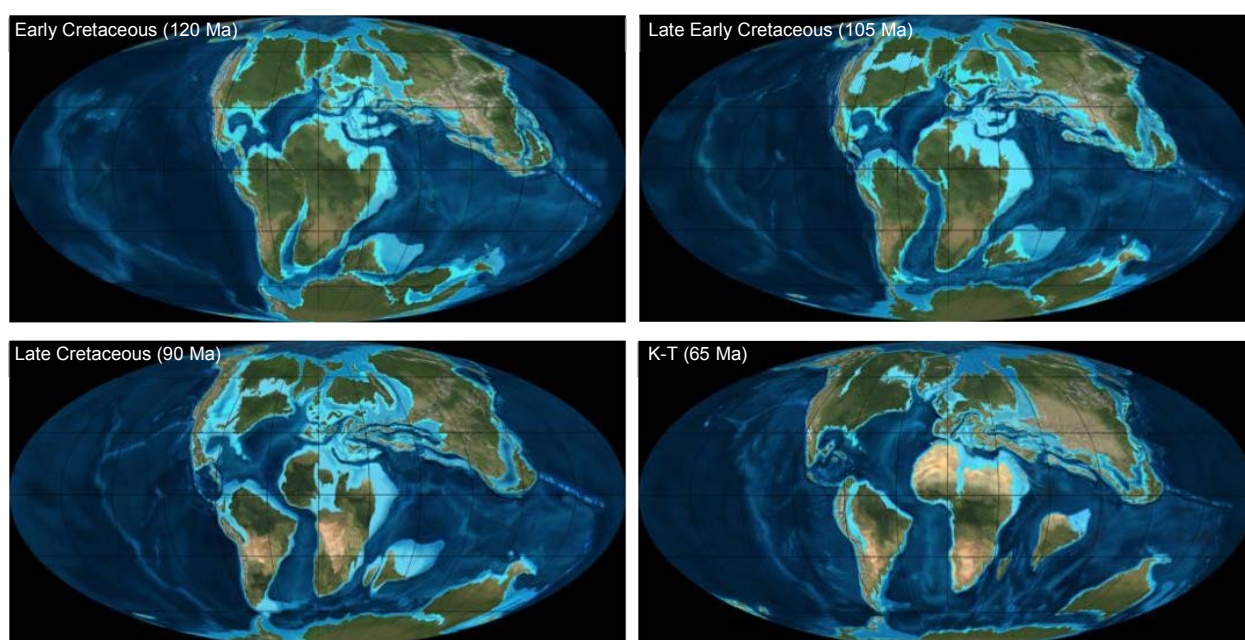


Figure 1. Paleogeographic evolution during the Cretaceous (from Blakey and Colorado Plateau Geosystems, INC, 2014) from the Early Cretaceous (c.a. 120 Ma) to the Cretaceous – Paleogene Boundary (K-T, c.a. 65 Ma).

and low paleolatitude Pacific seamount belt (e.g. Masse and Rossi, 1987; Gili *et al.*, 1995; Masse *et al.*, 1997; Huck *et al.*, 2010; Skelton and Gili, 2011). The analysis of carbonate platform evolution at global scale and low timescale resolution shows global patterns of growing and crisis events (e.g. Skelton and Gili, 2011). Crises are mirrored by strong ecological and biological changes (Masse and Fenerci-Masse, 2013a; Huck *et al.*, 2014). Numerous studies have related the carbonate platform crises with the development of Oceanic Anoxic Events (OAEs) recorded in deep environments (e.g. Masse and Philip, 1986; Ross and Skelton, 1993; Föllmi *et al.*, 1994; Weissert *et al.*, 1998; Burla *et al.*, 2008; Skelton and Gili, 2011). However, more complex framework emerges when analyzing carbonate platform evolution in the light of better stratigraphic resolution (e.g. Masse and Fenerci-Masse, 2011; Huck *et al.*, 2013).

Oceanic Anoxic Events (OAEs) were initially described by the recognition of apparently coeval Cretaceous marine carbon-rich sediments (primarily black shales, (Schlanger and Jenkyns, 1976). The “epithet” *anoxic* used in the definition of the OAEs has a genetic meaning. The OAEs constitute huge perturbations in the global carbon cycle during the Cretaceous. This feature is reflected in the particular signature of carbon stable isotopes, $\delta^{13}\text{C}$ (Scholle and Arthur, 1980; Menegatti *et al.*, 1998; Weissert *et al.*, 1998). Originally only two OAEs were recognized, namely, the Aptian-Albian (OAE 1) and the Cenomanian-Turonian (OAE 2). Advances in stratigraphy allowed a more precise dating resulting in the subdivision of the long OAE 1 interval into four subevents, out of which the Early Aptian OAE 1a is the only one of global extension (Fig. 3).

The OAE 1a event is referred as “Livello Selli” in Italy (Coccioni *et al.*, 1987), and “Niveau Goguel” in the SE of France (Bréhéret, 1988). From the study of its $\delta^{13}\text{C}$ signature in the Cismon section (N Italy), (Menegatti *et al.*, 1998) described it as the interval including two major positive $\delta^{13}\text{C}$ shifts (segments C4 and C6) with a main central segment (C5) corresponding to a period of temporary uniformity of $\delta^{13}\text{C}$. This pattern of $\delta^{13}\text{C}$ evolution is found on distant sections and it allows precise correlations in varied environmental settings (e.g. Huck *et al.*, 2010; Stein *et al.*, 2012).

Deciphering the mechanisms that triggered OAE 1a remain a challenging issue. The temporal proximity between the carbon excursions of the OAE 1a and the onset of intensified submarine volcanic activity (Ontong Java Plateau and the Manihiki Plateau) would suggest the imprint of volcanic degassing on global warming (e.g. Arthur *et al.*,

1985; Kuhnt *et al.*, 2011), on deep-ocean circulations and on plankton productivity (e.g. Erba, 1994). However, analyses of climate-sensitive sporomorphs around the OAE 1a period discard the hypothesis that variations in atmospheric pCO₂ account for a major shift in temperatures (Heimhofer *et al.*, 2004). Based on geochemical evidences, methane hydrate dissociation also has been proposed as responsible of the abrupt δ¹³C variations and reduced oxygen availability (e.g. Jahren *et al.*, 2001; Renard *et al.*, 2005). An alternative model was proposed on the basis of orbital forced alternations of the organic rich levels and marls (Herrle *et al.*, 2003; Kuypers *et al.*, 2004). Climatic cycles, alternating periods of higher temperatures and/or increased precipitation and runoff with cooler and drier periods, resulted in variations of the rate of deep water

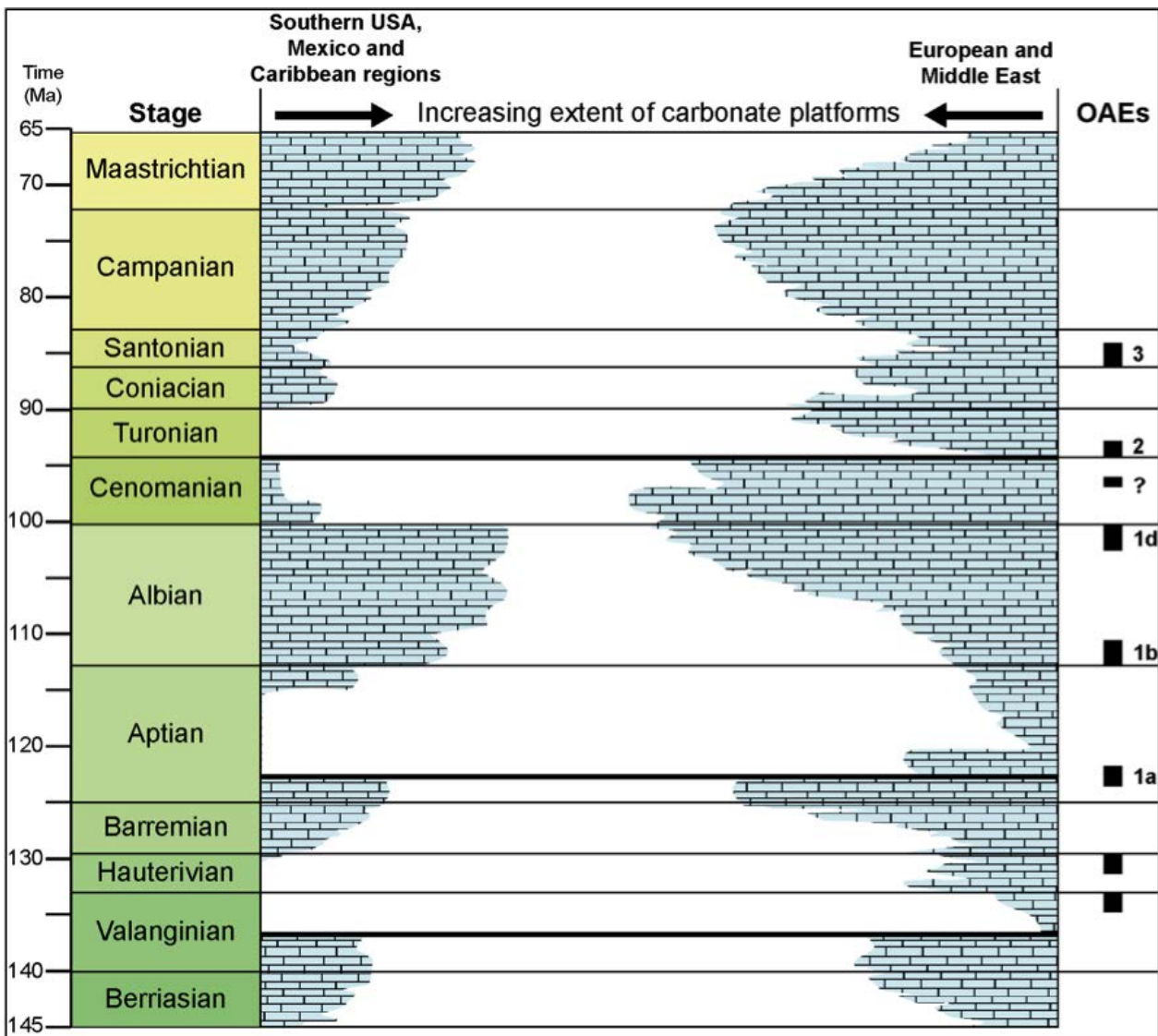


Figure 2. Synoptic history of Cretaceous carbonate platform development (blue tiled areas) in the European and Middle East regions and in the Southern USA, Mexico and Caribbean regions, major platform crises (bold horizontal lines) and timing and duration of oceanic anoxic events (modified from Skelton and Gili, 2011).

renewal and thus bottom water oxygenation and organic matter preservation (e.g. Tiraboschi *et al.*, 2009; Herrle *et al.*, 2010). Variations in the abundance and composition of microfossil assemblages recorded such variations in marine productivity (e.g. Erba, 1994; Bergen, 1998; Leckie *et al.*, 2002). The diversity of interpretations for the main Cretaceous events highlights the need for further multiproxy studies. The issue is about how specific paleoclimatic and paleoceanographic conditions are recorded over different oceanographic settings, from nearshore to the deep sea.

Study of the Iberian Massif Cretaceous history is of crucial interest for several reasons. From an oceanographic point of view, the Iberian Massif was in a key point between the Tethyan and Central Atlantic domains and witnessed the early opening of the proto-North Atlantic from the frontline (e.g. Soares *et al.*, 2012). During the Cretaceous the Iberian bloc experienced a counterclockwise rotation that led to its current position and modified the Atlantic / Tethyan connections (e.g. Gong *et al.*, 2008). The comparative study of the Cretaceous record in the Iberian Massif and in fully Tethyan settings, like the Southern Provence Basin, will allow us to differentiate between local, regional and global patterns.

1.2. New results and findings

The idea of a contrasted Cretaceous climate has been reinforced during recent years. Evidences of Cretaceous periods of global cooling and increased seasonality, of variations in the moisture, or the recognition of “cold snaps” during warm periods modulated the assumed equable Cretaceous climate (e.g. Price, 1999; Steuber *et al.*, 2005; Upchurch *et al.*, 2015; Galloway *et al.*, 2015). Progresses have been possible thanks to the development of detailed correlations among various sections from different regions for which the chronostratigraphic framework was well constrained and data from a dense sampling for different tracer analyses were available.

The different methodologies allowing dating, correlating, calibrating of durations or deciphering paleoenvironmental conditions are complementary, and integrative approaches facilitate the understanding of particular historical events. In many cases, biostratigraphy is the keystone for establishment of ages and correlations. Further detail may be reached by the use of magnetostratigraphic data and high-resolution curves of stable isotopes, as $\delta^{18}\text{O}$ and $\delta^{13}\text{C}$. The precise duration of the events may be

estimated through cyclostratigraphic calibrations. Description of environmental variations may be done through sedimentological, geochemical and paleontological data. Isotopic variations of elements such as oxygen and carbon reflect variations in environmental conditions like temperature and/or salinity, atmospheric $p\text{CO}_2$ and primary productivity. These environmental insights are complementary to paleoecological information obtained through the study of micropaleontological data. The abundance and distribution of microorganisms like foraminifers, ostracods, nanofossils or organic-walled dinoflagellate cysts (herein after dinocysts) may give indications about, for example, depth, oxygen availability and/or productivity. They may also be useful for identifying the development of gateways between different regions and the establishment of exchanges among water masses. Dinocyst are among the micropaleontological tracers having shown a great biostratigraphical utility. Because they are present from equatorial to polar, and onshore to offshore environments and their resistant organic composition makes them insusceptible to dissolution processes, they are abundant in many strata devoid of other fossils, especially in anoxic environments.



Figure 3. Geographic distribution of sections containing the OAE1a (black dots) and major igneous provinces active during the Cretaceous, red patches (modified after Tremolada *et al.*, 2007).

2. Dinoflagellates

Dinoflagellates are aquatic eukaryotic, unicellular organisms. Recent studies on molecular phylogeny group dinoflagellates and Apicomplexa, and their respective sister taxa, within the Myzozoa (Cavalier-Smith and Chao, 2004). The Myzozoa and the ciliates are the main members of Alveolata (Fig. 4) (Leander, 2008). Recent works suggested that alveolates, stramenopiles, Rhizaria and a clade consisting of criptomonads and Haptophyta (Hacrobia) constitute the Chromalveolata (Fast *et al.*, 2001; Harper and Keeling, 2003; Hackett *et al.*, 2007).

Although dinoflagellates may occur as coccoid cells, amoeboid cells, multinucleate cells, tentacle-bearing cells and filamentous and ribbon-like colonies of cells the most common are motile and biflagellate cells. The combined motion of both flagella imparts a unique spiral-like motion that inspired their name (from the Greek *dinos*, whirling rotation, and the Latin *flagellum*, small whip). Other key features in the assignment of an organism to the Dinoflagellata division are the presence of a dinokaryon, the possession of an amphisema and the presence of specific biomarkers (dinosterol and amphisterols). The dinokaryon is a nucleus containing constantly condensed chromosomes, without histones and in which the mitotic spindle is extranuclear. The amphisema is a complex outer region of the cell membrane characterized by the presence of a single layer of vesicles that may, or not, contain cellulosic plates (thecal

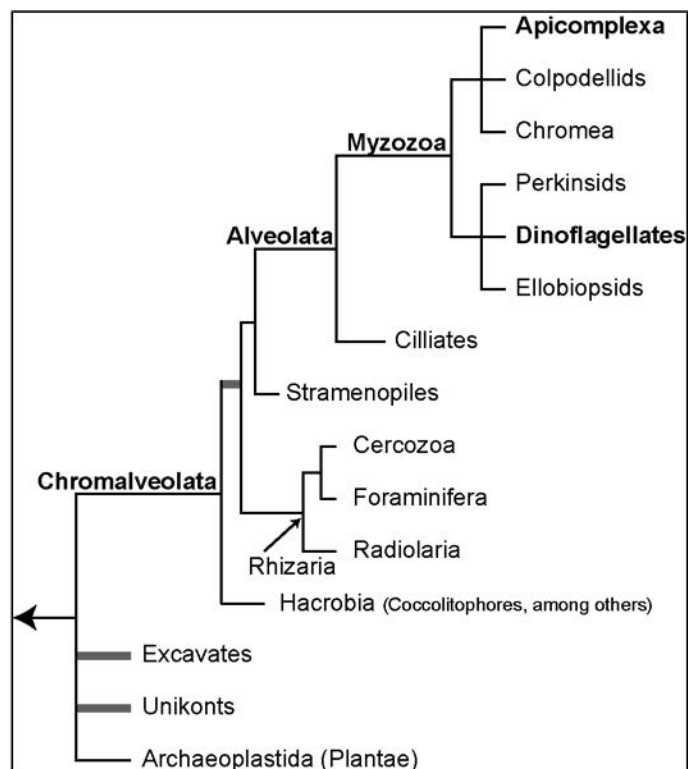


Figure 4. Phylogenetic tree including dinoflagellates (redrawn from Keeling *et al.*, 2009), solid grey lines indicate groups that may not be monophyletic. The basis for grouping the dinoflagellates within the Myzozoa (sucking life, Cavalier-Smith and Chao, 2004) it that both Dinozoa and Apicomplexa are commonly or ancestrally myzocytotic feeders. The Alveolata are characterized by showing a system of abutting membranous sacs called "alveoli; distinct micropores through the cell surface that function in pinocytosis; similar extrusive organelles (e.g. trichocysts; closed mitosis and/or tubular mitochondrial cristae (Leander, 2008). The groups comprised in the Chromalveolata clade share the widespread presence of plastids, all derived from secondary endosymbiosis with a red alga, additional support comes from molecular phylogenies (Keeling *et al.*, 2009).

plates) thus differentiating thecate taxa and athecate taxa (Dodge, 1987; Taylor, 1987; Fensome *et al.*, 1996). Dinoflagellates inhabit most aquatic environments at all latitudes from the Equator to Polar seas, from marine to open ocean to lakes or even sea ice. Up to a 90% of dinoflagellates are marine and (together with diatoms and coccolithophorids) they are one of the most important primary producers in marine environments but, together with diatoms, they also occur in freshwater habitats (e.g. Taylor and Pollinger, 1987).

The life cycle of dinoflagellates is complex (Fig. 5). Most of them have haplontic life cycles, which means that the vegetative state (experiencing growth) is haploid (n). Asexual reproduction is faster and is therefore the dominant form of reproduction when conditions are optimal. Sexual reproduction is essential for species adaptation because it enables genetic recombination (i.e. genetic variation). Asexual reproduction is brought out in different ways depending on species (Pfiester and Anderson, 1987). During the sexual phase two haploid gametes produced by the vegetative cells fuse to form a motile zygote (planozygote, 2n). Motile planozygotes can follow three different routes: (1) direct division (meiosis) that results in multiple haploid cells, (2) short encystment (temporary, cellulosic ecdysial cysts), or (3) long period encystment (resting cyst in dinosporin). The excystment occurs after a variable latency and may result in a planozygote (2n) or in multiple haploid, vegetative, motile cells (e.g. (Evitt, 1985; Figueroa and Bravo, 2005; Figueroa *et al.*, 2006). The temporary ecdysal cysts wall is cellulosic and easily degradable, thus ecdysal cysts are not prone to fossilization. The resting cyst wall consists of a highly resistant, macromolecular organic compound termed “dinosporin” (Fensome *et al.*, 1993), whose structure is still poorly known (e.g. (de Leeuw *et al.*, 2006; Versteegh *et al.*, 2007, 2012) and it is this resting cyst that is preserved in the geological record. A few species produce resistant cyst walls made of CaCO₃ or silica, but they are not discussed hereafter. Although not all living species produce fossilizable cysts, about 15-20% of all living dinoflagellate produce resting cyst (Head, 1996), up to 28% in temperate regions (Persson *et al.*, 2000).

The taxonomic identification of dinocyst relies on morphological characters that, to varying degrees, reflect aspects of the wall structure of their parent motile cells. The paracingulum is well represented in most dinocyst allowing the identification of the epicyst and the hypocyst, hosting the parasulcal notch. The plate distribution of motile forms is mirrored in the dinocyst paraplates distribution. Paraplates are distributed in quasi-latitudinal bands, parallel to the cinculum, along the epi- and hypocyst (Fig. 6),

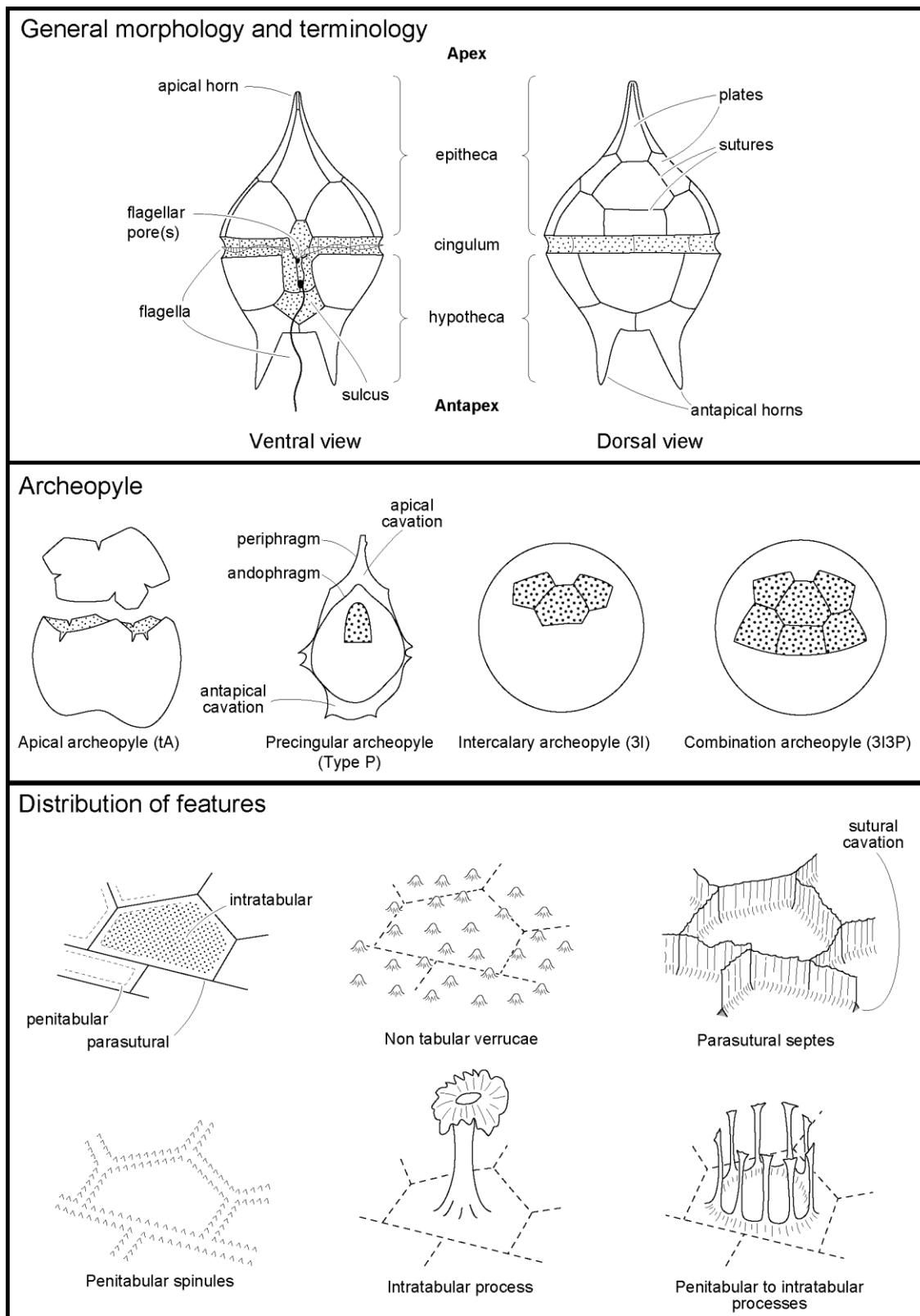


Figure 6. Main dinocyst morphological attributes used for their taxonomical classification (modified from Evitt, 1985).

2.1. Geographical and ecological distribution of dinocysts

Dinoflagellates are present at all latitudes and in all marine environments from inshore to offshore. General patterns in species geographical distribution of dinocysts were first recognized by Wall *et al.* (1977). The pioneer work of Wall *et al.* (1977) stirred up the community interest and since then a number of studies have been published (e.g. Harland, 1983; Goodman, 1987; Rochon *et al.*, 1999; Marret and Zonneveld, 2003; de Vernal *et al.*, 2005; Zonneveld *et al.*, 2013). From these studies it is empirically clear that dinocyst assemblages found on the sea floor offers a reliable picture of the planktonic dinoflagellate communities found at the sea surface. At a global scale, the distribution of modern organic walled dinoflagellate cyst is predominantly related to sea surface temperature (SST) and latitudinal patterns (Wall *et al.*, 1977; Harland, 1983; Dale, 1996; Zonneveld *et al.*, 2013). Another major trend reflects the inshore to offshore gradients along the continental margins that is related to the variations in nitrate, salinity, phosphate and bottom-water oxygen concentration (e.g. Wall *et al.*, 1977; Harland, 1983; Marret and Zonneveld, 2003).

The use of dinocyst in paleoceanographical studied increased in parallel to our knowledge about the environmental factors controlling their distribution. These studies led to the development or adaptation of quantitative approaches for the reconstruction of past oceanographical conditions from dinocyst data (e.g. Edwards *et al.*, 1991; Edwards, 1992; Mudie, 1992; de Vernal *et al.*, 1993, 1994; Marret *et al.*, 2001; Eynaud *et al.*, 2002; Solignac *et al.*, 2004; Pospelova *et al.*, 2008; Bonnet *et al.*, 2012). Reconstructions of hydrographical parameters using dinocyst data have been made using various approaches; the use of indices (e.g. relative abundance of warm water vs. cold water taxa); the application of transfer function (Imbrie and Kipp, 1971); the application of regression techniques or neural network approaches; and more recently the application of the best analogue method (Guiot, 1990) and the modern analogue technique (de Vernal *et al.*, 1994). However, the use of these quantitative approaches for the reconstruction of past oceanographical conditions is limited back in time by the unavailability of modern analogs for pre-Pliocene assemblages (de Vernal and Mudie, 1989).

Numerous studies have focused on the distribution of fossil dinocyst assemblages (pre-Pliocene). Most of them were founded in the relationship between sequence stratigraphy and the evolution of dinocyst assemblages, revealing that changes in assemblage composition and diversity may be used to determine

transgressive–regressive phases and can be related to changes in relative sea level (Haq *et al.*, 1987; Habib and Miller, 1989; Gregory and Hart, 1992; Brinkhuis and Biffi, 1993; Schiøler *et al.*, 1997; Jaramillo and Oboh-Ikuenobe, 1999; Dybkjær, 2004; Sluijs *et al.*, 2005). Initial investigations of Cretaceous diversity of dinoflagellate cysts focusing on larger scale patterns show that latitudinal distribution of taxa mirrored sea surface temperature (Masure and Vrielynck, 2009; Masure *et al.*, 2013).

3. Objectives and structure of the thesis

The environmentally driven biodiversity patterns described in extant dinocysts offer guidelines for the improvement of the traditional practice of biostratigraphy and environmental reconstructions in the deep time. The present thesis explores both aspects. On the one hand, it describes how differences in sampling sets, sampling resolution and operator practices may alter the chronostratigraphic interpretations. On the other hand, it aims at developing an adequate methodology for recognition of the environmental preferences of fossil dinocyst, and for characterization the environmental significance of dinocyst assemblages.

The first section of the thesis revisits the use of fossil dinocysts as chronostratigraphic tracer. It analyzes the dinocyst assemblages from the Cretaceous and Paleocene sections of the 959D DSDP site, located in proximity to the Côte d'Ivoire – Ghana transform margin. During the Cretaceous this region witnesses the opening of the South Atlantic. The studied interval is mostly devoid of calcareous microfossils, due to sedimentation below the carbonate compensation depth (CCD). Paleomagnetic data were too low to allow a magnetostratigraphy of the 959D cores (Shipboard Scientific Party, 1996). Under these conditions dinocyst are almost the only chronostratigraphical tracer for most of the studied interval (Masure *et al.*, 1998a and Oboh-Ikuenobe *et al.*, 1998). The two previous studies evidenced some biostratigraphic inconsistencies. In the present work, we re-analyzed a subset of the sample studied by Masure *et al.* (1998a), with two main objectives: (1) to discriminate the bias at the origin of the differences between the results of Masure *et al.* (1998a) and Oboh-Ikuenobe *et al.* (1998), and the data produced for the present study; and (2) to propose a consensual chronostratigraphic interpretation considering all available data (Kuhnt *et al.*, 1998a; Masure *et al.*, 1998a; Moullade *et al.*, 1998d; Oboh-Ikuenobe *et al.*, 1998; Watkins *et al.*, 1998).

The second section of the thesis is organized in two chapters, Chapters 2 and 3, and deals with the palaeoenvironmental distribution of fossil dinocysts. The Chapter 2 develops a methodology to associate dinocyst assemblages with specific environmental conditions. Because of the complexity of the question, it was essential to select an example in which the temporal sequences are robustly resolved. The availability of good information about depositional environments was also fundamental. Albian proximal deposits from the Atlantic Iberian Margin have been largely studied from a number of disciplines. Coastal and shallow shelf deposits are available in the Lusitanian basin (Rey, 1979; Hasenboehler, 1981; Heimhofer *et al.*, 2007, 2012; Dinis *et al.*, 2008; Horikx *et al.*, 2014). The 398D site from the Deep Sea Drilling Project (DSDP) records the same time slice under more distal conditions (Sibuet *et al.*, 1979). The comparative study of the 6 sections allows us to analyze the distribution and paleoecology of dinocyst species along an onshore-offshore transect. Almost all previous works that examined paleoecology of dinocysts in the deep time are based on qualitative analysis. In this study we examined the structure of the dataset through multivariate analysis. This approach assumes the existence of dinocyst associations indicative of species ecological affinities. The integration of our results with previous paleoenvironmental data (e.g. sedimentological, clay assemblages, and paleontological data) will link the dinocyst associations with particular paleoenvironmental conditions.

The third chapter aims at validating the methodology and to compare the results on the paleoenvironmental distribution of Albian fossil dinocysts with those found in other geological series. The Aptian series of the Southern Provence Basin and of the 398D DSDP site are considered. These sections are selected to extend the comparisons deeper in time and in a Tethyan province. Because the Aptian studied sections belong to different paleoceanographic regions, differences in their response to global trends and short-lived events can be tested. The studied sections from Southern Provence Basin define the historical Aptian stratotype and have been analyzed from a plethora of proxies. The integration of the new dinocyst data with previous multi-proxy analyses will allow us to strength our interpretations. The Aptian series record some of the more characteristic Cretaceous events, as the carbonate platform crisis and the OAE 1a. The response of dinocyst associations to these events will be analyzed in the Southern Provence Basin. The focus in our analyses on the taxa with a large

stratigraphical range allows us to test for conservative ecology of taxa during the ~20 million years of the Albian - Aptian interval.

Solving the paleoecological questions is of great interest for improving the reliability of dinocysts as biostratigraphic markers, and the resolution of distant section correlations. Meanwhile, the development of our knowledge about fossil dinocyst paleoenvironmental preferences will provide new evidences and constraints to paleoenvironmental and paleoclimatic reconstructions.

CHAPTER 1

Elucidation of the stage boundaries discrepancies from the ODP Hole 959D in the Gulf of Guinea

This chapter has been elaborated in collaboration with Masure E., Michoux, D. and Villier L.

1. <u>Introduction</u>	20
2. <u>Geological setting</u>	22
3. <u>Material and Methods</u>	24
4. <u>Dinoflagellate cysts and biostratigraphy</u>	25
4.1. Dinocyst biostratigraphy	25
4.2. Evolution of the Dinocyst assemblages, organofacies and palynofacies: a paleoenvironmental interpretation	31
5. <u>Discussion</u>	33
5.1. Density of sampling and biostratigraphic resolution	33
5.2. Rarity effect and the recognition of age markers	34
5.3. Taxonomic revisions and instability of stage boundaries	36
5.4. Influence of paleoenvironmental factors on the dinocyst stratigraphic record	37
6. <u>Conclusions</u>	38

1. Introduction

One of the most prominent events during the Cretaceous was the opening of the South Atlantic Ocean. The effective separation between Africa and South America continents lead to the connection between the Central and South Atlantic Oceans (e.g. Wagner and Pletsch, 1999; Pletsch *et al.*, 2001; Friedrich and Erbacher, 2006). The main paleobiological consequences of these events, was the exchange of marine biota between the Central and South Atlantic Oceans and the differentiation of African from South American faunas and floras (e.g. (eyment, 1969; Berggren and Hollister, 1974; Moullade and Guèrin, 1982). Numerous recent studies have focused on the paleoceanographic and paleoclimatic consequences of the establishment of a connection between the Central and South Atlantic (e.g. (immerman *et al.*, 1987; Jones *et al.*, 1995, 1995; Poulsen *et al.*, 2001; Friedrich and Erbacher, 2006; Förster *et al.*, 2007; Friedrich *et al.*, 2012).

Wegener (1915) first recognized the symmetry between the Atlantic margins of South America and Africa. The opening of the South Atlantic Ocean began with seafloor spreading in the southernmost part of the South Atlantic Ocean (e.g. Nürnberg and Müller, 1991; Channell *et al.*, 1995). The final breakup between South America and Africa took place between the upper Albian and the lower Cenomanian (e.g. Nürnberg and Müller, 1991; Granot *et al.*, 2012) leading to the establishment of shallow-water connection (e.g. Moullade and Guèrin, 1982; Friedrich and Erbacher, 2006). The area of final disjuncting is known as the Equatorial Atlantic Gateway (EAG). The Côte d'Ivoire – Ghana Transform Margin represents a continuation of the Romanche Fracture Zone, which is the southern boundary of the EAG (Basile *et al.*, 1998).

The position of the continental margins parallel to the equatorial fracture zones suggests that a large part of this opening history was accomplished by lateral movements of the South American and African plates (Wagner and Pletsch, 1999). However, the precise oceanographic history of the South Atlantic Ocean opening is still poorly known. The temporal and spatial changes in subsidence and block tilting over short distances along the transform margins lead to a fragmentary record. A long period of stable polarity of the geomagnetic field, the Cretaceous Normal Superchron (CNS), hampers the reconstruction of the early relative plate's motion.

Improving the chronological constraints of the sedimentary record in the different South Atlantic marginal basins is essential to decipher the complex evolution of the oceanic opening. Two previous studies (Masure *et al.*, 1998a; Oboh-Ikuenobe *et al.*, 1998) have evidenced the strengths and some inconsistencies of dinocyst biostratigraphy of the 959D site, placed in the Côte d'Ivoire – Ghana Transform Margin. In the present study we re-analyze a sample sub-set of Masure *et al.* (1998a). Biostratigraphy analyses the rocks from their fossil content, and aims at identifying stratigraphic sequences of fossils occurrences that could be of chronological significance (Berggren and van Couvering, 1978; Haq and Worsley, 1982). Biochronology expands the context of biostratigraphy by inferring, or interpolating, ages from the succession of taxa (e.g. Christopher and Goodman, 1996). Biostratigraphy is commonly the keystone for establishment of chronostratigraphic units, recognition of their boundaries, and inferences of correlations.

However, the geological record does not provide a straightforward representation of life evolution. The appearance, range and disappearance of taxa are not exclusively time-controlled. A number of palaeoecological, taphonomic, diagenetic and stratigraphic factors act on the geological record of the evolutionary dynamics of fossil taxa (e.g. Gradstein, 1985; Holland, 2000). The inherent properties of the paleontological record result in various biases:

- The incomplete record of a taxon's extension leads to gaps between its times of origination and extinction with its oldest and earliest occurrence as fossil;
- Collapse of a time sequence in condensed series, in which distinct evolutionary events could be considered coeval when they are not;
- When not recognized, the reworking of some fossils make its last occurrence younger than it actually is;
- The relative order of two evolutionary events may not necessarily be recorded in the right sequence, depending on paleoenvironmental conditions of the places and likelihood of taxon preservation as fossil.

Human biases can also add inconsistencies in the restoration of chronological information. The biostratigraphic study of dinocyst from the 959D site aims at testing how differences in sampling strategy, sampling resolution, and operator practices may alter the chronostratigraphic interpretations. A consensual chronostratigraphic

interpretation is proposed considering all available data (Masure *et al.*, 1998a; Moullade *et al.*, 1998d; Oboh-Ikuenobe *et al.*, 1998; Watkins *et al.*, 1998).

2. Geological setting

The ODP site 959D is located at 2100 m water depth on a small plateau that extends just north of the top of the Côte d'Ivoire – Ghana Marginal Ridge (CIGMR, Fig. 1.1) on the southern shoulder of the Deep Ivorian Basin (DIB) ($3^{\circ} 37.656'N$, $2^{\circ} 44.149'W$, (Shipboard Scientific Party, 1996). Both features, the CIGMR and DIB, were generated as a consequence of Early Cretaceous rifting of the northern south Atlantic (Fig. 1.2).

A simple three stage model may be used to describe the general margin development (Masclé and Blarez, 1987; Pletsch *et al.*, 2001). Until the Middle Albian, newly formatted isolated rift or strike-slip basins, with limited interconnection, characterized the margin (Fig. 1.3). An uplift event in the Middle-Late Albian led to the complete separation of the South American and African margins and to the establishment of permanent mid-water connection (Wagner and Pletsch, 1999; Pletsch *et al.*, 2001). The period of maximum uplift is marked by the deposition of shallow water reefal carbonates and clastic sediments (Masclé *et al.*, 1995, 1996). During this period strong differences in subsidence and basin morphology persisted along the Côte d'Ivoire – Ghana margin. During the oceanic opening stage, from the Middle

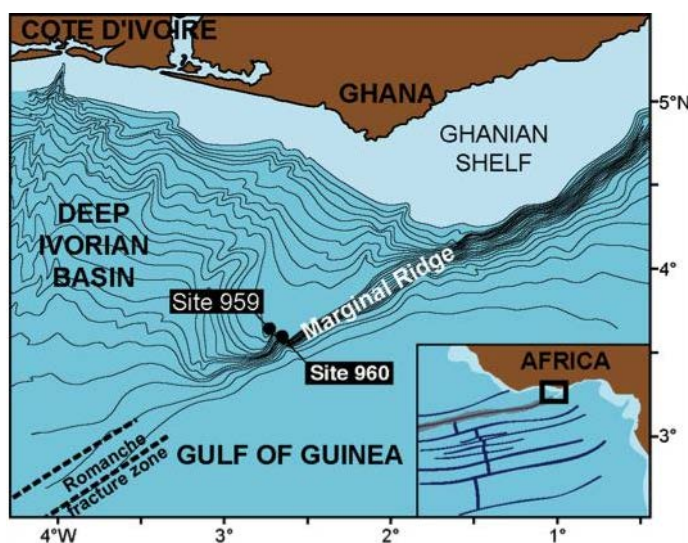


Figure 1.1. Location map of the 959D ODP site in the Côte d'Ivoire – Ghana Transform Margin area. The main physiographical features in the region are indicated (modified from Masclé *et al.*, 1998)

Coniacian after-wards, subsidence was permanent along the margin. Physiographical obstacles subsided sufficiently to allow continuous deep-water circulation (Wagner and Pletsch, 1999; Pletsch *et al.*, 2001).

The studied interval corresponds to the Oceanic opening stage from the Coniacian to the Paleogene. Cores 67R to 44R (1045.37 – 822 mbsf, meters below sea floor) sample the uppermost part of the lithologic Unit IVa and the

entire Unit III (Fig. 1.4). The top of the subunit IVa, consists of beds of sandy dolomite, limestone, and calcareous sandstone. The poorly sorted sandy limestone (67R-2) contains abundant foraminifers and nannofossils and scattered fragments of bivalve shells in quartz sand. Upper in the series, the lithologic Unit III is exclusively composed of organic rich black claystone. In the lowermost portion of lithologic Unit III (66R-CC to 66R-4) phosphatic hardgrounds and nodules floating in a nannofossils – clayey matrix are common (those levels were avoided for sampling). Bioturbated levels are present in the entire studied interval, but they are more common above 990 mbsf (Fig. 1.4). The presence of authigenic minerals (barite, pyrite, dolomite, glauconite and zeolite) is common along the studied section, but remain at low concentrations. In some intervals authigenic minerals appear associated to bioturbation (e.g. Cores 65 to 55, 995.4 to 937.1 mbsf). Thin laminae of concentrated authigenic minerals are common in some other intervals (e.g. Cores 54 to 51, 937.4 to 898.5 mbsf).

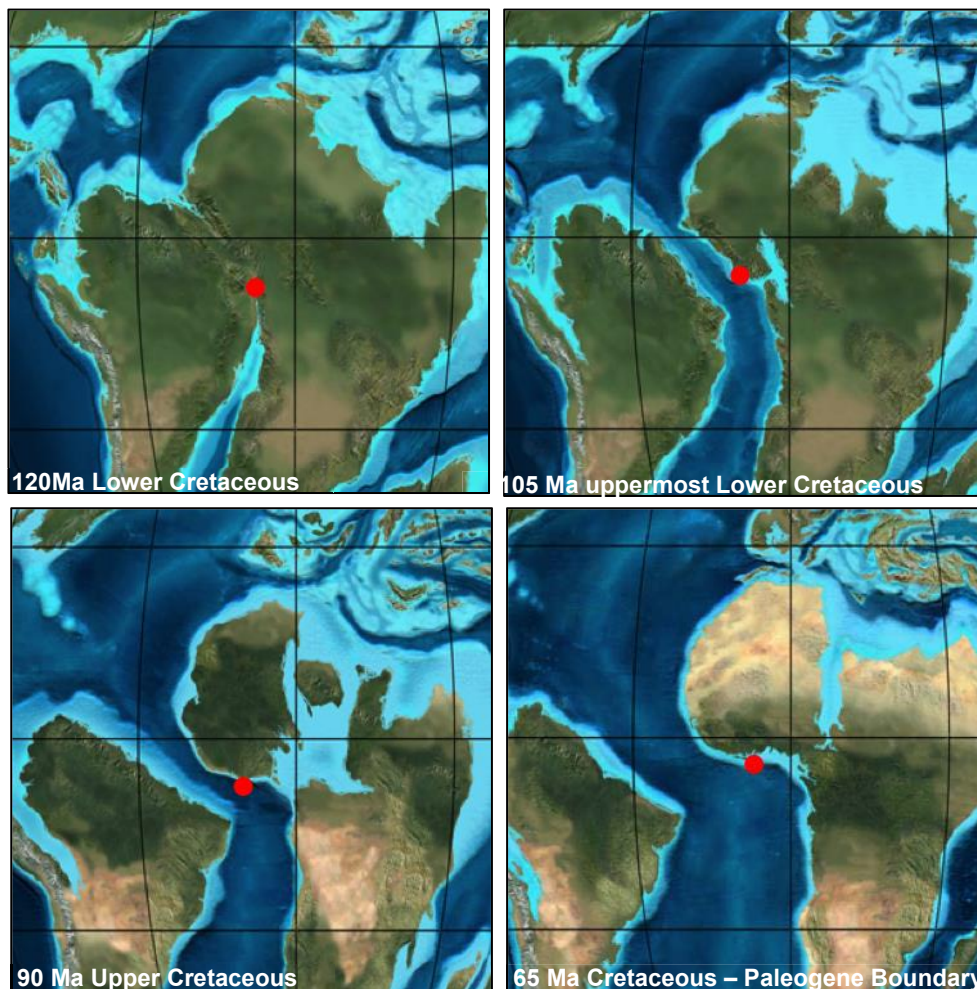


Figure 1.2. Paleogeographic evolution of the South Atlantic Ocean from the Lower Cretaceous (ca. 120 Ma) to the Cretaceous – Paleogene Boundary (ca. 65 Ma), maps from Blakey and Colorado Plateau Geosystems, INC, (2014). ODP Hole 959D position signaled by a red dot.

3. Material and Methods

All samples were processed following standard palynological preparation techniques, based on routine series of HCl – HF (70%) – HCl attacks (e.g. Traverse, 2007) followed by light oxidation with HNO₃ 50%. Sample volume was the same for all the analyzed levels, 20 ml. Organic residue was filtered over a 20 µm nylon mesh to eliminate the amorphous organic matter. At least two slides were mounted on glycerin jelly from the residue of each sample. The studied slides were all previously analyzed in Masure *et al.* (1998a). As glycerin jelly dehydrates with time, some slides were restored before analysis. Because cover slips get brittle with aging, restoring was not possible for the entire set of 56 samples of Masure *et al.* (1998a). The present study consider 23 samples from Cores 67R to 44R (1045.37 to 828.7 mbsf) of the 959D site.

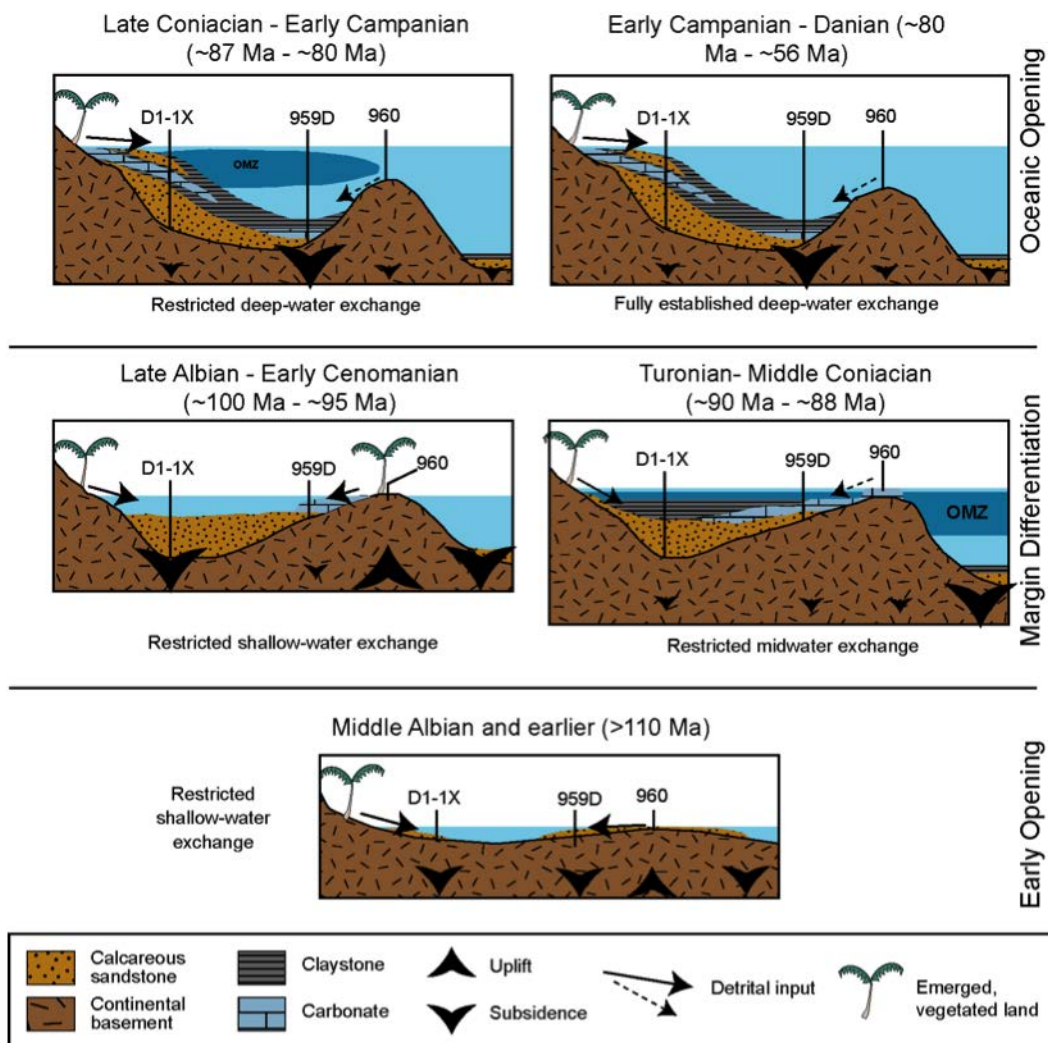


Figure 1.3. Schematic representation of the regional evolution of the Côte d'Ivoire – Ghana transform margin (modified from Wagner and Pletsch, 1999). Location of D1-1x and 960 ODP sites is also illustrated.

The complete list of analyzed samples is detailed in Table 1.1. Wherever possible a minimum of 250 palynomorphs was counted for each level and all available slides were then scanned for additional dinocyst taxa. The taxonomy of dinocysts is based on Fensome *et al.* (2008), a list of identified dinocyst taxa is given in Appendix A and the biostratigraphical distribution of dinocyst in the 959D site is given in Appendix B.1.

Table 1.1. ODP Hole 959D Sample list. All the listed samples were analyzed for quantitative dinocyst assemblage composition.

Core	Section	cm	Depth (mbsf)	Core	Section	cm	Depth (mbsf)
44R	6	060-062	828.7	56R	4	060-062	942.5
45R	1	034-039	831.94	57R	4	114-117	952.74
46R	2	018-023	842.48	58R	3	093-096	960.3
47R	1	035-037	851.25	59R	5	039-044	972.89
48R	3	065-068	864.25	60R	1	056-059	976.66
49R	4	133-137	876.03	60R	4	058-061	981.18
50R	5	098-101	886.88	62R	1	076-080	996.16
51R	4	008-011	893.78	63R	5	091-093	1011.91
52R	3	010-013	901.91	64R	1	092-095	1015.62
53R	6	018-020	914.97	66R	3	040-043	1037.1
54R	2	097-099	920.57	67R	2	057-061	1045.37
55R	3	083-085	930.39				

All counts and scans were performed with a Leica DM750 microscope, the slides were scanned along non-overlapping traverses using a 63x objective lens. Morphological identification of dinoflagellate cysts was performed using a 100x objective lens. Transmitted light photomicrographs (Plates I and II) were taken on a Leica DM750 microscope with a Leica ICC50 digital camera and the software Leica Application Suite.

4. Dinoflagellate cysts and biostratigraphy

4.1. Dinocyst biostratigraphy

The first occurrence of dinocyst in the studied sample set is located in the uppermost sample of the lithologic Subunit IVa Sample 67R-2, 57-61 cm (1045.4 mbsf, Fig. 1.5). Although dinocyst are still scarce in this sample and most of them are non-diagnostic long-ranging species, the presence of *Xenascus gotchii* (Fig. 1.5, 1.6; Pl. 1, Fig. 11) give some evidence for age determination. *X. gotchii* is known to appear

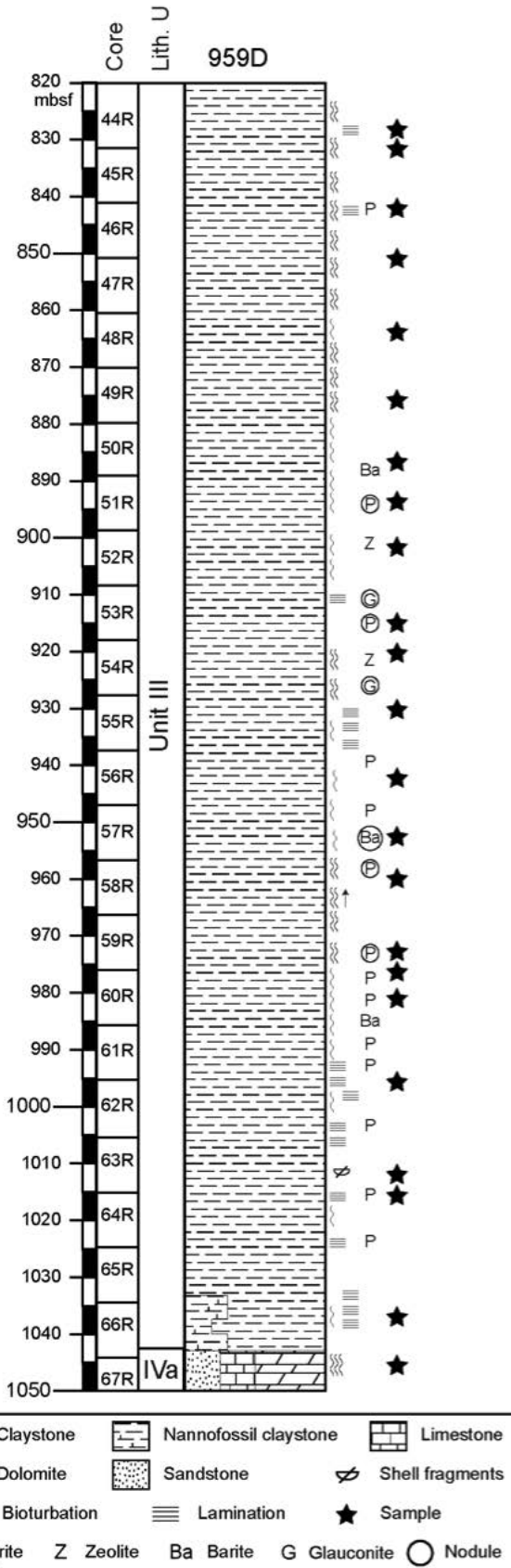


Figure 1.4. Lithology and lithological units defined within the studied interval from the 959D site (redrawn from Shipboard Scientific Party, 1996). Black stars indicate samples position.

during Senonian (Corradini, 1973), more precisely Coniacian-Santonian times according to (Kirsch, 1991). The following studied sample, Sample 66R-3, 40-43 cm (1035.1 mbsf) at the base of the lithologic Unit III, yields the only occurrence of *Cyclonephelium vannophorum* (Fig. 1.6). Since, the last occurrence (LO) of *C. vannophorum* occurs in Coniacian strata (Williams and Bujak, 1985, p. 900, fig. 19) the presence of both *X. gotchii* and *C. vannophorum* in the interval between 1045.4 mbsf and 1035.1 mbsf is here considered as indicative of Coniacian age (Fig. 1.6). This interpretation is consistent with the nannofossils (Watkins *et al.*, 1998) that identified the zones CC13a to CC15b, Late Turonian to Early Santonian in age, between 1053 mbsf and 1029.3 mbsf and placed the Turonian / Coniacian boundary in the center of the CC13a zone at 1045 mbsf.

No dinocyst markers of the Santonian stage were identified during the present study. However, Moullade *et al.* (1998d) recognized the stage in the Core 65 (1033.7 - 1024.1 mbsf, Fig. 1.6) from the association of dinocyst *Oboh-lkuenobe et al.* (1998), nannofossil (Watkins *et al.*, 1998) and planktonic foraminifer (Kuhnt *et al.*, 1998a).

In Sample 62R-1, 76-80 cm (996.16 mbsf) appears the first dinocysts indicative of a Campanian age, which includes the first occurrence (FO) of *Areoligera* (Fig. 1.5, 1.6; Pl. 2, Fig. 2). The *Areoligera* group is known from the Campanian of Gabon (Boltenhagen, 1977), from the Campanian stratotypic area in France (Masure, 1985) and from the Campanian of New Jersey (Aurisano, 1989). Dinocyst assemblage from sample, 60R-4, 58-61 cm (981.18 mbsf) is also characteristic of the Campanian. It records the FO of the genus *Andalusiella*, *Trichodinium castaneum* subsp. *bifurcatum* and *Palaeocystodinium lidiae* (Pl. 2, Fig. 8-9) and the only occurrence of *Phelodinium magnificum* (Fig. 1.6; Pl. 1, Fig. 3). The first appearance datum (FAD) of *P. magnificum* is Campanian in the world range charts of Williams and Bujak (1985, p. 901, fig. 19). The *Andalusiella* group is known in the Campanian of Gabon (as *Svalbardella* group, (Boltenhagen, 1977) and Egypt (Schrank, 1987) where *Trichodinium castaneum* subsp. *bifurcatum* is also present. The lower Campanian boundary is placed at 1024.1 mbsf (Fig. 1.6) following the benthic foraminifers (Moullade *et al.*, 1998d).

The FO of *Cerodinium diebelii* (Pl. 2, Fig. 7), the occurrence of *Andalusiella ivoirensis* (Pl. 2, Fig. 10) and the LO of the *Trichodinium castaneum* group (including *Trichodinium castaneum* subsp. *castaneum* and *Trichodinium castaneum* subsp. *bifurcatum*; Pl. 1, Fig. 10) are identified in Sample 57R-4, 114-117 cm (952.74 mbsf, Fig. 1.5, 1.6). The world range charts of Williams and Bujak (1985) proposes a Campanian age for FO of *C. diebelii* (p. 901, fig. 19 as *Ceratiopsis diebelii*) and a late Campanian age for the LO of *Trichodinium castaneum*. *A. ivoirensis* was described from the Maastrichtian of Ivory Coast (Masure *et al.*, 1996). The analysis of this sample by Masure (Masure *et al.*, 1998a) also evidenced the FO of the *Glaphyrocysta* group and *Alterbidinium varium* (Fig. 1.6), which suggest a Maastrichtian age. The co-occurrence of Campanian and Maastrichtian marker dinocyst suggests mixing in a condensed horizon or hiatus in the late Campanian and early Maastrichtian. The distribution of Campanian marker dinocysts recognized during our investigations is consistent with the conclusions of the synthesized data of biostratigraphic contributions by Moullade *et al.* (1998d), who placed the Santonian/Campanian boundary in section 65R-1, above 1024.1 mbsf (Fig. 1.6), and the Campanian/Maastrichtian boundary between the Sections 58R-3 and 57R-4 (i.e. between 956.82 mbsf and 952.74 mbsf).

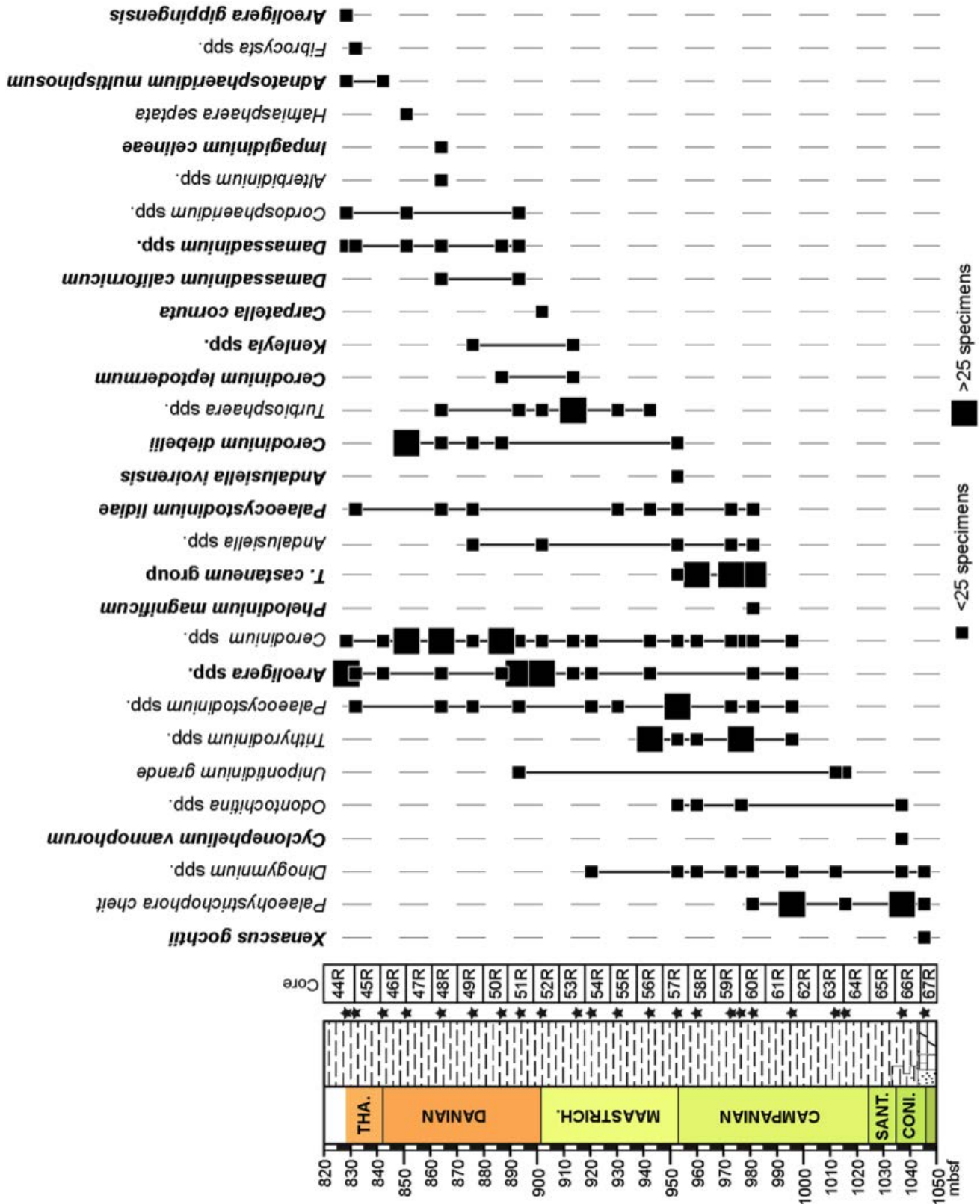


Figure 1.5. Stratigraphic distribution of selected dinocyst taxa in the 959D site. The considered taxa are important stratigraphic index species. For the lithological legend see Fig. 4. Black stars indicate sample positions. The chronostratigraphy column corresponds to the consensual biostratigraphy discussed in this study. CONI; - Coniacian; SANT. – Santonian; MAASTRICH. – Maastrichtian; THA. – Thanetian.

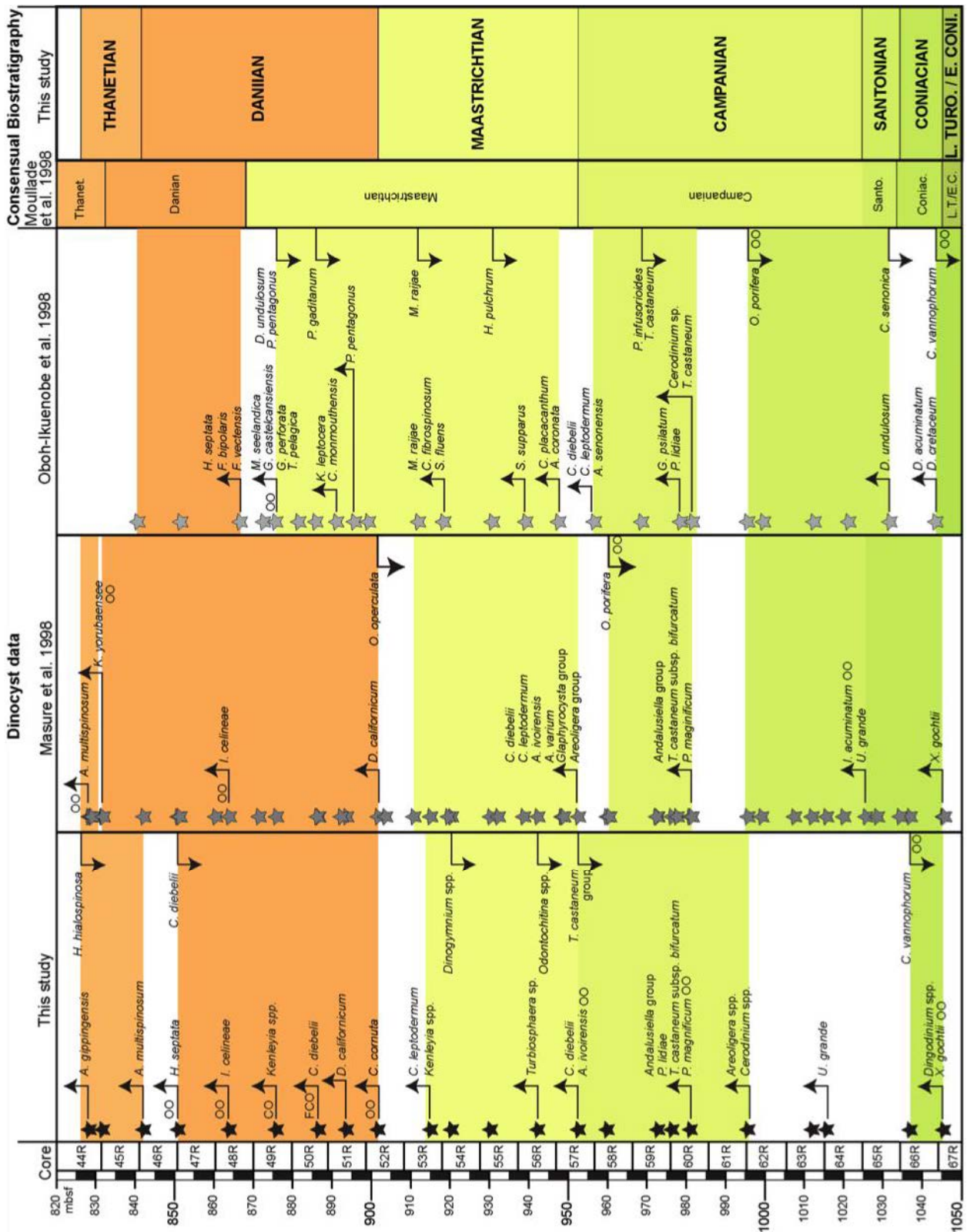


Figure 1.6. Main dinocyst events in 959D site samples. OO – Only occurrence; CO – Common Occurrence; FCO – First Common Occurrence; up-arrows – First occurrence (FO); down-arrows – Last Occurrence (LO). Stars present in each one of the dinocyst data columns indicate the sample positions for the associated study. L. TURO. / E. CONI. – L.T./E.C.– Late Turonian / Early Coniacian.

The first occurrence of Danian dinocyst markers are in Sample 52R-3, 10-13 cm (901.91 mbsf), where is observed the only occurrence of *Carpatella cornuta* (Fig. 1.6; Pl. 2, Fig. 4-5). In a previous analysis, Masure *et al.* (1998a) identified the FO of *Damassadinium californicum* in this sample (Fig. 1.6). Because *D. californicum* occurs in the basal Danian in Europe (Hansen, 1977, 1979a, 1979b), Morocco (Slimani *et al.*, 2010), Tunisia (Brinkhuis and Zachariasse, 1988) and Alabama (Habib *et al.*, 1992), this taxon is used as marker for the basal Danian on a worldwide scale (Williams and Bujak, 1985; Haq *et al.*, 1987; Williams *et al.*, 2004). The FO of *C. cornuta* is also considered a worldwide marker of the basal Paleocene. It has its FO in the basal Danian of several regions from both the Northern (Hansen, 1977, 1979b; Hultberg, 1986; Brinkhuis and Leereveld, 1988; Brinkhuis and Zachariasse, 1988; Habib *et al.*, 1996; Brinkhuis *et al.*, 1998; Vellekoop *et al.*, 2015) and Southern Hemispheres (Willumsen, 2000, 2004, 2006). *Impagidinium celineae* (Pl. 2, Fig. 3,6), which appears in the sample 48R-3, 65-68 cm (864.25 mbsf, Fig. 1.5, 1.6), was described from the Danian of Nigeria (Jan du Chêne and Adediran, 1985; Jan du Chêne, 1988) and Morocco (Slimani *et al.*, 2010). In Sample 47R-1, 35-37 cm (851.25 mbsf) occurs the LO of *Cerodinium diebelii* which is recognized to occur worldwide during the Danian (Williams and Bujak, 1985; Fig. 19, p. 901). Previous works (Moullade *et al.*, 1998d; Oboh-Ikuenobe *et al.*, 1998) placed the Maastrichtian/Danian boundary in Sample 49R-4, 99-102 cm (875.69 mbsf) because of the presence of 2-3 *Dinogymnium undulosum* cysts, a species whose LO is considered a worldwide marker of the Maastrichtian upper boundary (Williams and Bujak, 1985; p. 901, fig. 19). However, the presence of Paleocene dinocyst markers below this level suggests that they may be reworked. Reworking is evidenced in these levels by high maturity levels of organic matter, and the presence of pebbly mudstone beds (Wagner and Pletsch, 1999).

In Sample 46R-2, 18-23 cm (842.48 mbsf) is observed the FO of *Adnatosphaeridium multispinosum* (Fig. 1.5, 1.6; Pl. 2, Fig. 1). On global charts *A. multispinosum* is considered to be restricted to the Eocene (Williams and Bujak, 1985; Powell, 1992), however Jan du Chêne and Adediran (1985) found it in the Late Paleocene of Nigeria. The occurrence of *Areoligera gippingensis* in Sample 44R-6, 60-62 cm (828.7 mbsf, Fig. 1.5, 1.6) also points to a Thanetian age, since it was described from the Thanetian of eastern England (Jolley, 1992). The study of agglutinated foraminifers (Kuhnt *et al.*, 1998a) and calcareous nannofossils (Shafik *et al.*, 1998)

biostratigraphies in the core site 959D confirm a late Paleocene age, probably Thanetian, above 45R-1, 43-48 cm (874.6 mbsf, Fig. 1.6).

4.2. Evolution of the Dinocyst assemblages, organofacies and palynofacies: a paleoenvironmental interpretation

Dinocyst assemblages from the studied 959D samples are characterized by a relative high abundance of *Spiniferites* spp. and *Achomosphaera* spp. (Fig. 1.7), but successive rises and falls mark the history of the two genera. In the lower part of the studied interval (1045 – 1033.7 mbsf), Coniacian in age, *Palaeohystrichopora* spp. dominate and *Dinogymnium* spp. are also common. From the lower part of the Campanian (1011.91 mbsf) to the base of the Danian (893.8 mbsf) the taxa showing important peaks are; *Circulodinium* spp., *Trichodinium castaneum*, *Spinidinium* spp., *Trithyrodinium* spp., *Kallosphaeridium* spp. and *Areoligera* spp. In the upper part of the studied interval (from 886.8 mbsf to the top) dinocyst assemblages do not show clear peaks of dominance by a single taxon. The frequency distribution of taxa is more equitable in the assemblages.

Previous studies on the sedimentological, structural and paleoenvironmental evolution of the Côte d'Ivoire – Ghana transform margin suggest a first marked phase of deepening in the 959D site from the upper Coniacian to the lower Campanian (ca. 1035 to 1015 mbsf, Fig. 1.3) (Saint-Marc and N'Da, 1997; Basile *et al.*, 1998; Wagner and Pletsch, 1999; Pletsch *et al.*, 2001). The assemblages of benthic foraminifera from this interval suggest an extended oxygen minimum zone in the water column (Pletsch *et al.*, 2001; Friedrich and Erbacher, 2006). Subsidence rates of the CIGMR crest and, northern and southern flanks are different, and reworking processes are considered almost constantly active (Wagner and Pletsch, 1999). After the high subsidence interval and low oxygen availability, the deepening rate was lower and almost constant during most of the Campanian-Maastrichtian interval. From the early Campanian upwards, the initial reliefs of the sea bottom fall deep through the subsidence (Fig. 1.3), which allowed the deep-water circulation (Saint-Marc and N'Da, 1997; Pletsch *et al.*, 2001; Friedrich and Erbacher, 2006). Depth remained stable for the entire Paleogene (from ca. 890 mbsf to the top of the studied interval) (Pletsch *et al.*, 2001).

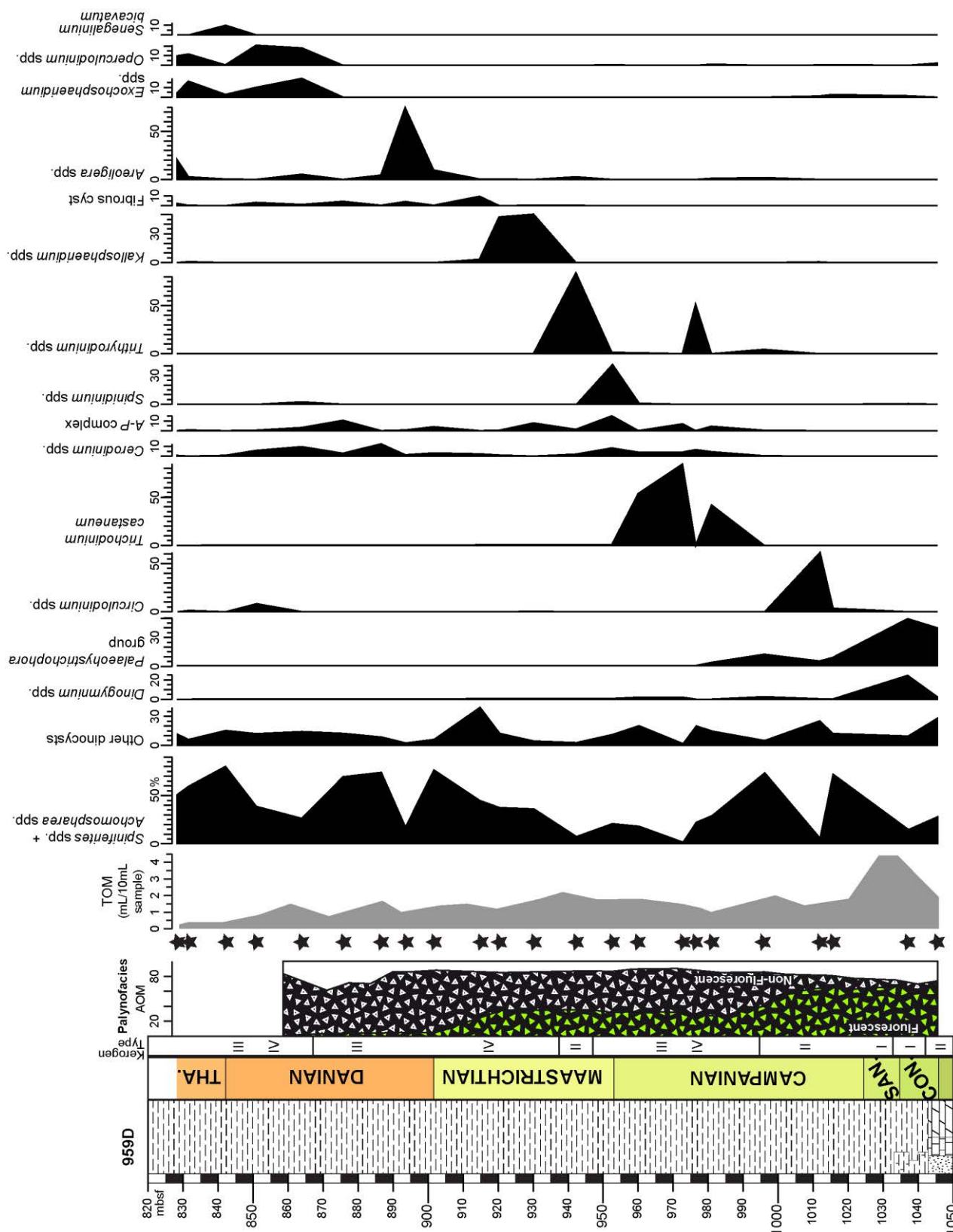


Figure 1.7. Summary of organic matter assemblage characteristics and relative abundance distribution of selected dinocyst from 959D site assemblages. Kerogen type after Wagner and Pletsch, (1999), palynofacies information from Oboh-Ikuenobe and Yepes (1997) and Total Organic Matter (TOM, volume of milliliters of organic residue in 10 milliliters of a sample) from Masure *et al.* (1998a). Black stars indicate sample positions. CON. - Coniacian, SAN. – Santonian, THA. – Thanetian. Kerogen Type I – Sapropelic origin; Type II – marine origin; Type III – Mixed marine – continental origin; Type IV – oxidized organic matter. *Palaeohystrichophora* group – Includes all the species from the genera *Palaeohystrichophora* and *Subilisphaera*; A-P complex – includes *Andalusiella* spp. and *Palaeocystodinium* spp.; Fibrous cyst include specimens from the genera *Cordosphaeridium*, *Turbiosphaeridium*, *Damassadinium* and *Fibrocysta*. For the lithological legend see Fig. 1.4.

The changes in the Côte d'Ivoire – Ghana transform margin are reflected in the sedimentary organic matter record. Marine productivity of organic matter is usually higher in neritic than in open marine environments. Contribution of marine, fluorescent organic matter in 959D samples was higher in the intervals interpreted as representing shallower conditions (Fig. 1.7, Oboh-Ikuenobe and Yepes, 1997; Pletsch *et al.*, 2001). The intervals of deep environments are enriched in mixed marine – continental and oxidized organic matter (Wagner and Pletsch, 1999; Pletsch *et al.*, 2001).

It may be possible that the succession of peaks of different dinocyst taxa represent the sequence of biological replacement due to the long term paleoenvironmental changes. The more equable frequency distribution of taxa in assemblages from the upper part of the studied interval (ca. 890 mbsf to the top of the studied interval) may reflect the structural and paleoenvironmental stabilization, posterior to the establishment of constant deep-water circulation and of normal oxygenation levels in the water column (Fig. 1.7).

5. Discussion

The differences between the results of Masure *et al.* (1998a), Oboh-Ikuenobe *et al.* (1998) and our own work, combines the effects of sampling biases and differences in worker's opinions.

5.1. Density of sampling and biostratigraphic resolution

Some interesting observations can be made from the comparison of sampling density, the stage boundaries position, the extension of intervals not assigned to any stage and the distance from the lower limit of stages proposed in each of the three studies herein considered to the lower limit of the stages proposed in the consensual biostratigraphy (Table 1.2, Fig. 1.6).

At a first sight it seems that the lower stratigraphic density of our samples prevents the identification of some stages, as the Santonian. Based on the co-occurrence of *Isabellidium acuminatum* and *Unipontidinium grande* (Pl. 1, Fig. 1-2) at 1025.37 mbsf (Fig. 1.6), Masure *et al.* (1998a) suggested a Santonian age for this level. Oboh-Ikuenobe *et al.* (1998) placed the lower Santonian boundary at 1031.7 mbsf because of the identification of FO of *Dingodinium undulosum*. The distance between the position of the lower Santonian boundary suggested from dinocyst

biostratigraphy by Masure *et al.* (1998a) and Oboh-Ikuenobe *et al.* (1998) and that suggested from the combination of all micropaleontological data by Moullade *et al.* (1998d) result in 7.8 m and 2.0 m of error in the boundary placement, respectively. In the present study the dinocyst assemblage at 1025.37 mbsf was not studied, *I. acuminatum* was not observed in any of the studied slides and the FO of *U. grande* was identified at 1015.62 mbsf, within the interval dated as Campanian. The non-observation of these taxa implies that we cannot define the Santonian stage from our dinocyst dataset and that the error associated to the lower Santonian boundary rises to 40.9m in the present study (Table 1.2).

However, sometimes it is not the sampling resolution that determines the precision of the stage boundaries placement but the sample position. Oboh-Ikuenobe *et al.* (1998) placed the upper Coniacian boundary at 1043.24 mbsf (Fig. 1.6), because of the observation of the only occurrence of *Cyclonephelium vannophorum*. In the present study the presence of *C. vannophorum* at 1037.10 mbsf lead us to place the upper Coniacian boundary at 1037.1 mbsf (Table 1.2). Although the sample resolution of the study by Oboh-Ikuenobe *et al.* (1998) was slightly higher (1 sample each 8.4 m) than in the present study (1 sample each 9.8 m) the error in the determination of the lower Coniacian boundary is higher from Oboh-Ikuenobe *et al.* (1998) results, 9.7 meters, than from our results, 3.4 m.

5.2. Rarity effect and the recognition of age markers

All dinocyst events identified by Masure *et al.* (1998a) and by the present study do not coincide exactly. The dinocyst events herein identified but not identified by Masure *et al.* (1998a), are the FO of *Areoligera* spp. and *Cerodinium* spp. at 996.16 mbsf; the FO of *Palaeocystodinium lidiae* at 981.18 mbsf; the FO of *Carpatella cornuta* at 901.9 mbsf; the FO of *Adnatosphaeridium multispinosum* at 842.48 mbsf and; the occurrence of *Areoligera gippingensis* at 828.7 mbsf. Obviously, the analysis by Masure *et al.* (1998a) also identified of some dinocyst events that have not been identified in the present study, like the FO of *Glaphyrocysta* group, *Alterbidinium varium* and *Cerodinium leptodermum* at 952.74 mbsf and the FO of *Damassadinium californicum* at 901.9 mbsf. When considering individually both studies these differences in the identification and placement of the dinoflagellate events would result in a difference of about 15 meters in the placing of the lower boundary of the Campanian and of about 14 meters for the lower boundary of the Thanetian.

Table 1.2. Comparison of sampling density, stage boundaries position, “gaps” and “errors” in Masure *et al.* (1998a), in the present study and in Oboh-Ikuenobe *et al.* (1998). Gap (m) refers to the intervals no assigned to any stage. Error (m) refers to the distance between the lower boundary of one of the stages in the consensual biostratigraphy herein proposed and the lower boundary identified from dinocyst in each of the studies herein compared.

		Masure <i>et al.</i> , 1998			This study			Oboh-Ikuenobe <i>et al.</i> , 1998					
Number of studied samples		49			23			25					
Studied interval (mbsf)		1045.71 - 828.7			1045.71 - 828.7			1043.4 - 841.37					
Mean distance between samples (m)		4.5			9.8			8.4					
Standard error (m)		3.6			4.4			3.7					
Recognized stages		Interval (mbsf)	Gap (m)	Error (m)	Interval (mbsf)	Gap (m)	Error (m)	Interval (mbsf)	Gap (m)	Error (m)			
	Thanetian	842.48 - 828.7	828.93 - 828.7	13.6	842.48 - 828.7	0	0			1.1			
	Danian	901.91 - 842.48	903.09 - 831.71	-1.2	901.91 - 851.25	13.1	0	866.97 - 841.37	8.7	39.4			
	Maastrichtian	952.74 - 901.91	960.03 - 910.97	-7.3	952.74 - 914.97	0	0	947.41 - 875.69	9.4	5.3			
	Campanian	1024.1 - 952.74	981.18 - 960.03	42.9	996.16 - 952.74	40.9	27.9	981.54 - 956.82	14.1	42.6			
	Santonian	1033.7 - 1024.1	1025.87 - 996.16	7.8			37.5	1031.7 - 995.61	11.7	2.0			
	Coniacian	1045.71 - 1033.7	1045.71 - 1028.68	-0.3	1045.71 - 1037.1		-0.3	1053.16 - 1043.4		-8.8			
Cumulative		28.5			73.1			62.8			65.8		
		28.5			73.1			62.8			65.8		
		32.2			94.7			32.2			94.7		

The inconsistencies in the placement of the K/T boundary are due to the effects of chance in taxon detections. Oboh-Ikuenobe *et al.* (1998) placed the upper Maastrichtian boundary in at 875.69 mbsf because of the LO of *Dinogymnium undulosum* and *Pierceites pentagonus*. The abundance of *Manumiella seelandica* in this level (10%) was also considered as indicative of the Maastrichtian / Danian boundary. In the present study we identify two Paleogene dinocyst events at 901.91 mbsf, with the only occurrence of *Carpatella cornuta* and the FO of *Damassadinium chibane* (Masure *et al.*, 1998a). The comparison of our dinocyst dataset with other studies of dinocyst biostratigraphy gives further evidences for the placement of the K/T boundary at 901.91 mbsf rather than at 875.69 mbsf. *P. pengatonous* was found in Danian sediments from Morocco by Slimani *et al.* (2010). In a bibliographic synthesis of the stratigraphical range of main dinocyst markers at the K/T boundary, Vellekoop *et al.* (2015) showed that *Dinogymnium* spp. crossed the boundary.

Within the dinocyst events considered for establishing the 959D site biostratigraphy (FO, FCO, LO and OO) in the three studies herein compared, “only occurrence” datums are very abundant (e.g. *Cyclonephelium vannophorum*, *Carpatella cornuta*, *Impagidinium celineae*, *Manumiella seelandica*, Fig. 1.6). This fact, combined with the high frequency of dinocyst events established from species represented by less than 4 specimens (species very rare, 2-3 specimens, and present, 1 specimen), evidences that most of the dinocyst useful as biostratigraphical markers are usually the less frequent (Table 1.3).

These remarks highlight the weight of chance in taxon detections in the differences observed among the biostratigraphic proposals from Masure *et al.* (1998a), Oboh-Ikuenobe *et al.* (1998) and from the present study.

Table 1.3. Frequency distribution of the abundance of dinocyst considered as biostratigraphical markers in Oboh-Ikuenobe *et al.* (1998) and/or in the present study. Data from Masure *et al.* (1998a) are not considered for this comparison because their publication contains exclusively presence / absence data.

	Dinocyst events	Present (1 cyst)	Very Rare (2-3 cyst)	Rare (4-9 cyst)	Common (10-24)	Abundant (25-49 cyst)	Very Abundant (50-99 cyst)	Dominant (>100 cyst)
TOTAL	41	16	12	8	4	1	0	0

5.3. Taxonomic revisions and instability of stage boundaries

Frequency distribution of the abundance of dinocyst considered as biostratigraphical markers in Oboh-Ikuenobe *et al.* (1998) and/or in the present study. Data from Masure *et al.* (1998a) are not considered for this comparison because their publication contains exclusively presence / absence data.

Frequency distribution of the abundance of dinocyst considered as biostratigraphical markers in Oboh-Ikuenobe *et al.* (1998) and/or in the present study. Data from Masure *et al.* (1998a) are not considered for this comparison because their publication contains exclusively presence / absence data.

The present study also evidences an example of personal observational bias. We identified Sample 56R-4, 60-62 cm (942.5 mbsf) the FO of *Turbiosphaera* sp. (Pl. 1, Fig. 9, 12-14). Specimens here identified as *Turbiosphaera* are similar to that identified by Oboh-Ikuenobe *et al.* (1998) as *Cordosphaeridium fibrospinosum* (illustrated in Pl. 3, Fig. 12, Oboh-Ikuenobe *et al.*, 1998). *Turbiosphaera* differs from *Cordosphaeridium* in having a more elongate body, wide and flat processes of which the apical and antapical processes are larger than the others and by having a paracingulum represented by a shelf-like projection (Stover and Evitt, 1978). From my point of view, the specimen illustrated by (Oboh-Ikuenobe *et al.*, 1998, Pl. 3, Fig. 12) as *C. fibrospinosum* possesses an antapical process larger than the others, which is a *Turbiosphaera* character, and processes are not expanded distally, which is a character for identifying *Cordosphaeridium*. So the specimens should all be considered as *Turbiosphaera*. Problems in indentifying the different fibrous dinocyst (as *Turbiosphaera*, *Cordosphaeridium*, *Damassadinium* and *Fibrocysta*) are well known (e.g. Soncini, 1990). These problems are illustrated by the fact that the type species of the genus *Turbiosphaera* (*T. filosa*, Archangelsky, 1969) was originally described as *Cordosphaeridium filosum* (Wilson, 1967). For these reason, it is advised not to use

problematic morphotypes (such as *Cordosphaeridium* and *Turbiosphaera*) as biostratigraphic markers. Fortunately, within the whole pool of considered dinocyst events problems on confidence of taxonomic identification are very rare and, in general terms, results obtained by different operators are reproducible (Mertens *et al.*, 2009).

The triple datum formed by the FO of *Hafniasphaera fluens*, *Manumiella rajiae* and *Cordosphaeridium fibrospinosum* at 918.47 mbsf, was considered by Oboh-Ikuenobe *et al.* (1998) as marker of the lower limit of the Upper Maastrichtian. Considering that our reinterpretation of *C. fibrospinosum* specimens as *Turbiosphaera* is correct, the FO of *H. fluens* at 918.47 mbsf might be considered an indication of the proximity to the K/T boundary (herein placed at 901.91 mbsf). *H. fluens* is present in the upper Maastrichtian of the United States and Mexico (Helenes, 1984; Habib and Miller, 1989), in Maastrichtian to Danian rocks in Denmark (Hansen, 1977), upper Maastrichtian to Danian rocks in South Scandinavia (Hultberg, 1986), and lower Maastrichtian to Paleocene rocks in Morocco (Soncini and Rauscher, 1988).

5.4. Influence of paleoenvironmental factors on the dinocyst stratigraphic record

Paleoenvironmental control on the dinocyst taxa relative frequency can impact the reconstruction of their stratigraphic distribution. The comparison of dinocyst distribution (Fig. 1.7) with the paleoenvironmental reconstructions proposed by previous studies shows a good fit see Wagner and Pletsch, 1999; Pletsch *et al.*, 2001; Friedrich and Erbacher, 2006. Modifications of environmental conditions have already been proposed for explaining variations in the distribution of dinocyst taxa along sedimentary sequences. For example, see surface temperature variations have been proposed as triggers of dinocyst frequency variations along the K/T boundaries from different regions (e.g. Brinkhuis *et al.*, 1998; Vellekoop *et al.*, 2015). They found that some of the chronobiostratigraphic dinocyst markers (as *Palynodinium grallator*, *Pierceites pentagonus*, *Phelodinium magnificum* or *Senegalinium bicavatum*) are influenced by SST variations. Improving our knowledge about how paleoenvironmental variation control dinocyst distribution is fundamental to realize the full potential of dinocyst as biostratigraphic markers.

6. Conclusions

The re-study of dinocyst biostratigraphy of the 959D ODP site, allow us to revise the chronostratigraphy, with higher consistencies among taxa and geological studies:

- The Late Turonian and Early Coniacian cannot be differentiated from dinocyst but are recognized from foraminifers in the lower part of the studied interval from 1050 to 1045.4 mbsf (Moullade *et al.*, 1998d).

- The presence of *Xenascus gochtii* and *Cyclonephelium vannophorum* confirm a Coniacian age for the lower part of the studied interval from 1045.4 to 1033.7 mbsf.

- The Santonian stage was evidenced from calcareous nannofossils and foraminifers from 1033.7 to 1024.1 mbsf (Moullade *et al.*, 1998d).

- The FO of *Areoligera* spp. marks the Campanian at 996.16 mbsf. The base of the Campanian proposed at 1024.1 mbsf by Moullade *et al.* (1998d) is herein conserved.

- The Campanian / Maastrichtian boundary is confirmed at 952.74 mbsf. The stacking of dinocyst evolutionary events at this level suggests a condensed or hiatus horizon.

- The appearance of Danian dinocyst markers, as *Carpatella cornuta* and *Damassadinium californicum*, at 901.91 mbsf argue in favor of placing a Maastrichtian / Danian boundary (K/T boundary) at this level.

- No Selandian biostratigraphic markers are recognized in the 959D samples.

- The base of the Thanetian is placed at 842.48 mbsf from the presence of *Adnatosphaeridium multispinosum*.

The comparison of our biostratigraphic dinocyst data with those published by Masare *et al.* (1998a) and Oboh-Ikuenobe *et al.* (1998) from the same cores allows some discussion on stage boundaries and time resolution. Because of the non-recognition of the Santonian stage in the present study, low sampling resolution, evaluated through the mean distance between samples, was thought as the main factor determining the major differences in the boundary limits placement. However, when analyzing the error in the placement of stage boundaries, evaluated through the distance in meters of the lower boundary of one stage in the consensual stratigraphy and in the individual dinocyst biostratigraphies herein considered, the present study

reaches the lowest cumulative error indicating that sampling density is not dramatically problematic for the precision of the boundaries placement. The low absolute frequency (less than 4 specimens) of most of the age marker dinocyst considered for determining the stage limits is the main factor that explains the differences among dinocyst biostratigraphic schemes.

The relative abundance distribution of dinocyst in the studied interval suggests that environmental conditions may influence their stratigraphic range. However, because of the complexity of paleoenvironmental signal recorded by the fossil group record, further work is necessary for assess the potential of fossil dinocyst as paleoenvironmental proxy.

CHAPTER 2

Spatio-temporal variability of Albian coastal and oceanic subtropical dinoflagellate cysts from the Iberian margin

This chapter has been elaborated in collaboration with Masure E., Rey, J. and Villier L.

1. <u>Introduction</u>	43
2. <u>Geological setting</u>	45
2.1. Coastal environments	47
2.2. Open marine distal environments	49
2.3. Biostratigraphical framework	50
3. <u>Material and methods</u>	51
3.1. Material	51
3.2. Methods	52
3.2.1. <i>Diversity analysis</i>	54
3.2.2. <i>Cluster Analysis</i>	55
3.2.3. <i>Seriation Analysis</i>	55
3.2.4. <i>Non-Parametric Multivariate ANalysis Of VAriance (NPMANOVA)</i>	56
3.2.5. <i>Correspondence Analysis (CA)</i>	56
4. <u>Results</u>	56
4.1 Diversity analysis	56
4.2. Differentiation of dinocyst associations between coastal and open marine distal environments	58
4.2.1. <i>Clusters of taxa and samples and Pairwise NPMANOVA</i>	58
4.2.2. <i>Correspondence Analysis</i>	63

4.3. Differentiation of dinocyst associations among shallow coastal environments.....	65
4.3.1. <i>Clusters of taxa and samples and Pairwise NPMANOVA.....</i>	65
4.3.2. <i>Correspondence Analysis.....</i>	68
4.4. Differentiation of distal open marine associations: analysis of the DSDP 398D cores	71
4.4.1. <i>Clusters of taxa and samples and pairwise NPMANOVA.</i>	71
4.4.2. <i>Correspondence Analysis.....</i>	74
5. <u>Interpretation and discussion</u>	75
5.1 Factors controlling taxa distribution.....	75
5.1.1 <i>Proximal - distal trends</i>	75
5.1.2 <i>Environmental stability - predictability</i>	76
5.1.3 <i>Imprints of heterogeneous coastal environments on dinocyst</i>	77
5.2 Paleoenvironmental significance of taxon associations	80
5.2.1. <i>Nearshore instable environments and associations.....</i>	80
5.2.2. <i>Neritic environments and associations</i>	83
5.2.3. <i>Open marine distal environments and associations</i>	85
5.2.4. <i>Variability of cyst morphology along environmental gradients.....</i>	89
5.3. Paleooceanographic and paleogeographic evolution of the western Iberian margin during the Albian	93
6. <u>Conclusions</u>.....	97

1. Introduction

The value of dinocyst in stratigraphic and paleoenvironmental studies has long been recognized. The general patterns in the geographical distribution of dinocysts, first recognized by Wall *et al.* (1977), are still obvious in the most recent syntheses “Atlas of modern dinoflagellate cyst distribution” (Marret and Zonneveld, 2003; Zonneveld *et al.*, 2013). These studies, and numerous others (e.g. Harland, 1983; Goodman, 1987; Rochon *et al.*, 1999; de Vernal *et al.*, 2005; Matthiessen *et al.*, 2005), allowed the identification of the individual loadings of the environmental parameters controlling the dinocyst distribution and confirmed that the geographical distribution of modern organic-walled dinoflagellate taxa is clearly constraint by oceanographic properties of the upper water masses.

The two editions of the “Atlas of modern dinoflagellate cyst distribution” (Marret and Zonneveld, 2003; Zonneveld *et al.*, 2013) identified the individual loading of the environmental factors controlling the dinocyst distribution on a global scale. Both compared dinocyst global distribution data with environmental datasets, but they differed in the spatio-temporal resolution considered. They both found that global temperature gradients explain the major biodiversity patterns, but their results differed in the identification of the remaining environmental parameters controlling the dinocyst distribution. The first edition found no clear influence of salinity in dinocyst distribution (Marret and Zonneveld, 2003). In the second edition, the resolution of dinocyst distribution and of the environmental dataset compared was higher (Zonneveld *et al.*, 2013). Using a finer scale they found that salinity becomes a prominent factor, explaining 34% of the variation in the dataset. They also found that, species are often tolerant to a wide range of environments but are abundant only in their optimal conditions (Marret and Zonneveld, 2003; and Zonneveld *et al.*, 2013). That reveals the importance (1) of the spatiotemporal resolution considered and (2) of analyzing the relative abundance of a taxon in dinocyst assemblages for extracting information on environments.

Spatiotemporal resolution becomes a central issue when working with fossil samples. A fossil assemblage can mix forms initially from different ages and environments. The resolution of the environmental signals can be recorded, but not necessarily, with several orders of magnitude lower that when working with modern

samples. So when attempting to reconstruct past environments it may be preferable to focus on their general characteristics than to try to establish a one-to-one relationship between environmental factors and fossil species. Most of the studies focused on the distribution of fossil dinocyst assemblages dealt with sequence stratigraphy revealing the value of dinocyst assemblages in reconstructing sea level changes (e.g. Haq *et al.*, 1987; Habib and Miller, 1989; Gregory and Hart, 1992; Brinkhuis and Biffi, 1993; Schiøler *et al.*, 1997; Jaramillo and Oboh-Ikuenobe, 1999; Dybkjær, 2004; Sluijs *et al.*, 2005). However, sequence boundaries are affected by condensation or hiatuses hampering the identification of the continuous replacement of dinocyst associations and the use of qualitative approaches difficult the identification of relative abundance distribution patterns of dinocyst taxa.

The first objective of the present study is to analyze the distribution of Albian dinocysts between different environments to determine whether or not they record the variations of environmental factors over small distances during a short period. Recent studies on the worldwide dinocysts distribution, during the Albian and the Aptian, confirm the major effect of temperature on the dinocyst distribution and allow distinguishing tropical, subtropical, subpolar and polar species (Masure and Vrielynck, 2009; Masure *et al.*, 2013). The comparison between dinocyst taxa latitudinal ranges and estimated temperatures (from $\delta^{18}\text{O}$ and TEX₈₆) provided their limit range temperatures (Masure and Vrielynck, 2009). In order to avoid the masking effect of temperature over other environmental factors with lower individual loadings, such as nutrient availability or salinity, the study sites herein considered were included in the same climatic belt during the Albian, at nearly 25-28°N (Hay *et al.*, 1999; Masse *et al.*, 2000) in the Northern mid-low latitude belt (Masure and Vrielynck, 2009). In order to maximize the potential record of environmental variations selected sites represent the inshore to offshore gradient, which constitutes the second major factor controlling modern dinocyst distribution (e.g. Wall *et al.*, 1977; Harland, 1983; Marret and Zonneveld, 2003). Five outcrops from the Lusitanian Basin have been selected for representing nearshore environments (e.g. Ribeiro, 1857; Choffat, 1885, 1891, 1904; Seifert, 1963; Rey, 1972, 1992; Rey *et al.*, 1977, 2006; Berthou and Schröder, 1979; Hasenboehler, 1981; Berthou and Hasenboehler, 1982; Berthou and Leereveld, 1990; Dinis *et al.*, 2002, 2008; Heimhofer *et al.*, 2007, 2012; Horikx *et al.*, 2014). The dinoflagellate cyst assemblages from these outcrops are compared with the dinocyst assemblages of samples from the 398D DSDP site, which recorded distal conditions

over the same time slice (e.g. de Graciansky and Chenet, 1979; Deroo *et al.*, 1979; Habib, 1979; Sibuet *et al.*, 1979; Masure, 1984; Taugourdeau-Lantz *et al.*, 1984).

The second objective of this study is to develop an appropriate methodology for identifying the dinocyst associations related to the different environmental conditions recorded. The assemblages diversity (taxa richness and evenness) is analyzed through methodologies that consider the effects of dilution/concentration of dinocyst in the samples due to variations in the sedimentation rate and the possibility of differential sampling effort. Dinocyst dataset have been analyzed through multivariate analysis to identify their structure and to determine whether or not natural taxon grouping is recorded. The results from the dinocyst dataset analyses are compared to all the sedimentological and paleontological data available to determine which are the environmental factors that acted on the Albian dinocyst distribution pattern.

2. Geological setting

During the Early Cretaceous, the studied area was located in the Iberian Massif at a paleolatitude of ~25°N (Hay *et al.*, 1999) to 28°N (Masse *et al.*, 2000), facing the proto-North Atlantic Ocean (Fig. 2.1). A continental break up and the opening of the North Atlantic Ocean characterize the Mesozoic history of the Iberian margin. Four successive rifting episodes structured the continental margin and the sedimentary record (Hiscott *et al.*, 1990; Rasmussen *et al.*, 1998). The production of oceanic crust between Iberia and Newfoundland started with the last extension episode during the Late Aptian – Early Albian interval (Boillot *et al.*, 1987; Tüchler *et al.*, 2004; Jagoutz *et al.*, 2007; Alves *et al.*, 2009; Soares *et al.*, 2012). The isostatic adjustment associated to the extensional episode caused the elevation of a large area of the Lusitanian Basin (Hiscott *et al.*, 1990), which resulted in the development of a major regional stratigraphic unconformity (Soares *et al.*, 2012). This erosional surface is pervasive onshore and can be traced offshore (Rey *et al.*, 2006; Soares *et al.*, 2012). In the Lusitanian Basin a mixed siliciclastic and carbonate sedimentary series was deposited above the erosional surface, during the Albian, while distal shale deposits dominated series recorded in the 398D site.

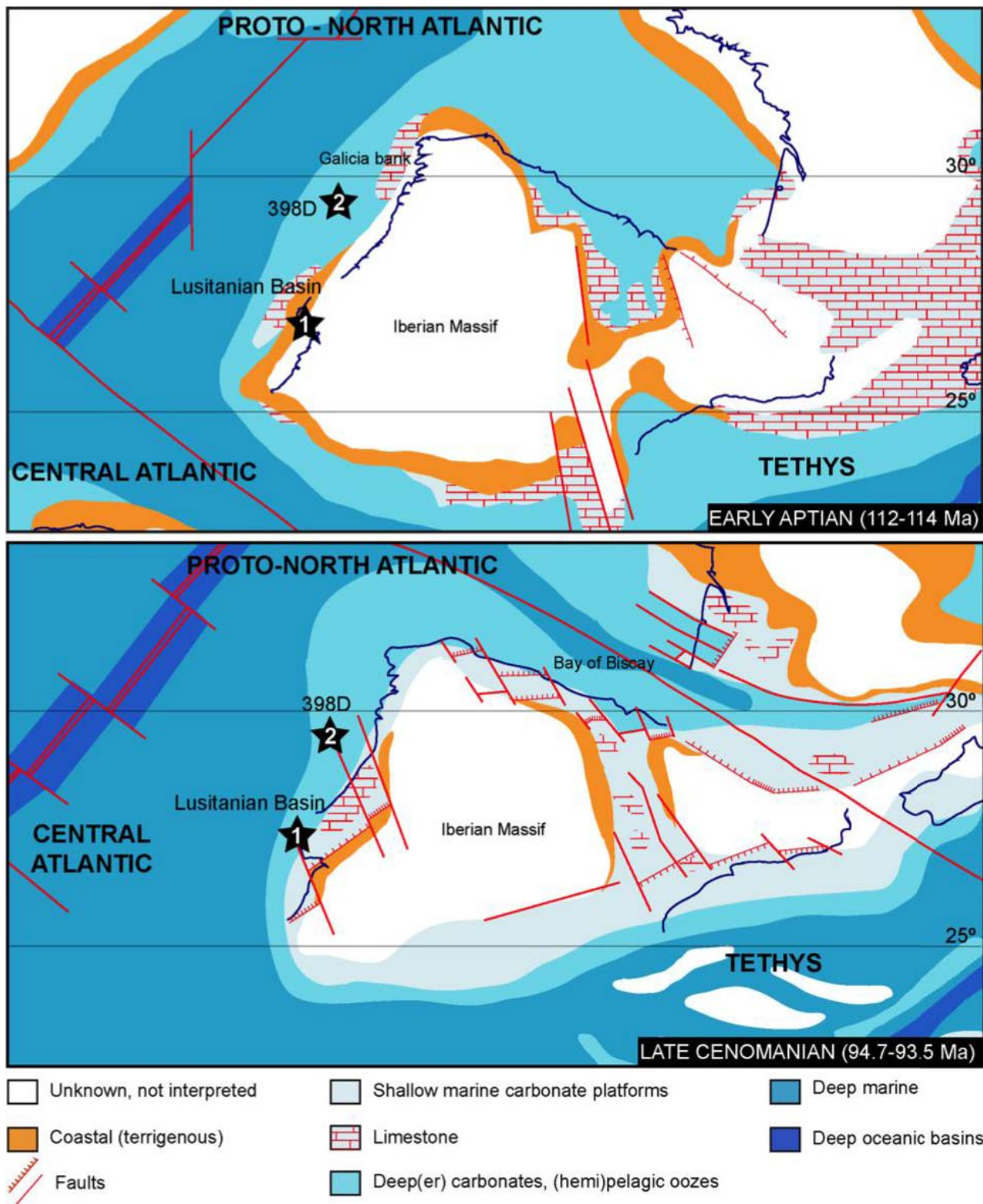


Figure 2.1. Paleogeographical position of Albian studied sites after Masse *et al.*, 2000. 1) Lusitanian Basin, 2) 398D DSDP Hole.

2.1. Coastal environments

The Albian series of the Lusitanian Basin were studied for over a century (Ribeiro, 1857; Choffat, 1885, 1891, 1904; Seifert, 1963; Rey, 1972). On the long-term, the Albian series records a global sea-level rise (Haq, 2014), modulated by the tectonic evolution of the Iberian margin. The Albian record starts with continental, fluvial deposits described as the Rodízio formation, followed by varied, marine, coastal environments of the Galé Formation, herein studied (Fig. 2.2). The Galé Formation was studied in detail for sedimentology biostratigraphy and sequence-stratigraphy, leading to the recognition of two members the Água Doce and the Ponta da Galé Members (Rey *et al.*, 1977, 2006; Berthou and Schröder, 1979; Berthou and Leereveld, 1990; Rey, 1992; Dinis *et al.*, 2002).

The lower limit of the Galé Formation corresponds to a transgressive surface and the first deposits are diachronic; being younger to the East and to the North (Rey, 1992). The lowermost part of the Água Doce Member is composed of alternating marl and bluish grey clayey limestones, with sparsely intercalated mudstone and silt- or sandstone beds. Mudstones are more common at the base of the member, they are strongly bioturbated and characterized by a rich macrofossil assemblages including oysters, gastropods, serpulids, thick-shelled bivalves and orbitolinids. Sandstone beds show ripple structures and fine lamination patterns. The middle and uppermost Água Doce Member is dominated by marly and sandy limestones, rich in macrofossil remains, large orbitolinids, gastropods and bivalves in the middle part, with the addition of oysters, echinoderms and miliolinids in the uppermost part (Rey, 1992; Heimhofer *et al.*, 2012). The high frequency of quartz grains, clays, and plant remains in the sediments reflects the influence of continental influx.

The limit between Água Doce et Ponta da Galé members is defined by the first limestone beds bearing rudists, which is not coeval throughout the basin (Fig. 2.2, (Dinis *et al.*, 2008; Horikx *et al.*, 2014). The Ponta da Galé Member shows a succession of varied sedimentary facies indicative of shallow marine environments, from base to top: limestones and marls rich in macrofossils (oysters, orbitolinids, bivalves, rudists and dasycladales); bioturbated sandy limestones; oosparitic granular limestones, oblique cross laminated; micritic limestones and marls evolving into sandy limestones, and containing rich and diverse assemblages of fossils (rudists, orbitolines, echinoderm debris and bivalves, Fig. 2.2). The top of the Galé Formation is truncated

by an oxidized surface on which lie bluish gray nodular sandy limestones of Cenomanian age (Rey, 1992).

The Galé Formation is associated to a high siliciclastic input from the northeast to the south east of the Lusitanian Basin. The influence of the fluvial systems on the

sedimentary dynamics slightly decreases trough time (Dinis *et al.*, 2008). According to the available paleoenvironmental data, the Água Doce Member represents shallow inner shelf to coastal conditions, influenced by continental influx. The Ponta da Galé Member is characterized by carbonates, including nerineid-rich sandy shoals, and rudist build-ups, that developed only under clear, oligotrophic waters. During the Albian, the facies belts shift north- and eastwards.

The Galé Formation covers two second-order transgressive-regressive (T-R) cycles (Dinis *et al.*, 2008) and eight third-order depositional sequences (Rey *et al.*, 2006). The first second order T-R cycle covers most of the Água Doce Member, in an age range of Middle Albian to the lower part of the Late Albian (Fig. 2.2). Its expression is probably triggered by the onset of oceanic crust production in the northern margin of Galicia (Malod and Mauffret, 1990). The second T-R cycle covers the upper part of the Água Doce Member and the Ponta da Galé Member, uppermost Late Albian

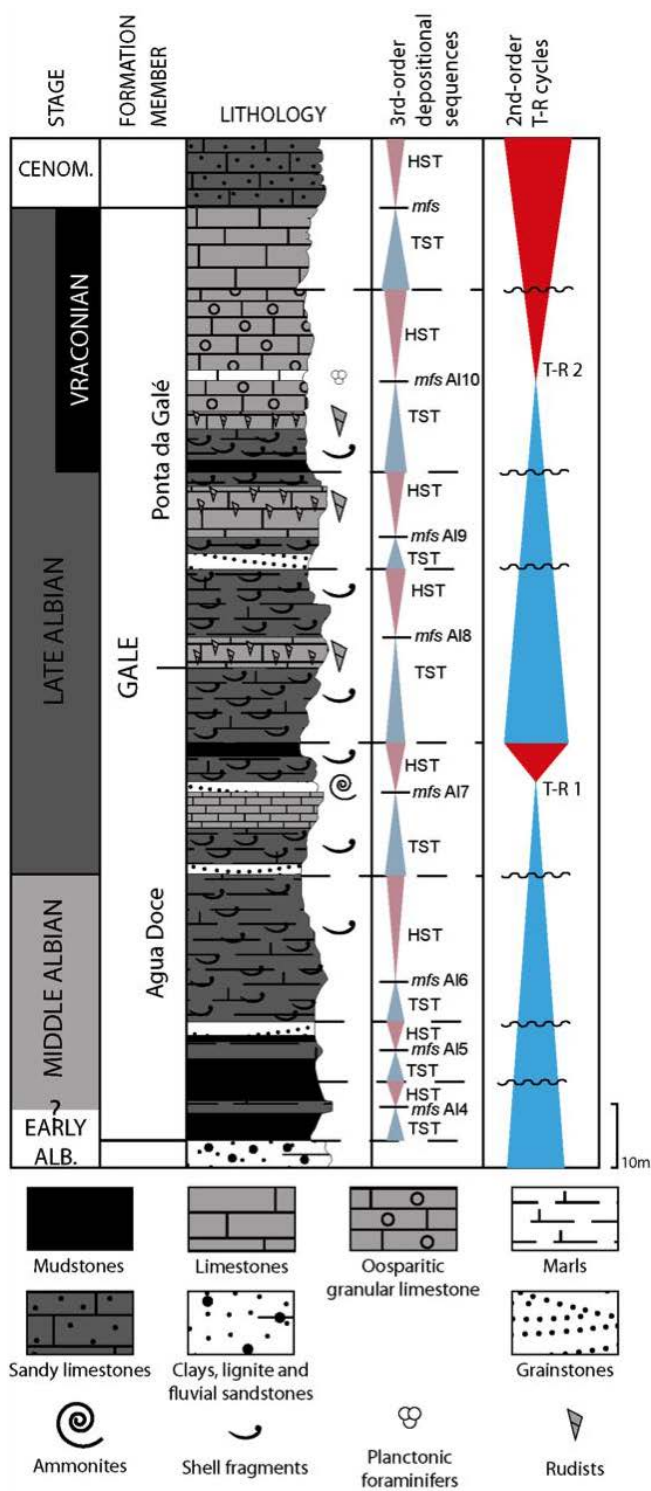


Figure 2.2. Synthetic column of the Galé Formation (modified from Rey *et al.*, 2006).

(Vraconian), and is probably linked with the onset of oceanic crust production in the eastern Bay of Biscay (Dinis *et al.*, 2008).

Five sections exposed in coastal outcrops near to Lisbon are selected to represent the proximal paleoenvironments in the southern part of the Lusitanian Basin, Portugal. São Julião - Falcão - Magoito (FM, Fig. 2.3) section starts, about 3 km South of Ericeira and extends southward up to Samarra beach. Magoito Aguda – Azenhas do Mar section (MA) is exposed along the coast immediately South of Magoito garrison, up to Azenhas do Mar cliffs. Guincho section (G) starts immediately North of the Cresmina fortress, at Ponta Alta, and extends through the Água Doce beach to the cliffs at the southern edge of Praia Grande do Guincho. Ponta do Sal section (PS) is located on the homonymous cape, western edge of the Baforeira bay, on the coast in front of São Pedro do Estoril. The southernmost section, Baforeira Rana section (BR), is located immediately to the West of PS section between the East edge of the Baforeira bay and the Carcavelos beach.

2.2. Open marine distal environments

The Deep Sea Drilling Project (DSDP) Hole 398D is selected to represent open marine distal conditions (Fig. 2.1). It is located 160 km off Portugal, West of Porto, in a small bathyal platform on the southern margin of Vigo Seamount. The hole was drilled on the western flank of a deep northeast-southwest trough in a region considered part of the passive margin of the eastern North Atlantic (Shipboard Scientific Party, 1979). The levels 1298.12 – 966.8 mbsf (meters below sea floor, cores 91 to 58) of the 398D core sample the age interval studied onshore in the Lusitanian Basin (Fig. 2.4). From the five lithological units described from the

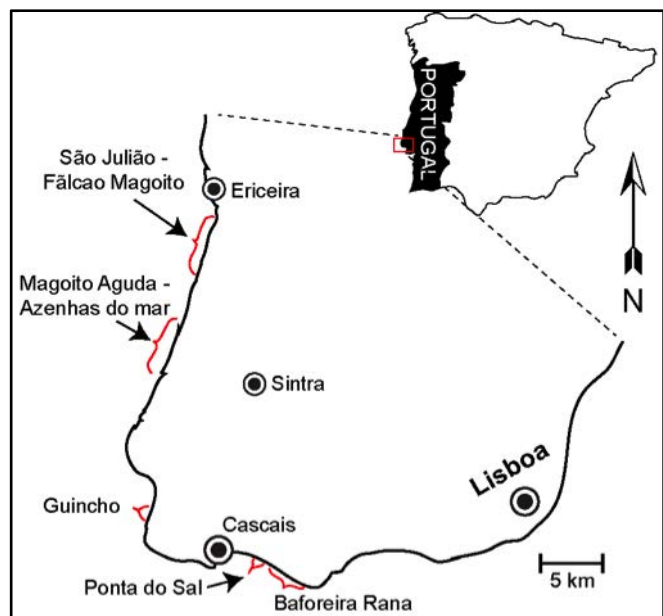


Figure 2.3. Location of Lusitanian Basin studied sections. São Julião – Falcão Magoito section is sometimes referred in the text by the abbreviation SJ-FM; Magoito Aguda – Azenhas do Mar by MA – AZ; Guincho by G; Ponta do Sal by PS; and Baforeira Rana by BR.

whole 398D site, the studied levels belongs to the lithological units 4B and 4A of (Sibuet *et al.*, 1979) and to the Hatteras formation (Jansa *et al.*, 1979; Masure, 1984).

The lower part of the studied section corresponds to lithological unit 4B (1306 to 1183 mbsf, cores 91 to 79, Fig. 2.4). Sedimentary facies consist predominantly of dark gray to black claystone (“black shales”) interbedded with greenish, gray mudstone, and calcareous mudstone (Shipboard Scientific Party, 1979). The carbonate content remains generally low; burrow traces and siderite are common, the organic carbon values are relatively high; ammonites and other mollusk debris are common (Arthur, 1979). Strong continental input is evidenced by the dominance of terrigenous clay and silt (de Graciansky and Chenet, 1979), Type III kerogen (Deroo *et al.*, 1979) and sporomorphs, bisaccates and structured palynodebris within the palynofacies assemblages (Habib, 1979). However, one level (90-5, 15-30 cm; 1293.7 mbsf) analyzed for organic compounds is rich in lipids of predominantly marine origin (Simoneit and Mazurek, 1979).

Levels 1183 to 964 mbsf (cores 78 to 58) fall within the Unit 4A (Fig. 2.4). The appearance of attapulgite marks the base of this unit (Chamley *et al.*, 1979). Lithological facies are composed mostly of laminated, black to dark gray mudstone and calcareous mudstone. The frequency of calcareous mudstone becomes more abundant and thicker to the top (Shipboard Scientific Party, 1979). Changes are also observed in the composition of organic matter. Type II kerogen is the main contributor to organic matter composition within the interval, the frequency of large plant debris decreases (Deroo *et al.*, 1979) and the abundance and diversity of dinoflagellate flora increases toward the top (Habib, 1979; Masure, 1984).

2.3. Biostratigraphical framework

Dinoflagellate cysts distribution was studied in the five outcrops of the Lusitanian Basin from a biostratigraphical perspective by Hasenboehler (1981) and Berthou and Hasenboehler (1982). Dinoflagellate cysts biostratigraphy in São Julião, Magoito Aguda and Guincho outcrops was also studied by Horikx *et al.* (2014) and by Heimhofer *et al.* (2007), respectively. The precise age of the base of the Galé Formation and of the boundary between the two members vary slightly among authors, the age differences emerging mainly as result of differences in the location of the first

occurrences of *Xiphophoridium alatum* and *Chichaouadinium vestitum*, two species considered as indicators of the transition from the Early to the Middle Albian (Heimhofer *et al.*, 2007, 2012; Horikx *et al.*, 2014). In the present work *X. alatum* is found in the lowest sample in the five sections so we consider that the base of the studied outcrops is not older than Middle Albian.

Dinoflagellate cysts distribution of the 398D samples was studied by Masure (1984). The results from dinoflagellate cyst biostratigraphy are consistent with those from foraminifera study (Sigal, 1979) regarding the position of the Early Albian – Middle Albian boundary. Middle Albian – Late Albian boundary and the lower boundary of the Vraconian (uppermost Late Albian) are placed lower with dinoflagellate data (Masure, 1984) than with foraminifera (Sigal, 1979) according the first occurrence of *Leberidocysta chlamydata* and *Cribroperidinium? intricatum*.

Pending a clearer resolution of age assignment, we retained a dating and correlation scheme based on dinoflagellate age markers. *Xiphophoridium alatum* and *Litosphaeridium arundum* are selected as markers for the Middle Albian interval, *Cribroperidinium? intricatum* and *Leberidocysta chlamydata* for the lower part of the Late Albian, and *Endoceratium dettmanniae*, *Litosphaeridium siphoniphorum*, *Ovoidinium verrucosum* and *Palaeohystrichophora cf. infusorioides* for the Vraconian. All species considered are among the most widespread across the Lusitanian margin and are recognized elsewhere as valuable for stratigraphic purposes (Davey and Verdier, 1971, 1973; Verdier, 1975; Davey, 1979; Fauconnier, 1979; Foucher, 1979; Monteil and Foucher, 1998; Oboh-Ikuenobe *et al.*, 2007; Gradstein *et al.*, 2012).

3. Material and methods

3.1. Material

Fifty samples were analyzed from the five sections of the Lusitanian Basin and twenty-two samples from the 398D DSDP hole. Seventeen samples were analyzed from de São Julião – Fãlcao Magoito outcrop, sixteen samples from Magoito Aguda – Azenhas do Mar, eight from Guincho, four from Ponta do Sal and five from Baforeira Rana outcrop. Lithology guided sampling strategy at outcrops. Gray to black colored marls, marly mudstones or mudstones were favored assuming a better preservation of

organic matter. Coarser, oxidized or diagenetized beds as well as green, red or yellow levels were avoided from sampling. Most of sampled beds are within the transgressive system tracks of the third order T-R cycles.

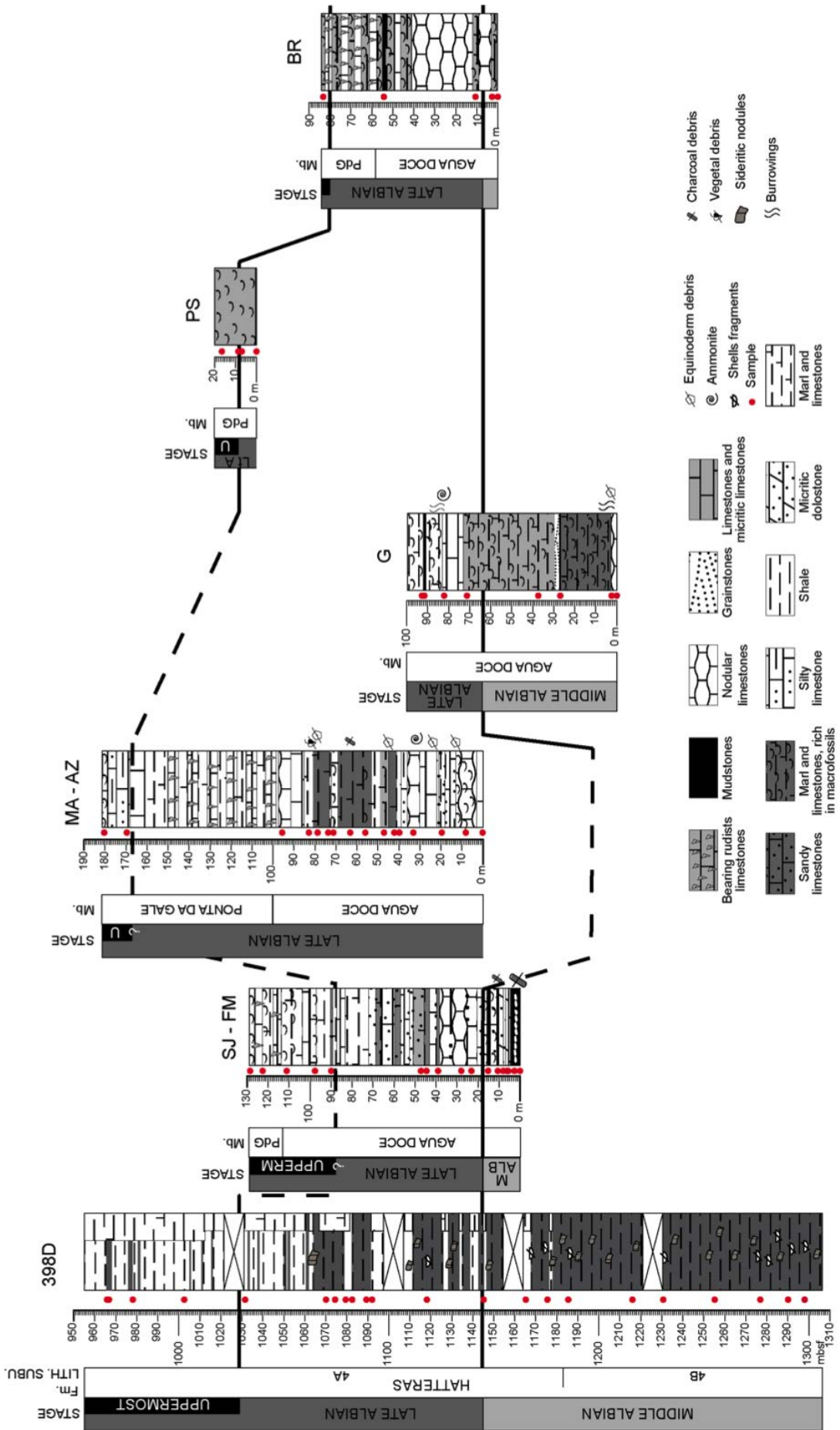
3.2. Methods

All samples were processed following standard palynological preparation techniques, based on routine series of HCl – HF (70%) – HCl attacks (e.g. Traverse, 2007) followed by filtering over a 10 µm nylon mesh to eliminate the amorphous organic matter. At least two slides were mounted for each sample from the organic residue. A minimum of 250 palynomorphs was counted from each level and all slides were then scanned for additional dinocyst taxa. The occurrence data tables were reconstructed from the initial counting sheets of previous biostratigraphic works (Hasenboehler, 1981; Masure, 1984), and checked on some slides. Every taxon list represents the assemblage of fossils found in one bed at one site. No samples were combined to create composite lists by geologic unit or location. The taxonomy of dinocysts follows Fensome *et al.* (2008), a list of identified dinocyst taxa is given in Appendix A and the biostratigraphical distribution of dinocyst in each studied section is given in Appendix B (B.2. to B.7).

Two diversity measures (Taxon richness and Evenness) were performed on all available dinoflagellate cyst data. Three primary analytical techniques (Seriation Analysis, Cluster Analysis and Correspondence Analysis, CA) and a measure of significance of clusters (Non-parametric Multivariate Analysis of Variance, NPMANOVA) were used in this study. The analyzed matrix excludes taxa with relative abundances under 2%, taxa occurring in a single sample, and taxa with a stratigraphical range limited, i.e. taxa with known ranges not covering the whole studied period. Multivariate analyses were carried out in order to describe the dataset structure. Primary analytical techniques and NPMANOVA were all performed using the PAST software package, v. 3.07 (Hammer *et al.*, 2001).

Figure 2.4. Simplified lithological log and correlation of the 398D hole with the outcrops of the Lusitanian Basin. Lithological information of the five outcrops from the Lusitanian Basin from Hasenboehler (1981). SJ – FM = São Julião – Magoito Aguda; MA – AZ = Magoito Aguda – Azenhas do Mar; G = Guincho; PS = Ponta do Sal; Br= Baforeira Rana. Samples name and height / depth in Appendix B.2. to B.7.

DINOCEST DISTRIBUTION IN AN INSHORE TO OFFSHORE TRANSECT IN THE WESTERN IBERIAN MARGIN



3.2.1. Diversity analysis

We used several quantitative analytical techniques to investigate fundamental components of taxonomic diversity, namely, the taxonomic richness and the evenness. The simplest possible diversity metric is the number of taxa present in the sample, known as taxonomic richness (S). However, it is important to remember that taxa richness will vary with sample size. In order to compensate for the effect of sample size, taxonomic richness was standardized using rarefaction analysis (Krebs, 1989; Adrain *et al.*, 2000) by using the PAST software package, v. 3.07 (Hammer *et al.*, 2001). Rarefaction analysis allows comparing the number of taxa in samples of different sizes by calculating the expected number of taxa in samples of any size less than the original sample, under assumptions of homogeneity and randomness (Sanders, 1968; Raup, 1975). As all rarefaction curves flattened above 30 individuals, we selected a sample size of 30 individuals (S_{30}) to compare the taxonomic richness among samples.

The evenness evaluates the assemblage diversity by analyzing distribution of individual frequency among taxa. Lower evenness values reflect the dominance of one or a few taxa among the whole association, whereas higher evenness values reflect that species proportions are equally distributed. Various metrics are available to evaluate sample evenness (e.g. Hammer and Harper, 2006; Bulinski, 2007). The different metrics define evenness in different ways, and the relative contributions from common and rare taxa are weighted differently from one metric to another (Hammer and Harper, 2006).

Four different metrics of evenness were evaluated: Pielou's J, Buzas & Gibson's (e^H/S), Probability of Interspecific Encounter (PIE) and Peter's E_{SS} . Pielou's J metric derives from the Shannon-Wiener diversity index and is a ratio that compares the observed distribution of taxa to the most even distribution possible in a given community (Pielou, 1969; Buzas and Hayek, 1996). Buzas & Gibson's e^H/S also derives from the Shannon-Wiener diversity index, values being normalized to the number of taxa present in the sample (Buzas and Gibson, 1969; Buzas and Hayek, 1996). The Probability of Interspecific Encounter (PIE) metric measures the probability that two individuals randomly sampled from a community belong to different taxa (Hurlbert, 1971). Peters's E_{SS} metric determines how much the proportion of taxa in a sample deviate from the mean proportion (Peters, 2001, 2003). We also calculated the

dominance (conceptually the inverse of evenness) in samples by using the Simpson's index λ which indicates the probability that two randomly picked individuals belong to the same taxa, whereby $\lambda = \sum(p_i^2)$ and p_i is the proportion of species i (Simpson, 1949).

Bulinski (2007) compared and evaluated the performance of evenness metrics according the variations of sample size and taxon frequency distributions. Her results suggest that PIE metric is the most stable at small sample sizes, but the E_{SS} metric may be preferable for segregation of groups of samples characterized by distinct evenness values (Bulinski, 2007). The five different metrics correlate well in our empirical data and we will only discuss PIE results.

3.2.2. Cluster Analysis

Cluster analysis is an exploratory tool which aims at sorting different taxa (or samples) into groups in a way that the degree of association between two taxa (or samples) is maximal if they belong to the same group and minimal otherwise. Cluster analysis can be used to discover structures in data without providing an explanation/interpretation (Saporta, 1990).

Clustering analysis was carried out using two-way hierarchical, agglomerative, UPGMA (Unweighted Pair-Group Method using arithmetic Averages) method (Legendre and Legendre, 1998), with Raup-Crick coefficient as similarity measure (Raup and Crick, 1979). Raup-Crick coefficient was selected to avoid the possible problems of Jaccard coefficient when comparing two samples in which one has many more species than the other. Clusters from the R-mode analysis group taxa that usually appear together in samples. Clusters from the Q-mode analysis group samples that share similar taxa assemblages.

3.2.3. Seriation Analysis

Dendograms resulting from cluster analysis can be affected by the order of taxa in the data matrix, we used unconstrained seriation analysis to standardize the results before interpretation. In its unconstrained version, data matrix is arranged such that the presences of taxa are concentrated along the diagonal; this is just a simple graphical technique (Cleal, 2008).

3.2.4. Non-Parametric Multivariate ANalysis Of VAriance (NPMANOVA)

Cluster analysis on its own provides no measure of significance of the difference between any two clusters that it reveals (Anderson, 2001; Cleal, 2008). However, the Non-parametric Multivariate Analysis of Variance (NPMANOVA) allows obtaining Bonferroni-corrected P-values using permutation to evaluate if the null hypothesis is true and the groups are not really different (Anderson, 2001). We used this technique to evaluate if clusters resulting from the UPGMA cluster analysis were statistically different (Bonferroni-corrected $p < 0.05$).

3.2.5. Correspondence Analysis (CA)

Correspondence Analysis (CA) (Benzécri, 1973) is an ordination method that allows graphical representations of relationships between taxa and samples in a multidimensional space. Applied to occurrence matrices, the method assumes that the distribution of taxa among samples responds to a few ecological gradients, such that complex sets of data may be reduced to a limited number of axes of variation that can be represented in a geometrical plot and that can be interpreted in terms of ecological habits (Dale and Dale, 2002). CA assumes that taxa have unimodal responses to the underlying parameters.

One important condition in which the various ordination methods differ is in the way they assign mathematical weights to the taxa. In CA, an average of a set of taxon scores is used. This means that in CA even rare species may have high scores (Dale and Dale, 2002).

4. Results

4.1 Diversity analysis

The standardized taxonomic richness, S_{30} , in the Lusitanian Basin ranges between 13.1 and 1 in the São Julião section, 10.8 and 2.8 taxa in Magoito Aguda, 11 and 5.6 taxa in Guincho, 6.8 and 2.8 taxa in the Ponta do Sal and between 10.7 and 4.8 taxa in Baforeira Rana, and between 12.1 and 4.8 taxa in the 398D hole samples.

Evenness in the Lusitanian Basin sections, estimated through the Probability of Interspecific Encounter (PIE), ranges between 0.92 and 0. In the 398D assemblages PIE has a much lower variability, ranging between 0.96 and 0.81, with the exception of one sample with an evenness of 0.43.

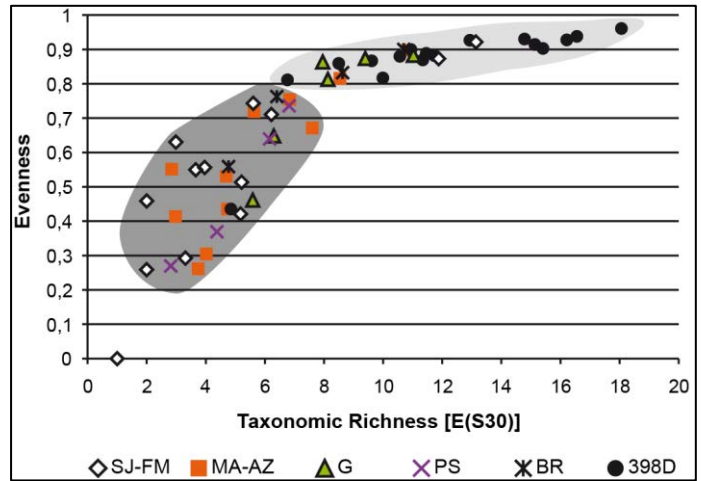


Figure 2.5. Crossplot of Taxonomic Richness, $E(S_{30})$, and Evenness values from Lusitanian Basin and 398D DSDP site samples. São Julião - Falcao Magoito (SJ-FM), Magoito Aguda - Azenhas do mar (MA-AZ), Guincho (G), Ponta do Sal (PS) and Baforeira Rana (BR).

Plotting Taxonomic Richness vs. Evenness from samples of the different studied

sections reveals two major types of samples in function of their assemblage structure (Fig. 2.5). Samples from Lusitanian Basin sections show low values of taxonomic richness and a wide range of evenness values. Samples from 398D hole are characterized by high values of evenness as well as the highest values of taxonomic richness within the dataset.

No temporal or environmental trend is clear within the biodiversity data when analyzed at the sample level. Some information appears when samples are merged by time intervals (Fig. 2.6). The species richness remains stable or increases slightly between the Middle and the Late Albian and the transition to the Vraconian interval records a decrease in taxonomic richness of the most distal sections (SJ-FM, MA-AZ),

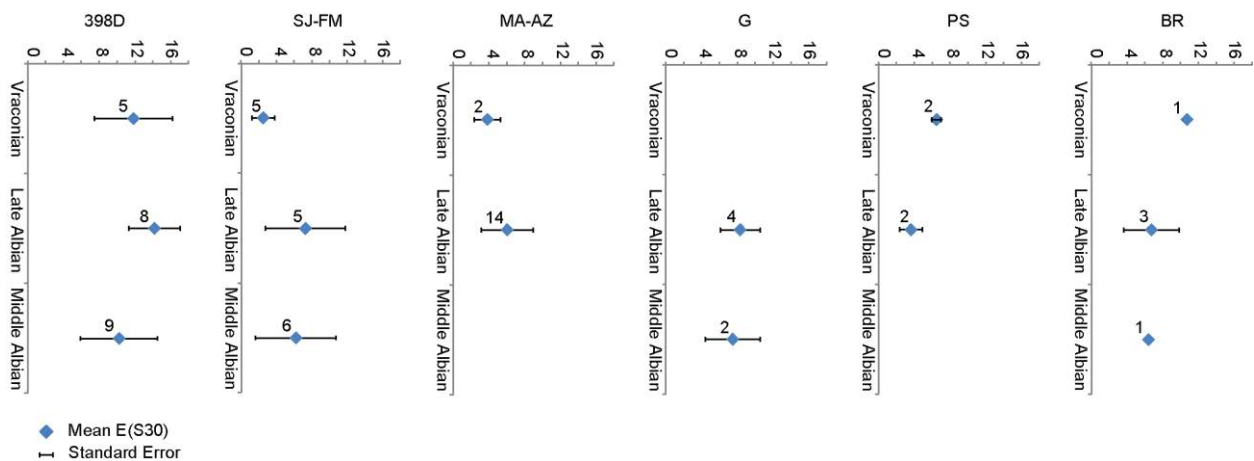


Figure 2.6. Lusitanian Basin and 398D site sample taxonomic richness, $E(S_{30})$ merged by time intervals

including the 398D core. Whereas the richness increases in the most proximal sections (PS and BR).

The patterns of evenness are similar for the northern most sections from the Lusitanian Basin (SJ-FM, MA-AZ and G) and for the 398D, with increasing values between the middle and the upper Albian and stability or a slight decrease into the Vraconian (Fig. 2.7). In the southern most Lusitanian Basin sections (PS and BR) the evenness decreases between the Middle and Late Albian, and then reaches its higher mean values during the Vraconian.

4.2. Differentiation of dinocyst associations between coastal and open marine distal environments

4.2.1. Clusters of taxa and samples and Pairwise NPMANOVA.

The joint analysis of the data derived from the Lusitanian Basin and DSDP 398D hole allows testing the differentiation of dinocysts associations between the coastal and the neritic / oceanic environments. The data table contains 52 taxa and 69 samples. R-mode cluster analysis of the whole dataset reveal three clusters of taxa (Fig. 2.8), and the Q-mode analysis segregates two clusters of samples (Fig. 2.9). Results from the pairwise NPMANOVA analyses reveal Bonferroni-corrected p values below 0.005, which suggests that none of the retained clusters is likely originated by chance.

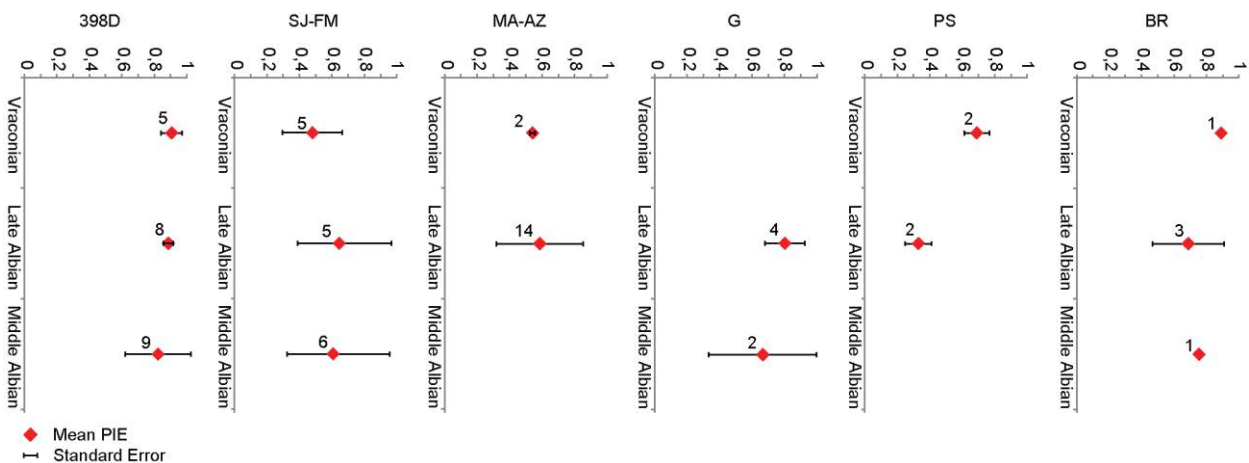


Figure 2.7. Lusitanian Basin and 398D site sample Evenness (PIE) merged by time intervals.

DINOCYST DISTRIBUTION IN AN INSHORE TO OFFSHORE TRANSECT IN THE WESTERN IBERIAN MARGIN

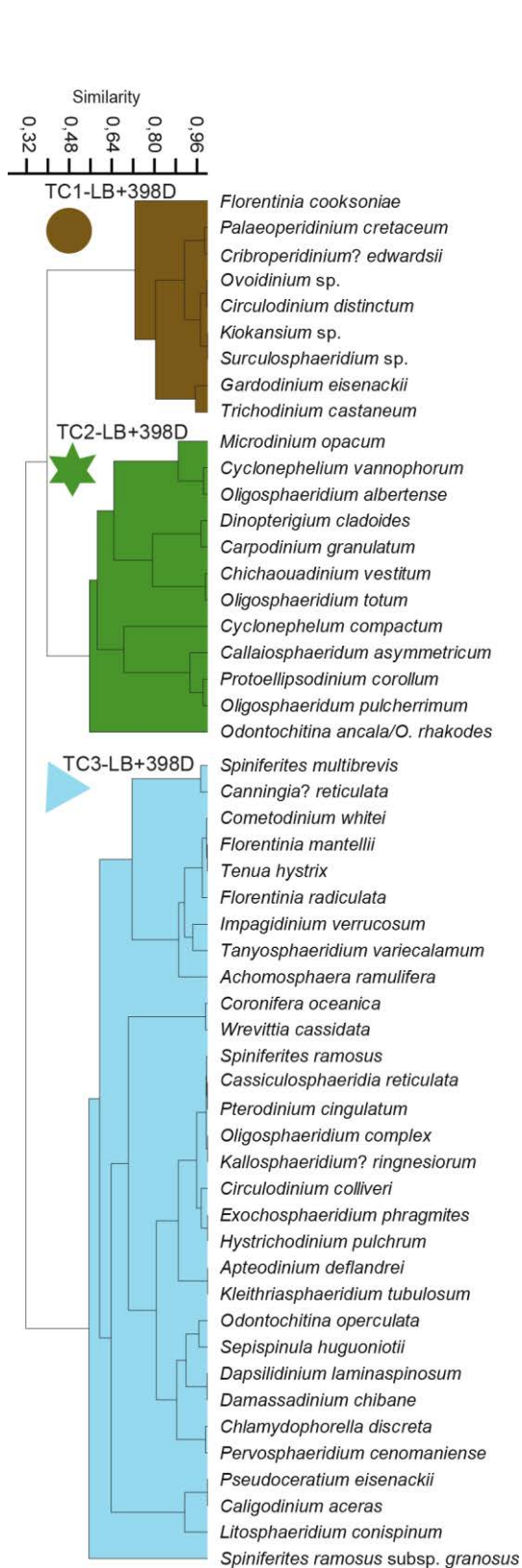


Figure 2.8. UPGMA R-mode cluster analysis of Lusitanian Basin and 398D data, using Raup-Crick coefficient as similarity measure. Grouped taxa usually appear together in samples.

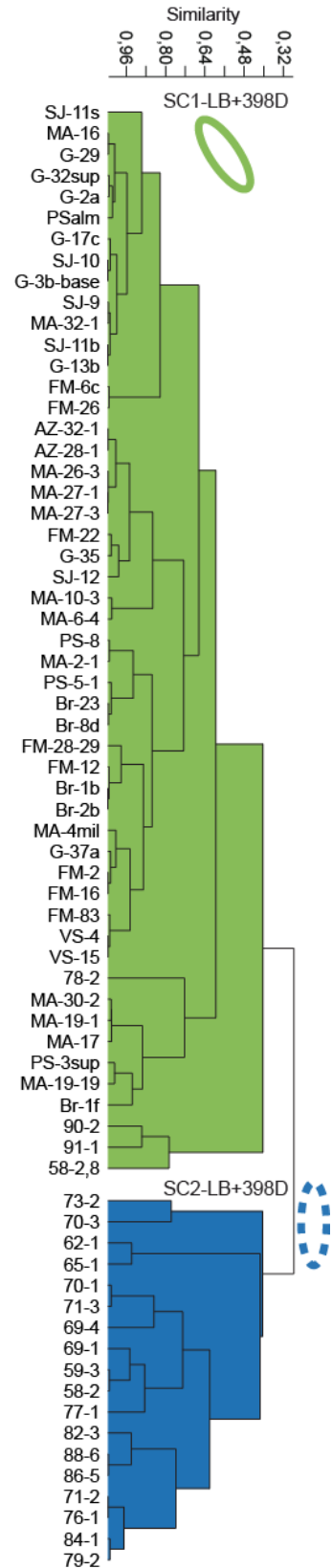


Figure 2.9. UPGMA Q-mode cluster analysis of Lusitanian Basin and 398D data, using Raup-Crick coefficient as similarity measure. Clustered samples share similar taxon assemblages.

R mode – clustering taxon associations

First cluster of taxa, TC1-LB+398D associates 9 taxa (Fig. 2.8): 4 taxa occurring exclusively in Lusitanian Basin samples (*Florentinia cooksoniae*, *Kiokansium* sp., *Ovoidinium* sp. and *Surculosphaeridium* sp.) and 4 taxa occurring both in the Lusitanian Basin and in the 398D sites samples (*Circulodinium distinctum*, *Cribroperidinium? edwardsii*, *Gardodinium eisenackii*, *Palaeoperidinium cretaceum* and *Trichodinium castaneum*). The taxon list counts 2 peridiniinean and 7 gonyaulacinean taxa (Table 2.1). The most frequent taxon (*T. castaneum*) occurs in 36 samples with an average abundance of 23% (max. 90%). Abundance of the taxa clustered in TC1-LB+398D was higher in the Lusitanian Basin samples (Figure 2.10).

Table 2.1. Taxa included in TC1-LB+398D, 53 samples contained taxa included in this cluster.

	Number of samples in which it occurs	Mean relative abundance (%)	Max relative abundance (%)	Order	Suborder
<i>Circulodinium distinctum</i>	22	6	18	Gonyaulacales	Gonyaulacineae
<i>Cribroperidinium? edwardsii</i>	23	9	24	Gonyaulacales	Gonyaulacineae
<i>Florentinia cooksoniae</i>	5	5	7	Gonyaulacales	Gonyaulacineae
<i>Gardodinium eisenackii</i>	8	7	20	Gonyaulacales	Uncertain
<i>Kiokansium</i> sp.	2	6	8	Gonyaulacales	Gonyaulacineae
<i>Ovoidinium</i> sp.	10	25	93	Peridinales	Peridiniineae
<i>Palaeoperidinium cretaceum</i>	20	23	83	Peridinales	Peridiniineae
<i>Surculosphaeridium</i> sp.	3	8	17	Gonyaulacales	Gonyaulacineae
<i>Trichodinium castaneum</i>	36	23	90	Gonyaulacales	Gonyaulacineae

Cluster of taxa TC2-LB+398D groups 12 taxa (Fig. 2.8). This cluster includes 5 taxa occurring exclusively with representation over 2% in Lusitanian Basin samples (*Callaiosphaeridium asymmetricum*, *Carpodinium granulatum*, *Microdinium opacum*, *Oligosphaeridium pulcherrimum* and *Oligosphaeridium totum*) and 7 taxa occurring both in Lusitanian Basin and 398D sites (*Chichaouadinium vestitum*, *Cyclonephelium compactum*, *Cyclonephelium vannophorum*, *Dinopterigium cladoides*, *Odontochitina ancala/O. rhakodes*, *Oligosphaeridium albertense* and *Protoellipsoidinium corollum*). TC2-LB+398D cluster groups 1 ceratiinean taxon, 1 cladopyxiinean taxon, 1 peridiinean taxon and 9 gonyaulacinean taxa (Table 2.2). The most frequent taxa are *Odontochitina ancala/O. rhakodes*, *Cyclonephelium vannophorum*, *Protoellipsoidinium corollum* and *Cyclonephelium compactum* (Table 2.2). The frequency of the taxa that characterize TC2-LB+398D was higher in the Late Albian of the Lusitanian Basin sections than in the 398D site.

DINOCYST DISTRIBUTION IN AN INSHORE TO OFFSHORE TRANSECT IN THE
WESTERN IBERIAN MARGIN

Table 2.2. Taxa included in TC2-LB+398D, 58 samples contained taxa included in this cluster.

	Number of samples in which it occurs	Mean relative abundance (%)	Max relative abundance (%)	Order	Suborder
<i>Callaiosphaeridium asymmetricum</i>	5	6	13	Gonyaulacales	Gonyaulacineae
<i>Carpodinium granulatum</i>	9	8	17	Gonyaulacales	Gonyaulacineae
<i>Chichaouadinium vestitum</i>	16	39	86	Peridinales	Peridiniineae
<i>Cyclonephelium compactum</i>	23	7	23	Gonyaulacales	Gonyaulacineae
<i>Cyclonephelium vannophorum</i>	26	13	65	Gonyaulacales	Gonyaulacineae
<i>Dinopterygium cladoides</i>	20	8	21	Gonyaulacales	Goniodimineae
<i>Microdinium opacum</i>	7	14	55	Gonyaulacales	Cladopyxiineae
<i>Odontochitina ancala/O. rhakodes</i>	29	20	81	Gonyaulacales	Ceratiineae
<i>Oligosphaeridium albertense</i>	14	9	23	Gonyaulacales	Gonyaulacineae
<i>Oligosphaeridium pulcherrimum</i>	7	10	18	Gonyaulacales	Gonyaulacineae
<i>Oligosphaeridium totum</i>	5	7	12	Gonyaulacales	Gonyaulacineae
<i>Protoellipsodinium corollum</i>	26	18	67	Gonyaulacales	Gonyaulacineae

Third cluster of taxa, TC3-LB+398D, groups 31 taxa (Fig. 2.8) out of which 8 are present in both the Lusitanian Basin and the 398D sections (*Circulodinium colliveri*, *Chlamydophorella discreta*, *Cometodinium withei*, *Coronifera oceanica*, *Exochosphaeridium phragmites*, *Odontochitina operculata*, *Spiniferites multibrevis*, and *Spiniferites ramosus*) and 23 taxa occurring exclusively in 398D site samples (*Achomosphaera ramulifera*, *Apteodinium deflandrei*, *Caligodinium aceras*, *Canningia reticulata*, *Cassiculosphaeridia reticulata*, *Damassadinium chibane*, *Dapsilidinium laminaspinosum*, *Florentinia mantellii*, *Florentinia radiculata*, *Hystrichodinium pulchrum*, *Impagidinium verrucosum*, *Kallosphaeridium? ringnesiorum*, *Kleithriasphaeridium tubulosum*, *Litosphaeridium conispinum*, *Oligosphaeridium complex*, *Pervosphaeridium cenomaniense*, *Pseudoceratium eisenackii*, *Pterodinium cingulatum*, *Sepispinula? huguoniotii*, *Spiniferites ramosus* subsp. *granosus*, *Tanyosphaeridium variecalamum*, *Tenua hystrix* and *Wrevittia cassidata*). TC3-LB+398D is composed exclusively of gonyaulacaleans, among them 2 ceratiinean taxa (Table 2.3). Taxa included in TC3-LB+398D predominate in all the samples from the 398D site but they also occur in the Lusitanian Basin outcrops at a relatively low frequency (usually less than 10 %). They reach a maximum during the Middle Albian at the Guincho section, with up to 20% of the taxon composition (Fig. 2.10).

Table 2.3. Taxa included in TC3-LB+398D, 45 samples contained taxa included in this cluster.

	Number of samples in which it occurs	Mean relative abundance (%)	Max relative abundance (%)	Order	Suborder
<i>Achomosphaera ramulifera</i>	5	7	13	Gonyaulacales	Gonyaulacineae
<i>Apteodinium deflandrei</i>	4	12	25	Gonyaulacales	Gonyaulacineae
<i>Caligodinium aceras</i>	2	37	71	Gonyaulacales	Uncertain
<i>Canningia reticulata</i>	2	16	26	Gonyaulacales	Gonyaulacineae
<i>Cassiculosphaeridia reticulata</i>	8	4	7	Gonyaulacales	Uncertain
<i>Chlamydothrella discreta</i>	7	6	12	Gonyaulacales	Uncertain
<i>Circulodinium colliveri</i>	12	12	32	Gonyaulacales	Gonyaulacineae
<i>Cometodinium whitei</i>	12	8	30	Gonyaulacales	Gonyaulacineae
<i>Coronifera oceanica</i>	5	5	9	Gonyaulacales	Gonyaulacineae
<i>Damassadinium chibane</i>	5	4	8	Gonyaulacales	Gonyaulacineae
<i>Dapsilidinium laminaspinosum</i>	6	6	9	Gonyaulacales	Uncertain
<i>Exochosphaeridium phragmites</i>	13	5	8	Gonyaulacales	Uncertain
<i>Florentinia mantellii</i>	3	6	8	Gonyaulacales	Gonyaulacineae
<i>Florentinia radiculata</i>	3	4	4	Gonyaulacales	Gonyaulacineae
<i>Hystrichodinium pulchrum</i>	10	9	22	Gonyaulacales	Gonyaulacineae
<i>Impagidinium verrucosum</i>	2	20	28	Gonyaulacales	Gonyaulacineae
<i>Kallosphaeridium? ringnesiorum</i>	7	15	38	Gonyaulacales	Gonyaulacineae
<i>Kleithrasphaeridium tubulosum</i>	9	7	13	Gonyaulacales	Gonyaulacineae
<i>Litosphaeridium conispinum</i>	4	12	25	Gonyaulacales	Gonyaulacineae
<i>Odontochitina operculata</i>	12	9	25	Gonyaulacales	Ceratiineae
<i>Oligosphaeridium complex</i>	13	7	18	Gonyaulacales	Gonyaulacineae
<i>Pervosphaeridium cenomaniense</i>	6	9	15	Gonyaulacales	Gonyaulacineae
<i>Pseudoceratium eisenackii</i>	3	9	15	Gonyaulacales	Ceratiineae
<i>Pterodinium cingulatum</i>	12	14	29	Gonyaulacales	Gonyaulacineae
<i>Sepispinula? huguoniotii</i>	5	15	31	Gonyaulacales	Gonyaulacineae
<i>Spiniferites multibrevis</i>	12	9	17	Gonyaulacales	Gonyaulacineae
<i>Spiniferites ramosus</i>	35	12	46	Gonyaulacales	Gonyaulacineae
<i>Spiniferites ramosus</i> subsp. <i>granosus</i>	3	5	7	Gonyaulacales	Gonyaulacineae
<i>Tanyosphaeridium variecalamum</i>	3	5	7	Gonyaulacales	Uncertain
<i>Tenua hystrix</i>	3	4	5	Gonyaulacales	Gonyaulacineae
<i>Wrevittia cassidata</i>	3	9	14	Gonyaulacales	Gonyaulacineae

Q mode – Samples clustering

The cluster SC1-LB+398D associates all of the 47 samples from the Lusitanian Basin and 4 samples from the DSDP site 398D (Fig. 2.9). The samples are associated to varied sedimentary environments in the Lusitanian Basin: calcareous sandstones bearing vegetal remains or microfossil bearing marls and limestones. The 398D site samples clustered within SC1-LB+398D are black shales alternating with beds bearing fragmented shells and siderite nodules (1175.48 mbsf, 1290.32 mbsf and 1298.12 mbsf) or mixed marly chalk – shale level (966.08 mbsf).

The cluster SC2-LB+398D is composed of 18 samples from the 398D cores (Fig. 2.9) mainly characterized as shales. Black shales dominate the lower part of the series (from 1277.2 to 1070.15 mbsf), whereas the upper part (1031.68 mbsf to 966.85 mbsf) is characterized as mixed marly chalk – shale levels. Levels bearing shell fragments and siderite nodules are common.

4.2.2. Correspondence Analysis.

Correspondence analysis (CA) points out the correlation between the clusters of taxa and the clusters of samples (Fig. 2.11). The first two axes represent 18.3% of the total variance of data, but are the only two axes that can be easily interpreted in terms of paleoenvironments.

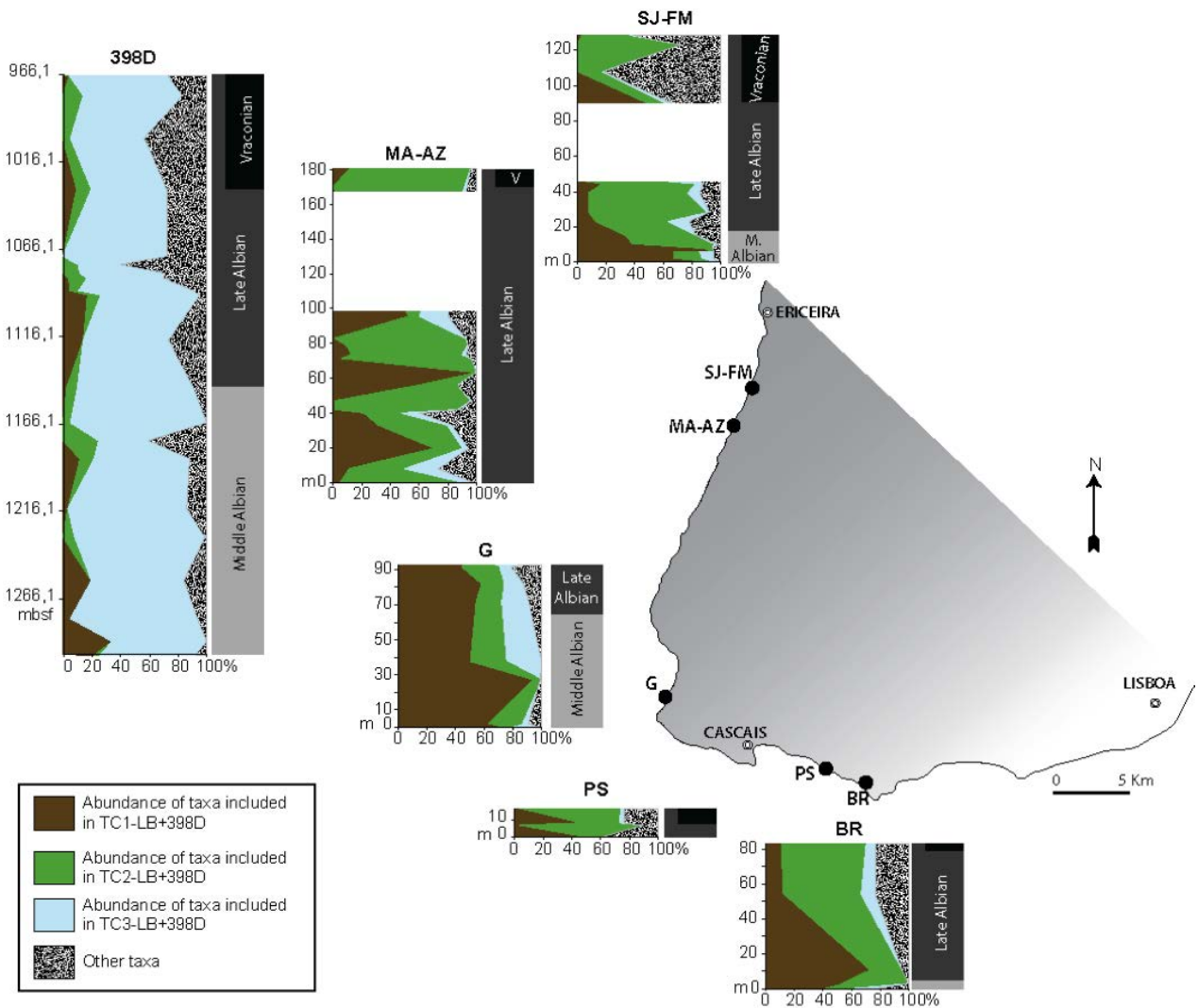


Figure 2.10. Taxa clusters abundance along the Lusitanian Basin outcrops and the 398D hole. São Julião - Falcao Magoito (SJ-FM), Magoito Aguda - Azenhas do Mar (MA-AZ), Guincho (G), Ponta do Sal (PS) and Baforeira Rana (BR). Black smoky areas represent the relative abundance of all the taxa no taken into account for the analysis.

The plotting of taxon and sample clusters together in the multivariate space of the CA shows that SC2-LB+398D and TC3-LB+398D strongly overlap and are characterized by negative values on the first axis (Fig. 2.11). The distribution of SC1-LB+398D samples overlaps TC1-LB+398D and TC2-LB+398D, sharing all positive values on the first axis. TC1-LB+398D and TC2-LB+398D are however segregated along the second axis, the first cluster associated to negative values and the second cluster to positive ones (Fig. 2.11).

Representing the main lithological features of studied samples within the CA evidences that TC1-LB+398D is associated to samples that contain black colored sand, clays, and plant remains (Fig. 2.12). Taxa grouped in this cluster may be related to proximal environments receiving inputs of siliciclastic sediments and continental organic matter from estuaries. Taxa included in TC2-LB+398D plot with the samples characterized as marl, limestone, levels containing microfossils remains (oysters, rudists). The association is thus indicative of shallow water environments. The high carbonate content and occurrence of rudists suggests a low siliciclastic flux, and potentially a lower nutrient input than for TC1-LB+398D. Taxa included in TC3-LB+398D seem to be indicative of clay deposits, in open marine, distal environments.

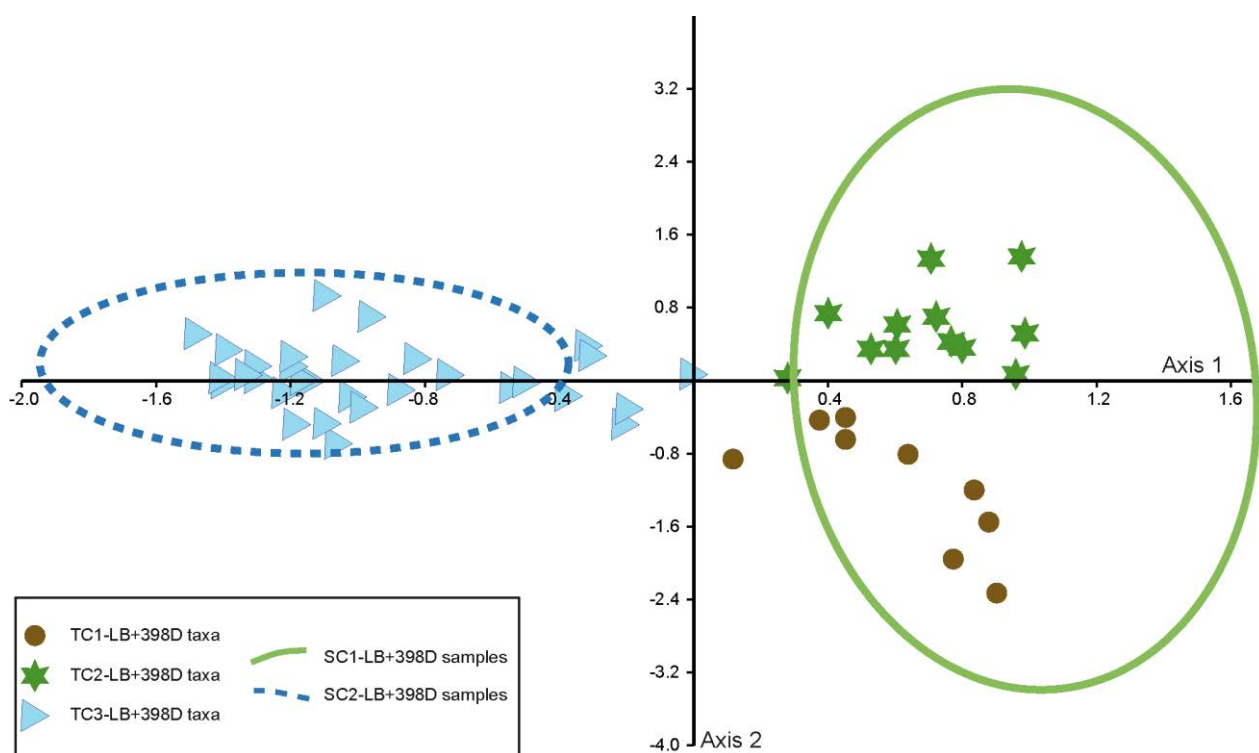


Figure 2.11. Plotting of taxon and sample clusters together in the scatter diagram of CA from Lusitanian Basin and 398D site data. The ellipses outline the distribution of samples included in the clusters.

4.3. Differentiation of dinocyst associations among shallow coastal environments

4.3.1. Clusters of taxa and samples and Pairwise NPMANOVA.

In the analysis of the whole dataset, the samples derived from sections at the Lusitanian coast are mixed in a single sample cluster and two taxon clusters. While considered without the 398D core data, the data are reduced to 29 taxa and 47 samples. The R and Q-mode cluster analyses reveal 3 clusters of taxa (TC1-LB, TC2-LB and TC3-LB, Fig. 2.13) and 3 clusters of samples (SC1-LB, SC2-LB and SC3-LB, Fig. 2.14). Pairwise NPMANOVA analyses suggest that none of the cluster is likely to arise from random (Bonferroni-corrected $p < 0.02$). Thus, the splitting of the initial groupings allows refinement of paleoecological interpretation for the association found in coastal environments.

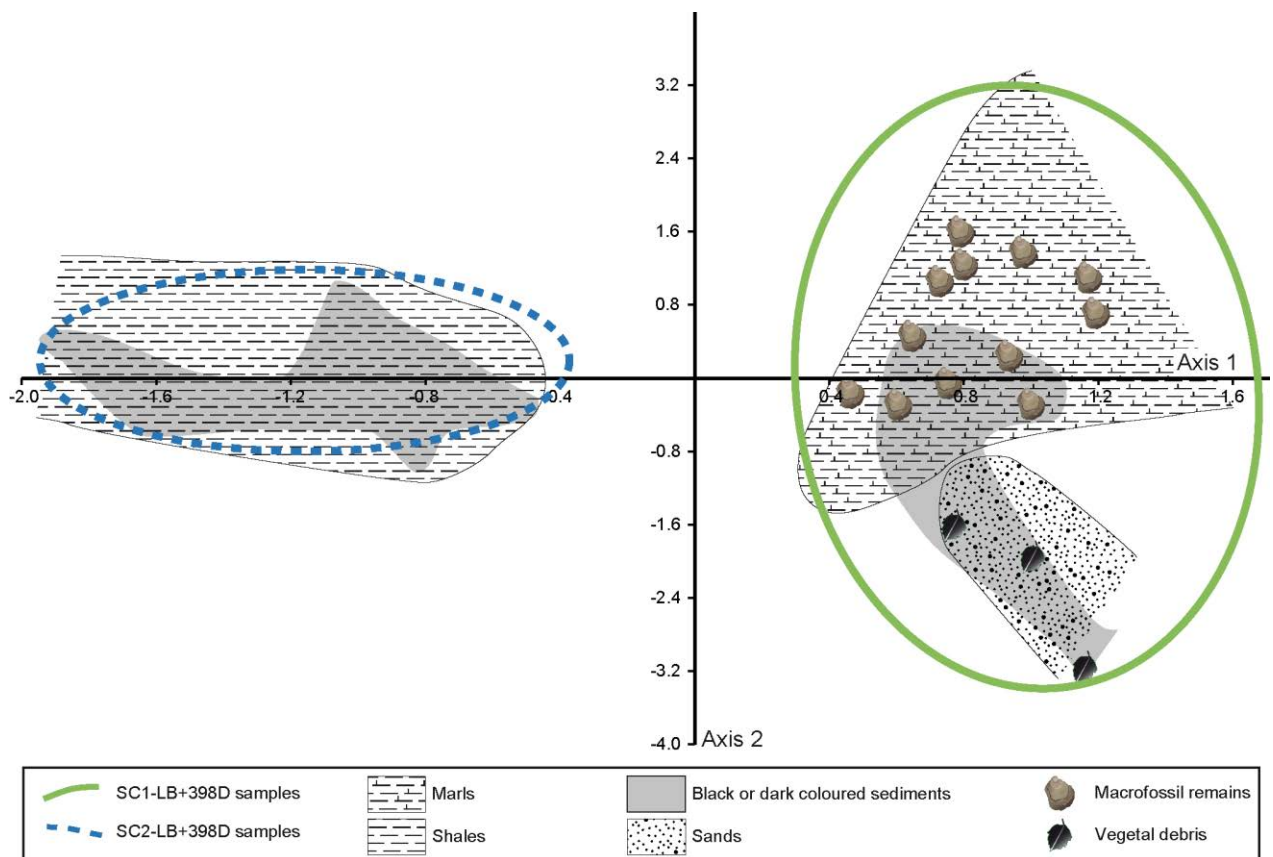


Figure 2.12. Plotting the clusters of samples from the Lusitanian Basin and the 398D site together with their sedimentological and paleontological properties in the CA scattergram. Green ellipse outlines the distribution of SC1-LB+398D and dotted blue ellipse the distribution of SC2-LB+398D. Lithological patterns reflect the main characteristics of samples plotting in the area, main macrofossils found on these levels are represented.

R mode – Taxa clustering

First cluster of taxa (TC1-LB) groups 9 gonyaulacalean taxa and 2 peridinialean taxa (Fig. 2.13, Table 2.4). Within the gonyaulacalean taxa *Trichodinium castaneum* is the most common taxon occurring in 28 samples with an average abundance of 28% (max. 90%). Taxa included in TC1-LB are more abundant in the lower part of Lusitanian Basin sections (Fig. 2.15), during the Middle Albian, and became less common through the Late Albian.

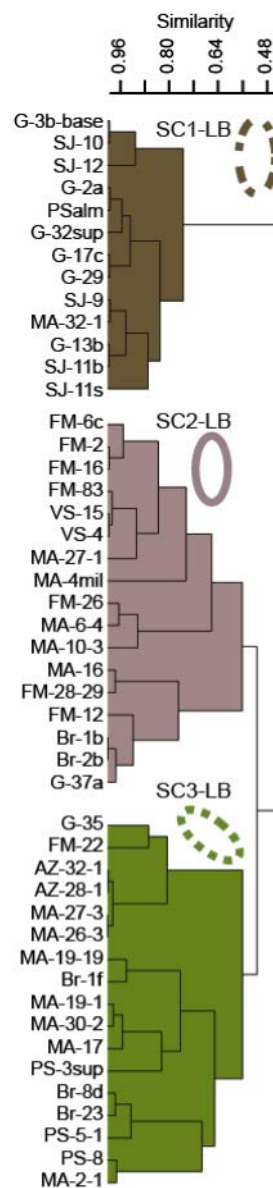
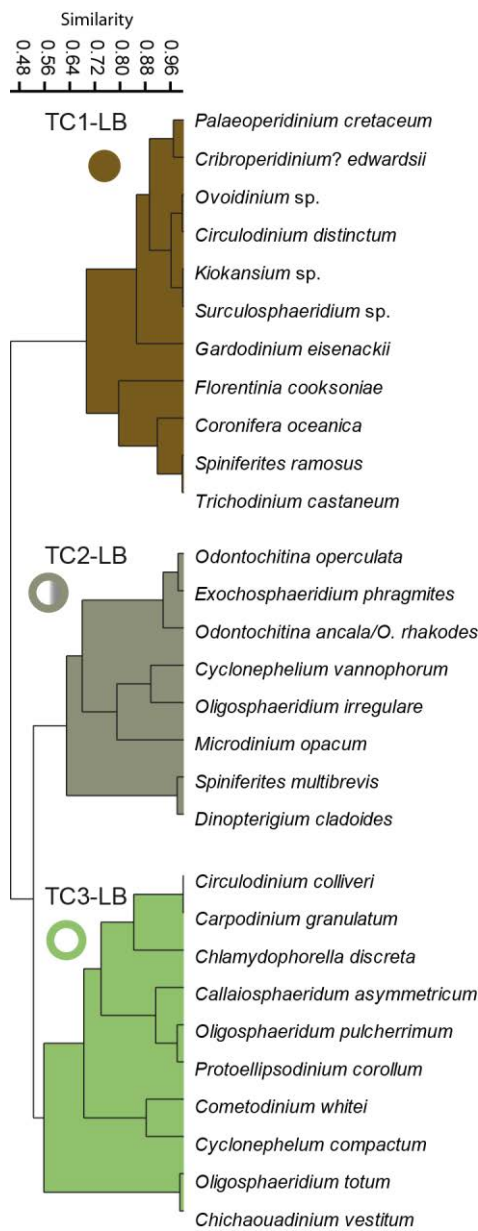


Figure 2.13. UPGMA R-mode cluster from Lusitanian Basin data, using Raup-Crick coefficient as similarity measure. Taxa associated in a cluster usually appear together.

Figure 2.14. UPGMA Q-mode cluster from Lusitanian Basin data, using Raup-Crick coefficient as similarity measure. Clustered samples share similar taxon assemblages.

DINOCYST DISTRIBUTION IN AN INSHORE TO OFFSHORE TRANSECT IN THE
WESTERN IBERIAN MARGIN

Table 2.4. Taxa included in TC1-LB, 40 samples contained taxa included in this cluster.

	Number of samples in which it occurs	Mean relative abundance (%)	Max relative abundance (%)	Order	Suborder
<i>Circulodinium distinctum</i>	17	6	13	Gonyaulacales	Gonyaulacineae
<i>Coronifera oceanica</i>	3	4	4	Gonyaulacales	Gonyaulacineae
<i>Cribroperidinium? edwardsii</i>	18	9	19	Gonyaulacales	Gonyaulacineae
<i>Florentinia cooksoniae</i>	5	5	7	Gonyaulacales	Gonyaulacineae
<i>Gardodinium eisenackii</i>	5	7	20	Gonyaulacales	Uncertain
<i>Kiokansium</i> sp.	2	6	8	Gonyaulacales	Gonyaulacineae
<i>Ovoidinium</i> sp.	10	25	93	Peridiniales	Peridiniineae
<i>Palaeoperidinium cretaceum</i>	18	23	83	Peridiniales	Peridiniineae
<i>Spiniferites ramosus</i>	15	12	28	Gonyaulacales	Gonyaulacineae
<i>Surculosphaeridium</i> sp.	3	8	17	Gonyaulacales	Gonyaulacineae
<i>Trichodinium castaneum</i>	28	28	90	Gonyaulacales	Gonyaulacineae

The second cluster of taxa (TC2-LB) groups 8 taxa, including all the ceratiinean and cladopyxiinean taxa in the dataset, and no peridiinean (Fig. 2.13, Table 2.5). The most common taxa are *Cyclonephelium vannophorum* and *Odontochitina ancala/O. rhakodes*, occurring both in 24 samples with mean relative abundances of 13.19% and 22.33 % respectively. There is not a clear distributional pattern of the frequency of taxa grouped in TC2-LB among the Lusitanian Basin sections (Fig. 2.15).

Table 2.5. Taxa included in TC2-LB, 39 samples contained taxa included in this cluster.

	Number of samples in which it occurs	Mean relative abundance (%)	Max relative abundance (%)	Order	Suborder
<i>Cyclonephelium vannophorum</i>	24	13	65	Gonyaulacales	Gonyaulacineae
<i>Dinopterygium cladoides</i>	17	9	21	Gonyaulacales	Goniodimineae
<i>Exochosphaeridium phragmites</i>	3	4	4	Gonyaulacales	Uncertain
<i>Microdinium opacum</i>	7	14	55	Gonyaulacales	Cladopyxiineae
<i>Odontochitina ancala/O. rhakodes</i>	24	22	81	Gonyaulacales	Ceratiineae
<i>Odontochitina operculata</i>	5	6	14	Gonyaulacales	Ceratiineae
<i>Oligosphaeridium albertense</i>	12	10	23	Gonyaulacales	Gonyaulacineae
<i>Spiniferites multibrevis</i>	6	10	17	Gonyaulacales	Gonyaulacineae

Third cluster of taxa (TC3-LB) groups 10 taxa and is mainly composed of gonyaulacalean taxa and only 1 peridinialean taxon (Fig. 2.13, Table 2.6). The most frequent taxa of the cluster are *Protoellipsodinium corollum*, *Cyclonephelium compactum*, *Chichaouadinium vestitum* and *Carpodinium granulatum* (Table 2.6). Taxa of TC3-LB were more abundant in the Upper Albian of the São Julião, Magoito Aguda and Ponta do Sal sections (Fig. 2.15), whereas they were of secondary importance in Guincho and Baforeira Rana.

Table 2.6. Taxa included in TC3-LB, 32 samples contained taxa included in this cluster.

	Number of samples in which it occurs	Mean relative abundance	Max relative abundance	Order	Suborder
<i>Callaiosphaeridium asymmetricum</i>	5	6	13	Gonyaulacales	Gonyaulacineae
<i>Carpodinium granulatum</i>	9	8	17	Gonyaulacales	Gonyaulacineae
<i>Chichaouadinium vestitum</i>	13	45	86	Peridinales	Peridiniineae
<i>Chlamydothorea discreta</i>	2	4	4	Gonyaulacales	Uncertain
<i>Circulodinium colliveri</i>	4	4	8	Gonyaulacales	Gonyaulacineae
<i>Cometodinium whitei</i>	6	7	13	Gonyaulacales	Gonyaulacineae
<i>Cyclonephelium compactum</i>	17	8	23	Gonyaulacales	Gonyaulacineae
<i>Oligosphaeridium pulcherrimum</i>	7	10	18	Gonyaulacales	Gonyaulacineae
<i>Oligosphaeridium totum</i>	5	7	12	Gonyaulacales	Gonyaulacineae
<i>Protoellipsodinium corollum</i>	19	21	67	Gonyaulacales	Gonyaulacineae

Q mode – Samples clustering

A first cluster of samples (SC1-LB) groups 13 samples from the lower part of São Julião section and all but one sample from Guincho (Fig. 2.14). The samples are characterized by a sandy lithology (sands, sandy marls), often bearing plant remains or a black color due to the occurrence of organic matter.

A second cluster of samples (SC2-LB) associates 17 samples from the middle and upper part of São Julião section with samples from the lower part of Magoito Aguda and Baforeira Rana sections (Fig. 2.14). The SC2-LB samples vary in their lithology between limestones and marlstones, usually bearing fossils (oysters, gastropods, cardiids and mytilids), and some with dark color.

The third Cluster of samples (SC3 – LB) groups 17 samples from the upper part of Magoito Aguda, and Baforeira Rana sections, and all the samples from Ponta do Sal section, except the lowest one (Fig. 2.14). Most samples are marls bearing macrofossils (oysters, rudists, echinoderms).

4.3.2. Correspondence Analysis.

The scatter diagram resulting from the correspondence analysis of the Lusitanian Basin data points out the congruence between the clusters of taxa and the clusters of samples (Fig. 2.16). The percentage of variation represented by the two first axes reach the 21.2% of the total variation.

Taxa from TC1-LB and samples from SC1-LB share negative values on the first axis and span almost the whole recorded variability on the second axis (Fig. 2.16). On the scatter diagram of the CA analysis, TC1-LB taxa plot with sandy and clayey samples. They also share their distribution with black and plant remains bearing levels (Fig. 2.17). These taxa may be indicative of nearshore environments, influenced by continental runoff and organic matter inputs.

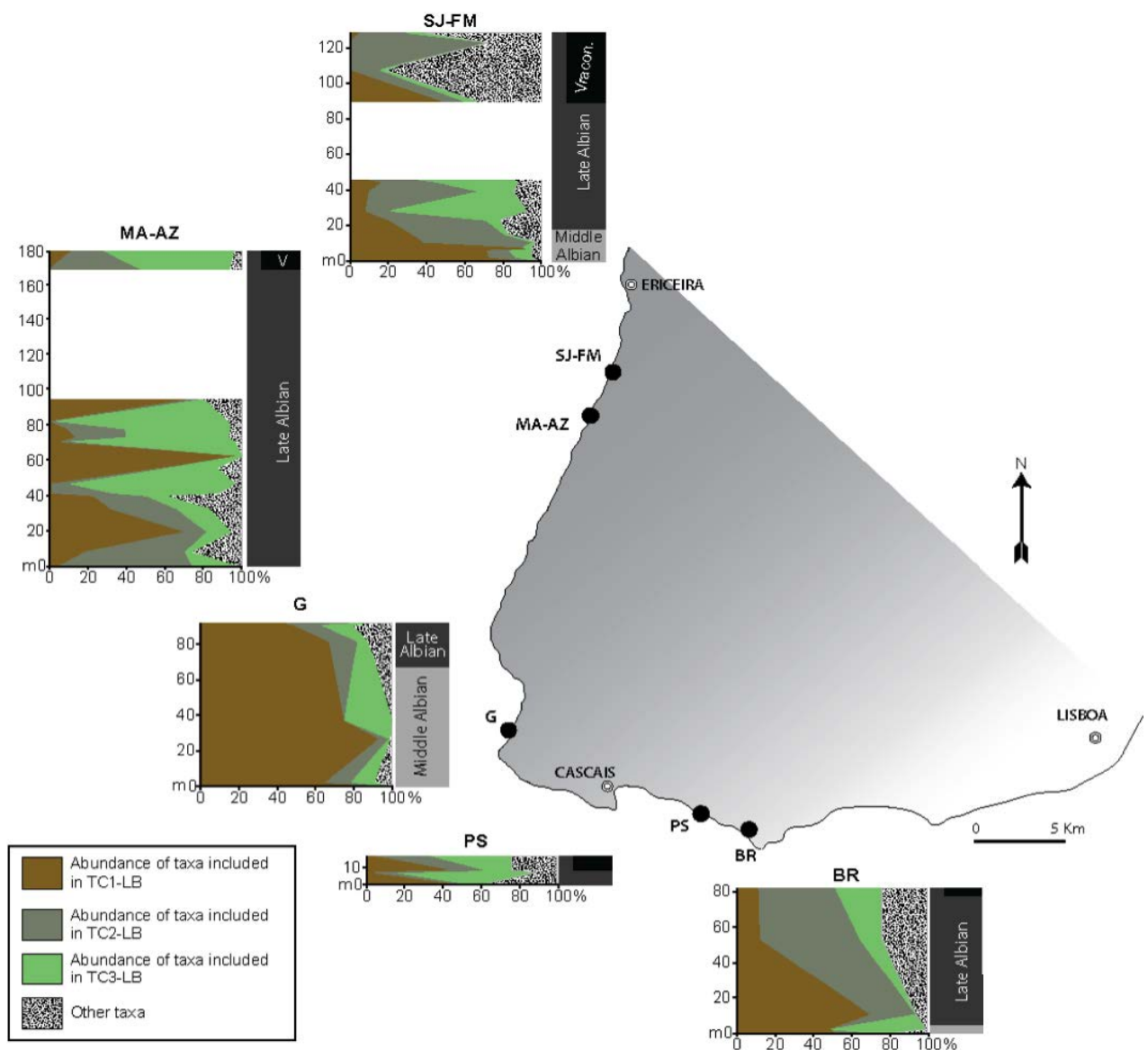


Figure 2.15. Taxon clusters abundance along the Lusitanian Basin outcrops. São Julião - Falcao Magoito (SJ-FM), Magoito Aguda - Azenhas do Mar (MA-AZ), Guincho (G), Ponta do Sal (PS) and Baforeira Rana (BR). Black smoky areas represent the relative abundance of all the taxa no taken into account for the analysis.

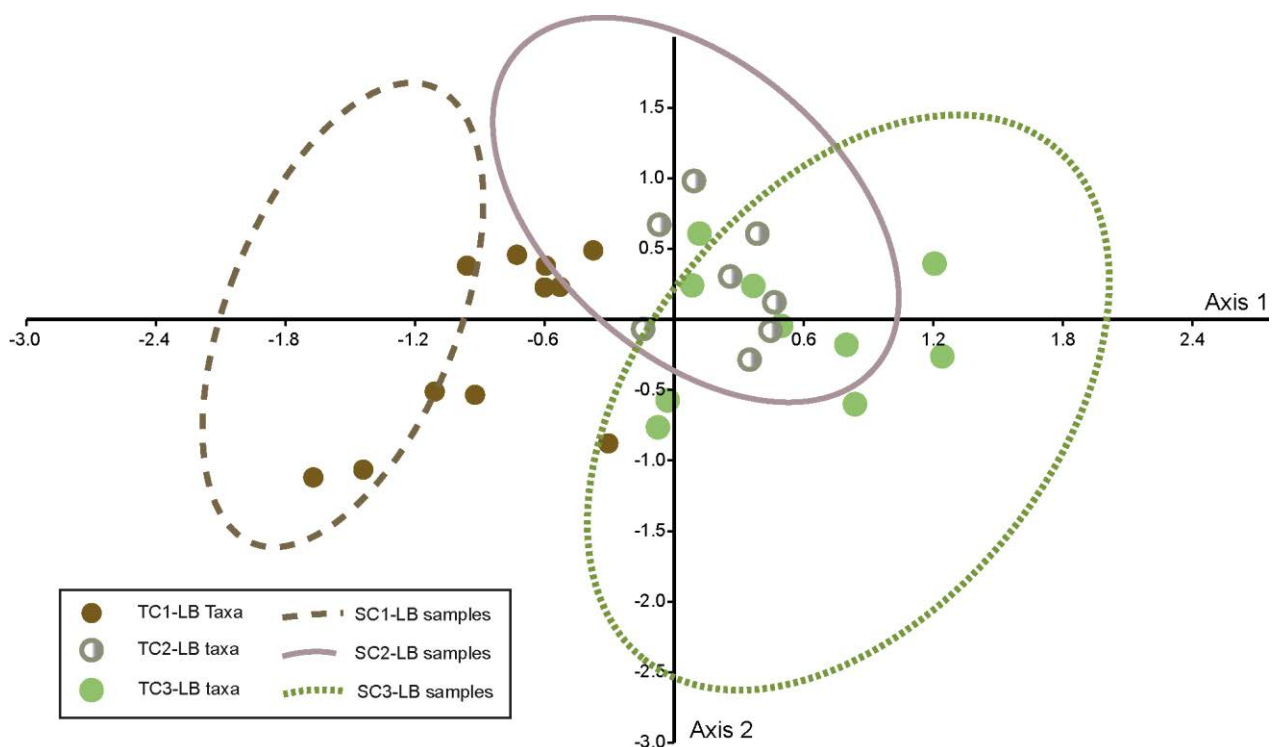


Figure 2.17. Scatter diagram of Correspondence analysis for the Lusitanian outcrops data. The ellipses outline the distribution of samples included in the clusters.

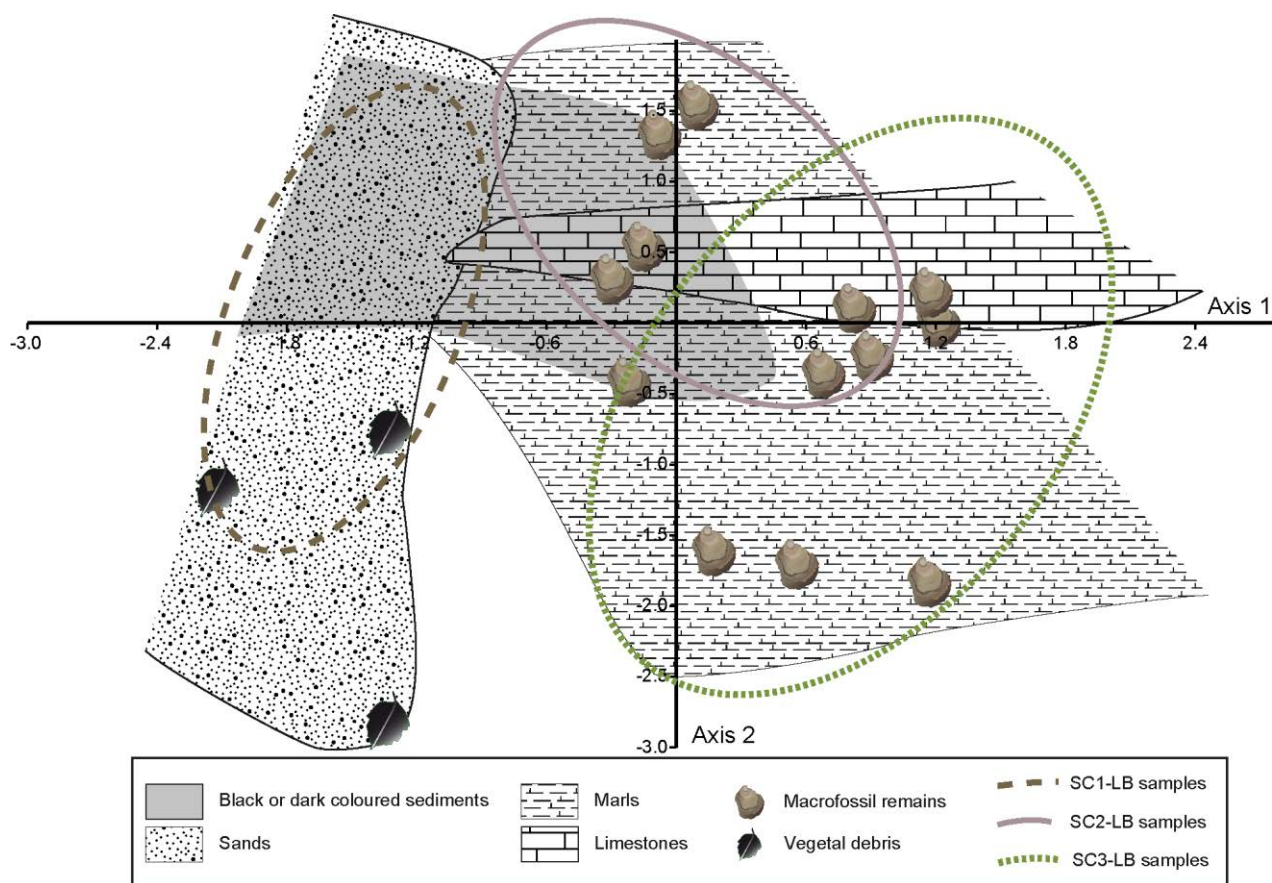


Figure 2.17. Plotting of the clusters of samples from the Lusitanian Basin together with their sedimentological and paleontological properties in the CA scattergram. The ellipses outline the distribution of samples included in the cluster specified in the legend. Lithological patterns reflect the main characteristics of samples plotting in the area, main macrofossils found on these levels are represented.

TC2-LB taxa and SC2-LB samples plot around the center of the CA scatter diagram (Fig. 2.16). Samples plotting near to TC2-LB taxa are limestones and marls,

but they also show a slight relationship with dark colors and levels rich in microfossil remains (Fig. 2.17).

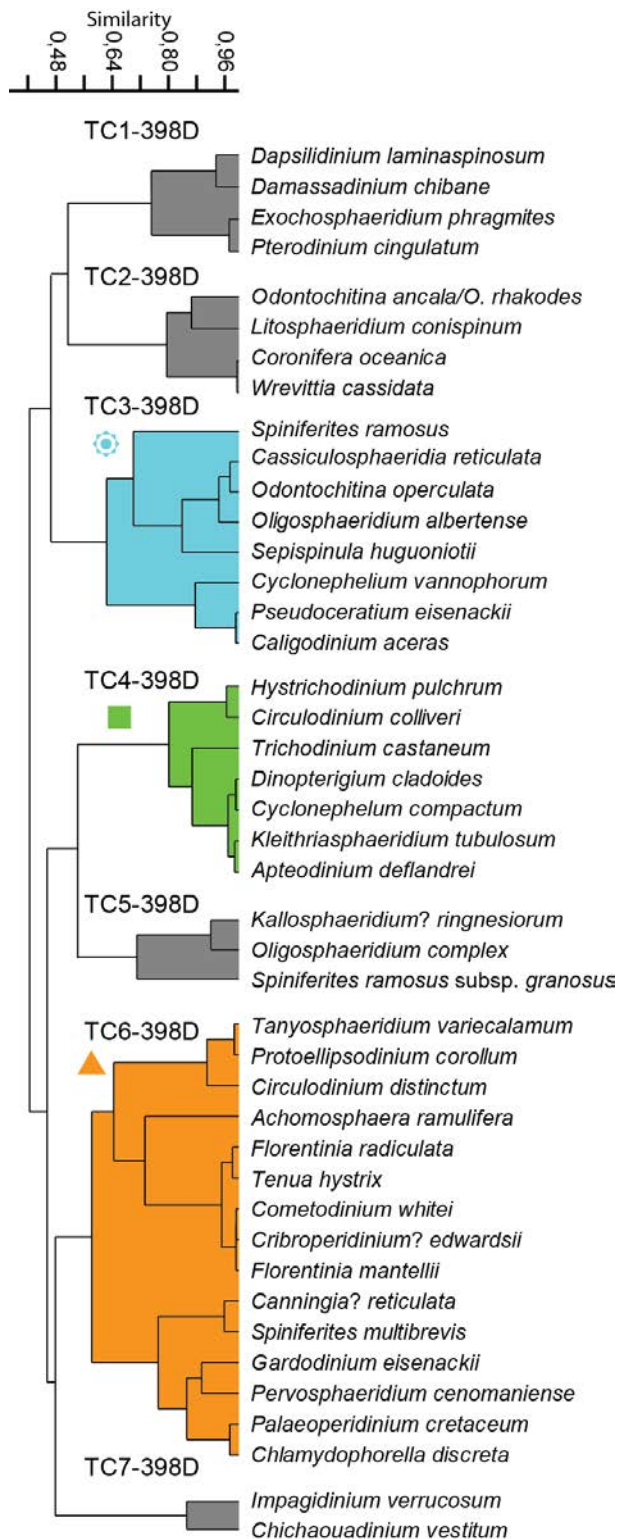


Figure 2.18. UPGMA R-mode cluster from 398D hole data, using Raup-Crick coefficient as similarity measure. Taxa associated in a cluster usually appear together in samples.

Taxa grouped in TC3-LB and samples included in SC3-LB mainly have positive scores on the axes (Fig. 2.16). Samples distributed near to TC3-LB taxa on the CA scatter diagram are mostly limestones, marls, and rich in microfossils remains (Fig. 2.17).

The distribution of the samples on the first axis of the scatter diagram can be understood as reflecting the distance to the shoreline. However, interpretation of the second axis from the lithological and sedimentological information remains difficult.

4.4. Differentiation of distal open marine associations: analysis of the DSDP 398D cores

4.4.1. Clusters of taxa and samples and pairwise NPMANOVA.

The database created from the 398D hole data considers 43 taxa and 22 samples. R and Q-mode cluster analysis from the dataset reveal seven clusters of taxa, named TC1-398D to TC7- 398D

(Fig. 2.18), and six clusters of samples, named SC1-398D to SC6- 398D (Fig. 2.19).

Results of the pairwise NPMANOVA analyses suggest that most of the clusters may not be robust (Bonferroni-corrected $p > 0.05$). Only a few clusters receive a support from pairwise comparisons; TC3-398D, TC4-398D and TC6-398D for the taxa, and SC2-398D and SC3-398D for the samples.

R mode – Taxa clustering

Cluster TC3-398D groups 8 taxa (Fig. 2.18), all gonyaulacalean, and among them two ceratiinean taxa. The most frequent taxa are *Spiniferites ramosus*, *Cassiculosphaeridia reticulata* and *Odontochitina operculata* (Table 2.7). The contribution of TC3-398D to main assemblages remains higher in the mixed marly chalk of the upper part of the sections than in the black shale of the base (Fig. 2.20). The highest values of relative abundances of TC3-398D are associated to levels (from 1175 mbsf to 1145 mbsf) described in the literature as reflecting continental inputs, within a global sequence of pelagic sediments (Sigal, 1979).

Table 2.7. Taxa included in TC3-398D, 20 samples contained taxa included in this cluster

	Number of samples in which it occurs	Mean relative abundance (%)	Max relative abundance (%)	Order	Suborder
<i>Caligodinium aceras</i>	5	14	71	Gonyaulacales	Uncertain
<i>Cassiculosphaeridia reticulata</i>	8	3	2	Gonyaulacales	Uncertain
<i>Cyclonephelium vannophorum</i>	2	12	19	Gonyaulacales	Gonyaulacineae
<i>Odontochitina operculata</i>	7	10	22	Gonyaulacales	Ceratiineae
<i>Oligosphaeridium albertense</i>	2	3	4	Gonyaulacales	Gonyaulacineae
<i>Pseudoceratium eisenackii</i>	3	7	11	Gonyaulacales	Ceratiineae
<i>Sepispinula? huguoniotii</i>	5	10	22	Gonyaulacales	Gonyaulacineae
<i>Spiniferites ramosus</i>	20	9	38	Gonyaulacales	Gonyaulacineae

Cluster of taxa TC4-398D groups 7 gonyaulacinean taxa (Fig.2.18). *Hystrichodinium pulchrum*, *Kleithriasphaeridium tubulosum* and *Circulodinium colliveri* are among the most frequent (Table 2.8). They contribute with high relative abundances to the taxon association between 1230.7 mbsf and 1185 mbsf, at 1145 mbsf, 1089.86 mbsf and 1070.15 mbsf (Fig. 2.20). Higher values of relative abundance of TC4-398D are associated to black shale intervals. Low values of TC4-398D relative abundance are associated to mixed marly chalk.

DINOCYST DISTRIBUTION IN AN INSHORE TO OFFSHORE TRANSECT IN THE
WESTERN IBERIAN MARGIN

Table 2.8. Taxa included in TC4-398D, 16 samples contained taxa included in this cluster.

	Number of samples in which it occurs	Mean relative abundance (%)	Max relative abundance (%)	Order	Suborder
<i>Apteodinium deflandrei</i>	4	10	18	Gonyaulacales	Gonyaulacineae
<i>Circulodinium colliveri</i>	8	13	28	Gonyaulacales	Gonyaulacineae
<i>Cyclonephelium compactum</i>	6	4	5	Gonyaulacales	Gonyaulacineae
<i>Dinopterygium cladoides</i>	3	4	6	Gonyaulacales	Goniodimineae
<i>Hystrichodinium pulchrum</i>	10	8	19	Gonyaulacales	Gonyaulacineae
<i>Kleithrasphaeridium tubulosum</i>	9	6	10	Gonyaulacales	Gonyaulacineae
<i>Trichodinium castaneum</i>	8	4	7	Gonyaulacales	Gonyaulacineae

Cluster TC6-398D groups 15 taxa out of which 14 gonyaulacalean and 1 peridinialean (Fig. 2.18). The taxa occurring in most samples are *Protoellipsodinium corollum*, *Cometodinium whitei*, *Pervosphaeridium cenomaniense* and *Spiniferites multibrevis* (Table 2.9). Cluster TC6-398D is more abundant in the lower part of the section, between 1298.12 mbsf and 1255.5 mbsf (Fig. 2.20). The pattern of variation of the relative abundance of TC6-398D is opposite to that of TC4-398D. The highest relative abundance of TC6-398D corresponds to shell-rich black shale levels.

Table 2.9. Taxa included in TC6-398D, 17 samples contained taxa included in this cluster.

	Number of samples in which it occurs	Mean relative abundance (%)	Max relative abundance (%)	Order	Suborder
<i>Achomosphaera ramulifera</i>	5	5	9	Gonyaulacales	Gonyaulacineae
<i>Canningia reticulata</i>	2	13	22	Gonyaulacales	Gonyaulacineae
<i>Chlamydophorella discreta</i>	5	5	9	Gonyaulacales	Uncertain
<i>Circulodinium distinctum</i>	5	6	17	Gonyaulacales	Gonyaulacineae
<i>Cometodinium whitei</i>	6	8	28	Gonyaulacales	Gonyaulacineae
<i>Cribooperidinium? edwardsii</i>	5	8	20	Gonyaulacales	Gonyaulacineae
<i>Florentinia mantellii</i>	3	6	7	Gonyaulacales	Gonyaulacineae
<i>Florentinia radiculata</i>	3	3	4	Gonyaulacales	Gonyaulacineae
<i>Gardodinium eisenackii</i>	2	7	5	Gonyaulacales	Uncertain
<i>Palaeoperidinium cretaceum</i>	2	19	27	Peridinales	Peridiniineae
<i>Pervosphaeridium cenomaniense</i>	6	7	14	Gonyaulacales	Gonyaulacineae
<i>Protoellipsodinium corollum</i>	7	7	17	Gonyaulacales	Gonyaulacineae
<i>Spiniferites multibrevis</i>	6	6	11	Gonyaulacales	Gonyaulacineae
<i>Tanyosphaeridium variecalamum</i>	3	3	4	Gonyaulacales	Uncertain
<i>Tenua hystrix</i>	3	3	4	Gonyaulacales	Gonyaulacineae

Q mode – Samples clustering (Fig. 2.19)

Cluster SC2-398D groups 7 samples from the lower part of the core (from 1277.2 mbsf to 1185.86 mbsf, 1145 mbsf and 1089.86 mbsf), mostly from black shales where siderite nodules are common (Fig. 2.4).

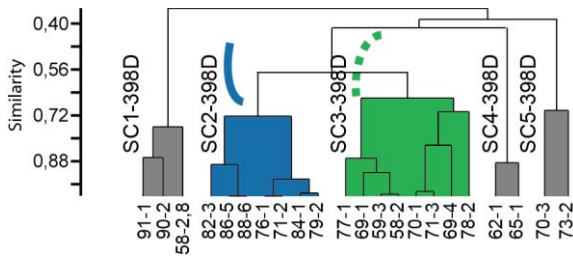


Figure 2.19. UPGMA Q-mode cluster from Hole 398D data, using Raup-Crick coefficient as similarity measure. Clustered samples share similar taxon assemblages.

The third cluster of samples SC3-398D groups 8 samples from the upper half of the core (from 1175.48 mbsf to 996.85 mbsf). All samples but two (1175.48 and 1165.2 mbsf), are dated as Upper Albian. The corresponding sedimentary facies are mixed marly chalk – shales (Fig. 2.4).

4.4.2. Correspondence Analysis.

The correspondence analysis of the 398D core samples illustrates 21.9% of the total variation on the two first axes. Despite the similar level variation explained to the CA made of the whole dataset and of the data from the Lusitanian sections alone, the interpretation of dispersion patterns remains difficult.

As revealed by the pairwise NPMANOVA analysis of clusters, the scatter diagram resulting from the correspondence analysis points out that there is not a good fit between the clusters of taxa and samples (Fig. 2.21).

However, when only considering clusters supported by the pairwise NPMANOVA (TC3-398D, TC4-398D and TC6-398D; SC2-398D and SC3-398D), then the link between clusters and lithology emerges (Fig. 2.22). Taxa included in TC3-398D plot near to samples from SC3-398D, mainly described as mixed marly levels.

TC4-398D taxa plot in the intersection zone between the ellipses delimiting the

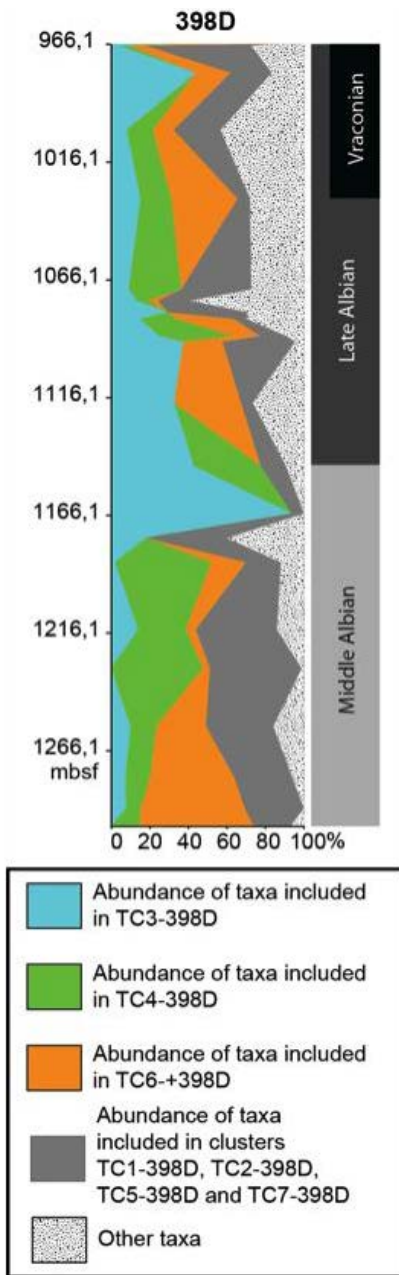


Figure 2.20. Taxa clusters abundance distribution along the 398D site. Black smoky areas represent the relative abundance of all the taxa no taken into account for the analysis

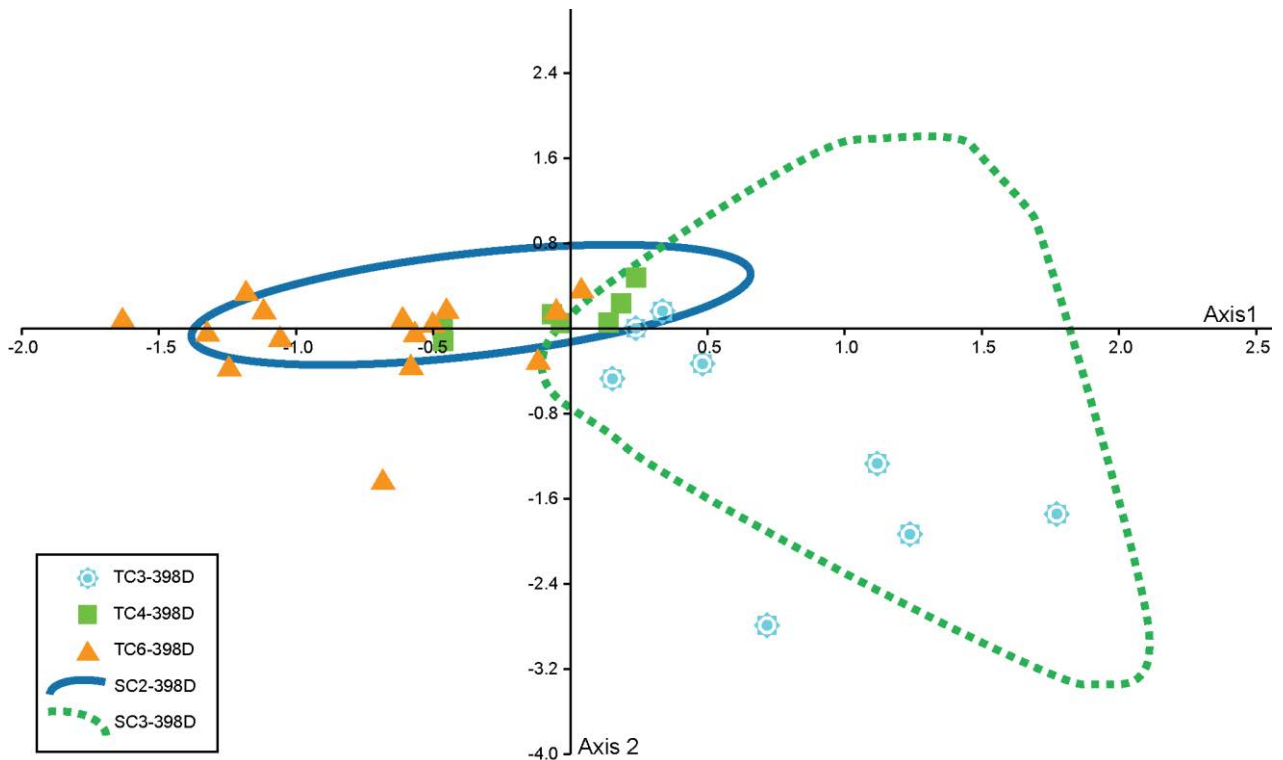


Figure 2.21. Scatter diagram of Correspondence analysis from 398D site data and cluster analysis. The ellipses outline the distribution of samples included in the cluster specified in the legend.

distribution of SC2-398D (mainly black-shales) and SC3-398D (mainly mixed marly chalk – shales) samples. Cluster of taxa TC6-398D was related to samples included in SC2-398D, mainly characterized as black shales, coming from levels where siderite nodules were common.

5. Interpretation and discussion

5.1 Factors controlling taxa distribution

5.1.1 Proximal - distal trends

The taxon associations of the Lusitanian Basin sections are clearly distinguished from those of the 398D core site by lower values of the diversity estimates and by the taxon associations (Fig. 2.6, Fig. 2.10). In the multivariate analysis of the whole dataset, samples from the Lusitanian Basin all share positive values on the first axis, whereas samples from 398D site have negative values (Fig. 2.11). The proximal character of Lusitanian Basin sections has been evidenced (e.g. Rey, 1979; Dinis *et al.*, 2008; Heimhofer *et al.*, 2012). Fully marine conditions are well known for the succession from the 398D site (e. g. de Graciansky and Chenet, 1979;

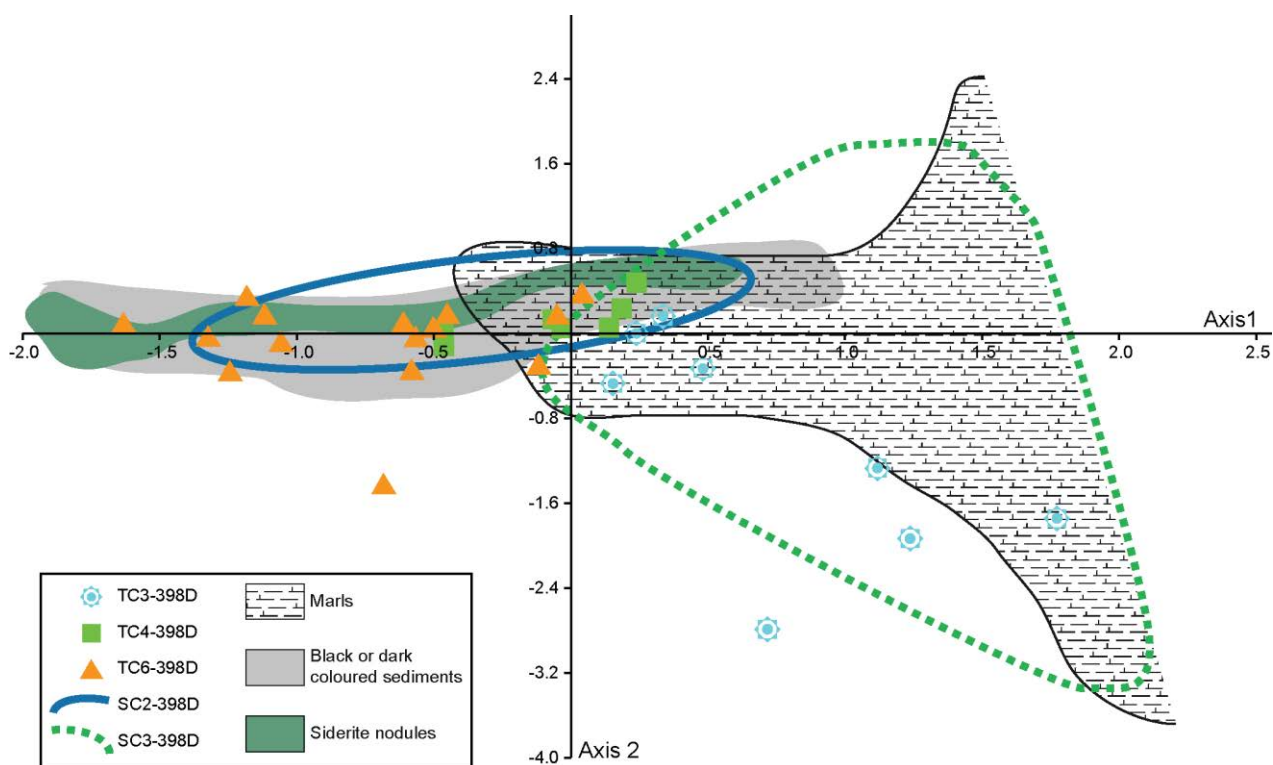


Figure 2.22. Plotting of the clusters of samples from the 398D site together with the main lithological characteristics of samples plotting in the area. Only clusters recognized by the NPMANOVA analysis as being statistically different are represented. Lithological patterns reflect the main characteristics of samples plotting in the area

Sibuet *et al.*, 1979; Meyers and Shaw, 1996). Thus, the first axis of the CA from the whole dataset could be understood as an inshore-offshore gradient.

In the Recent, it is well established that the diversity of dinoflagellate cysts is structured along the inshore to offshore gradient (Wall *et al.*, 1977; Harland, 1983; Marret and Zonneveld, 2003). In itself, the distance to the coast summarize a wide range of environmental variations that constraint the development of species. The prevalence of factors remains unclear, but nutrient availability (nitrate, phosphate), salinity, bottom-water oxygen concentration (Zonneveld *et al.*, 2013), and stability of environmental conditions should be considered.

5.1.2 Environmental stability - predictability

Taxonomic richness and evenness reflect distinct diversity structures between Lusitanian Basin outcrops and the in 398D site. Assemblages of 398D site samples are homogeneous in structure and more diverse (high values of taxonomic diversity and evenness, Fig. 2.5) whereas assemblages from Lusitanian Basin sections were more heterogeneous in structure and less diverse (in general terms, values of taxonomic diversity and evenness were lower and more variable, Fig. 2.5). This is

consistent with the data structure revealed by cluster analysis. Samples reflecting environmental stability recorded over time (398D site) will show close taxon associations, whereas samples recording unstable environments over time (Lusitanian Basin) will lead to more varied assemblages. So, taxa and samples from stable environments will group in weak clusters (see section 4.4.1), but those from unstable environments will group in robust clusters (see section 4.3.1.). The 398D site recorded relatively stable open marine environments and that of Lusitanian Basin outcrops recorded nearshore unstable to neritic environments. The increasing stability gradient from the Lusitanian Basin outcrops to the 398D site can also be interpreted as increasing distance to the shoreline.

As dinocysts diversity strongly depends on the stress in the ecosystems and stress is often related to relative shoreline proximity, Sluijs *et al.* (2005) already proposed that the relative dinocyst diversity should also be indicative of position along an inshore offshore transect. A study of Early Oligocene assemblages from the Upper Rhine Graben revealed that dinocyst diversity and equitability increase with distance from the shoreline (Pross and Schmiedl, 2002). The analysis of dinocysts diversity in three Cenomanian – Turonian sections from the Castilian Platform revealed increasing diversity from inner to outer neritic settings (Peyrot *et al.*, 2011). Harris and Tocher (2003) also found the same pattern when analyzing the diversity gradient within different sections of the Late Cretaceous from the Western Interior Basin.

5.1.3 Imprints of heterogeneous coastal environments on dinocyst

As seen in section 5.1.1. the inshore – offshore gradient was the main factor controlling the dinocyst distribution in the Iberian margin during the Albian. The first axis of the CA from the whole dataset is identified as representing the inshore – offshore gradient, with proximal conditions represented on positive values of the axis and distal conditions on negative values.

The mapping of the lithological data on the scattergram of the CA from the whole data set, suggest that the second axis of the multivariate analysis may reflect the magnitude of continental siliciclastic inputs (Fig. 2.12). As seen in section 4.2.1, the cluster analysis of the whole dataset identifies two clusters of samples; SC1-LB+398D grouping all the information from Lusitanian Basin sections, and SC2-LB+398D exclusively composed of samples from the 398D site. The cluster analysis of the Lusitanian Basin alone allows refinement on the analysis of assemblages from

proximal settings (Fig. 2.14, 2.17). When plotting the clusters of samples from the Lusitanian Basin alone on the scatter diagram of the correspondence analysis of the whole data set, the three clusters of samples identified are segregated along the second axis. Samples in SC1-LB are associated to negative values, SC2-LB samples plot around the central values and samples in SC3-LB fall mainly within positive values (Fig. 2.23).

The relay of dominating clusters during the Albian in the analyzed sections of the Lusitanian Basin, from cluster SC1-LB to SC3-LB (see description of Q-mode clusters in section 4.3.1), reflects the evolution of paleoenvironments during the long-term eurybatic sea-level rise (Haq, 2014). The eurybatic rise during the Albian shifted the Lusitanian Basin shoreline westward and modified the hydrological and sedimentological regimes (Dinis *et al.*, 2008). Nearshore Albian deposits of the Galé Formation are linked with siliciclastics on the northeast, representing large fluvial systems draining to SW. Whereas, during the Cenomanian a large carbonate platform extended far inland (Dinis *et al.*, 2008). The effects of sea-level variations are more noteworthy on coastal areas. Thus the higher dispersion of Lusitanian Basin data along the second axis reflect the higher magnitude of environmental changes associated to the sea-level variations in proximal settings, Lusitanian Basin, than in distal settings, 398D site.

The distribution of cysts on the scattergram of the CA from the whole dataset analysis and their relationship with the different lithologies reveal further evidences of the signature of coastal conditions. Taxa plotting on the lower right quadrant and recognized as cluster TC1-LB+398D are characterized by the highest ratio of peridiniacean taxa (Table 2.1, Fig. 2.11, Appendix B.2 to 7). High proportions of peridiniacean taxa as *Palaeoperidinium cretaceum* and *Ovoidinium* sp. could be understood as evidence of enhanced nutrient supply, their peaks reflecting peaks of primary production. Modern high productivity areas are usually characterized by the dominance of heterotrophic dinocysts as *Protoperidinium* (e.g. Lewis *et al.*, 1990; Hamel *et al.*, 2002; Radi and de Vernal, 2004). All modern peridinioids are not heterotrophic (e.g. Dale and Fjellså, 1994), so the assumption of a complete equivalence between the terms “peridinioid” and “heterotrophic” is a simplification that may be misleading in some cases (Sluijs *et al.*, 2005). However, peridinioid cysts still represent the closest approximation to heterotrophic dinoflagellates and their

abundance can be considered indicative of palaeoproductivity (Sluijs *et al.*, 2005; Prauss, 2012b).

The clear relationship between the taxa included in TC1-LB+398D and sandy facies suggest that another environmental control may acted on the distribution of dinocyst along the studied series. The preservation of organic matter into a sediment, and thus of dinocysts, is affected by the oxygen concentration in bottom and pore waters of the sediments, the sedimentation rate and the sediments permeability. The aerobic decay of organic matter is especially important in areas characterized by oxygen-rich bottom waters, low sedimentation rates (preventing rapid burial) and / or highly permeable sediments. The best conditions for preservation of dinocysts occur in oxygen-depleted muds and the worse conditions are found in sandy levels associated to riverine inputs. Previous studies on dinocysts preservation as function of oxidative processes have already show that some taxa are more sensitive than other to oxygen-related decay, and thus that the preservation of biodiversity structure can be affected (Dodsworth, 2000; Versteegh and Zonneveld, 2002; Zonneveld *et al.*, 2008).

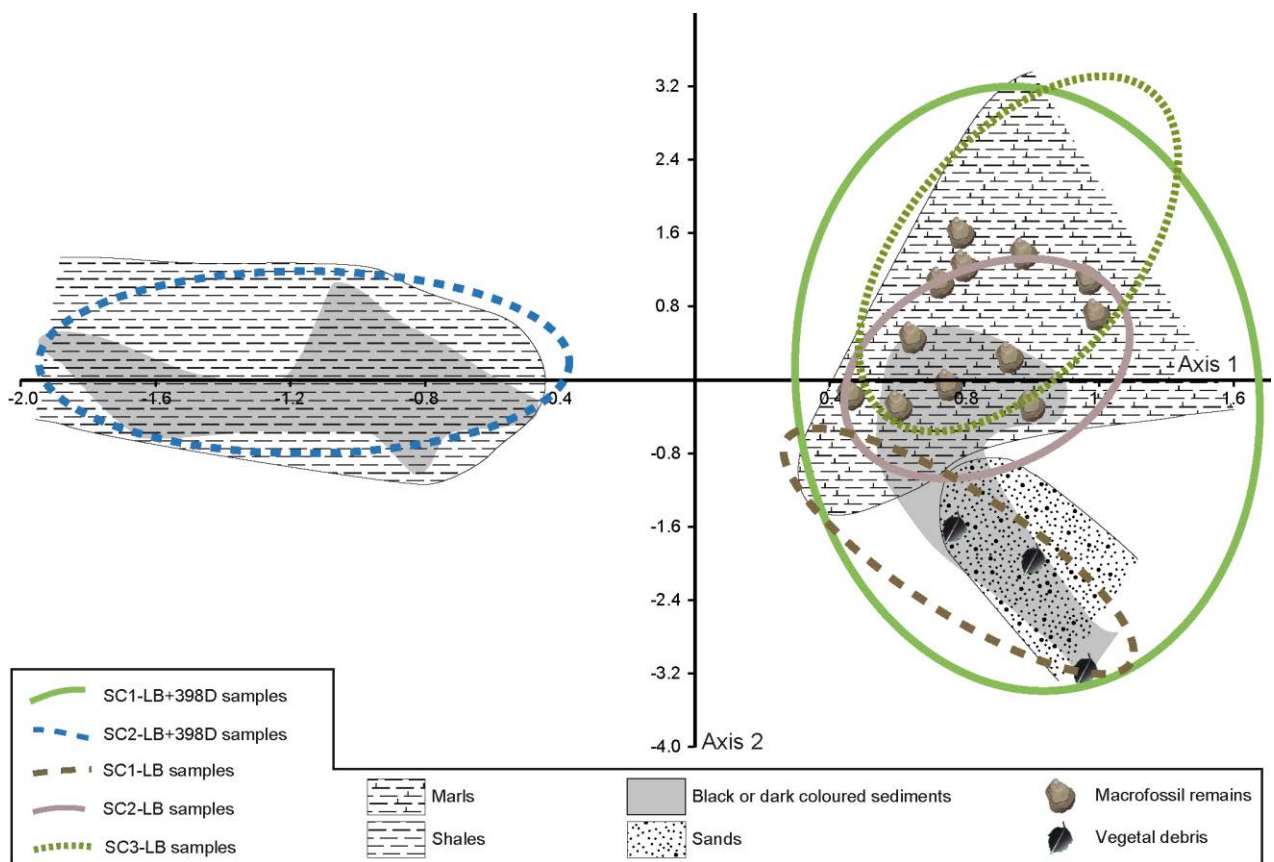


Figure 2.23. Plotting the clusters of samples from the analysis of the whole dataset (SC1-LB+398D and SC2-LB+398D) together with those from the Lusitanian Basin alone (SC1-LB, SC2-LB and SC3-LB) in the CA scattergram from the whole dataset. Ellipses outline the distribution of samples included in the clusters. Lithological patterns reflect the main characteristics of samples plotting in the area.

Dodsworth (1995) shown that in some cases, a higher proportion of fossil peridiniacean taxa was the result of selective aerobic degradation of gonyaulacacean taxa. The distribution of peridinioid taxa on the cluster analysis and in the scattergram of the CA from the whole dataset analysis may result from both high nutrient availability and oxygen related decay.

The second axis of the correspondence analysis of the whole dataset (Fig. 2.11, 2.12 and 2.23) likely reflects a complex combination of salinity, nutrients variations and taphonomic bias due to oxidation, rather than a linear variation of siliciclastic continental influx.

5.2 Paleoenvironmental significance of taxon associations

Although not representing the entire planktonic community, the assemblages of fossil dinocysts are excellent source of paleoenvironmental conditions (Goodman, 1987). However, the interpretation of the occurrence of a given taxon, and / or relative abundance of dinocyst forms in a sample is not straightforward (Pearce *et al.*, 2003). High dominance of one form can be the result of either favorable or stressful conditions or the consequences of selective taphonomic processes. Nevertheless, it is possible to identify some taxa indicative of a specific environment and some other taxa showing higher relative abundances in one environment and occasional occurrences in others. The degree of species tolerance to environmental conditions and the recognition of empirical clusters of species assemblages can become relevant indicators of salinity, nutrients, pH or oxygen availability in the sediment water interface and in the upper part of the sediments.

5.2.1. Nearshore instable environments and associations

Within the range of paleoenvironments recorded on the studied sections, nearshore environments influenced by riverine inputs, recorded in the Lusitanian Basin sections, were the most variable and stressful. The analysis of the Lusitanian Basin data allows the identification of two clusters of taxa indicating clearly proximal instable environments, those are the cluster TC1-LB+398D (from the analysis of the whole Albian dataset, Fig. 2.8) and the cluster TC1-LB (from the analysis of the Lusitanian Basin data alone, Fig. 2.13).

The cluster TC1-LB+398D includes four taxa occurring exclusively in Lusitanian Basin samples (*Florentinia cooksoniae*, *Kiokansium* sp., *Ovoidinium* sp. and

Surculosphaeridium sp.) and five taxa occurring both in Lusitanian Basin and 398D sites samples (*Circulodinium distinctum*, *Cribroperidinium? edwardsii*, *Gardodinium eisenackii*, *Palaeoperidinium cretaceum* and *Trichodinium castaneum*). Species included in TC1-LB+398D dominated assemblages at the base of Lusitanian Basin sections and presented low relative abundances in the 398D site (Fig. 2.10).

Heimhofer *et al.* (2012) analyze the evolution of vegetation patterns and climate, from the palynological and clay mineral assemblages at Guincho section. They associate the fluctuations in terrestrial plant communities to variations in the regional moisture availability, which may be related to variations in riverine discharge. The dinocysts association of the cluster TC1-LB+398D occurs at Guincho at levels recognized as recording humid climates by Heimhofer *et al.* (2012). The detailed stratigraphical study of São Julião section by Horikx *et al.* (2014) made it possible to correlate accurately this section to Guincho and to map on it the climatic trends of Heimhofer *et al.* (2012). At São Julião, the association of the cluster TC1-LB+398D also occurs with humid conditions on the emerged lands.

The study of the sedimentary organic matter, palynofacies and pyrolysis analysis on the 398D site samples (de Graciansky *et al.*, 1978; Deroo *et al.*, 1979; Habib, 1979) reveals that organic matter of continental origin accumulates mainly in the lower part of the section. The general variation pattern of the cluster TC1-LB+398D abundance along the 398D cores shows a gradual decrease from the base to the top of the studied interval (Fig. 2.20). This pattern does not correlate with any of the continental influx index from the 398D site. Therefore, the occasional presence of taxa from the TC1-LB+398D cluster in the 398D site should reflect local ecological conditions, but no transport or reworking from the inshore. The most likely explanation for the ecological significance of the cluster TC1-LB+398D is the environmental variability triggered by occasional input of fresh water and terrestrial material.

The most representative taxa of TC1-LB are *Trichodinium castaneum*, *Cribroperidinium? edwardsii*, *Circulodinium distinctum*, *Palaeoperidinium cretaceum*, and *Spiniferites ramosus* (see section 4.3.1 and Table 2.4 for more details). Species of the cluster TC1-LB occur more often in the lower part of the series (Fig. 2.15). They dominated the assemblages during the Middle Albian and became less important through the Late Albian. The general trend of TC1-LB abundance at Guincho is similar to that of kaolinite content, and at São Julião it covaries with the regional humidity

(Heimhofer *et al.*, 2012; Horikx *et al.*, 2014). The occurrence of taxa from the TC1-LB cluster is influenced by riverine run off and the input of continental organic matter (Fig. 2.17).

We consider that high abundances of *Trichodinium castaneum*, *Cribroperidinium? edwardsii*, *Circulodinium distinctum*, *Palaeoperidinium cretaceum* and *Gardodinium eisenackii*, of TC1-LB+398D and TC1-LB clusters in assemblages can be interpreted as indicating highly unstable conditions, in which only the most tolerant taxa were able to proliferate or to be preserved. These taxa are not restricted to marginal environments, but they are encountered in varied conditions, including the deep settings of the 398D core samples. Because they can occur in many paleoenvironmental conditions, we consider them as the most tolerant to a wide range of environmental conditions. Since these species dominate samples taken from sandy levels we also consider them the less vulnerable to oxygen-related decay and so, to have a high preservation potential. Other taxa present in the nearshore assemblages were *Kiokansium* sp., *Ovoidinium* sp., and *Surculosphaeridium* sp. but, since the only data concerning these taxa were given in (Hasenboehler, 1981), it is not possible to make reliable comparisons.

Previous paleoecological interpretations of *T. castaneum*, *P. cretaceum* and *C. distinctum* as well as taxa from *Cribroperidinium* genus vary widely among studies. *T. castaneum* has been described as characteristic of fluvial to shallow marine environments (Helenes and Somoza, 1999), as dominant in outer environments (Peyrot *et al.*, 2011) or even as not showing environmental preference (Harris and Tocher, 2003). *P. cretaceum* was listed as euryhaline indicator, despite widespread occurrences by Harris and Tocher (2003). The same authors (Harris and Tocher, 2003) suggested that *C. distinctum* may be more indicative of increases in water depth or salinity whereas, Wilpshaar and Leereveld (1994) considered the genus *Circulodinium* as characteristic of inner neritic and restricted marine environments. The genus *Cribroperidinium* is described as characteristic of inner neritic environments by some authors (Peyrot *et al.*, 2011 and references therein), but as tolerant to different environments by others (Lebedeva, 2010). The inconsistencies on paleoenvironmental preferences suggested by previous authors reveal the high tolerance of these species to environmental conditions.

5.2.2. Neritic environments and associations

All the dinocyst taxa found in levels recognized as representing inner/middle neritic paleoenvironments were grouped in clusters TC2-LB+398D, TC2-LB and TC3-LB. Among taxa included in these clusters two main patterns were identified in function of their geographical distribution. Some taxa were restricted to the Lusitanian Basin sections, whereas others were present in both the Lusitanian Basin sections and in the 398D site.

The species restricted to the Lusitanian Basin sections were: *Callaiosphaeridium asymmetricum*, *Carpodinium granulatum*, *Microdinium opacum*, *Oligosphaeridium pulcherrimum* and *Oligosphaeridium totum*. Their distribution in the multivariate analysis matches the distribution of mixed carbonate/siliciclastic deposits. Calcareous marls rich in microfossils (Rey, 1979, 1992) are recognized as typical of inner/middle neritic settings (Figs. 2.16 and 2.17). Because there is no direct evidence of riverine influx (sandy levels bearing plant remains), the conditions could be considered mesotrophic and stenohaline.

Inner to middle neritic preferences have also been alluded for *Microdinium* genus (Lebedeva, 2010), in particular for *M. opacum* (Lister and Batten, 1988), and *O. pulcherrimum* (Lister and Batten, 1988; Helenes and Somoza, 1999; Harris and Tocher, 2003). (Harris and Tocher, 2003) described *O. totum* as being more abundant in environments with stable salinities but occurring in all the studied sites.

The taxa with a widespread distribution that occur in the mid neritic environments of the Lusitanian Basin but also in the deeper settings represented in the 398D DSDP cores are: *Cyclonephelium compactum*, *Cyclonephelium vannophorum*, *Dinopterygium cladoides*, *Odontochitina ancala/O. rhakodes*, *Oligosphaeridium albertense* and *Protoellipsodinium corollum*. All these taxa were more abundant in the Late Albian from the Lusitanian Basin, interpreted as representing inner-middle neritic conditions, but they were also present during the whole Middle and Late Albian and in all studied sections. Considering their widespread distribution, and their peak of abundance in the inner/middle neritic environments, they must be tolerant to some variations in salinity and nutrient availability.

Large tolerances to environmental parameters variations are described in the bibliography for *C. vannophorum* (Lister and Batten, 1988; Helenes and Somoza,

1999; Harris and Tocher, 2003) and *C. compactum* (Harris and Tocher, 2003), although the environmental parameters controlling their distributions are not yet identified. Helenes and Somoza (1999) also considered *D. cladoides* as preferring middle neritic environments and noted that it was able to reach outer neritic depths. *Odontochitina ancala* and *O. rhakodes*, were both described from the Albian Kiowa formation, by (Bint, 1986), which represents neritic environments (Scott, 1970).

Cluster of taxa TC2-LB+398D dominates Lusitanian Basin assemblages during Late Albian and it is present with low relative abundances in the 398D site (Fig. 2.10). Variations of TC2-LB+398D relative abundance do not show a clear correlation with the palynological or clay mineral assemblages in Guincho section, or with the organic matter or palynofacies in the 398D site. Contribution of TC2-LB+398D in the 398D site samples rarely exceeds 15% (Fig. 2.10).

The cluster TC2-LB+398D association indicates inner/middle neritic environments. If associated to high abundances of *Callaiosphaeridium asymmetricum*, *Carpodinium granulatum*, *Microdinium opacum*, *Oligosphaeridium pulcherrimum* and *Oligosphaeridium totum* mesotrophic conditions can be suggested. On the other hand, if high representation of TC2-LB+398D is associated to high abundances of *Cyclonephelium compactum*, *Cyclonephelium vannophorum*, *Dinopterygium cladoides*, *Odontochitina ancala/O. rhakodes*, *Oligosphaeridium albertense* and *Protoellipsodinium corollum* more instable conditions are suggested, instability being related to salinity and nutrients availability.

Abundance pattern of taxa grouped in TC2-LB was variable within the Lusitanian Basin sections (Fig. 2.15). On the CA scatter diagram of Lusitanian Basin alone, TC2-LB taxa plot around limestones and marls, but they also show a slight relationship with dark colored and abundance of microfossil remains (Fig. 2.16, 2.17). Relative frequency of TC2-LB in Guincho does not correlate to changes in kaolinite content, but shows a general trend similar to that of mica content (Heimhofer *et al.*, 2012). Most of the taxa contributing with high relative abundances to TC2-LB representation (*Odontochitina ancala/O. rhakodes*, *C. vannophorum*, and *O. albertense*, Table 2.5) are characterized as preferring inner/middle neritic habitats and being tolerant to variations of environmental factors. Thus we interpret TC2-LB as characteristic of slightly variable inner/middle neritic environments.

Species of the cluster TC3-LB are more abundant in the Late Albian of the São Julião, Magoito Aguda and Ponta do Sal sections (Fig. 2.15), whereas they are of secondary importance at Guincho and Baforeira Rana. Abundance of TC3-LB in Guincho does not correlate to changes in any of the clay minerals studied by Heimhofer *et al.* (2012). Most of the taxa in TC3-LB can be interpreted as preferring mesotrophic inner/middle neritic environments (*C. asymmetricum*, *C. granulatum*, *O. pulcherrimum* and *O. totum*). However, the main contributors to TC3-LB are *Chichaouadinium vestitum*, interpreted as cosmopolitan preferring meso- to eutrophic conditions (see discussion in section 5.2.3), and *C. compactum* and *P. corollum*, characterized as preferring inner/middle neritic habitats and being tolerant to variations. We consider high abundances of TC3-LB as indicative of inner/middle neritic conditions, stable mesotrophic conditions are suggested when *C. asymmetricum*, *C. granulatum*, *O. pulcherrimum* and *O. totum* are present.

5.2.3. Open marine distal environments and associations

The cluster TC3-LB+398D includes 23 taxa occurring exclusively in 398D site samples (*Achomosphaera ramulifera*, *Apteodinium deflandrei*, *Caligodinium aceras*, *Canningia reticulata*, *Cassiculosphaeridia reticulata*, *Damassadinium chibane*, *Dapsilidinium laminaspinosum*, *Florentinia mantellii*, *Florentinia radiculata*, *Hystriodinium pulchrum*, *Impagidinium verrucosum*, *Kallosphaeridium? ringnesiorum*, *Kleithriasphaeridium tubulosum*, *Litosphaeridium conispinum*, *Oligosphaeridium complex*, *Pervosphaeridium cenomaniense*, *Pseudoceratium eisenackii*, *Pterodinium cingulatum*, *Sepispinula? huguoniotii*, *Spiniferites ramosus* subsp. *granosus*, *Tanyosphaeridium variecalamum*, *Tenua hystrix* and *Wrevittia cassidata*) and 8 taxa present in both the Lusitanian Basin and the 398D site (*Chlamydothorella? discreta*, *Circulodinium colliveri*, *Cometodinium withei*, *Coronifera oceanica*, *Exochosphaeridium phragmites*, *Odontochitina operculata*, *Spiniferites ramosus*, and *Spiniferites multibrevis*).

Within the taxa included in the cluster TC3-LB+398D some were more common and abundant in the 398D hole than in the Lusitanian Basin sections: *Chlamydothorella discreta*, *Circulodinium colliveri*, *Cometodinium whitei*, *Exochosphaeridium phragmites* and *Odontochitina operculata*. Occurrences of these species in the Lusitanian Basin were occasional and rarely exceeded the 2% of relative abundance, whereas they occurred in almost the entire 398D hole where they

represents usually about 10% of the assemblages (peaking sometimes up to 20%). Their distribution patterns observed in our study suggest that these taxa prefer stable outer neritic environments but tolerate some fluctuations of environmental conditions.

This interpretation is compatible with suggestions made from other studies on fossil dinocysts. When analyzing dinocyst distribution along a proximal – distal transect, Harris and Tocher (2003), observed that *E. phragmites*, *C. colliveri* and *C. discreta* were present along the whole transect. Harris and Tocher (2003) considered *E. phragmites* and *C. colliveri* as euryhaline indicators and *C. discreta* as offshore indicator. Other authors proposed the genus *Exochosphaeridium* and *Circulodinium* to be indicative of marginal marine environments (Wilpshaar and Leereveld, 1994; Lebedeva, 2010). Smelror and Leereveld (1989) considered *C. discreta* as being representative of outer neritic – oceanic environments. The genus *Odontochitina*, and *O. operculata* in particular, was assumed as eurybiontic or cosmopolitan taxon (Pearce *et al.*, 2009; Lebedeva, 2010), as indicative of eutrophic environments (Coccioni *et al.*, 1993) or as marker of open marine environments (Marshall and Batten, 1988). Helenes and Somoza (1999) interpreted *O. operculata* and *C. whitei* as preferring mainly middle neritic environments with occasional shifts to outer neritic.

Spiniferites ramosus, *Spiniferites multibrevis* and *Chichaouadinium vestitum* are other taxa common in both the Lusitanian sections and the 398D cores, occurring in a wide range of environmental conditions. *S. ramosus* and *S. multibrevis* have a relatively continuous record in the 398D core and in the Lusitanian Basin sections, where they are more abundant in the Late Albian levels, especially at Guincho. Our data match the interpretation of *S. ramosus* as ubiquitous taxon. Even if it is less common, *S. multibrevis* shows a distribution is similar to that of *S. ramosus*. Thus, a similar ecology can be assumed for the two species. In the literature, *S. ramosus* has received different paleoecological interpretations. Some authors consider *S. ramosus* an ubiquitous form associated to stable marine environments (e.g. Pross and Schmiedl, 2002; Prince *et al.*, 2008), others note that *S. ramosus* is often associated with high-productivity, peridinioid-dominated assemblages from upwelling areas (Harris and Tocher, 2003) and others found it more abundant in inner than in outer carbonated platform environments (Peyrot *et al.*, 2011). The diverse abundance patterns of *S. ramosus* and *S. multibrevis* noticed by other authors fits with our interpretation of these species as ubiquitous.

Within the whole dataset here analyzed, *Chichaouadinium vestitum* occurs in many samples from shallow to deep environments, often as a dominant taxon, exceeding 70% of the identified cysts in some samples. *C. vestitum* shows high variations of abundance, with higher and more frequent peaks in the Lusitanian Basin than in the 398D cores. As previously referenced, peridinioid taxa as *C. vestitum*, are assumed as analogs of modern heterotrophs dominating in areas rich in nutrients. We consider *C. vestitum* a cosmopolitan taxon under mesotrophic to eutrophic conditions. Its distribution was positively correlated to the nutrient availability but independent to variations of other parameters associated to the distance from the shoreline.

Impagidinium verrucosum and *Pterodinium cingulatum* are within the taxa occurring exclusively in the 398D site. Other taxa characteristic of 398D site assemblages share similar distribution patterns with *I. verrucosum* and *P. cingulatum*: *Achomosphaera ramulifera*, *Cassiculosphaeridia reticulata*, *Dapsilidinium laminaspinosum*, *Hystrichodinium pulchrum*, *Kallosphaeridium? ringnesiorum*, *Kleithrisphaeridium tubulosum* and *Oligosphaeridium comple.g.* Because their pattern of occurrence and relative abundance are consistent among studies, species from the genus *Impagidinium* and *Pterodinium* are demonstrated as indicative of oceanic conditions (e.g. Wall *et al.*, 1977; Marshall and Batten, 1988; Smelror and Leereveld, 1989; Dale, 1996; Prince *et al.*, 1999, 2008; Harris and Tocher, 2003; Crouch and Brinkhuis, 2005). The joint occurrence of the group (*A. ramulifera*, *Cassiculosphaeridia reticulata*, *D. laminaspinosum*, *H. pulchrum*, *K.? ringnesiorum*, *K. tubulosum* and *O. complex*) in the assemblages together with *I. verrucosum* and *P. cingulatum* is here considered to also reflect outer neritic conditions.

Similar distribution of these species has been found in several studies on fossil dinocyst distribution. *A. ramulifera*, *H. pulchrum* and *D. laminaspinosum* occurred in the Western Interior Basin during the Upper Cretaceous, where they are considered indicators of offshore conditions (Harris and Tocher, 2003), even if not restricted to distal environments. *A. ramulifera*, *H. pulchrum* and *D. laminaspinosum* also occur in the open marine facies of the Upper Cretaceous English Chalk (Prince *et al.*, 1999, 2008). Among other taxa, Marshall and Batten (1988) included *P. cingulatum* and *H. pulchrum* in a deep settings “*Spiniferites* association” for the Cenomanian and Turonian of Lower Saxony. In the data of Marshall and Batten (1988), it appears that

A. ramulifera, *K.? ringnesiorum*, *D. laminaspinosum* and *O. complex* also occur in levels dominated by the “*Spiniferites* association”. Helenes and Somoza (1999) found that the distribution of *K.? ringnesiorum* in Cretaceous sediments from eastern Venezuela is mainly associated to middle and outer neritic paleoenvironments.

Presence of *Apteodinium deflandrei*, *Damassadinium chibane*, *Canningia reticulata*, *Lithosphaeridium conispinum*, *Pervosphaeridium cenomaniense* and *Spiniferites ramosus* subsp. *granosus* was also restricted to the 398D site but their abundance distribution pattern was different to that showed by *I. verrucosum* and *P. cingulatum*. In fact, *A. deflandrei* and *D. chibane* showed higher relative abundances in the carbonate depleted black shale levels. Whereas, *Canningia reticulata*, *L. conispinum*, *P. cenomaniense* and *S. ramosus* subsp. *granosus* were more abundant in mixed marl – chalky levels. It seems that the same factor/s triggered the lithological change and the dinocyst assemblage composition, but more information is required.

In the multivariate analyses, TC3-LB+398D departs from all shallow marine assemblages. Taxa included in TC3-LB+398D dominated assemblages in the 398D hole and showed low abundances in the Lusitanian Basin sections (Fig. 2.10). The relative abundance of species included in TC3-LB+398D is lower in the part of the São Julião interpreted as humid, than in the part interpreted as arid. General variation pattern of TC3-LB+398D abundance in Guincho does not show a clear correlation with palynological or clay mineral assemblages described by Heimhofer *et al.* (2012). In the 398D site, TC3-LB+398D abundance does not show a pattern correlatable to changes in organic matter or palynofacies (de Graciansky and Chenet, 1979; Deroo *et al.*, 1979; Habib, 1979). Thus, high abundances of TC3-LB+398D are understood as representing open marine, stable outer neritic environments, without coastal influence.

Clusters derived from the analysis of the 398D core samples suggest that some refinements are possible in paleoenvironmental interpretation. *Circulodinium colliveri*, *Hystrichodinium pulchrum* and *Kleithriasphaeridium tubulosum* are the main contributors to TC4-398D abundance. *C. colliveri* prefers stable outer neritic environments although it is tolerant to some variations of environmental parameters. *H. pulchrum* and *K. tubulosum* are typical of outer neritic conditions. This cluster also includes *A. deflandrei*, that it is more abundant in the mixed marly – chalk levels deposited under pelagic conditions (Sigal, 1979). We consider that among all the

significant cluster of taxa from 398D site data TC4-398D represents the strongest open marine signal.

TC6-398D includes among others *Palaeoperidinium cretaceum*, *Circulodinium distinctum* and *Cribooperidinium? edwardsii*, characterized as highly tolerant to environmental variations, and *Protoellipsodinium corollum*, that occurs preferentially in inner/middle neritic conditions. Taxa indicative outer neritic conditions are less common in TC6-398D. Thus, TC6-398D is probably the cluster of taxa that better illustrates the influence of environmental variability at the 398D site.

TC3-398D includes *Cyclonephelium vannophorum*, *Odontochitina operculata*, *Cassiculosphaeridia reticulata* and *Spiniferites ramosus* that tolerate a considerable range of environmental conditions. The strongest contributor to TC3-398D is *S. ramosus*, an ubiquitous species. Among the outer neritic conditions, TC3-398D is supported but open marine species are mixed with more tolerant forms.

5.2.4. Variability of cyst morphology along environmental gradients

It is noteworthy that some species from the same genus, mainly differentiated by the processes length and width and by presence / absence of perforations on their processes, were distributed along the investigated environmental gradients. Morphological variations found within our material can be related to changes in environmental regimes.

Morphological differences between the four species of the genus *Oligosphaeridium* here considered are restricted to variations of the processes morphology and are represented in Fig. 2.24. *O. complex* processes present cylindrical bases and stems, and slightly funnel-shaped distal extremities bearing spines. Processes of *O. irregulare* are flared from their bases and distal extremities present recurved spines. *O. pulcherrimum* processes consists on processes with cylindrical

	<i>O. complex</i>	<i>O. pulcherrimum</i>	<i>O. albertense</i>	<i>O. totum</i>
Ornamentation of distal extremities	 distal spines or branches, straight (patulate), orthogonal or recurved	 sharply fenestrated with spinous margins sometimes connected by small trabeculae	 recurved spines	 perforated and slightly denticulated
Stem morphology	Tubiform to tapering	Flared from the upper half	Flared from the base	
Base of the processes	Tubiform to tapering		Flared from the base	

Figure 2.24. Morphological differences between the four species of the genus *Oligosphaeridium* here considered. *Oligosphaeridium* genus cysts are chorate; central body subspherical in shape and subcircular ambitus. The wall is composed of a endophragme and a usually smooth periphragme. The periphragme develops intratabular (one per paraplaque) hollow tubular process. Paracingular processes absent. The arqueopyle is apical type (tA). Operculum free.

bases, flared from their upper half and sharply fenestrated distal extremities bearing spines. *O. totum* processes are shapely flared from their bases and perforated slightly denticulated extremities.

Oligosphaeridium complex is associated to outer neritic environments whereas *O. albertense*, *O. pulcherrimum* and *O. totum* to inner/middle neritic environments (Fig. 2.25). We suggest that reduced processes length and the presence of perforations and fenestrations in distal extremities may represent responses to increasing environmental stress within the four species of the genus *Oligosphaeridium* here considered.

Morphological differences between the three species of the genus *Odontochitina* here considered are represented in Fig. 2.26. Bint (1986) suggested that “*O. ancala* could have developed from *O. operculata* by introduction of the elbow in the

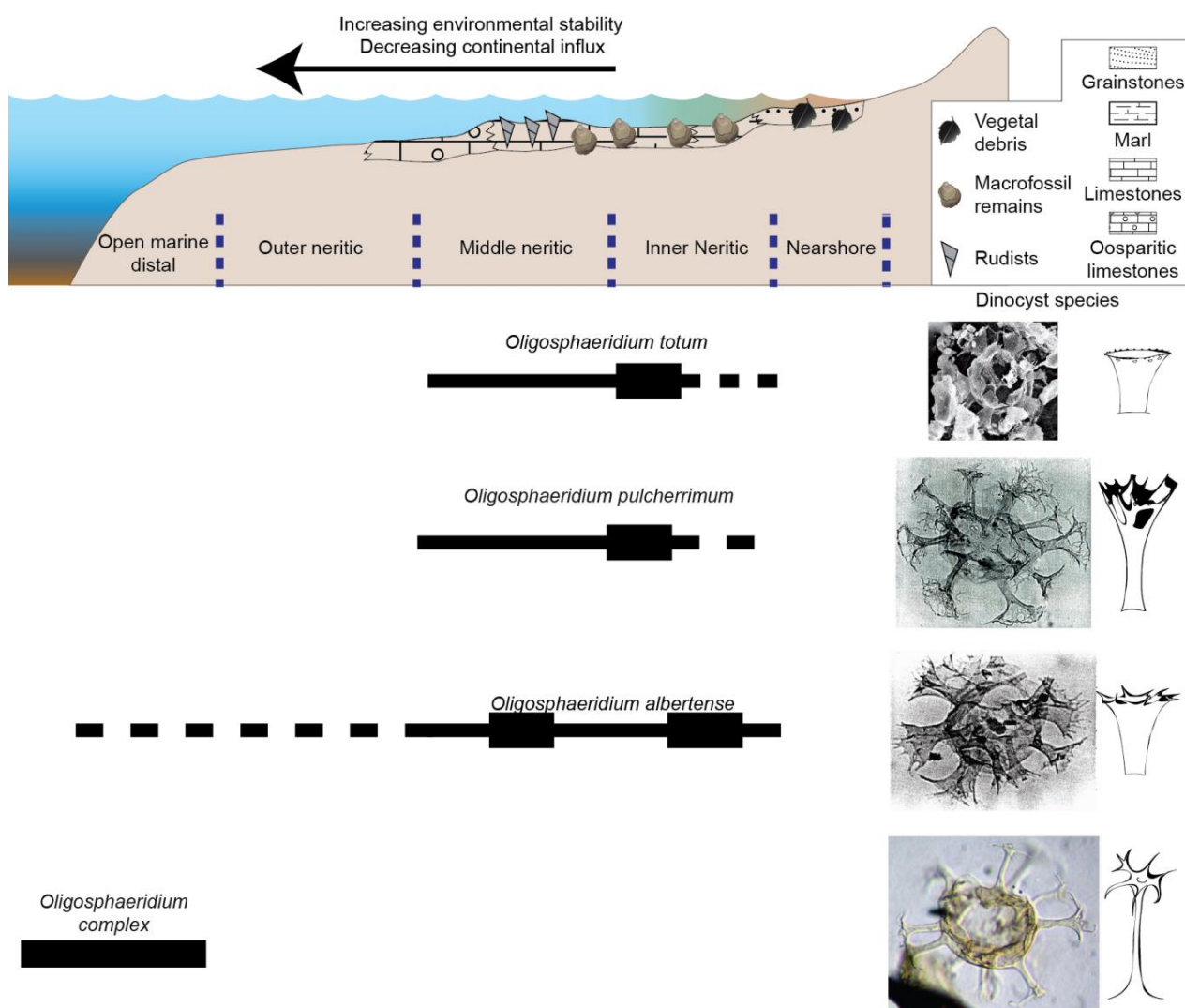


Figure 2.25. Distribution of species from the genus *Oligosphaeridium* along the inshore – offshore studied transect.

lateral horn and progressive development of the localized perforations and antapical pericoel extension” and that “*O. rhakodes* could have developed from *O. ancala* by removal of the distal portions of the horns beyond the localized perforations”. *Odontochitina operculata* is herein identified as associated to outer neritic environments whereas *Odontochitina ancala*/*O. rhakodes* (which includes *O. ancala* and *O. rhakodes*) are associated to inner/middle neritic environments (Fig. 2.27). Here we propose that

	<i>Odontochitina operculata</i>	<i>Odontochitina ancala</i>	<i>Odontochitina rhakodes</i>
Horn profil	Straight	Elbow in the right lateral horn	
Perforations	No	localized about midway along the horns	blunted horns, distally ragged and perforate
Distal extremity	Pointed	constricted immediately beyond their perforate portion	distal portion of the horn absent

Figure 2.26. Morphological differences between the three considered species of the genus *Odontochitina*. Cyst of the *Odontochitina* genus are described as large ceratioid Cornucavate cysts with three prominent horns: one apical, one antapical and one right lateral postcingular. The endocyst may be subspherical or protrude into the base of the horns. Although cavation is usually restricted to the horns, a larger antapical pericoel may be present. Apical archeopyle, type tA.

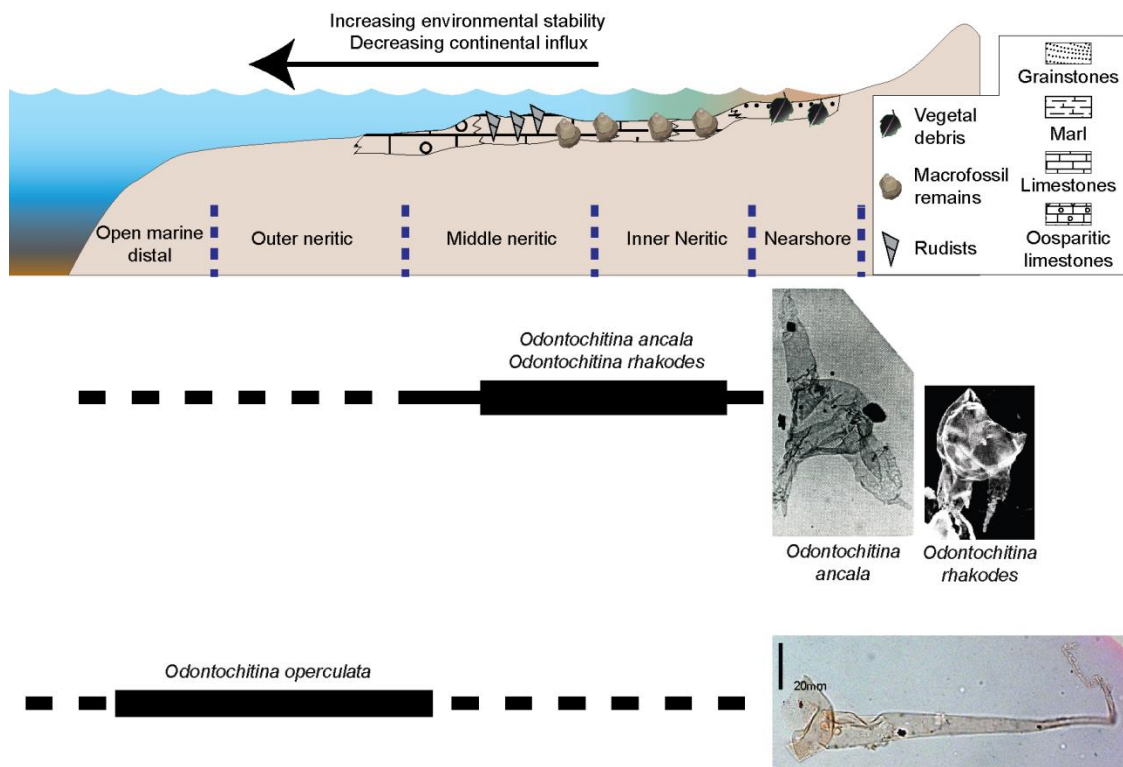


Figure 2.27. Distribution of species from the genus *Odontochitina* along the inshore – offshore studied transect.

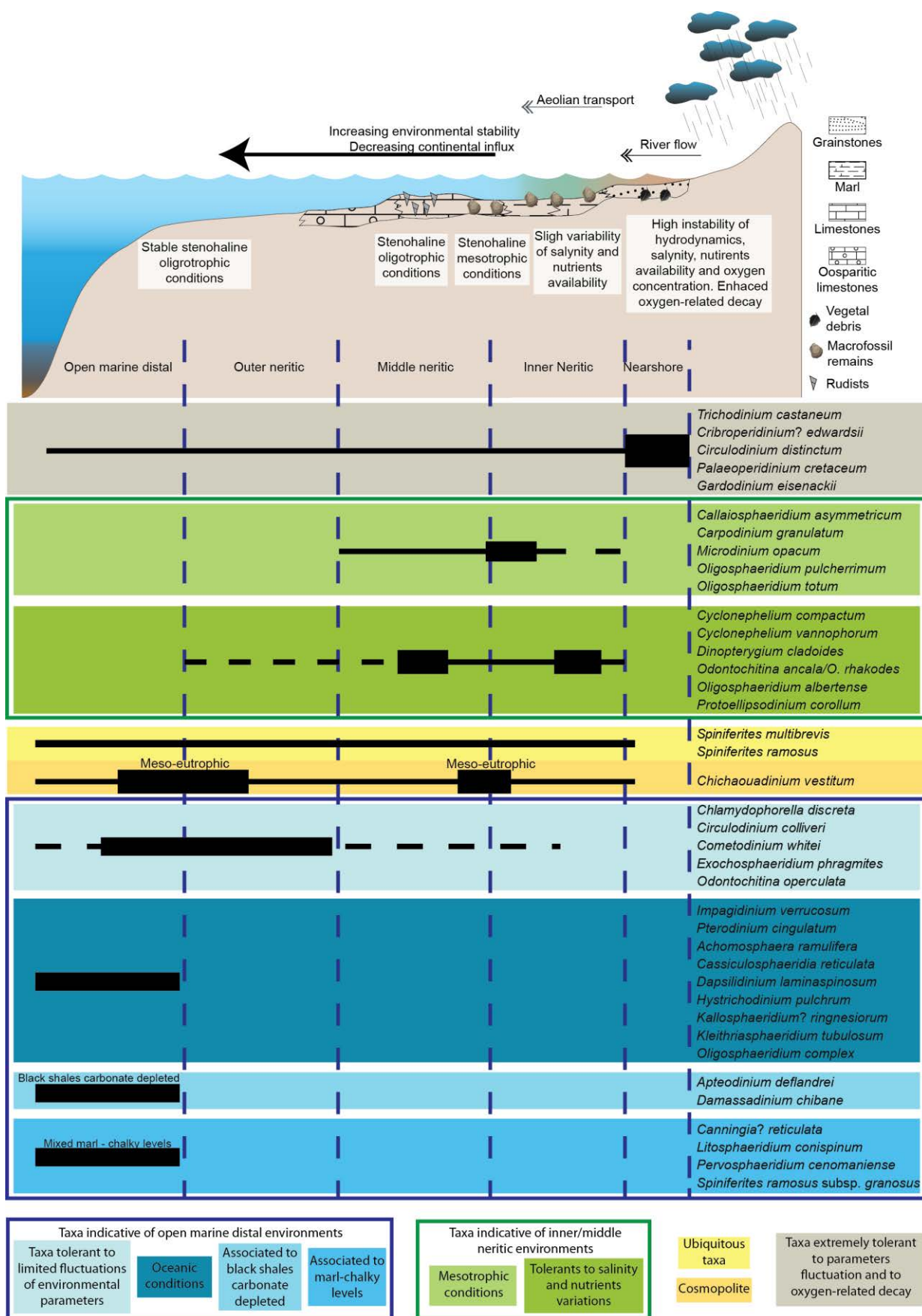


Figure 2.28. Distribution of the dinocyst associations recognized in function of their environmental preferences.

morphological differences between *O. operculata*, *O. ancala* and *O. rhakodes* do not the result of a gradual evolution but instead they reflect increasing environmental stress.

The data suggest that morphological differences between *Oligosphaeridium complex*, *O. pulcherrimum*, *O. albertense* and *O. totum* and between *Odontochitina operculata* and *Odontochitina ancala/O. rhakodes* reflect the environmental variability. Several studies on dinocyst assemblages of different ages and geographical origins also evidenced the influence of environmental variations on dinocysts morphology. Wall *et al.* (1977) found that under unstable-unpredictable regimes the more cosmopolitan modern dinocysts tend to exhibit subtle changes in cyst morphology, e.g. variations in spine length, ornament and size. Numerous studies on modern dinocysts have attempted to correlate the morphological variations of individual dinocyst taxa to environmental factors, such as density or turbulence, suggesting that morphology can be used for paleoceanographic reconstructions (e.g. Ellegaard *et al.*, 2002; Zonneveld and Susek, 2007; Mertens *et al.*, 2011; Jansson *et al.*, 2014). Riding *et al.* (1985) suggested that the geographical distribution of individual taxonomic components of ctenidodinioid cysts reflects the supposed salinity levels of Bathonian surface waters. Marshall and Batten (1988) also proposed that the morphological variations of representatives of the genus *Aptea* in the early Cretaceous Weald Clay may be physiological responses to ambient conditions, more precisely to salinity gradient.

5.3. Paleoceanographic and paleogeographic evolution of the western Iberian margin during the Albian

The relative position of samples included in each cluster of samples from Lusitanian Basin data analysis make it possible to associate the sequence SC1-LB > SC2-LB > SC3-LB to the infilling of the basin during the sea-level rise. The scatter diagram of Correspondence Analysis revealed the congruence between the clusters of taxa and the clusters of samples (Fig. 2.11 and 2.16) suggesting that the distribution and frequency of taxa along the studied successions may also reflect the effects of the Albian sea-level rise in the Lusitanian Basin and the 398D site the infilling of the Lusitanian Basin. Previous studies based on sedimentological and paleontological information recognize the evolutionary trend of paleoenvironments associated to the infill of the depositional space in the basin and to the Albian long-term sea-level rise

(e.g. Rey, 1979; Dinis *et al.*, 2002; Heimhofer *et al.*, 2012; Horikx *et al.*, 2014). The Lusitanian Basin achieved full infill by the Cenomanian (Dinis *et al.*, 2008).

We identified two main groups of taxa in function of their environmental preferences; 1) Taxa preferring inner- to middle-neritic environments; 2) Taxa preferring open marine environments. We also identified several sub-groups of taxa, within the two main groups above mentioned, in function of their tolerance to variations of environmental factors; a group of taxa highly tolerant to variations in environmental factors and resistant to oxygen-related decay; and some taxa ubiquitous and cosmopolite (Fig. 2.28).

Middle Albian levels from the Lusitanian Basin recorded nearshore environments with important shifts in salinity and nutrient availability, due to the influence of fluvial systems. They were dominated by taxa extremely tolerant to environmental parameters fluctuations and by taxa indicative of inner/middle neritic conditions, tolerant to salinity and nutrient variations (Fig. 2.28, Fig. 2.29). *Palaeoperidinium cretaceum*, here included within the taxa highly tolerant to environmental fluctuations, and *Chichaouadinium vestitum*, identified as cosmopolitan under mesotrophic conditions, showed important peaks of relative abundance during this period, which could be related to high nutrient availability due to continental influx. During this interval dinocyst assemblages from the 398D site were dominated by taxa identified as characteristic of open marine distal environments. Relative abundance of marine taxa tolerant to limited fluctuations of environmental parameters was also considerable. The abundance of this later group of taxa may be a consequence of the instability generated by the elevated continental influx in the Lusitanian Basin. High nutrient availability during the Middle Albian was also evidenced by the peaks of relative abundance of *P. cretaceum*, responsible of all the abundance peaks of the taxa extremely tolerant to environmental fluctuations at the 398D site, and by the contributions of *C. vestitum*.

During the Late Albian the importance of the continental influx diminished which, together with the influence of the long-term sea-level rise, allowed the development of inner /middle neritic conditions in the Lusitanian Basin. High relative abundance of taxa tolerant to high environmental fluctuations and peridiniacean, as *P. cretaceum* and *C. vestitum*, reflect the late pulses of continental influx (Fig. 2.28, Fig.

DINO CYST DISTRIBUTION IN AN INSHORE TO OFFSHORE TRANSECT IN THE WESTERN IBERIAN MARGIN

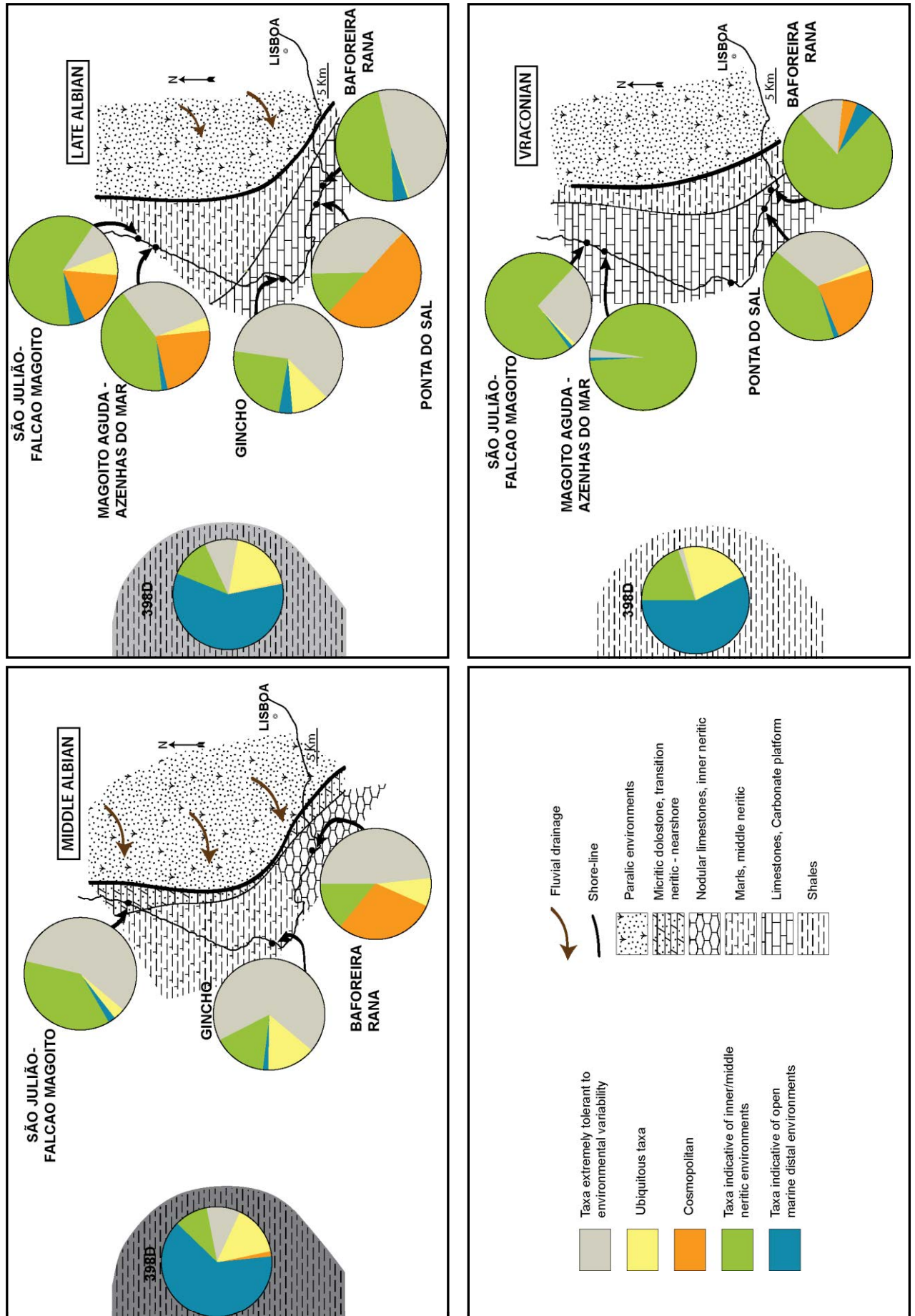


Figure 2.29. Maps of dinocyst associations distribution related to the depositional environments during the Middle Albian to the Vraconian (uppermost Upper Albian) in the western Iberian margin.

2.29). However, the abundance of taxa indicative of inner/middle neritic conditions increased and taxa indicative of open marine environments, but tolerant to limited fluctuations of environmental parameters, were also present. This indicates that the continental influx during the Late Albian in the Lusitanian Basin was lower and less constant than during the Middle Albian. Dinocyst associations in the 398D site also reflect this environmental evolution during the Late Albian. Relative abundance of taxa tolerant to high environmental fluctuations in the 398D site was lower than in the Middle Albian and taxa indicative of enhanced nutrient availability were almost absent.

Vraconian (uppermost Late Albian) dinocyst associations from the Lusitanian Basin reflect the establishment of a carbonate platform, larger in the northern outcrops area than in the southern area. Taxa indicative of neritic conditions dominated the assemblages (Fig. 2.28, Fig. 2.29). In the northern outcrops (São Julião – Falcao Magoito and Magoito aguda – Azenhas do Mar), the absence of taxa indicative of mesotrophic neritic conditions reflects the oligotrophic conditions on the area due to the northeast shift of the paleo-shoreline, and so the increased distance to the nutrient source.

Taxa indicative of open marine environments were also absent from the northern outcrops suggesting that the platform was large enough in this area to allow the development of a neritic environment isolated from direct open marine influence. However, in the southern outcrops (Ponta do Sal and Baforeira Rana outcrops) higher nutrient availability was indicated by the presence of *C. vestitum*. During the Vraconian, dinocyst associations from the 398D site reflect the absence of continental influx and the influence of the carbonate platform development. Taxa included in the different groups representatives of open marine conditions, together with the ubiquitous *S. ramosus*, dominated the associations whereas taxa representative of the group tolerant to large environmental fluctuations were almost absent. Relative abundance of taxa indicative of neritic environments was higher than in previous intervals, probably reflecting the influence of the carbonate platform in the paleoceanography of distal environments.

6. Conclusions

The cluster analysis of the dinocyst assemblages from different Albian sections from the Iberian margin (Lusitanian Basin sections and 398D DSDP site) reveals that the co-occurrence of taxa supports associations clearly indicative of paleoenvironmental conditions. Multivariate Correspondence Analysis analyses help at deciphering the hierarchy of paleoenvironmental factors that constraint species occurrences and relative abundance. The integration of sedimentological data to the analysis of dinocyst assemblages allows characterizing the environmental preferences of dinocyst species.

The main patterns of species distribution are related to the distance from the shore, (inshore – offshore trend). From the analysis of Lusitanian Basin and 398D site data three dinocyst associations are recognized, characterizing coastal highly unstable conditions, inner/middle neritic environments, and stable outer neritic environments.

Biodiversity structure of assemblages is controlled by the stress associated to environmental instability, increasing from the offshore toward the inshore and marked by a decrease in taxonomic richness and evenness. The assemblages recorded offshore in the 398D DSDP site are typical of outer neritic environments some species are recognized as typical of open stable marine conditions, species tolerant to slight variations of environmental factors are also common in these environments. The pattern of species distribution is more complex in the Lusitanian Basin. The proximity to the shore and the instability of environmental conditions are identified as the main factors controlling the segregation of dinocyst associations in proximal settings. The input of fresh waters and siliciclastic sediments in coastal environments imply a complex combination of salinity and nutrients variations, which account for the main differences between the Lusitanian Basin assemblages.

Coastal environments under highly unstable conditions are characterized by the dominance the most tolerant taxa to variations of environmental parameters (like salinity and nutriment availability), those are; *Trichodinium castaneum*, *Cribroperidinium? edwardsii*, *Circulodinium distinctum*, *Palaeoperidinium cretaceum* and *Gardodinium eisenackii*.

Stable and mesotrophic inner/middle neritic environments are interpreted for assemblages in whom *Callaiosphaeridium asymmetricum*, *Carpodinium granulatum*,

Microdinium opacum and *Oligosphaeridium pulcherrimum* and *O. totum* are abundant. When *Cyclonephelium compactum*, *Cyclonephelium vannophorum*, *Dinopterygium cladoides*, *Odontochitina ancala/O. rhakodes* and *Protoellipsodinium corollum* are present and abundant they are indicative of more unstable inner/middle neritic environments.

The wide distribution of *Spiniferites ramosus* and *Spiniferites multibrevis* make it possible to consider them ubiquitous taxa. *Chichaouadinium vestitum* is considered as cosmopolitan taxon under mesotrophic to eutrophic conditions because its wide distributed and often expresses peaks of abundance in the Lusitanian Basin.

Some taxa as, *Chlamydothorella discreta*, *Circulodinium colliveri*, *Cometodinium whitei*, *Exochosphaeridium phragmites* and *Odontochitina operculata* were more abundant in the 398D site assemblages although they were also present in the Lusitanian Basin. They are thus considered as living preferentially in stable outer neritic environments, although they can tolerate limited fluctuations of environmental conditions.

Outer neritic conditions are widely accepted for *Impagidinium verrucosum* and *Pterodinium cingulatum*. As they show similar patterns of occurrence, restricted to the 398D site, *Achomosphaera ramulifera*, *Cassiculosphaeridia reticulata*, *Dapsilidinium laminaspinosum*, *Hystriodinium pulchrum*, *Kallosphaeridium? ringnesiorum*, *Kleithriasphaeridium tubulosum* and *Oligosphaeridium complex* are also considered indicative of outer neritic conditions.

The oceanographic conditions that triggered the lithological change observed in the 398D site from black-shales to mixed marly-chalk levels also controlled the distribution of some dinocyst species. *Apteodinium deflandrei*, and *Damassadinium chibane* were present during the deposition of black shale levels, whereas *Canningia reticulata*, *Litosphaeridium conispinum*, *Pervosphaeridium cenomaniense* and *Spiniferites ramosus* subsp. *granosus* were present during the deposition of mixed marly – chalk levels. However, more information is necessary to identify the specific factors involved.

CHAPTER 3

Spatio-temporal variability of Aptian dinoflagellate cysts

This chapter has been elaborated with the collaboration of Masure E. and Villier L.

1. <u>Introduction</u>	101
2. <u>Geological setting</u>	103
2.1. Southern Provence Basin	103
2.2. Site 398D Deep Sea Drilling Project (DSDP)	106
2.3 Biostratigraphical framework	109
3. <u>Material and methods</u>	110
3.1. Material	110
3.2. Methods	110
3.2.1. <i>Diversity analysis</i>	111
3.2.2. <i>Paleoproductivity estimation: The Peridinioid/Gonyaulacoid (P/G) ratio</i>	112
3.2.3. <i>Statistical analyses (Seriation Analysis, Cluster Analysis, Correspondence Analysis, and Non-Parametric Multivariate Analysis of Variance)</i>	112
3.2.4. <i>Structured Sedimentary Organic Matter (SOM)</i>	112
4. <u>Results</u>	114
4.1 Diversity analysis	114
4.2. Peridinioid / Gonyaulacoid (P/G) ratio	115
4.3. Differentiation of dinoflagellate cyst associations	116
4.3.1. <i>Dinocyst assemblages identified in the Southern Provence Basin</i>	116
4.3.1.1. <i>Clusters of taxa and samples and Pairwise NPMANOVA</i>	117
4.3.1.2. <i>Correspondence Analysis</i>	119
4.3.2. <i>Dinocyst associations from the Southern Provence Basin and the 398D site</i>	121
4.3.2.1. <i>Clusters of taxa and samples and Pairwise NPMANOVA</i>	121
4.3.2.2. <i>Correspondence Analysis</i>	124

4.4. Structured Sedimentary Organic Matter (SOM) assemblage analysis	124
4.4.1. <i>Southern Provence Basin</i>	124
4.4.2. <i>Structured SOM from the DSDP 398D site</i>	128
4.5. Marks of paleoenvironmental changes in the Southern Provence Basin.	129
4.5.1. <i>Early Aptian: a phase of carbonate platform demise.</i>	129
4.5.2. <i>Oceanic Anoxic Event 1a in the Southern Provence Basin, the Goguel event.</i>	130
4.5.3. <i>The White Level (Niveau Blanc)</i>	131
4.5.4. <i>Early Late Aptian</i>	131
4.5.5. <i>The Fallot Level.....</i>	133
5. <u>Interpretation and discussion</u>	134
5.1. Factors controlling dinocysts distribution	134
5.1.1. <i>Dinocyst distribution in the Southern Provence Basin during the Aptian</i>	134
5.1.2. <i>Stability and predictability</i>	135
5.2. Paleoenvironmental significance of the dinocyst associations ...	137
5.2.1. <i>Early Aptian conditions: Intrashelf Basin surrounded by carbonate platforms</i>	137
5.2.2. <i>Late Aptian conditions: Intrashelf Basin without carbonate platforms</i>	139
5.3. The OAE 1a, the White Level and the Fallot Level: record in the Southern Provence Basin of global and regional events	142
5.3.1. <i>Oceanic Anoxic Event 1a (OAE 1a) - Niveau Goguel</i>	142
5.3.2. <i>White Level (Niveau Blanc)</i>	144
5.3.3. <i>Niveau Fallot.....</i>	145
5.4. Validity of the paleoenvironmental model on a larger scale	146
5.5 Paleooceanographic and paleogeographic evolution of the Southern Provence Basin during the Aptian	147
6. <u>Conclusions</u>.....	148

1. Introduction

During the Cretaceous period a long-term sea level rise (Steuber, 2002; Haq, 2014) favored the widespread development of extensive carbonate platforms (e.g. Masse and Rossi, 1987; Gili *et al.*, 1995; Masse *et al.*, 1997; Huck *et al.*, 2010; Skelton and Gili, 2011). The carbonate platforms record several crisis phases that modified their morphologies and altered the ecosystem they sheltered (e.g. Masse and Fenerci-Masse, 2013a; Huck *et al.*, 2014). Some of these crises, also called drowning events, were close in time to periods of major perturbations of the carbon cycle as is the case of the Oceanic Anoxic Events (OAEs, e.g. Masse and Philip, 1986; Ross and Skelton, 1993; Föllmi *et al.*, 1994; Weissert *et al.*, 1998; Burla *et al.*, 2008; Skelton and Gili, 2011).

Extensive carbonate platforms affected by successive drowning events and major perturbations of the carbon cycle are characteristic features of the Aptian (e.g. Schlanger and Jenkyns, 1976; Masse and Philip, 1986; Arthur *et al.*, 1990; Ross and Skelton, 1993; Skelton and Gili, 2011; Masse and Fenerci-Masse, 2013a). Because all these features are particularly well recorded in the northwestern Tethys sector, and the SE France in particular, numerous studies have focused on the Aptian conditions in this region (e.g. Masse, 1976, 1993; Arnaud-Vanneau *et al.*, 1979; Arnaud-Vanneau, 1980; Arnaud *et al.*, 1995, 1998; Moullade *et al.*, 1998c, 2005, 2015; Herrle *et al.*, 2003; Heimhofer *et al.*, 2004, 2006; Renard *et al.*, 2005, 2007; Beltran, 2006; Babinot *et al.*, 2007; Beltran *et al.*, 2007; Kuhnt and Moullade, 2007; Baudin *et al.*, 2008; Moullade and Tronchetti, 2010; Kuhnt *et al.*, 2011; Stein *et al.*, 2012; Lorenzen *et al.*, 2013; Masse and Fenerci-Masse, 2013a, 2013b, 2013c; Westermann *et al.*, 2013). The North Provence carbonate platform experienced four drowning events from the Late Barremian to the uppermost Early Aptian (Masse and Fenerci-Masse, 2011, 2013a). These drowning events were associated to the physiographical transformation of the carbonate platforms to a ramp model and to a switch in the organisms dwelling in (Masse and Fenerci-Masse, 2013a, 2013b, 2013c). In the SE France, the Southern Provence Basin was filled by a continuous Aptian hemipelagic series that document the complete transformation, not only the carbonate platform drowning events, but also the posterior evolution of the region (Moullade *et al.*, 2005; Beltran *et al.*, 2007, 2009; Kuhnt and Moullade, 2007; Renard *et al.*, 2007; Baudin *et al.*, 2008). The Southern Provence Basin series also records the global and regional events of perturbation of

the carbon cycle, like the OAE 1a and Fallo level respectively (e.g. Bréhéret and Delamette, 1988; Bréhéret, 1995; Baudin *et al.*, 2008).

During the Aptian carbonate platforms and OAEs were global features. However, the image is not constant all over the world (e.g. Huck *et al.*, 2010, 2013; Skelton and Gili, 2011). Aptian records in the western Iberian Margin are different from those of SE France (Burla *et al.*, 2008; Huck *et al.*, 2012, 2014). Distal records of the Aptian events in the western Iberian Margin reveal the importance of continental inputs in the region and their variability (Cornford, 1979; de Graciansky and Chenet, 1979; Deroo *et al.*, 1979; Habib, 1979). The great exposition to the Central Atlantic Ocean of carbonate platforms in the western Iberian Margin influenced their evolution, continental inputs were buffered by oceanic dilution resulting in a long and gradual demise of carbonate platforms (Huck *et al.*, 2012, 2014). The position of the Iberian Margin between the Tethyan and Central Atlantic domains, together with the early opening of the proto-North Atlantic (Soares *et al.*, 2012) and the counterclockwise rotation of the Iberian bloc (Gong *et al.*, 2008) during the Aptian confer a crucial interest to the study of this region.

The comparative study of the dinocyst Aptian record in the western Iberian Margin and in the Southern Provence Basin will allow us to identify the similarities and differences in their paleoenvironmental evolution. Most previous studies focused on the middle and lower part of the water column providing important information about oxygenation state, which controls the organic matter preservation (e.g. Bralower *et al.*, 1993; Pletsch *et al.*, 2001; Friedrich *et al.*, 2003; Friedrich and Erbacher, 2006). As dinocyst dwell the uppermost part of the column water, the study of dinocyst associations may provide key information about changes in the water surface, as salinity or nutrient availability. In the previous chapter, dinocyst associations were identified through the multivariate analysis of Albian data. The comparison of the resulting dinocyst associations with the sedimentological and paleontological available data allowed us to define their environmental preferences and tolerances. In the present chapter, the same methodology is applied to Aptian dinocyst data to analyze whether the composition of the identified dinocyst assemblages was stable through different geographies and during long time intervals. The comparison of dinocyst data with structured sedimentary organic matter (SOM) assemblage data is used for identifying changes in the influence of continental inputs, and associated salinity and nutrient variations.

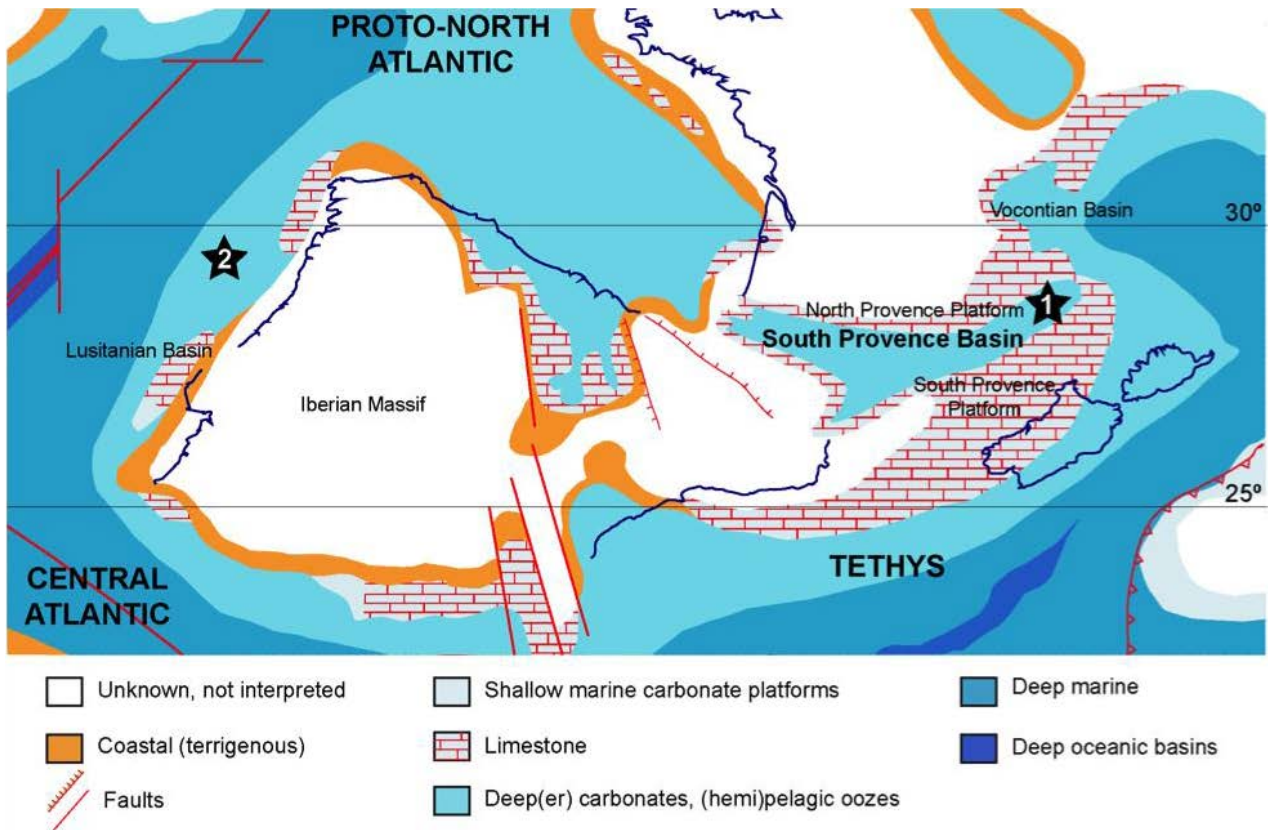


Figure 3.1. Early Aptian (112-114 Ma) palaeogeographic reconstruction with location of the studied sections redrawn after Masse *et al.* (2000). During the Early Cretaceous, the (1) Southern Provence Basin and the (2) DSDP site 398D were located at a paleolatitude of $\sim 25^{\circ}\text{N}$ (Hay *et al.*, 1999) to 28°N (Masse *et al.*, 2000).

2. Geological setting

During the early Cretaceous, the studied areas were located at a paleolatitude of $\sim 25^{\circ}\text{N}$ (Hay *et al.*, 1999) to 28°N (Masse *et al.*, 2000) (Fig. 3.1).

2.1. Southern Provence Basin

The studied series from the Southern Provence Basin includes part of the Early Aptian (uppermost lower and upper Bedoulian) and of the Late Aptian (early and middle Gargasian). We analyzed the dinocyst content of samples from the historical Bedoulian stratotype, cropping out between Cassis and La Bédoule (Fig.3.2). The Late Aptian is studied at La Marcouline Quarry. The analyzed sections are correlated lithostratigraphically and biostratigraphically, with three other close sections, extensively studied during the past years using a wide range of methods: Les Tocchis outcrop and two drill cores in the Bedoulian stratotype (LB1 and LB3) (Moullade *et al.*,

2004, 2015; Lorenzen *et al.*, 2013). The sedimentary record is continuous without sedimentary or tectonic unconformities.

The Early Aptian beds from the Cassis – La Bédoule historical stratotype area were described in detail by Moullade *et al.* (1998a, 2004) and Masse (1998) on the basis of a composite set of discrete sections (Fig. 3.2, Fig. 3.3). The Early Aptian studied interval corresponds to the upper 70 m from the Cassis – La Bédoule succession. The first 40 m (samples 122 to 146) record a sedimentary succession in which carbonated facies are represented by monotonous micritic limestones, containing calcareous nannofossils, small benthic and planktonic foraminifers. Higher in the series, a first thin marl bed appears isolated by an overlying thin limestone bed (sample 150) followed by 9,5 m thick marly interval (which comprises sample 155c). The upper interval of the Cassis – La Bédoule succession is composed by nearly 20 m of marl dominated beds, of variable induration. Near to the top of the series a light colored marl bed constitutes a stratigraphical mark-bed throughout the region, it is known as the White Level (bed 170, Moullade and Tronchetti, 2010). The La Marcouline succession exhibits a rhythmic alternation of gray marl and light-gray marly limestone beds (Moullade and Tronchetti, 2010). All the levels studied at La Marcouline are of Late Aptian age.

At Cassis, La Bédoule and La Marcouline, the weathering of the rock section leads to alternation of beds with positive and negative reliefs. Prominent beds have been interpreted as limestone beds, and softer beds interpreted as marl beds (e.g. Moullade *et al.*, 1998a; Stein *et al.*, 2012). However, analysis of the CaCO₃ content (Masse, 1998; Renard *et al.*, 2007) revealed that variations in the weathering profile do not correspond exactly to the limestone/marl alternations described in the field. The

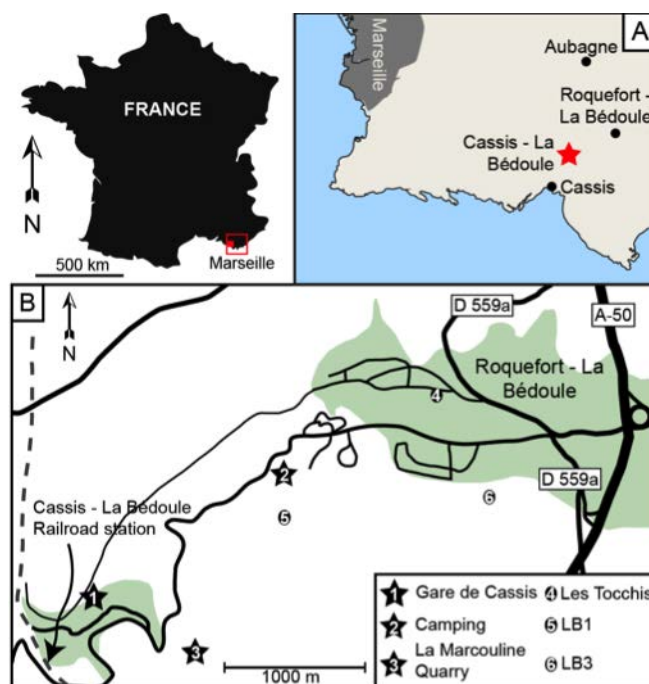


Figure 3.2. Location of the studied outcrops from the Southern Provence Basin, which are part of the composite section from Gare de Cassis outcrop, Camping Section at Roquefort – La Bédoule and La Marcouline Quarry, and the Les Tocchis section and the cores LB1 and LB3 used to correlate the studied successions (modified from Lorenzen *et al.*, 2013; Moullade *et al.*, 2015, 2004).

differences between the field aspect and the CaCO₃ content of the beds are especially obvious in the Cassis – La Bédoule succession. The study of three drill cores from the Bedoulian stratotype area showed that changes in the sediment composition are much more gradual than inferred by field observations (Lorenzen *et al.*, 2013; Moullade *et al.*, 2015). Moullade *et al.* (2015) realized that “small differences in chemical composition of the rocks are artificially accentuated by surface diagenesis, erosion and differential weathering”.

During the Upper Barremian a vast carbonate platform developed in the southeastern France, the so-called Urgonian carbonate platforms. A drowning event during the middle Upper Barremian (during the *Gerhardtia sartousiana* ammonite zone), modulated by the regional tectonic deformations triggered the formation of a deep-marine corridor that evolved into the Southern Provence Basin during the uppermost Barremian (*Imerites giraudi* ammonite zone) (Masse and Fenerci-Masse, 2013b, 2013c). The Southern Provence Basin was located at 27-28° North (Masse *et al.*, 2000), isolated from the Vocontian Basin to the northeast by the North Provence Platform and bounded to the south by the Southern Provence Platform (Fig. 3.1). The Southern Provence Basin received hemipelagic sediments from the latest Barremian onwards, offering a continuous record up to the Late Aptian (Masse and Fenerci-Masse, 2013a).

During the earliest Early Aptian (*Deshayesites weissi* – *D. deshayesi* ammonite zones transition) a drowning event of the carbonate platforms lead to the replacement of pure limestones by marls and marly limestones in the studied area (Masse and Fenerci-Masse, 2013a). Higher in the series, the Oceanic Anoxic Event 1a (OAE 1a) is recorded within the *Roloboceras hambrovi* ammonites subzone, and it is locally recognized as the Goguel Level. The onset of event is expressed by a marked decrease in $\delta^{13}\text{C}_{\text{carb}}$ followed by a positive excursion (Kuhnt *et al.*, 2011; Lorenzen *et al.*, 2013). The $\delta^{18}\text{O}$ fluctuations between the beds 146 and 158 may relate to transient episodes of cooler/drier and warmer/wetter climates at the scale of the northwestern margin of the Tethys (Stein *et al.*, 2012). The lack of consistent RSTE enrichments and low C_{org}:P_{tot} ratios indicate that the Southern Provence Basin remained oxic during the OAE 1a (Stein *et al.*, 2012). At the onset of the OAE 1a a third event drowned up the carbonate platforms surrounding the South Provence Basin, followed by a deepening of the basin and of the surrounding platforms (Masse and Fenerci-Masse, 2013a).

The latest Early Aptian records a late drowning event at the transition from the *Deshayesites grandis* ammonites subzone to the *Dufrenoya furcata* ammonites zone). It is associated to the homogenization of the sedimentary environments at the regional scale, with deposition of deep water marls, which is recognized as the onset of the Gargas marls (Masse and Fenerci-Masse, 2013a). During this interval the climate was warm temperate to subtropical with a contrasted seasonality of alternating dry and pluvial periods, revealed by the floristic (Masure *et al.*, 1998b) and clay assemblages (Stein *et al.*, 2012). Analysis of the oxygen isotopes also reveals higher temperatures during the Early Aptian (Kuhnt *et al.*, 1998b, 2011). Foraminiferal assemblages recovered from the late Early Aptian, mainly within the *D. furcata* ammonite zone, reveal that this interval corresponds to the maximum paleodepth in the Southern Provence Basin (Moullade *et al.*, 1998b, 2015; Moullade and Tronchetti, 2010).

The Late Aptian interval records hemipelagic conditions over the Provence region. Spectral analysis of the marl / marly limestone bedding rhythms suggests orbitally-forced fluctuation of the sediments (Beltran, 2006; Kuhnt and Moullade, 2007), which is interpreted as resulting in a monsoon-controlled precipitation pattern (e.g. (Herrle *et al.*, 2003). The analysis of the carbonated fraction shows that Nannoconids were responsible of up to 90% of the pelagic carbonate sedimentation (Beltran *et al.*, 2009). Deposition of marls is interpreted as the consequence of increased fertility, resulting from an increase in runoff during periods of lower surface water salinity associated to increasing temperatures and precipitations (Beltran *et al.*, 2007; Kuhnt and Moullade, 2007). The deposition of marly-limestones is interpreted as the consequence of diminished runoff, and therefore lower nutrient input and fertility, during drier and cooler periods (Beltran *et al.*, 2007; Kuhnt and Moullade, 2007).

2.2. Site 398D Deep Sea Drilling Project (DSDP)

The site 398D DSDP experienced different oceanographic conditions to those of the Southern Provence Basin. The comparison between both regions will allow testing the robustness of the model developed from the South Provence Basin data and whether it is transposable to other regions. During the Aptian, the 398D site was in the Central Atlantic domain under the influence of the growing proto-North Atlantic (Fig.3.1). The 398D site is located 160 km off Portugal, west of Porto, in a small bathyal platform on the southern margin of Vigo Seamount. The hole was drilled on the western flank of a deep northeast-southwest trough in a region considered part of the

continental passive margin of the eastern North Atlantic (Sibuet *et al.*, 1979). The Cores 127 to 111 (1637 to 1484 mbsf, meters below sea floor) record rocks of Aptian age similar to that of the fully tethyan Cassis – La Bédoule and La Marcouline successions (Fig. 3.3). From the five lithological units described from the 398D site, the studied time interval is found within the lithological sub-unit 4C of (Sibuet *et al.*, 1979).

The sub-unit 4C is lithologically complex. It is composed of dark mudstone, claystone, and calcareous claystone ranging from black to dark gray to olive-green-gray with various interbedded mud and limestone pebble debris flows, and mud-supported conglomerates (containing Tithonian clasts), turbiditic mudstones, and thin to thick turbiditic sandstones and siltstones (Fig. 3.3). The lower interval of the studied section, Cores 127 to 118 (1639 to 1544 mbsf), within the *Globigerinelloides blowi* foraminiferal zone (Fig. 3.3), is characterized by the dominance of kerogen Type III (Deroo *et al.*, 1979), the predominance of first cycle organic matter (Cornford, 1979) and by presenting by the greatest abundance of structured palynodebris, sporomorphs, and sporomorph species richness of the whole 398D cores (Habib, 1979). Whereas the upper interval of the studied section comprising the *Schackoina cabri*, *Praehedbergella luterbacheri* and the lower part of the *Globillerinoides ferreolensis* foraminiferal zones, Cores 117 to 111 (1544 to 1477.5 mbsf), is characterized by kerogen Type III in association to a poor hydrogen index (Deroo *et al.*, 1979), which is dominated by redeposited organic matter (Cornford, 1979). Organic carbon values decrease rapidly above Core 117 (Sibuet *et al.*, 1979). Palynofacies in this upper interval, Cores 117 to 111, are characterized by the dominance of nearly equidimensional carbonaceous particles, low numbers of palynomorphs and slightly higher proportion of phytoplankton to sporomorphs than in the precedent interval (Habib, 1979).

In the lower part of the section, in the *G. blowi* foraminiferal zone, the sedimentological sequences and the high content of continental debris represent transport by turbiditic currents (Fig. 3.3) possibly related to deltaic progradation (Habib, 1979) or build-out of a deep-sea fan complex (de Graciansky and Chenet, 1979). Changes in sedimentological sequences and palynofacies composition reflect the decrease of terrigenous input (Habib, 1979) associated to a “foot of slope” environment in the upper part of the section (de Graciansky and Chenet, 1979), from the uppermost part of the *G. blowi* foraminiferal zone to the top of the studied interval (Fig. 3.3).

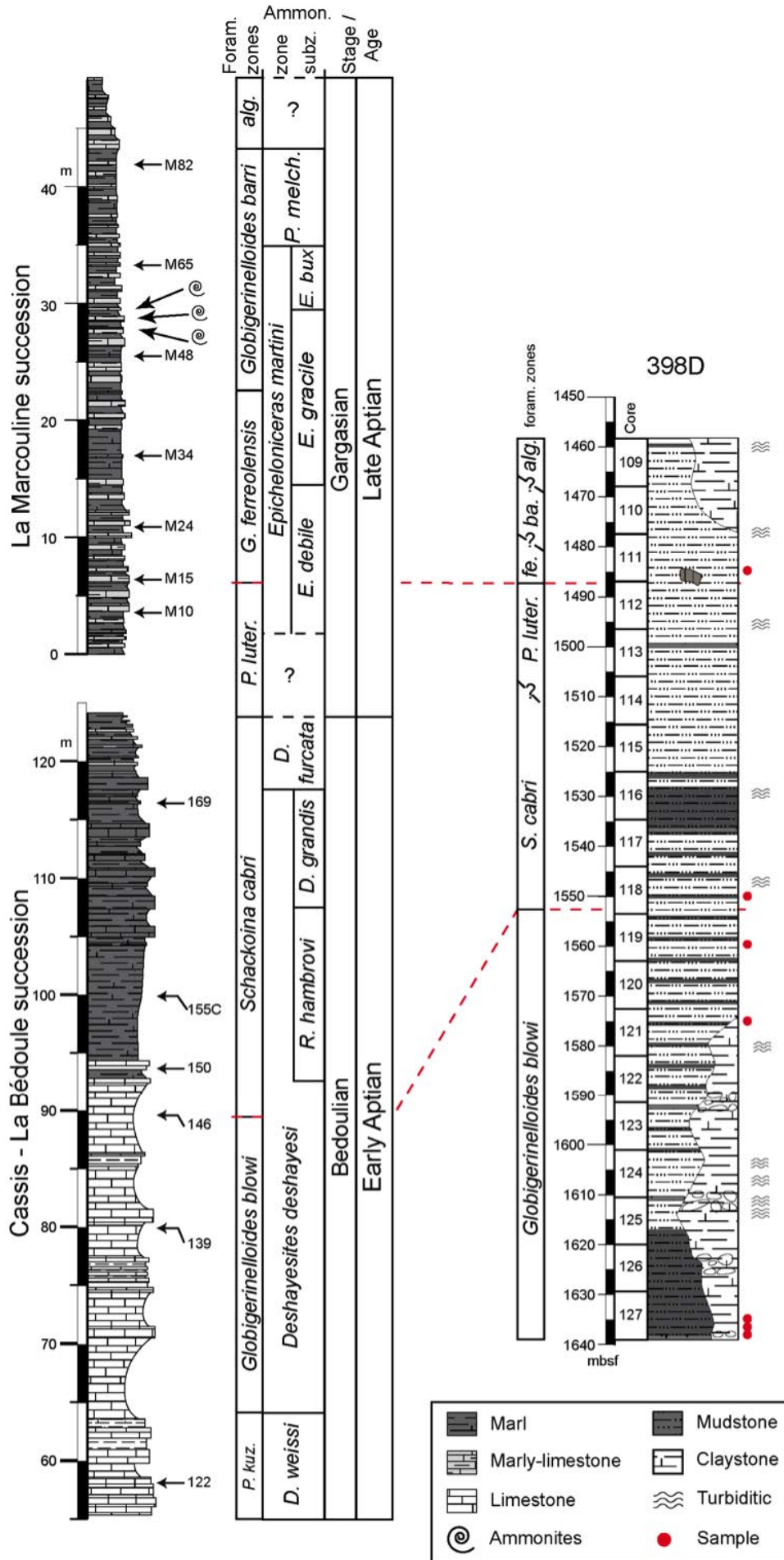


Figure 3.3. Composite section from Gare de Cassis section, La Marcouline Quarry, and Camping Section at Roquefort – La Bédoule from the South Provence Basin, and its biostratigraphical correlation with the 398D DSDP site. For the South Provence Basin the ammonites zonation follows Ropolo *et al.* (2008, 2006, 1998) and “the Kilian group” Reboulet *et al.*, (2011), and Moulade *et al.* (2008, 2005, 1998b) for the foraminiferal zonation. Foraminiferal datums for the 398D DSDP site foraminiferal were obtained from Sigal (1979). Foraminiferal zones; Ammon. – ammonites, subz. – subzone. *D. weissii* – *Deshayesites weissii*; *R. hambrovi* – *Roboloceras hambrovi*; *D. grandis* – *Deshayesites grandis*; *D. furcata* – *Dufrenoyia furcata*; *E. debile* – *Epicheloniceras debile*; *E. gracile* – *Epicheloniceras gracile*; *E. bux.* – *Epicheloniceras buxtorfi*; *P. melch.* – *Parahopites melchioris*; *P. kuz.* – *Praehedbergella kuznetsovae*; *P. luter* – *Praehedbergella luterbacheri*; *G. ferreolensis*, *ba.* – *Globigerinelloides ferreolensis*; *ba.* – *Globigerinelloides barri*; *alg.* – *Globigerinelloides algerianus*

2.3 Biostratigraphical framework

Dinoflagellate cysts distribution of the Cassis – La Bédoule succession was studied from a biostratigraphical perspective by Davey and Verdier (1974) and by Masure *et al.* (1998b). Masure (1984) studied the dinoflagellate cyst distribution in 398D Cores 111 to 46. Unfortunately, the scarcity of dinoflagellate cyst in the 398D samples did not allow the identification of either the Early Aptian or the Late Aptian. No biostratigraphical studies based on the dinoflagellate cysts distribution is available for La Marcouline succession.

Masure *et al.* (1998b) recognized three dinocysts zones within the Cassis – La Bédoule succession: (1) The base of the *Pseudoceratium securigerum* zone is defined by the first appearance data (FAD) of *P. securigerum* and its upper limit corresponds to the FAD of *Tehamadinium sousense*. The last appearance data (LAD) of *Hystriodinium ramoides* and *Heslertonia herlertonensis* are documented within the *Pseudoceratium securigerum* zone. The FAD of *Ovoidinium diversum* is suggested as an alternative mark of the base of this zone in the Tethyan realm, if *P. securigerum* is absent. The time interval represented by the *Pseudoceratium securigerum* zone matches the *Deshayesites weissii* and part of the *Deshayesites deshayesi* ammonites zone, the *Globigerinelloides blowi* foraminifera zone and the nannofossils sub-zones NC6A and part of the NC6B. (2) The FAD of *Tehamadinium sousense* defines the lower boundary of the *T. sousense* zone. Its upper boundary is established at the FAD of *Tehamadinium tenuiceras*. The LAD of *Ctenidodinium elegantulum* and *Rhynchodiniopsis aptiana* in the Tethyan domain are associated to the base of this zone. This zone is equivalent to the upper part of the *D. deshayesi*, the whole *Roloboceras hambrowi* and *Deshayesites grandis* ammonite zones; the upper part of *G. blowi* and the lower part of *S. cabri* foraminifera zones and to a part of the NC6B nannofossil subzone. (3) The FAD of *Tehamadinium tenuiceras* marks the base of the *T. tenuiceras* zone. The top of this zone is not formally defined. However, it is in the Late Aptian series, above the studied levels (Masure *et al.*, 1998b). *T. tenuiceras* zone is equivalent to the upper part of the *D. grandis* and part of the *Dufrenoyia furcata* ammonites zones, to the upper part of the *S. cabri* and the whole *Praedbergella luterbacheri* foraminifera zone, and to the lower part of the NC7 nannofossil subzone.

Numerous studies published during the last decades focused on ammonites and foraminifera helped at drawing a precise chronostratigraphic framework for the South

Provence Basin of the Early Aptian and Late Aptian series. However, there exist controversies regarding the lower limit of the *Deshayesites deshayesi* ammonite zone and the placement of the *Roloboceras hambrovi* ammonite subzone (see discussion in Moreno-Bedmar *et al.*, 2009, and in Masse and Fenerci-Masse, 2013a), with consequences regarding the location of the boundary between the Early and Late Aptian and the correlation between the international units and the historical stages Bédoulien and Gargasien, defined in Provence (Reboulet *et al.*, 2011; Kuhnt *et al.*, 2011; Moullade *et al.*, 2015). Our biostratigraphical scheme follows the contributions of Ropolo *et al.* (1998, 2006, 2008) for the ammonite zonation and Moullade *et al.* (1998b, 2005, 2008) for the foraminiferal zonation (Fig. 3.3).

The foraminiferal data of Sigal (1979) allow correlation between the 398D cores and the series from the Southern Provence Basin (Fig. 3.3). The base of the *Globigerinelloides blowi* zone is placed at 1639 mbsf (base of Core 127). A foraminifer association common to the *Schackoina cabri* and *Praehedbergella luterbacheri* zones appears from 1553.3 mbsf to 1496.5 mbsf (cores 118 to 113). The occurrence of *Globillerinoides ferreolensis* at 1408.5 mbsf suggests an age of *G. ferreolensis*, *Globigerinelloides barri* and/or *Globigerinelloides algerianus* foraminiferal zones from 1496.5 to 1408.5 mbsf (cores 112 to 109, Sigal, 1979).

3. Material and methods

3.1. Material

Thirteen samples were analyzed from the Southern Provence Basin and seven from the 398D site. Both hard (“limestones”) and soft (“marls”) levels were equally sampled at the South Provence Basin. Previous biostratigraphical and geochemical studies guided the selection of samples at La Bédoule – Cassis and La Marcouline outcrops. At the 398D site, samples in intervals described as turbiditic were avoided.

3.2. Methods

The palynological processing methodology is described in Chapter 2. Two simultaneous counting were performed on each sample: a semi-quantitative analysis of dinocysts assemblages by counting at least 300 individuals, when possible, and a rough palynofacies analysis carried by counting of at least 500 particles (including

phytoclasts, wood and leaves fragments, spores, pollen grains, dinocysts, acritarchs and foraminiferal linings). All palynological analysis have been conducted under a Zeiss Axioplan 2 microscope equipped with bright field, differential interference contrast, and phase contrast optics. The microscope slides were scanned along non-overlapping traverses using a 63x objective lens. Morphological identification of dinoflagellate cyst has been performed using a 100x objective lens. The seven samples selected from the 398D site were considered for the study of the organic matter, but only two brought enough dinocysts to consider them for paleoenvironmental comparisons. A taxon list was produced for every fossil assemblage found in one bed at one site. No samples were combined to create composite lists by geologic unit or location. The taxonomy of dinocysts is based on Fensome *et al.* (2008). The list of identified dinocyst taxa is given in Appendix A and the biostratigraphical repartition of dinocyst in each studied section is given in Appendix B.8 and B.9.

Assuming that methods used in the analysis of dinocyst distribution in Albian sediments from the Lusitanian Basin and 398D hole, described in Ch. 2, allow the identification of dinocyst associations sharing environmental preferences we have applied strictly these same analyses to the new Aptian dataset. The Aptian dataset was designed for paleoenvironmental analysis and produced by my personal observations, which contrasts with the Albian dataset extracted from the literature. This implied the possibility of counting structured sedimentary organic matter content, and to obtain of data prone for evaluation of the paleoproductivity (P/G ratio).

3.2.1. Diversity analysis

As for Albian data, we used two quantitative analytical techniques to investigate the taxonomic richness and the evenness (see Section 3.2.1 in Chapter 2 for more details). Counting of the dinocyst diversity was considered at Genus level.

The taxonomic richness in Aptian samples from La Bédoule – Cassis and La Marcouline successions and from the 398D site was calculated by rarefaction analysis (Krebs, 1989; Adrain *et al.*, 2000), using the PAST software package, v. 3.07 (Hammer *et al.*, 2001). As all rarefaction curves flattened above 212 individuals, we selected a sample size of 212 individuals (S_{212}) to compare the taxonomic richness between the different samples.

3.2.2. Paleoproductivity estimation: The Peridinioid / Gonyaulacoid (P/G) ratio

Peridinioid cysts represent a proxy for heterotrophic dinoflagellates and their abundance can be considered related to paleoproductivity (Sluijs *et al.*, 2005; Prauss, 2012b, see section 5.1.3 chapter 2). The most relevant qualitative estimates of paleoproductivity are based on the ratio of peridinioid (P) versus gonyaulacoid (G) cyst abundance (e.g. (Lewis *et al.*, 1990; Powell *et al.*, 1992; Eshet *et al.*, 1994, p. 199; Prauss, 2012b). We applied the formula of Versteegh (1994) whereby $P/G = nP/(nP+nG)$, and n = number of specimens.

3.2.3. Statistical analyses (Seriation Analysis, Cluster Analysis, Correspondence Analysis, and Non-Parametric Multivariate Analysis of Variance)

For detailed justification and a precise description of the statistical methodology see section 3.2 in chapter 2. For paleoecological analyses, the analyzed matrix excludes all taxa with relative abundances lower than 2%, taxa present in a single sample, and taxa with a stratigraphical range limited to a single stratigraphical unit. Dinocyst were identified to the species levels when possible. Some dinocyst data were considered at the genus level for comparisons and analysis because of too often difficulties with species identification due to (1) preservational bias, (2) the abundance of inter-specific grading morphologies and (3) the limited overlap of species pool between Provence and Lusitanian Margin. Paleoecological analyses were performed on dinocyst data from the South Provence Basin alone and from the whole Aptian dataset, data from the South Provence Basin and from the 398D site. The dinocyst data from the Aptian 398D samples alone were not submitted to paleoecological analysis because only two samples furnished reliable data.

3.2.4. Structured Sedimentary Organic Matter (SOM)

Palynofacies analyses consider the changes in relative abundance of sedimentary organic matter (SOM) types and can be used as tracer for paleoenvironmental and hydrographic interpretation (e.g. Lewis *et al.*, 1990; Tyson, 1995; Batten, 1996).

Slides were treated and mounted to facilitate the study of palynomorphs, so they were filtered over a 20 μm mesh to eliminate the amorphous organic matter. Our study is thus limited to structured SOM. A minimum operational diameter of 20 μm was established for counting phytoclasts (Tyson, 1995). The definition, biological sources and constituents of 16 categories are listed in Table 3.1. and can be summarized in five main groups:

- Total phytoclast; includes all the phytoclast categories counted;
- Total sporomorphs; includes spores, pollen grains and pseudo-amorphous sporomorphs;
- Total dinoflagellate cysts; includes dinocysts and pseudo-amorphous dinocysts;
- Foraminiferal linings;
- Other constituents; includes acritarchs and other algae.

Table 3.1. Structured sedimentary organic matter categories (in bold) counted in the samples with indication of their biological sources and constituents (modified from Tyson, 1995).

Group	Source	Category	Constituent	
Palynomorphs	Zoomorphs	foraminiferal linings	Benthonic and planktonic foraminifera	
	Organic-walled phytoplankton	dinoflagellate cysts		
		acritarchs		
		other algae		
	Sporomorphs	pollen spores	Bisaccates and <i>Classopolis</i> spp. dominant	
		pseudo-amorphous sporomorphs pseudo-amorphous dinocyst pseudo-amorphous palynomorphs	Sporomorphs with <50% of surface intact Dinocysts with <50% of surface intact <50% of surface intact and non-identifiable as sporomorph or dinocyst	
Phytoclasts	Macrophyte plant debris	Opaque	Equidimensional	Oxidized or carbonized woody tissues. Black particle. Long axis less than twice the short axis. Without internal biostructures. Oxidized or carbonized woody tissues. Black particle. Long axis more than twice the short axis. Without internal biostructures.
			Lath	
		Translucent	Wood tracheids with pits	Brown particle from wood tracheid with visible pits.
	Cuticle (Cu)		Thin cellular sheets, epidermal tissue.	
	Membranes (Mb)		Thin, non-cellular, transparent sheets of probable plant origin.	
		Pseudo-amorphous phytoclasts	Translucent phytoclasts with no definitive biostructure.	
	Fungal debris	Fungi	hyphae	

4. Results

4.1 Diversity analysis

The standardized taxonomic richness per sample, $E(S_{212})$, ranges between 29 and 14 taxa at Cassis – La Bédoule and between 37 and 23 taxa at La Marcouline (Fig. 3.4). The two samples from the 398D site show values of 30 and 20 (Fig. 3.5).

Evenness in Cassis – La Bédoule assemblages, estimated through the Probability of Interspecific Encounter (PIE), ranges between 0.87 and 0.67 in the Cassis – La Bédoule samples and between 0.90 and 0.82 in the La Marcouline samples (Fig. 3.4). Evenness values in the two samples from the 398D site are 0.89 and 0.55 (Fig. 3.5).

The standardized taxonomic richness along the Provence successions shows a slight increase from the base to the top, interrupted by a marked decrease in the samples 146 and 150. Assemblage evenness shows nearly constant values along the studied interval (Fig. 3.4).

Plotting Taxonomic Richness vs. Evenness (Fig. 3.6) from all the samples studied suggests similar structures for all assemblage of Cassis – La Bédoule and La Marcouline sections. From the two samples of the 398D site analyzed, one

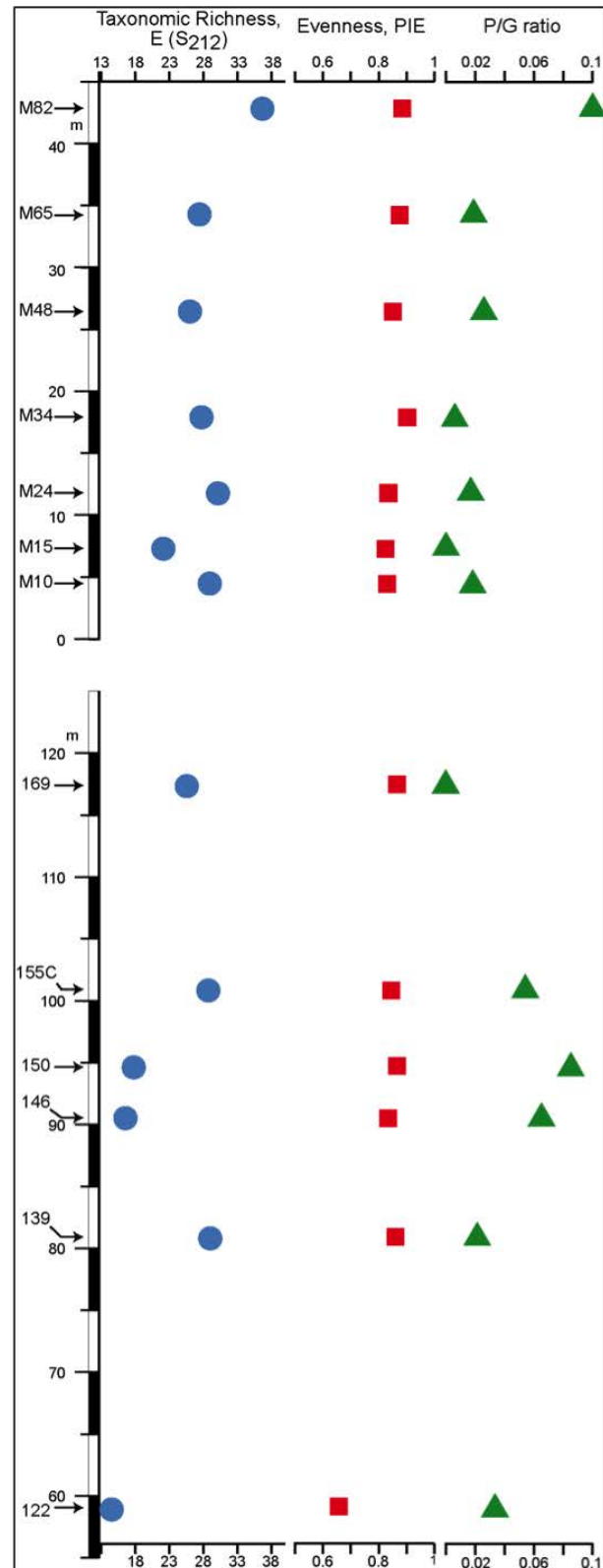


Figure 3.4. Values of diversity metrics, Taxonomic Richness $E(S_{212})$ and evenness (PIE), and estimation of paleoproductivity (P/G) from the Cassis – La Bédoule studied samples. Standard errors associated to the samples Taxonomic Richness are not shown because they are smaller than the diameter of the blue dots.

shows a structure similar to that shown by samples from the South Provence Basin (118-4), whereas the other (111-5) shows the lowest value of Evenness found in the studied samples.

4.2. Peridinioid / Gonyaulacoid (P/G) ratio

The P/G ratio ranges between 0 and 0.085 in the Cassis – La Bédoule samples and between 0 and 0.1 in La Marcouline samples (Fig. 3.4). The two samples from the 398D hole show values of 0.02 and 0.33 for the P/G ratio (Fig. 3.5).

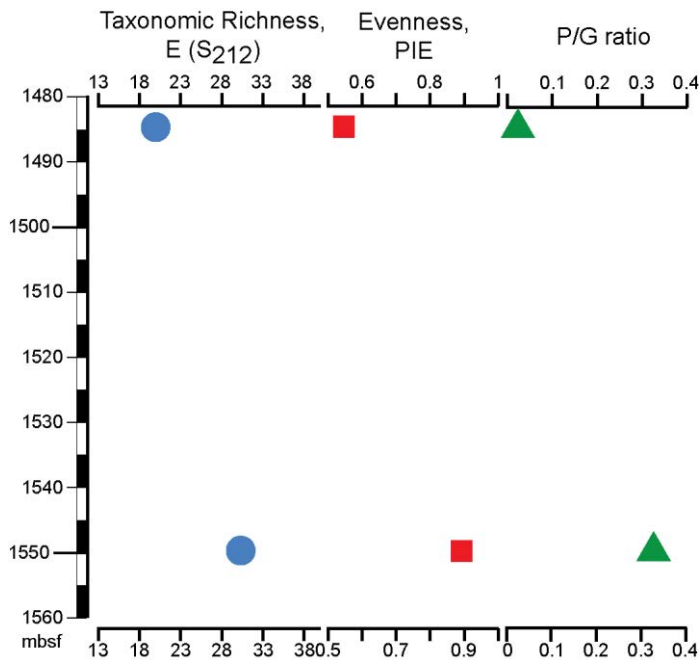


Figure 3.5. Values of diversity metrics, Taxonomic Richness E(S212) and evenness (PIE), and estimation of paleoproductivity (P/G) in studied samples from the 398D .

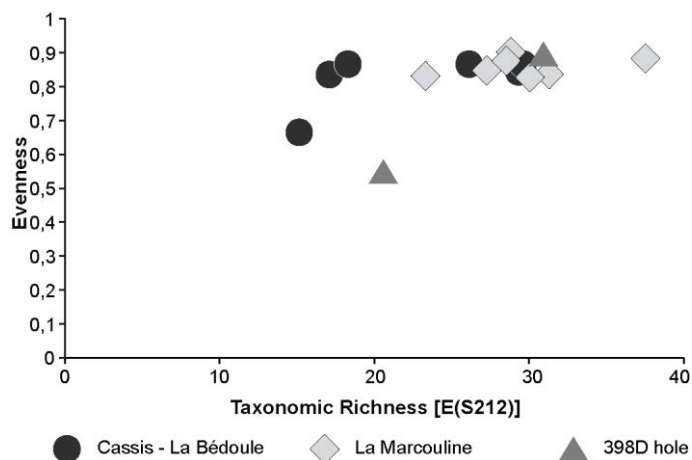


Figure 3.6. Crossplot of Taxonomic Richness, E(S212), and Evenness values Cassis – La Bédoule and La Marcouline successions and 398D DSDP hole samples.

P/G ratio values remain low throughout the successions of the South Provence Basin. However, a decreasing trend characterizes the Cassis – La Bédoule succession interrupted by a marked increase in samples 146 to 155. In the La Marcouline succession P/G ratio values oscillate within a narrow range except for sample MA82 that reaches a much higher value (Fig. 3.4). P/G ratio values in marl levels are slightly higher than in limestone beds.

Seriation of the P/G ratio values calculated from South Provence Basin samples and from 398D site samples, highlights the otherwise suggested differences (Fig. 3.7). Most of the samples showing the lower P/G ratio values come from the La Marcouline succession, whereas higher P/G ratio values are associated to the

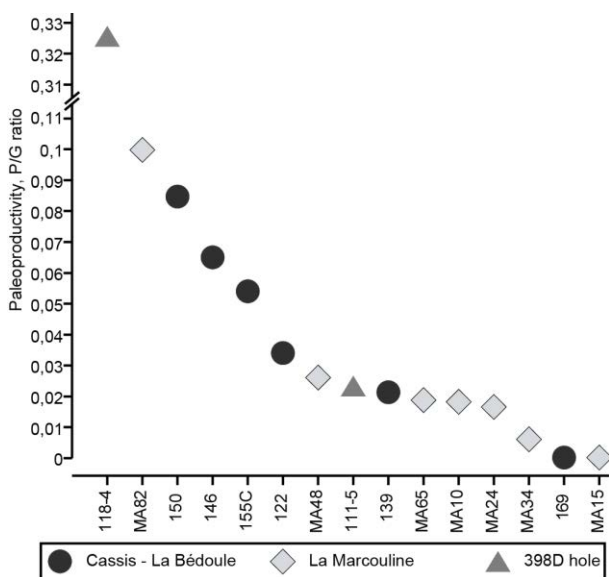


Figure 3.8. Seriation of paleoproductivity values estimated for the Cassis – La Bédoule and La Marcouline successions and for the 398D hole samples

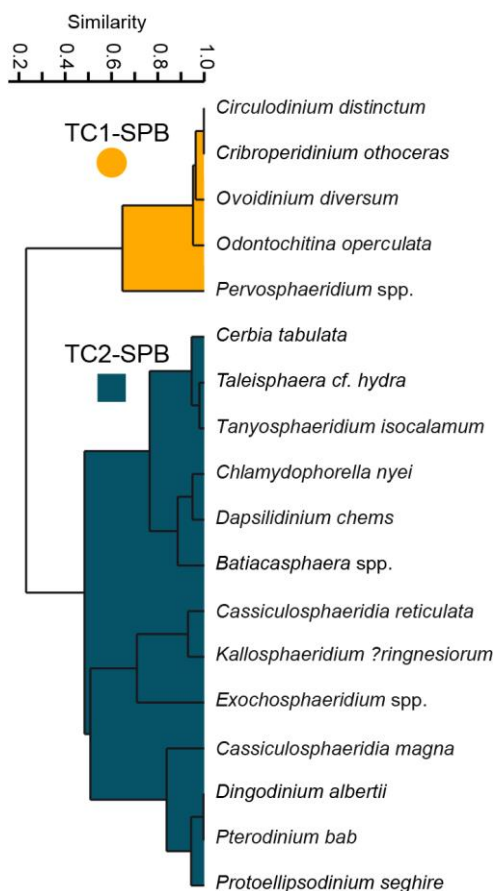


Figure 3.7. UPGMA R-mode cluster analysis of Southern Provence Basin data, using Raup-Crick coefficient as similarity measure. Taxa associated in a cluster usually appear together in samples.

Cassis – La Bédoule samples. Samples from the 398D site show highly contrasted P/G ratio values. P/G ratio value of sample 111-5 (0.02) is intermediate between those of Cassis – La Bédoule succession and La Marcouline successions. However, P/G ratio value of sample 118-4 (0.33) stands out from the rest of the analyzed samples, which is associated to the high relative abundance of *Subtilisphaera* spp. (25.5%).

These results can be interpreted as indicating higher paleoproductivity in the South Provence succession during the Early Aptian (Cassis – La Bédoule succession) than during the Late Aptian (La Marcouline succession), marl levels recording higher productivity than marly-limestone levels. In the 398D hole the highest dinocyst production is estimated in sample 111-5 from the 398D hole, whereas in sample 118-4 estimated paleoproductivity was similar to that recorded at La Marcouline.

4.3. Differentiation of dinoflagellate cyst associations

4.3.1. Dinocyst associations identified in the Southern Provence Basin

The analysis of the data derived from the South Provence Basin allows

testing the differentiation of two dinocyst associations during the Early Aptian and the Lower Late Aptian (Early and middle Aptian). 21 taxa were present in at least two of the 13 samples with relative abundance >2%. *Spiniferites* spp. and *Oligosphaeridium complex* are excluded for the multivariate analysis because they

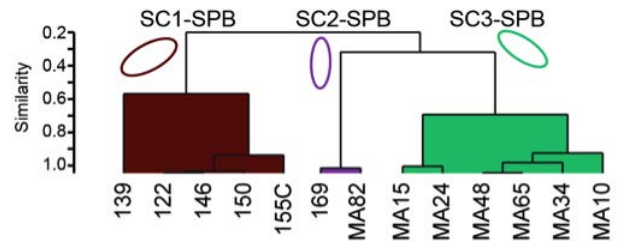


Figure 3.9. UPGMA Q-mode cluster analysis of Southern Provence Basin data, using Raup-Crick coefficient as similarity measure. Samples clustered share similar taxon assemblages

occurred in all the studied samples. Thus the datatable used for multivariate analysis contains 19 taxa and 13 samples. R-mode cluster analysis of the dataset reveals two cluster of taxa (Fig. 3.8), and the Q-mode analysis segregates three clusters of samples (Fig. 3.9). Results from the NPMANOVA analyses are significant for all the pairwise analyses except for those concerning SC2-SPB (Bonferroni-corrected p values >0.05). All of the retained clusters are statistically robust, except SC2-SPB that may be originated by chance.

4.3.1.1. Clusters of taxa and samples and Pairwise NPMANOVA.

R mode – clustering taxon associations

First cluster of taxa, TC1-SPB associates 5 taxa (Fig. 3.8, Table 3.2) present in 7 samples: *Circulodinium distinctum*, *Cribroperidinium orthoceras*, *Odontochitina operculata*, *Ovoidinium diversum*, and *Pervosphaeridium* spp. TC1-SPB groups three gonyaulacinean with the only peridiniinean (*O. diversum*) and ceratiinean (*O. operculata*) on the dataset. The most representative taxon of the cluster is *Circulodinium distinctum*, which is present in six of the seven samples with a mean relative abundance of 27% (max. 50%). Abundance of taxa clustered in TC1-SPB was higher in the Cassis – La Bédoule succession (from the bottom to the base of the *Roboceras hambrovi* ammonite subzone, Fig. 3.10).

Table 3.2. Taxa included in TC1-SPB.

	Number of samples in which it occurs	Mean relative abundance (%)	Max relative abundance (%)	Order	Suborder
<i>Circulodinium distinctum</i>	6	27	50	Gonyaulacales	Gonyaulacineae
<i>Cribroperidinium orthoceras</i>	6	7	13	Gonyaulacales	Gonyaulacineae
<i>Odontochitina operculata</i>	4	6	10	Gonyaulacales	Ceratiineae
<i>Ovoidinium diversum</i>	4	6	9	Peridinales	Peridiniineae
<i>Pervosphaeridium</i> spp.	2	3	3	Gonyaulacales	Gonyaulacineae

Cluster TC2-SPB includes 13 taxa distributed among 11 samples (Fig. 3.8, Table 3.3). All taxa grouped in this cluster are gonyaulacales, with the most taxa being *Dingodinium albertii*, *Pterodinium bab*, and *Chlamydophorella nyei*. The frequency of taxa grouped in TC2-SPB is higher in the lower 30 m of La Marcouline section (Fig. 3.10).

Table 3.3. Taxa included in TC2-SPB.

	Number of samples in which it occurs	Mean relative abundance (%)	Max relative abundance (%)	Order	Suborder
<i>Batiacasphaera</i> spp.	4	3	7	Gonyaulacales	Uncertain
<i>Cassiculosphaeridia magna</i>	2	2	2	Gonyaulacales	Uncertain
<i>Cassiculosphaeridia reticulata</i>	5	3	5	Gonyaulacales	Uncertain
<i>Cerbia tabulata</i>	5	5	6	Gonyaulacales	Gonyaulacineae
<i>Chlamydophorella nyei</i>	6	6	17	Gonyaulacales	Uncertain
<i>Dapsilidinium chems</i>	5	8	13	Gonyaulacales	Uncertain
<i>Dingodinium albertii</i>	6	17	36	Gonyaulacales	Uncertain
<i>Exochosphaeridium</i> spp.	5	3	5	Gonyaulacales	Uncertain
<i>Kallosphaeridium?</i> <i>ringnesiorum</i>	2	5	7	Gonyaulacales	Gonyaulacineae
<i>Pterodinium bab</i>	6	9	16	Gonyaulacales	Gonyaulacineae
<i>Protoellipsodinium seghire</i>	3	3	3	Gonyaulacales	Gonyaulacineae
<i>Taleisphaera cf hydra</i>	2	4	4	Gonyaulacales	Goniodomaceae
<i>Tanyosphaeridium isocalamum</i>	3	3	4	Gonyaulacales	Uncertain

As indicated above, *Spiniferites* spp. and *Oligosphaeridium complex* occur in almost all studied samples (Table 3.4). Their general patterns of relative abundance are similar (Fig. 3.10), increasing slightly from the base to the top of the studied interval.

Table 3.4. Other taxa occurring with relative abundances over 2% in more than two samples.

	Number of samples in which it occurs	Mean relative abundance (%)	Max relative abundance (%)	Order	Suborder
<i>Oligosphaeridium complex</i>	12/13	8	18	Gonyaulacales	Gonyaulacineae
<i>Spiniferites</i> spp.	13/13	22	36	Gonyaulacales	Gonyaulacineae

Q-mode – Samples clustering

The cluster SC1-SPB associates all the Early Aptian samples, except the uppermost sample 169 (Fig. 3.9). All the samples included in this cluster are characterized as limestone levels by their CaCO₃ content (Masse, 1998). Note that no data are available for CaCO₃ in sample 155C that is found in intermediate position between the lower, limestone dominated, interval and the upper, marl dominated, interval.

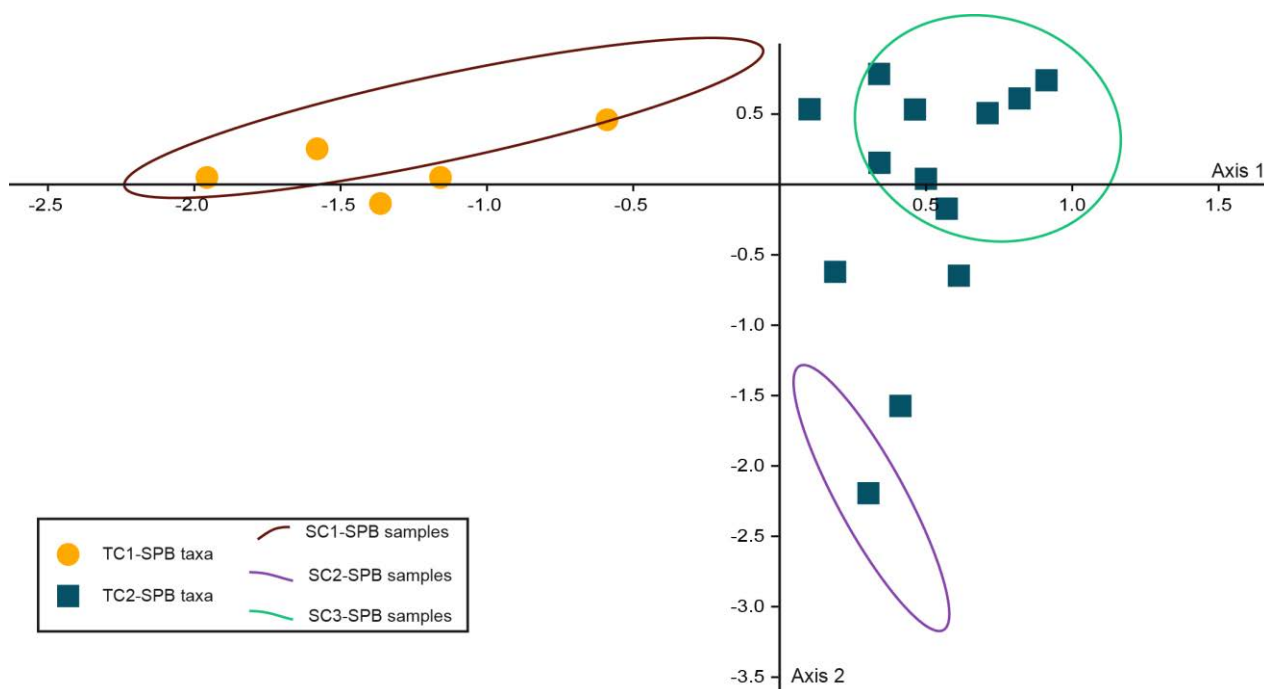


Figure 3.12. Plotting of taxon and sample clusters together in the scatter diagram of CA from the Southern Provence Basin data. The ellipses outline the distribution of samples included in the cluster specified in the legend. The first two axes represent 51% of the total variance of data

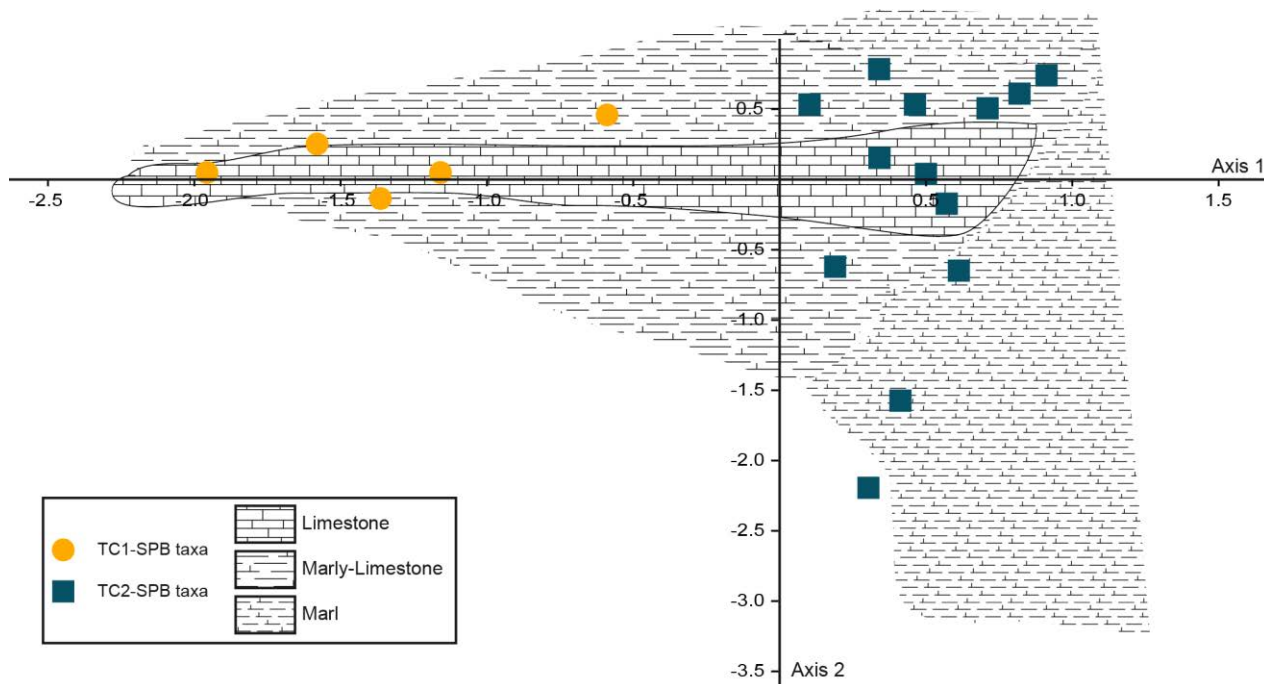


Figure 3.11. Plotting the clusters of taxa from the Southern Provence Basin samples together with the sedimentological properties of the studied samples in the scatter diagram from the Correspondence Analysis.

However, NPMANOVA analysis of clusters points out the weakness of SC2-SPB. The distance between the samples 169 and MA82 that form SC2-SPB is much higher than the distance among samples of SC1-SPB or SC3-SPB.

Plotting of the lithological data on the CA does not show a clear relationship between cluster distribution and lithology (Fig. 3.12).

4.3.2. Dinocyst associations from the Southern Provence Basin and the 398D site.

4.3.2.1. Clusters of taxa and samples and Pairwise NPMANOVA.

The combined analysis of the data derived from the South Provence Basin and the 398D site allows testing the differentiation of dinocysts associations between the Tethyan and Central Atlantic domains. From the 15 considered samples, 21 taxa were present in at least two samples with relative abundance >2%. *Spiniferites* spp. and *Oligosphaeridium complex* were not considered in the multivariate analysis because they occurred in all but one samples. All the *Pterodinium* forms (including *Pterodinium bab*) have been considered together as *Pterodinium* spp. to prevent the loss of environmental information associated with *Pterodinium* genus. Morphological variability in the representatives of *Pterodinium* in the 398D site is much higher than in the Southern Provence Basin. Considering *Pterodinium* specimens at the species level resulted in their disappearance from the datatable, because the relative abundance of individual species does not exceed 2%. The datatable used for multivariate analysis contains therefore 19 taxa and 15 samples. R-mode cluster analysis of the dataset reveals two clusters of taxa (Fig. 3.13), and the Q-mode analysis segregates three clusters of samples (Fig. 3.14). Results of the NPMANOVA analyses support all clusters with Bonferroni-corrected p values under 0.05 except for SC2-SPB.

Clusters resulting for the join analysis of dinocyst data from the South Provence Basin and the 398D hole are highly similar to those obtained for the analysis of the South Provence Basin alone. In the following sections we only detail the remarkable differences.

R mode – clustering taxon associations

Composition of the two taxon clusters obtained from the R-mode analysis was almost the same that for those obtained for the South Provence Basin alone.

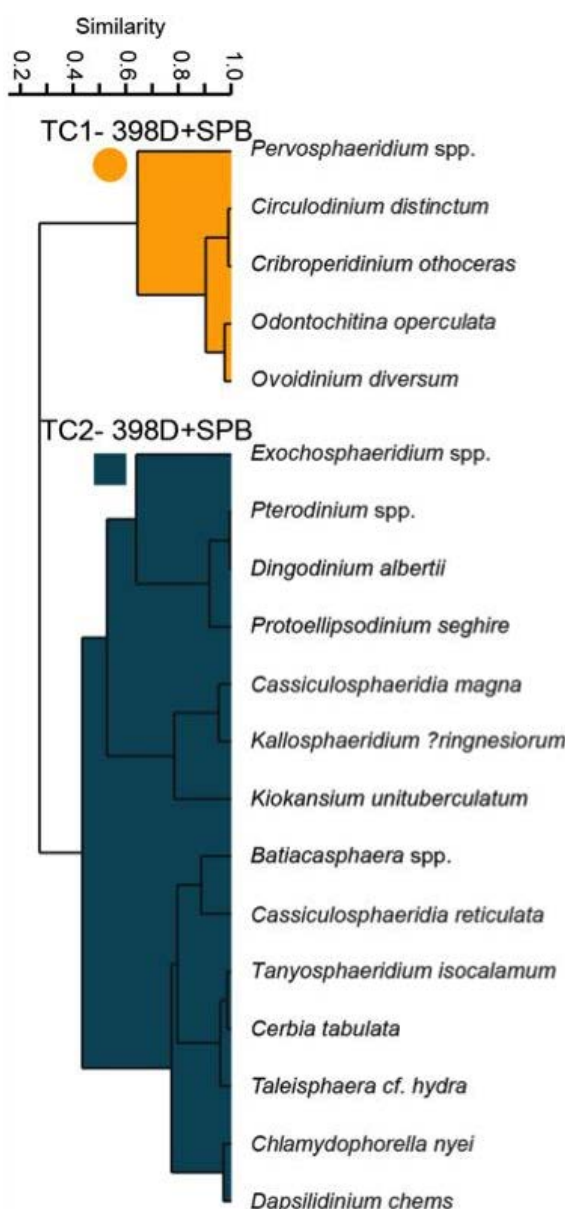


Figure 3.13. UPGMA R-mode cluster analysis of Southern Provence Basin and 398D hole data, using Raup-Crick coefficient as similarity measure. Taxa associated in a cluster usually appear together in samples.

First cluster of taxa, TC1-398D+SPB associates the same 5 taxa as TC1-SPB (Fig. 3.14, Table 3.5): *Circulodinium distinctum*, *Cribroperidinium orthoceras*, *Ovoidinium diversum*, *Odontochitina operculata*, and *Pervosphaeridium* spp. These taxa were present in 9 samples. Distribution of the taxa clustered in TC1- 398D+SPB in the South Provence Basin was the same as described in section 4.2.1 (Fig. 3.4). In the 398D hole, taxa included in TC1-398D+SPB were slightly more abundant in sample 118-4 than in 111-5 (Fig. 3.15).

Cluster TC2- 398D+SPB includes 14 taxa distributed among 13 samples (Fig. 3.13, Table 3.6). This cluster includes all the taxa included in TC2-SPB plus *Kiokansium unituberculatum*, which occurs in both samples from the 398D with a mean relative abundance of 4%. Distribution of TC2- 398D+SPB in the

South Provence Basin was the same as described for TC2-SPB in section 3.2.1 (Fig. 3.10). Taxa included in TC2-398D+SPB represent 26% of the assemblage in the lower sample (118-4) whereas they dominate the assemblage in the upper sample (111-5) with a representation of 76% (Fig. 3.15). *Pterodinium* spp., with a relative abundance of 67%, is responsible for the high frequency of TC2 – 398D+SPB in sample 111-5.

Spiniferites spp. is a considerable contributor to 398D assemblages. Its contribution to assemblages decreases from 14% in the lower sample to 5% in the upper one. *Oligosphaeridium complex* was absent from the upper sample and showed a relative abundance of 3% in the lower sample (Fig. 3.15, Table 3.7).

Table 3.5. Taxa included in TC1- 398D+SPB.

	Number of samples in which it occurs	Mean relative abundance (%)	Max relative abundance (%)	Order	Suborder
<i>Circulodinium distinctum</i>	6	27	50	Gonyaulacales	Gonyaulacineae
<i>Cribroperidinium orthoceras</i>	6	7	13	Gonyaulacales	Gonyaulacineae
<i>Odontochitina operculata</i>	4	6	10	Gonyaulacales	Ceratiineae
<i>Ovoidinium diversum</i>	4	6	9	Peridinales	Peridiniineae
<i>Pervospaeridium</i> spp.	2	3	3	Gonyaulacales	Gonyaulacineae

Table 3.6. Taxa included in TC2- 398D+SPB.

	Number of samples in which it occurs	Mean relative abundance (%)	Max relative abundance (%)	Order	Suborder
<i>Batiacasphaera</i> spp.	4	3	7	Gonyaulacales	Uncertain
<i>Cassiculosphaeridia magna</i>	2	2	2	Gonyaulacales	Uncertain
<i>Cassiculosphaeridia reticulata</i>	5	3	5	Gonyaulacales	Uncertain
<i>Cerbia tabulata</i>	5	5	6	Gonyaulacales	Gonyaulacineae
<i>Chlamydothorea nyei</i>	6	6	17	Gonyaulacales	Uncertain
<i>Dapsilidium chems</i>	5	8	13	Gonyaulacales	Uncertain
<i>Dingodinium albertii</i>	6	17	36	Gonyaulacales	Uncertain
<i>Exochosphaeridium</i> spp.	5	3	5	Gonyaulacales	Uncertain
<i>Kallosphaeridium?</i> ringnesiorum	2	5	7	Gonyaulacales	Gonyaulacineae
<i>Kiokansium unituberculatum</i>	2	3	4	Gonyaulacales	Gonyaulacineae
<i>Pterodinium bab</i>	6	9	16	Gonyaulacales	Gonyaulacineae
<i>Protoellipsodinium seghire</i>	3	3	3	Gonyaulacales	Gonyaulacineae
<i>Taleisphaera cf hydra</i>	2	4	4	Gonyaulacales	Goniodomaceae
<i>Tanyosphaeridium isocalamum</i>	3	3	4	Gonyaulacales	Uncertain

Table 3.7. Other taxa occurring with relative abundances over 2% in more than two samples.

	Number of samples in which it occurs	Mean relative abundance (%)	Max relative abundance (%)	Order	Suborder
<i>Oligosphaeridium complex</i>	13/15	8	17	Gonyaulacales	Gonyaulacineae
<i>Spiniferites</i> spp.	15/15	21	36	Gonyaulacales	Gonyaulacineae

Q-mode – Samples clustering

Composition of the three clusters of samples obtained from the Q-mode cluster analysis was almost the same that for those obtained for the South Provence Basin alone.

The first cluster, SC1- 398D+SPB associates all the samples included in SC1-SPB, most of samples from the La Marcouline succession, and sample 115-5 from the 398D site (Fig. 3.14).

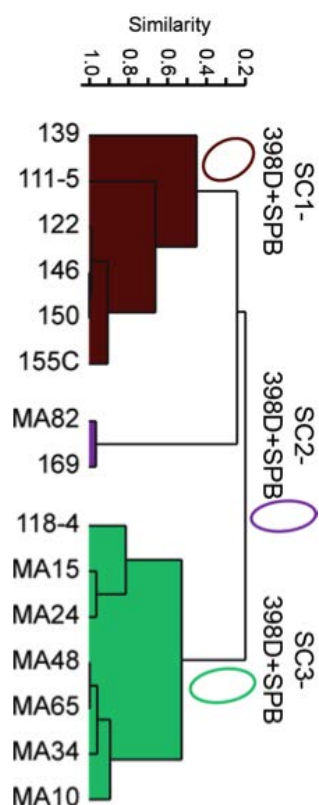


Figure 3.14. UPGMA Q-mode cluster analysis of Southern Provence Basin and 398D data, using Raup-Crick coefficient as similarity measure. Samples clustered share similar taxon assemblages

The cluster SC2- 398D+SPB groups the same two samples as SC2-SPB (169 and MA82, Fig. 3.14).

Third cluster of samples, SC3-398D+SPB is composed of the same samples as SC3-SPB and also includes sample 118-4 from the 398D site (Fig. 3.14).

4.3.2.2. Correspondence Analysis.

Correspondence analysis (CA) points out the congruence between the clusters of taxa and the clusters of samples (Fig. 3.16).

In general terms, the plotting position of taxa and samples is the same than in the scatter diagram resulting of the CA of the South Provence Basin alone (Fig. 3.11). Samples from the 398D site plot in low negative values on the first axis and in positive values on the second axis. *Kiokansium unituberculatum*, which occurred over 2% of relative abundance exclusively in the 398D site samples, is the only taxon included in TC2-398D+SPB plotting in negative values on the first axis.

4.4. Structured Sedimentary Organic Matter (SOM) assemblage analysis

4.4.1. Southern Provence Basin

All the residues were characterized by abundant structured phytoclasts and sporomorphs (see Appendix D.1 for data). Preservation of palynomorphs was good in most samples, allowing the identification of at least the 60% of the observed sporomorphs and dinocysts (Fig. 3.17).

Total Phytoclast category dominates the structured SOM assemblages (Fig. 3.17), ranging between (46% and 86%). Opaque, equidimensional phytoclasts is the

most abundant category. Dinocysts are the second contributor in abundance to the total assemblage (6% to 37%), they dominate in a few samples (155C, MA10 and MA48). Foraminiferal linings are a rare constituent of the assemblages showing usually a relative abundance between 0 and 4%, with a peak at 13% in sample 155C.

The Total Phytoclast category is clearly higher in the lower part of the studied interval, Cassis – La Bédoule succession, showing relative abundances over 69% (max 86%) in all the samples except in sample 155C (46%). The contribution of each phytoclast category is almost constant in this part, opaque, equidimensional phytoclasts being dominant. Wood tracheids are rare. Fungal remains occur in the samples 139 to 155C. Sporomorphs have low abundance in the lower Aptian. Their relative abundance shows an increase

from the base to the top of the Cassis – La Bédoule succession, but sporomorphs never exceeding 6% of the total assemblage. Pollen grains are more abundant than spores in most samples. Total dinocyst contribution increases from the base to the top of the series reaching a maximum of 37% in sample 155C followed by a marked decrease in sample 169, to 6%. The ratio of spores, pollen and dinocyst identifiable to the pseudo-amorphous palynomorphs increases continuously from base to top (Fig. 3.17). Sample 155C is also remarkable regarding its maximum of foraminiferal lining abundance. Other components as zooclasts, acritarchs and other algae were absent from the assemblages of the Cassis – La Bédoule succession.

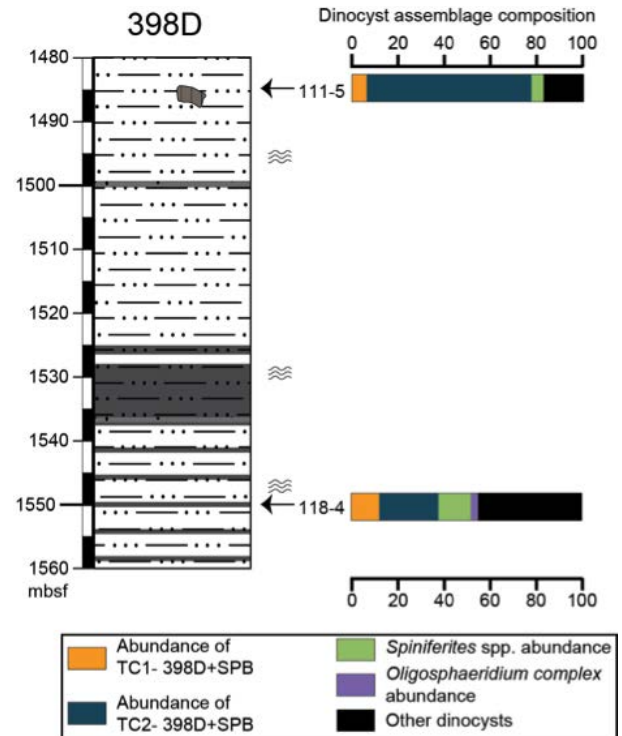


Figure 3.15. Temporal changes in dinocyst associations in the 398D samples (counted as % of specimens assigned to each taxon cluster). TC1- 398D+SPB includes *Circulodinium distinctum*, *Cribroperidinium orthoceras*, *Odontochitina operculata*, *Ovoidinium diversum* and *Pervosphaeridium* spp. and TC2- 398D+SPB includes *Batiacasphaera* spp., *Cassiculosphaeridia magna*, *Cassiculosphaeridia reticulata*, *Cerbia tabulata*, *Chlamydothorea nyei*, *Dapsilidinium chems*, *Dingodinium albertii*, *Exochosphaeridium* spp., *Kallosphaeridium? ringnesiorum*, *Kiokansium unituberculatum*, *Pterodinium bab*, *Protoellipsodinium seghire*, *Taleisphaera cf .hydra*, and *Tanyosphaeridium isocalamum*.

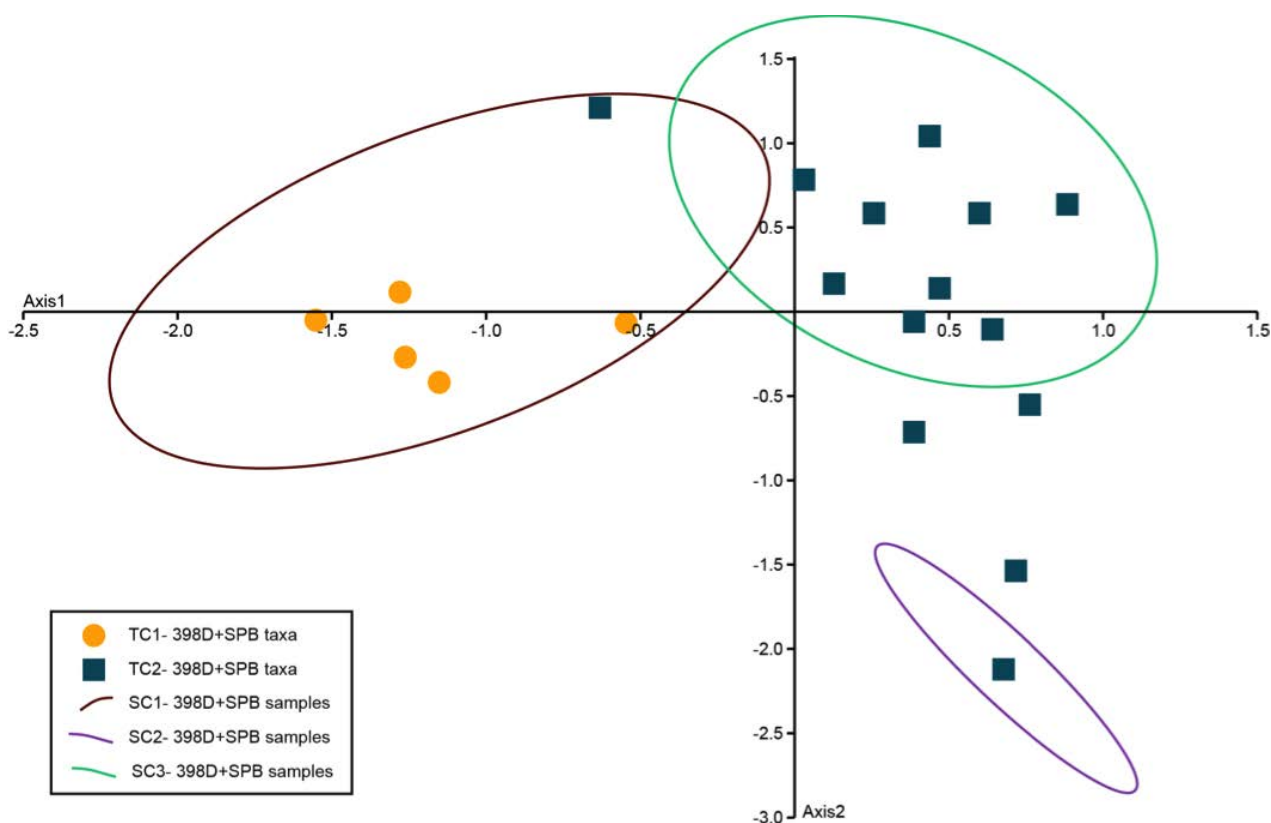


Figure 3.16. Plotting of taxon and sample clusters together in the scatter diagram of CA from Southern Provence Basin and 398D data. The ellipses outline the distribution of samples included in the cluster specified in the legend. The first two axes represent 44% of the total variance of data.

The Total phytoclast category is also dominant in La Marcouline succession (48% to 65% of the structured SOM content), but it does not reach the highest values observed at Cassis - La Bédoule. The relative abundance of wood tracheids never exceeds 3% but they usually occur in La Marcouline samples. Fungal remains are scarce. Sporomorphs reach a maximum of 22% in sample MA82, in which bisaccates exhibit a much higher abundance than in any other studied samples. The relative abundance of dinocysts is almost constant (23 – 36%), interrupted by a low value in sample MA65 (13%). The relative frequency of pseudo-amorphous palynomorphs increases continuously from the base of La Marcouline section up to MA65, compared to identifiable sporomorphs and dinocysts. Foraminiferal linings show low abundances (1 – 4%) but they contribute more constantly to the assemblage in La Marcouline than in the La Cassis – La Bédoule successions. Other elements, as zooclast, acritarchs and algae are present in all the samples, except in MA65, but they never represent more than 3% of the total assemblage.

SPATIO-TEMPORAL VARIABILITY OF APTIAN DINOFLAGELLATE CYSTS

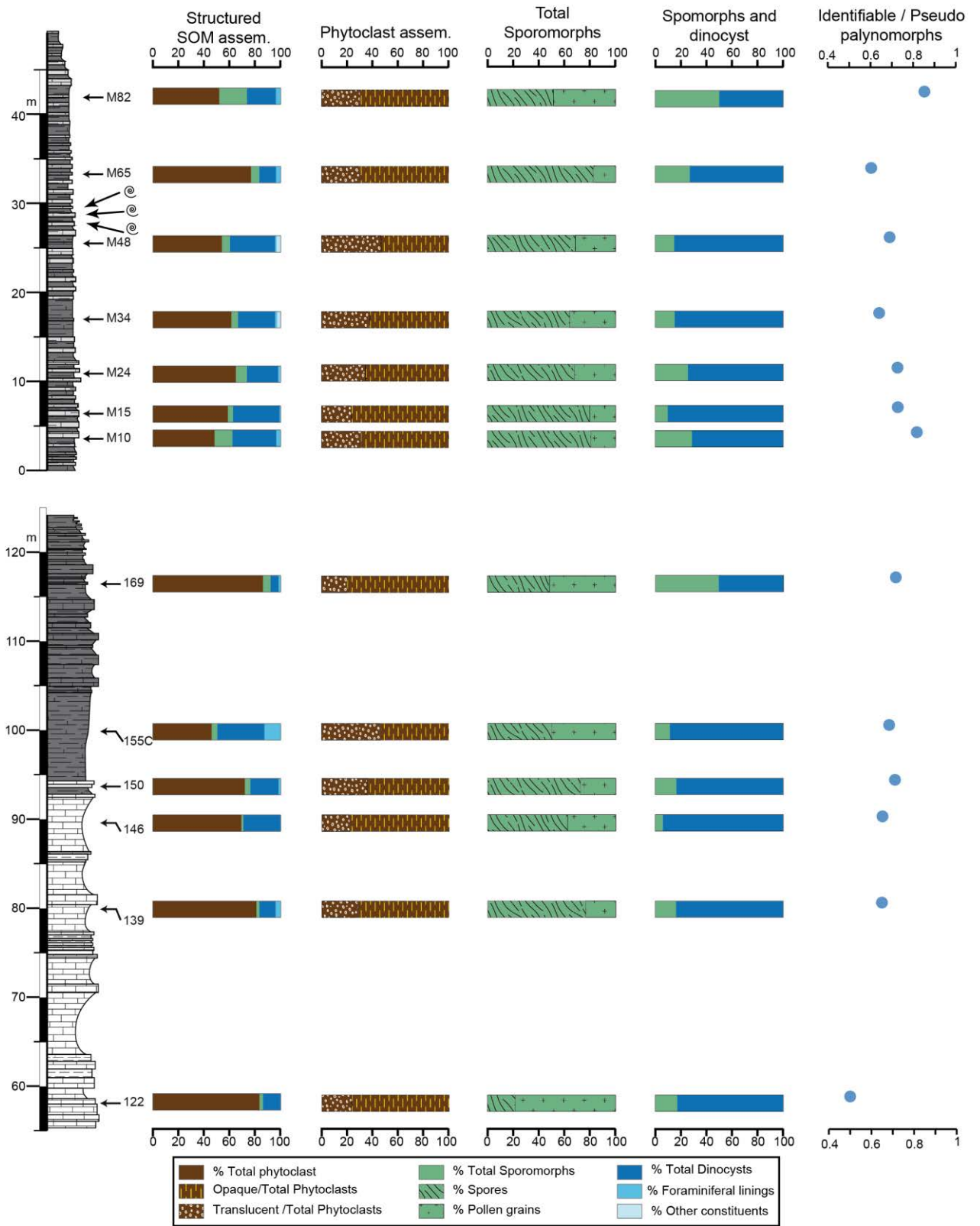


Figure 3.17. Properties of the structured sedimentary organic matter during the Aptian of the Southern Provence Basin (Cassis – La Bédoule and La Marcouline successions). Composition of the Total Phytoclast and Total Sporomorphs categories and Merged Dinocyst and Sporomorphs assemblages and the ratio of Identifiable palynomorphs over pseudo-amorphous palynomorphs.

4.4.2. Structured SOM from the DSDP 398D site

Abundance and preservation of structured SOM is variable among the studied samples. 50% to 97% of the sporomorphs can be identified, dinocysts are rare (Fig. 3.18).

The Total Phytoclast category strongly dominates the assemblages in the 398D samples, ranging between (42% and 94%, Fig. 3.13, see Appendix D.2. for data). Sporomorphs are the second major contributor (5% to 40%). Foraminiferal linings are scarce or absent. Other components (zooclast, acritharch and algae) are absent from all the analyzed samples.

Translucent phytoclast is the most abundant category (Fig. 3.18), membranes

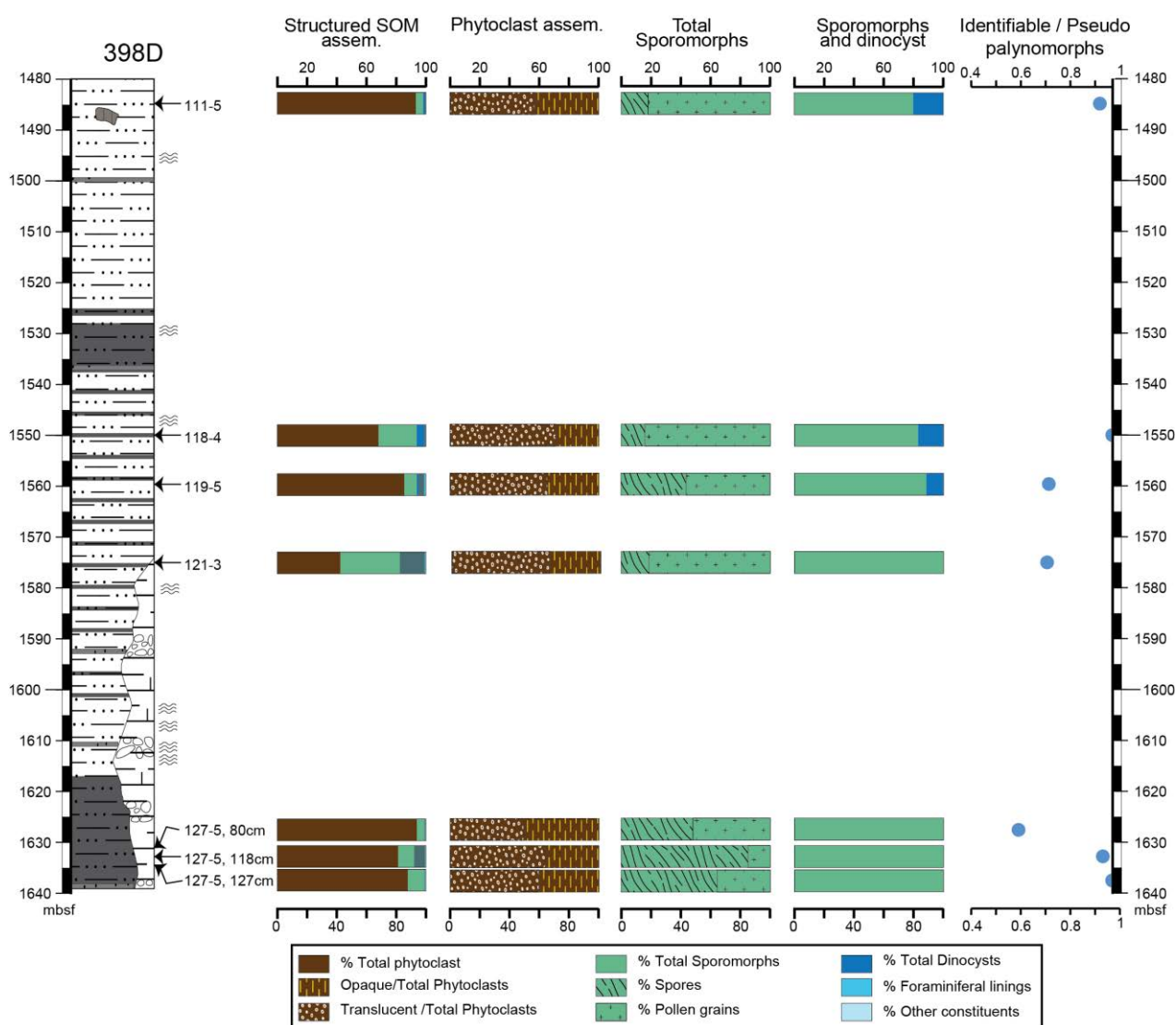


Figure 3.18. Properties of the structured sedimentary organic matter during the Aptian of the 398D site. Composition of the Total Phytoclasts and Total Sporomorphs categories and Merged Dinocyst and Sporomorph assemblages, and ratio of identifiable palynomorphs over pseudo-amorphous palynomorphs.

and pseudo-amorphous phytoclasts being the most common elements. Opaque phytoclasts are the second major contributor in terms of abundance to the total assemblage (15 – 41%), equidimensional phytoclasts are more common than lath phytoclasts. The relative abundance of wood tracheids never exceeded 1% in any of the analyzed samples. No clear trend appears in phytoclast distribution. The total abundance of palynomorphs (Total sporomorphs and dinocysts and pseudo-amorphous palynomorphs) ranges between 6 – 18%, except in two samples where it peaks to 32% (118-4) and 57% (121-3). These two peaks are associated with peaks in bisaccate pollen grains (Fig. 3.18). Sporomorphs dominate over pollen grains in the lower part of the studied interval, but the situation reverses in the upper part. Bisaccate pollen grains are the more common pollen type. Dinocysts occur only in the three uppermost samples.

4.5. Marks of paleoenvironmental changes in the Southern Provence Basin.

The characteristics of the dinocyst and structured SOM assemblages allow the differentiation of five intervals: one represented by the single sample 122; one for the lower part of the section (interval 1); the sample 169; one for the upper part (interval 2) of the stratigraphic succession; and the sample MA82 (Fig. 3.10, Fig. 3.17). The variations of dinocyst diversity (taxonomic richness and evenness) and paleoproductivity (P/G ratio) are fully consistent with the discrimination of these 5 stratigraphical sets of samples (Fig. 3.19). Both the taxonomic richness, $E(S_{212})$, and the evenness show an increasing trend from the base to the top of the succession (Fig. 3.19). Paleoproductivity long-term variations show a more complex pattern. The 5 stratigraphical set of samples, discriminated from their dinocyst and structured SOM assemblages, highlight the regional and global paleoenvironmental changes recognized by other studies in the Southern Provence Basin.

4.5.1. Early Aptian: a phase of carbonate platform demise.

The first stratigraphical set discriminated consists exclusively in Sample 122 of the Cassis – La Bédoule succession. Sample 122 shows extremely particular dinocysts and structured SOM assemblages (Fig. 3.10, Fig. 3.17). Dinocyst assemblage is dominated by TC1-SPB taxa (57%) and by *Rhynchodiniopsis* sp. (29%), which is not taken into account for multivariate analyses because it only occurs

in this sample. From the structured SOM analysis it is shown that opaque phytoclasts dominate the assemblage. It is also remarkable, that preservation of palynomorphs is worse than in any other studied sample (Fig. 3.17). Sample 122 also shows the lowest values of taxonomic richness and evenness in the studied interval (Fig. 3.19).

4.5.2. Oceanic Anoxic Event 1a in the Southern Provence Basin, the Goguel event.

The “*interval 1*” includes four samples from the lower part of the studied series (sample 139 to sample 155C). The samples come from the limestone-dominated interval in Cassis – La Bédoule succession. Taxa included in TC1-SPB dominated the assemblages (Fig. 3.10) showing relative abundances between 17% and 62%. Relative abundance of taxa included in TC2-SPB did not exceed 17%, *Spiniferites* spp. and *Oligosphaeridium complex* ranged between 2% - 29% and 2% - 11%, respectively. Study of structured SOM revealed that samples included in interval 1 are characterized by decreasing abundance of phytoclasts and low relative abundance of sporomorphs (Fig. 3.17). Within the palynomorphs assemblage, dinocyst dominate whereas sporomorphs were of secondary importance. An upwards increase in the abundance of pollen grains is observed, although spores remain more abundant than pollen grains in the *interval 1*. Foraminiferal test linings are rare in these samples, with the exception of

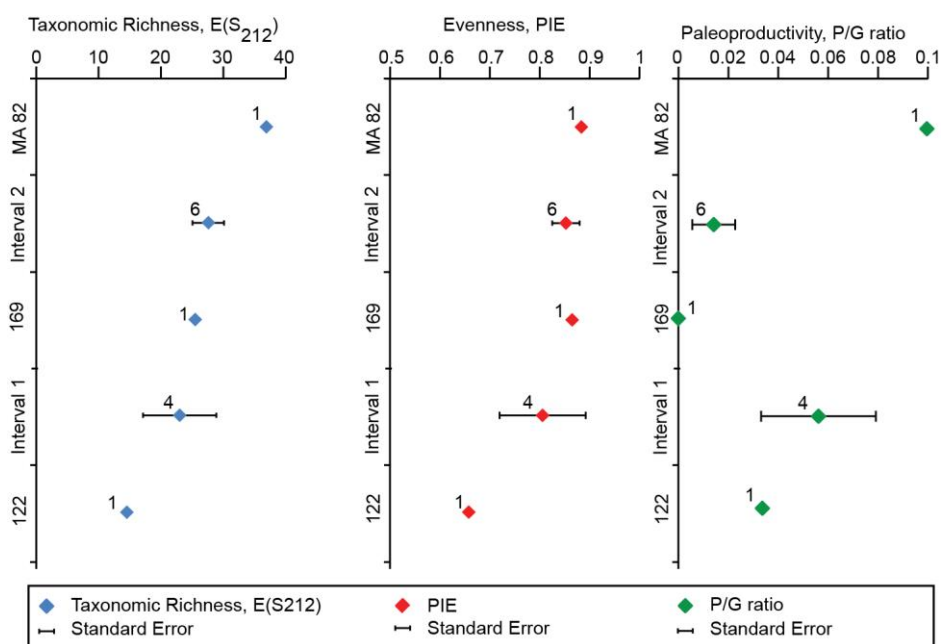


Figure 3.19. Diversity values, taxonomic richness, $E(S_{212})$, and evenness, and paleoproductivity from Cassis – La Bédoule and La Marcouline samples merged by interval. Estimation of paleoproductivity was calculated with the P/G ratio proposed by (Versteegh, 1994). Numbers next to symbols indicate the number of samples take into account for calculation of mean values.

sample 155C (13%). Samples grouped in this interval show the highest relative abundances of fungal remains from the entire studied series, with relative abundances around 2% - 3%, whereas wood tracheids show their minimal abundances.

Structure of dinocyst assemblages expresses a high variability in the interval 1. Dinocyst assemblages have low values of taxonomic richness and evenness (Fig. 3.19). Furthermore, variability (standard error) of both the taxonomic richness and the proportional frequency of taxa (evenness) is high. Paleoproductivity in the interval 1, estimated through the P/G ratio, show high values increasing markedly from sample 139 to sample 150 and slightly decreasing in sample 155C.

Samples grouped in the interval 1 (samples 139 to 155C) are grossly coeval with the OAE 1a Interval, recognized through the analysis of the $\delta^{13}\text{C}$ curve (Moullade *et al.*, 2015).

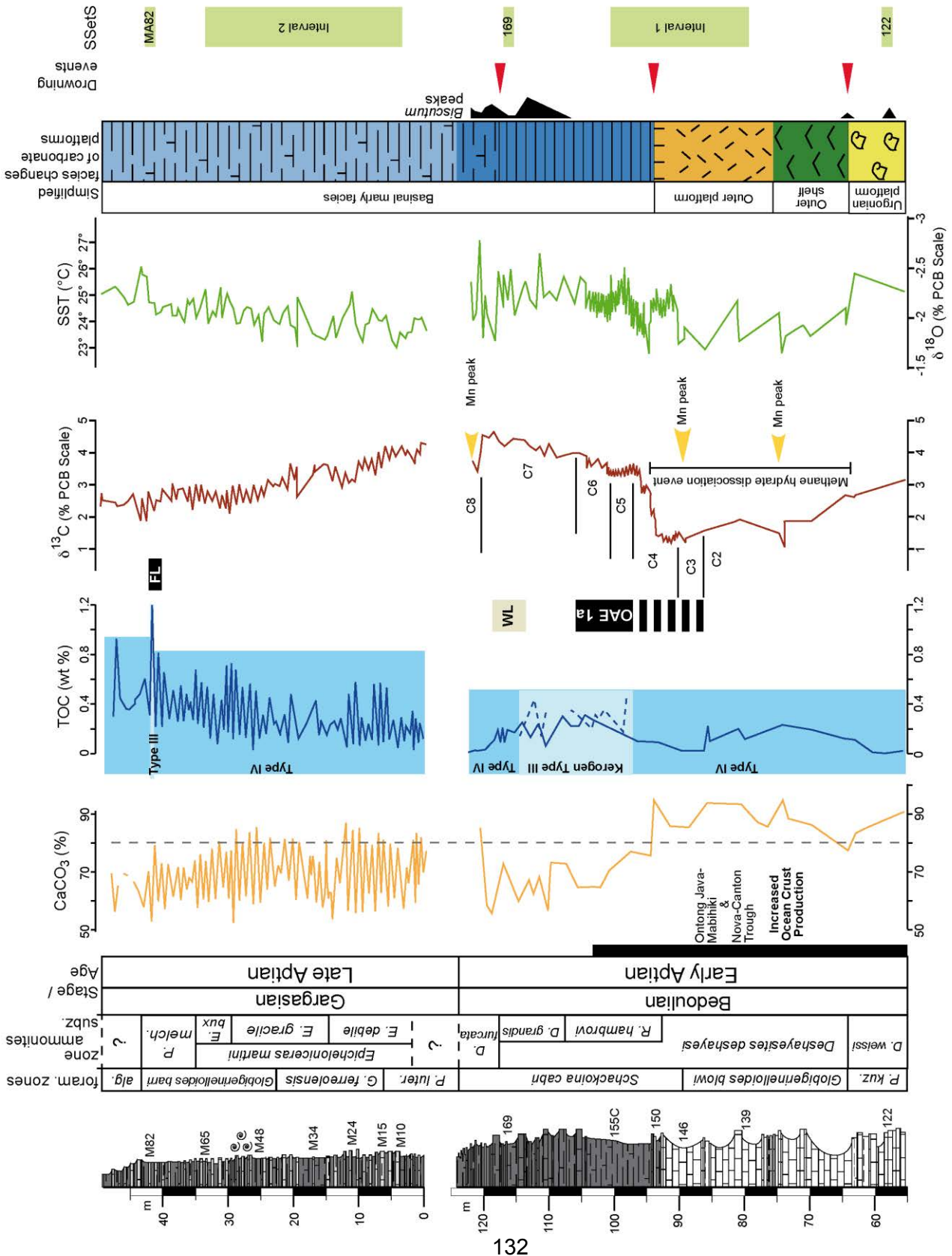
4.5.3. The White Level (Niveau Blanc)

Sample 169 is discriminated by its particular structured SOM assemblage (Fig. 3.17): with the lowest value of dinocyst abundance from the structured SOM assemblage (6%), associated to the absolute maximum of continental constituents (92%) in the whole interval. Within the structured SOM opaque phytoclast is dominant (69%). The dinocyst assemblage shows a transitional composition between the underlying samples TC1-SPB taxa-dominated and the overlying samples TC2-SPB taxa-dominated. Diversity estimation, taxonomic richness and evenness, express medium values. The estimated paleoproductivity is equal to 0 because of the total absence of peridinioids in this sample. Moullade and Tronchetti (2010) suggest that beds 166 to 170 from in the Cassis – La Bédoule succession correspond to the so called “White Level”.

4.5.4. Early Late Aptian

Samples MA10 to MA65 from the La Marcouline succession are included in the upper “interval 2”. Three of them come from marly-limestone beds (MA15, MA34 and MA65) and the three other from marl beds (MA10, MA24 and MA48). Taxa included in TC2-SPB dominate the assemblages, their representation ranging between 32% and 53% (Fig. 3.10). Taxa included in TC1-SPB are absent, except from MA10 were it represented 3% of the assemblage. *Spiniferites* spp. was an important contributor to dinocyst assemblages during this interval showing relative abundances between 15%

and 36%. Relative abundances of *Oligosphaeridium complex* during the interval 2 were more variable than in the rest of the series (0-18%). Study of structured SOM shows that the samples included in the interval 2 are characterized by an increase in elements of continental origin (Total phytoclast and Total sporomorphs) and,



consequently, by a decrease in the frequency of marine groups (Dinocysts, Foraminiferal linings and other constituents) (Fig. 3.17).

Dinocyst assemblage structure of samples included in the interval 2 is characterized by high diversity values (high values of taxonomic richness and evenness) associated to small variations among samples (low standard error) (Fig. 3.19). In the interval 2, the mean P/G ratio and its associated variability, appear much lower than in the interval 1.

4.5.5. The Fallot Level

The uppermost discriminated interval includes exclusively Sample MA82 of the La Marcouline section. Sample MA82 exhibits an extremely high abundance of sporomorphs (22%) that reaches its absolute maximum in this sample (Fig. 3.17). *Spiniferites* spp. and *Oligosphaeridium complex* were the main contributors to the dinocysts assemblage (27% and 16%, respectively) (Fig. 3.10). Bisaccate pollen grains is the major Sporomorph category. It is remarkable that even if the abundance of the total sporomorph group increases, the contribution of continental particles (Total phytoclasts and Total sporomorphs) to the total structured SOM assemblage decreases. It is also noteworthy that this increase in pollen grains is not coincident with an increase in the abundance of dinocysts, a usual pattern (Fig. 3.17). Sample MA82 showed the highest values of taxonomic richness and paleoproductivity, and a high value of evenness (Fig. 3.19).

Baudin *et al.* (2008) recognized the Fallot level (Bréhéret and Delamette, 1988) in beds 77 and 79 (sample MA82) at the La Marcouline section.

Figure 3.20. Synthesis of published data in the Early – Late Aptian studied interval from the South Provence Basin. Lithological legend of the Cassis – La Bédoule succession and biostratigraphical details in Fig. 3. Carbonate content curve from the Cassis – La Bédoule after Masse and Machhour, (1998) and Renard and de Rafélis (1998) and after Renard *et al.* (2007) for the La Marcouline succession, the grey dashed line at 80% indicate the boundary between marls and limestones after Masse (1998). Total organic carbon content (TOC, weight %) and kerogen type information from the Cassis – La Bédoule after Masse and Machhour (1998) and Stein *et al.* (2012) and after Baudin *et al.* (2008) for the La Marcouline succession and for the position of the Fallot Level (FL). Kerogen Type III is usually related to terrestrial higher plant debris, whereas Type IV is indicative of residual deeply altered organic matter. The White (WL) Level is placed following Moullade and Tronchetti (2010). Carbon and oxygen isotope records after Kuhnt *et al.*, (2011, 1998b), limits of the carbon segments defined by Menegatti *et al.*, (1998) after Lorenzen *et al.* (2013). Identification of the position of the OAE 1a after Lorenzen *et al.* (2013). The manganese (Mn) peaks are placed after Renard *et al.* (2005). Estimation of Sea Surface Temperature (SST) after Kuhnt *et al.* (2011). The simplified facies during the Early Aptian and the placement of the drowning events are redrawn after Masse and Fenerci-Masse (2013a). Peaks of abundance of the nannofossil genus *Biscutum* after Bergen, (1998). Stratigraphical set of samples identified in function of their dinocyst and structured SOM assemblages characteristics, see section 5.5. Basinal marly facies drawn in light blue on the simplified facies column are here proposed for the Late Aptian in the North Provence platform area.

5. Interpretation and discussion

5.1. Factors controlling dinocysts distribution

5.1.1. Dinocyst distribution in the Southern Provence Basin during the Aptian

There is an abrupt shift in dinocyst associations at the Early – Late Aptian boundary in Southern Provence Basin. During the Early Aptian assemblages are dominated by dinocysts of the cluster TC1-SPB, but its relative abundance fall down in the uppermost Early Aptian. The decline of the species pool supporting TC1-SPB is associated to a replacement by dinocyst species of TC2-SPB (Fig. 3.10). This marked segregation in the distribution of the two identified associations is reflected in the Correspondence Analysis (Fig. 3.11), where TC1-SPB taxa plot on negative values of the first axis and TC2-SPB taxa plot on the positives ones.

A similar pattern of taxon replacement is recorded for benthic and planktonic foraminifera, and for ostracods. In order to facilitate the comparison with dinocysts, an UPGMA cluster analysis was performed on the foraminiferal datasets published by Moullade *et al.* (1998b, 2005) (Fig. 3.21, see Appendix E for cluster compositions). Cluster analyses of benthic and planktonic foraminifera both reveal two clusters of taxa and two clusters of samples. All the Early Aptian samples are grouped in one cluster and are dominated by one of the taxon clusters. Similarly, all the Late Aptian samples are clustered together and are dominated by the other cluster of taxa (Fig. 3.21). Babinot *et al.* (2007) studied the ostracods of the Early – Late Aptian boundary in Provence. They recognized two associations, one for the latest Early Aptian and the other characterizing the earliest Late Aptian, sharply separated by an episode of impoverished fauna at the base of the Late Aptian (Babinot *et al.*, 2007).

Numerous studies have analyzed the Aptian of the Southern Provence Basin (e.g. Kuhnt *et al.*, 1998b, 2011; Masse and Machhour, 1998; Renard and de Rafélis, 1998; Beltran *et al.*, 2007, 2009; Renard *et al.*, 2007; Baudin *et al.*, 2008; Stein *et al.*, 2012). None of the investigated sedimentological or geochemical proxies ($\delta^{13}\text{C}_{\text{carb}}$, $\delta^{18}\text{O}$, P content, redox-sensitive and trace elements, composition of the clay fraction assemblages...) show a pattern similar to that shown by micropaleontological associations of dinocyst, foraminifers and ostracods.

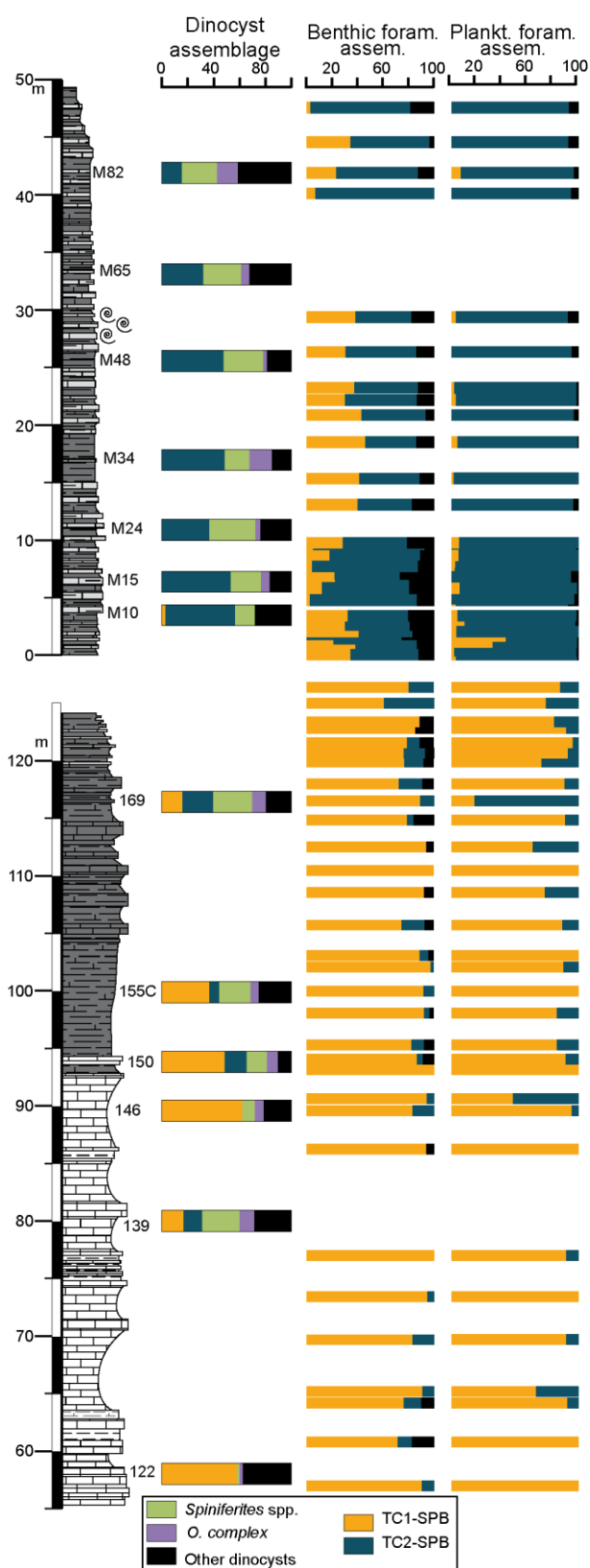
The shift in the composition of microfaunal assemblages is coeval to the last drowning phase of the North Provence carbonate platform, at the *Deshayesites grandis* – *Dufrenoya furcata* transition (Fig. 3.3 and 3.20) (Masse and Fenerci-Masse, 2011, 2013a). Changes in the physiography of carbonate platforms bordering the South Provence Basin are here regarded as the main factor controlling the distribution of dinoflagellate communities. The first axis of the CA of dinocyst data (Fig. 3.11) may reflect the switch of paleoceanographic conditions associated to the offset of the North Provence platform.

5.1.2. Stability and predictability

The high values of taxonomic richness and evenness from the Southern Provence Basin and 398D samples (Fig. 3.6) confirm that the studied Aptian dinocyst assemblages were associated to marine stable conditions (see discussion in section 5.1.2 from Chapter 2 for details on the interpretation of relative diversity values). However, some details must be discussed.

Aptian dinocyst assemblages from the Southern Provence Basin are characterized by high values of taxonomic richness and evenness, i.e. assemblages were composed by numerous different taxa showing balanced relative frequencies (Fig. 3.4). A trend toward higher taxonomic richness and evenness is observed from the base to the top of the series (Fig. 3.19). Furthermore, standard errors of diversity values are lower in the interval 2 than in interval 1 indicating lower environmental variability during the Late Aptian than during the Early Aptian. These changes mirror the long-term paleoenvironmental evolution of the Southern Provence Basin and of its the bordering carbonate platforms during the Aptian.

The central part of the Southern Provence Basin received hemipelagic sedimentation during its early Cretaceous history (Masse and Fenerci-Masse, 2013a). The extension and physiography of the adjacent carbonate platform and the paleoceanography of the Basin are strongly linked. During the *Deshayesites deshayesi* ammonites zone (Early Aptian) three drowning phases of the carbonate platforms are reflected in the stratigraphical succession. They are associated to the replacement of rudist biofacies on the platforms by biocalcarenites and cherty limestones indicating the environmental evolution from infralittoral to relatively deep circalittoral environments (Masse and Fenerci-Masse, 2011, 2013a). The third drowning phase



was followed by the development of basinal marly facies over the entire Northern Provence platforms (Masse and Fenerci-Masse, 2013a).

The increasing water depth over the Northern Provence platform modified the conditions in the Basin. Water masses properties over relatively shallow carbonate platforms are influenced by enhanced evaporation rates that condition the density of water masses, allowing the establishment of strong fronts between water masses (Patterson and Walter, 1994). With drowned platforms, water exchanges with the basin are facilitated and the fronts may weaken. These changes led to the development of more stable and homogeneous conditions.

The two samples from the 398D that yielded reliable dinocyst data show different assemblage structures (Fig. 3.5). Assemblage structure from the lowermost sample (118-4) is equivalent to the assemblage structure in samples from the Southern Provence Basin during stable marine conditions, whereas the uppermost sample (111-5) was characterized by low values of evenness (0.55), as consequence of the dominance of *Pterodinium* (67% of dinocysts).

Figure 3.21. Comparison of the distribution of dinocysts associations, with the distribution of benthic and planktonic foraminifera associations along the Cassis – La Bédoule and the La Marcouline successions. The dinocyst assemblage takes into account the TC1-SPB and TC2-SPB taxa, *Spiniferites* spp. and *Oligosphaeridium complex* abundance and taxa under 2% of representation or occurring in only one assemblage. Benthic and planktonic foraminifera assemblages take into account TC1-SPB and TC2-SPB taxa abundances and taxa under 2% of representation or occurring in only one sample.

Pterodinium is widely recognized as indicative of stable open marine environments (e.g. Wall *et al.*, 1977; Marshall and Batten, 1988; Smelror and Leereveld, 1989; Dale, 1996; Prince *et al.*, 1999, 2008; Harris and Tocher, 2003; Crouch and Brinkhuis, 2005), usually characterized by high values of taxonomic richness and equable frequency among individual dinocyst. We did not found a reasonable ecological/environmental explanation for the outstanding dominance of *Pterodinium* spp. in sample 111-5.

5.2. Paleoenvironmental significance of the dinocyst associations

We compared dinocyst presence/absence datasets, with the relative abundance distributions, sedimentological information, stable isotopes ($\delta^{13}\text{C}$ and $\delta^{18}\text{O}$) and trace elements to identify the paleoenvironmental significance of the taxa. Dinocysts are excellent source for paleoenvironmental interpretations (Goodman, 1987) even if they do not represent the entire planktonic community and even if the interpretation of the occurrence and/or abundance of taxa is not straightforward (Pearce *et al.*, 2003).

The environmental preferences and the tolerances to variations of the environmental conditions of some dinocyst taxa are analyzed in Chapter 2. The stratigraphic range of all the dinocyst taxa considered in the Albian study includes the Aptian period. The paleoecological and paleoenvironmental models derived for the Albian dinocysts fauna can be directly tested on the Aptian data.

5.2.1. Early Aptian conditions: Intrashelf Basin surrounded by carbonate platforms

During the time of widespread extension of the carbonate platforms, dinocyst assemblages were dominated by taxa included in the cluster TC1-SPB (Fig. 3.10): *Circulodinium distinctum*, *Cribroperidinium orthoceras*, *Odontochitina operculata*, *Ovoidinium diversum* and *Pervosphaeridium* spp. None of these taxa reach a relative abundance of 2% in the La Marcouline succession, except *Pervosphaeridium* spp. in sample MA10. The interval dominated by TC1-SPB taxa was also characterized by low diversity values (low taxa richness and evenness) and high P/G ratio values (Fig. 3.4).

It is likely that the limited distribution of *Circulodinium distinctum*, *Cribroperidinium orthoceras*, *Odontochitina operculata*, *Ovoidinium diversum* and *Pervosphaeridium* spp. to the interval of carbonate platform demise, reveals their

tolerance to certain environmental factor variations (such as temperature and/or salinity) and preference for mesotrophic conditions. These species were suggested by other authors as tolerant to environmental variations and indicative of mesotrophic conditions. The genus *Circulodinium* was considered as characteristic of inner neritic and restricted marine environments by Wilpshaar and Leereveld (1994), whereas Harris and Tocher (2003) suggested it may be indicative of increasing in water depth or salinity. The environmental tolerance of the genus *Cribroperidinium* is suggested by the disparity on the environmental preferences assigned to him by different authors. (Peyrot *et al.*, 2011) and references therein) described *Cribroperidinium* as characteristic of inner neritic environments, but Lebedeva (2010) considered it as tolerant to various environments. From the analysis of the dinocyst distribution in the Cenomanian of the Western Interior Basin, Harris and Tocher (2003) found *Cribroperidinium orthoceras* at all investigated sites but more common in offshore sites. Previous interpretations of environmental preferences for the genus *Odontochitina*, and *O. operculata* in particular, vary from preferring mainly middle neritic environments (Helenes and Somoza, 1999) to marker of open marine environments (Marshall and Batten, 1988), and from eurybiontic or cosmopolitan (Pearce *et al.*, 2009; Lebedeva, 2010; Masure *et al.*, 2013) to indicative of eutrophic environments (Coccioni *et al.*, 1993). As previously discussed, peridinioids, like *Ovoidinium diversum*, are considered analogs to modern heterotrophic dinocysts like *Protoperidinium* (e.g., Lewis *et al.*, 1990; Hamel *et al.*, 2002; Radi and de Vernal, 2004) and thus, are indicative of enhanced paleoproductivity (Sluijs *et al.*, 2005; Prauss, 2012b). Davey (1979) suggested oceanic preferences for *O. diversum*. Lister and Batten (1988) accepted *O. diversum* as indicative of oceanic influx but they reported the species in the Late Aptian of SE England in inner – mid shelf paleoenvironments. The occurrence of *O. diversum* in a variety of environmental conditions is rather indicative of tolerance to some environmental variations despite preferences for open stable marine environments.

The increase of terrigenous inputs from beds 128-129 to the top of the Cassis – La Bédoule succession might be coeval to an increase of nutrient supply, which is supported by peaks in the abundance of nannofossils of the genus *Biscutum* (Bergen, 1998), a positive excursion of strontium (Renard and de Rafélis, 1998), low values of $\delta^{18}\text{O}$ and an increasing trend of $\delta^{13}\text{C}$ (Kuhnt *et al.*, 1998b; Lorenzen *et al.*, 2013). Increasing nutrient availability is also alluded as trigger of the biotic replacement on

carbonate platforms, from rudist to orbitolinids, and associated communities (Föllmi *et al.*, 1994; Vilas *et al.*, 1995; Föllmi and Gainon, 2008, p. 200; Huck *et al.*, 2013; Masse and Fenerci-Masse, 2013a). However, Masse and Fenerci-Masse (2013a) noted that the development of the *Palorbitolina* community may also result of the replacement of a stenotopic biota after environmental perturbations.

Environmental preferences of *Circulodinium distinctum*, *Cribroperidinium orthoceras*, *Odontochitina operculata* and *Ovoidinium diversum* evidenced in the Aptian of Provence agree with those made for the Albian data of the Iberian margin in Chapter 2. *Circulodinium distinctum*, *Odontochitina operculata* and the representative of the genus *Cribroperidinium* (*C.? edwardsii*) were identified in the Albian as tolerant to environmental conditions. Peridinioids, as *Ovoidinium diversum*, were consistently associated to meso- to eutrophic conditions. The single *Ovoidinium* species present in the analyzed Albian samples, *Ovoidinium* sp. (Hasenboehler, 1981), was restricted to levels directly influenced by riverine inputs.

Pervosphaeridium is represented by *P. cenomaniense* in Albian samples from the Iberian margin, which is restricted to marly-chalk levels of the 398D site. *P. cenomaniense* was characterized as preferring open marine environments. The carbonate, Sr and TOC content are similar in the Aptian levels (Masse and Machhour, 1998; Renard and de Rafélis, 1998) in which *Pervosphaeridium* spp. occurred and in the Albian levels (Chamley *et al.*, 1979) in which *P. cenomaniense* occurred. The tolerance to environmental fluctuations and the preference for mesotrophic conditions here proposed to *Pervosphaeridium* spp. may also be applied to *P. cenomaniense*.

5.2.2. Late Aptian conditions: Intrashelf Basin without carbonate platforms

Late Aptian dinocysts assemblages from the La Marcouline succession are characterized by the dominance of taxa included in cluster TC2-SPB: *Batiacasphaera* spp., *Cassiculosphaeridia magna*, *Cassiculosphaeridia reticulata*, *Cerbia tabulata*, *Chlamydophorella nyei*, *Dapsilidinium chems*, *Dingodinium albertii*, *Exochosphaeridium* spp., *Kallosphaeridium? ringnesiorum*, *Protoellipsoidinium seghire*, *Pterodinium bab*, *Taleisphaera cf. hydra* and *Tanyosphaeridium isocalamum*. In general terms, samples from the Late Aptian interval are also characterized by high diversity values (highest taxa richness and evenness) and low paleoproductivity values (P/G ratio) (Fig. 3.4).

Representation of the TC2-SPB cluster is of minor importance during the Early Aptian, with punctual occurrences of *Chlamydophorella nyei*, *Cassiculosphaeridia reticulata*, *Dapsilidinium chems*, *Exochosphaeridium* spp., *Kallaiosphaeridium? ringnesiourm* and *Pterodinium bab*. Three taxa included in TC2-SPB cluster are absent from all the Early Aptian studied samples, *Cassiculosphaeridia magna*, *Dingodinium albertii* and *Protoellipsodinium seghire*, and four other taxa occur only in the uppermost Early Aptian (sample 169): *Batiacasphaera* spp., *Cerbia tabulata*, *Taleisphaera* cf. *hydra* and *Tanyosphaeridium isocalamum*.

This distribution may be related to the fact that the Southern Provence Basin originated from the Provence carbonate platforms by a tectonic phenomenon (Masse, 1976; Machhour *et al.*, 1998; Masse and Fenerci-Masse, 2013a) and direct water exchange with other deep environments was limited until the last drowning event during the late Early Aptian. Aging of water masses over carbonate platforms modifies their properties. Among other modifications, the evaporation modifies salinity and organism respiration changes CO₂ concentration and $\delta^{13}\text{C}$ values of water masses over actual carbonate platforms (Patterson and Walter, 1994). The organisms that prefer stable marine environments are usually stenotopic, it is therefore possible that the segregation of offshore and inshore communities was linked to the limited access of dinocyst species with open marine preferences to shallow water carbonate platforms.

We propose that open marine oligotrophic conditions trigger the distribution and abundance of *Batiacasphaera* spp., *Cassiculosphaeridia magna*, *Cassiculosphaeridia reticulata*, *Cerbia tabulata*, *Chlamydophorella nyei*, *Dapsilidinium chems*, *Dingodinium albertii*, *Exochosphaeridium* spp., *Kallosphaeridium? ringnesiorum*, *Protoellipsodinium seghire*, *Pterodinium bab*, *Taleisphaera* cf. *hydra*, *Tanyosphaeridium isocalamum*. This interpretation is compatible with other studies on fossil dinocysts. Because their pattern of occurrence and relative abundance are consistent among studies, species from the genus *Pterodinium* are demonstrated as indicative of oceanic conditions (e.g. Wall *et al.*, 1977; Marshall and Batten, 1988; Smelror and Leereveld, 1989; Dale, 1996; Prince *et al.*, 1999, 2008; Harris and Tocher, 2003; Crouch and Brinkhuis, 2005). Among other taxa, Marshall and Batten (1988) included a species from the genus *Pterodinium*, *P. cingulatum*, in a deep settings “*Spiniferites* association” for the Cenomanian and Turonian of Lower Saxony. It appears in the data of Marshall and Batten (1988) that *K.? ringnesiorum* and a species from the genus *Dapsilidinium*, *D. laminaspinosum*,

also occur in levels dominated by the “*Spiniferites* association”. Helenes and Somoza (1999) found that the distribution of *K. ringnesiorum* in Cretaceous sediments from eastern Venezuela is mainly associated to middle and outer neritic paleoenvironments. Harris and Tocher (2003) consider *D. laminaspinosum* indicator of offshore conditions, even if not restricted to distal environments. *D. laminaspinosum* is also found in the open marine facies of the Upper Cretaceous English Chalk (Prince *et al.*, 1999, 2008).

When analyzing dinocyst distribution along a proximal – distal transect, Harris and Tocher (2003), observed that *E. phragmites* was found at all sites but was more abundant in environments considered euryhalines. Other authors proposed the genus *Exochosphaeridium* to be indicative of marginal marine environments (Wilpshaar and Leereveld, 1994; Lebedeva, 2010).

From the analysis of dinocysts assemblages from the early Cretaceous of the North West Siberia, Lebedeva and Nikitenko (1999) found that moderate abundances of genus *Dingodinium*, *Cassiculosphaeridia*, *Chlamydophorella*, *Oligosphaeridium* and *Spiniferites* are characteristic of the deeper water facies. The distribution of *Dingodinium* and *Chlamydophorella* in the Upper Bathonian to Lower Oxfordian is interpreted as representing the deeper part of the shelf by Smelror and Leereveld (1989). Prauss (2012a and references therein) also suggests open surface marine water preference for *Chlamydophorella* from the palynological study of the Cenomanian/Turonian boundary in the Tarfaya Basin (Morocco). Stable open marine preferences can be inferred for *C. nyei* in the Late Aptian of SE England (Lister and Batten, 1988). Lister and Batten (1988) also found that species of *Cerbia*, *Tanyosphaeridium*, *Protoellipsodinium* and *Batiacasphaera* were more abundant in the mid-outer shelf environments than in inner shelf environments. *Batiacasphaera* is considered indicative of offshore conditions (Pearce *et al.*, 2003; Pross and Brinkhuis, 2005; Prince *et al.*, 2008).

Basinal conditions developed in Northern Provence platform during the latest Early Aptian, after the last drowning event (Masse and Fenerci-Masse, 2013a). Evolution of the paleoenvironmental conditions during the Late Aptian at the La Marcouline fit our interpretation of a stable oligotrophic open marine environment and deposition under pelagic conditions. Nannoconids were responsible for up to 90% of the pelagic sedimentation (Beltran *et al.*, 2009). Because of the absence of signals of burial diagenesis, the values of bulk carbonates $\delta^{13}\text{C}$ likely reflect a primary signature

and record environmental changes (Beltran *et al.*, 2009). The general trend of decreasing $\delta^{13}\text{C}$ values during the Late Aptian may reflect decreasing fertility. The study of TOC content in the La Marcouline succession revealed a mean value around 0.30%, which is in the range of average values compiled for recent marine sediments deposited in oxic pelagic conditions, and kerogen type IV (deeply altered organic matter (Tyson, 1995; Baudin *et al.*, 2008).

Not all the taxa found in the studied Aptian levels were present in the Albian levels, but, in both series, the open marine oligotrophic conditions are constantly marked by the abundance of *Batiacasphaera* spp., *Cassiculosphaeridia magna*, *Cassiculosphaeridia reticulata*, *Cerbia tabulata*, *Chlamydothorella nyei*, *Dapsilidinium chems*, *Dingodinium albertii*, *Exochosphaeridium* spp., *Kallosphaeridium? ringnesiorum*, *Protoellipsodinium seghire*, *Pterodinium bab*, *Taleisphaera cf. hydra* and *Tanyosphaeridium isocalamum*.

5.3. The OAE 1a, the White Level and the Fallot Level: record in the Southern Provence Basin of global and regional events

5.3.1 Oceanic Anoxic Event 1a (OAE 1a) - Niveau Goguel

An increase in temperature and precipitations accompanied by modifications of the paleoceanographic circulation pattern are suggested as responsible of the dinocyst and structured SOM assemblage characteristics of samples 139 to 155C. Changes in the paleoceanographic circulation pattern may explain the observed differences between the structured SOM of this interval and the preceding sample 122 and the increasing abundance of pollen grains in the sporomorphs assemblage. Increased precipitations reduce the time of exposure of vegetal debris to atmospheric related oxidative processes, and it accelerates the transport of vegetal debris, leading to an increase of translucent phytoclast contribution to the total phytoclast group (Fig. 3.17). Under warmer and more humid climates degradative processes of vegetal debris change from oxidative to fungal related, explaining the increase in the abundance of fungal remains and the associated decrease of wood tracheids. Furthermore, enhanced runoff increase the nutrient input and consequently the marine productivity as reflected by (1) the increase in the relative abundance of dinocysts, (2) the increase

of the P/G ratio (Fig. 3.4, Fig. 3.19), and (3) the dominance of mesotrophic TC1-SPB taxa (Fig. 3.12).

The presence of kaolinite in the clay assemblage and the notable presence of glauconite in the *D. deshayesi* ammonite zone are interpreted as an increase of continental weathering and may be related to an increase of nutrient availability (Masse, 1998, and references therein). The increase in $\delta^{13}\text{C}$ values between levels 139 and 155C (Fig. 20, Kuhnt *et al.*, 1998b, 2011) agrees with an increase in productivity. Renard *et al.* (2005) suggested that the marked negative shift in $\delta^{13}\text{C}$, coincident with a considerable manganese peak (Fig. 3.20), might be related to the dissociation of isotopically light methane gas-hydrates. However, this mechanism involve the development of anoxic conditions in bottom waters, but the analysis of redox-sensitive trace elements show no marked variations indicating that this region remained oxic during OAE 1a (Stein *et al.*, 2012). In the Cassis – La Bédoule succession the $\delta^{18}\text{O}$ curve in the lower part of this interval is characterized by considerable variations. The $\delta^{18}\text{O}$ curve slope becomes negative from sample 150 onwards, which can be related to increasing temperatures (Fig. 3.20, Kuhnt *et al.*, 1998b, 2011).

The climatic and oceanographic conditions triggering the OAE 1a are still matter of debate. The most common proposed scenario suggests that intensified submarine volcanic activity (Ontong Java Plateau and the Manihiki Plateau, Fig. 3.20), and the accompanying volcanic degassing, may have triggered a phase of global warming (e.g. Arthur *et al.*, 1985; Erba, 1994; Larson and Erba, 1999; Kuhnt *et al.*, 2011). However, the climate-sensitive sporomorphs display minor fluctuations and the estimated variations in pCO₂ levels across the OAE 1a cannot account for a major shift in temperatures (Heimhofer *et al.*, 2004). Changes in paleoceanographic circulation are suggested as responsible of the slight variations observed in the sporomorphs assemblages (Heimhofer *et al.*, 2004). This proposal is compatible with an alternative model, which suggests that under a monsoonal climate system an increase in temperature, eccentricity-driven, and the concomitant strengthening of wind speed increased surface water mixing and precipitation, and thus surface water productivity (Herrle *et al.*, 2003). Our data fit better with the model proposed by Herrle *et al.* (2003).

5.3.2 White Level (Niveau Blanc)

In the levels identified as corresponding to the White Level (beds 166 to 170, Moullade and Tronchetti, 2010) high continental inputs are evidenced by the increase in the abundance of continental constituents within the structured SOM assemblage and by the low abundance of dinocyst and other marine constituents (Fig. 3.17). However, the estimated paleoproductivity of sample 169 is the lowest in the studied Early – Late Aptian studied succession (Fig. 3.19). The combination of a low paleoproductivity in sample 169 with the lowest abundance of marine elements suggests that marine primary productivity was disturbed by an increase in the runoff.

Increased humidity and continental weathering from level 167 onwards was already suggested from the palynomorph assemblages of Cassis – La Bédoule succession (Masure *et al.*, 1998b), as well as from the study of the organic carbon content that suggested a continental origin of organic matter (Masse and Machhour, 1998). The $\delta^{18}\text{O}$ values between levels 166 and 170 are low and variable (Fig. 3.20, Kuhnt *et al.*, 1998b), they may result from increasing temperatures or decreasing salinities. Kuhnt *et al.* (2011) interpret the low $\delta^{18}\text{O}$ values of the Cassis – La Bédoule succession as indicating temperatures between 26-27°C. The observed increase in continental elements and the low abundance of marine elements corresponds better to the interpretation of low values of $\delta^{18}\text{O}$ resulting from an increase in the runoff, a salinity decrease (Beltran *et al.*, 2007; Moullade *et al.*, 2011). The $\delta^{13}\text{C}$ curve during this interval shows a slight decrease within an interval characterized high values (Fig. 3.20, Kuhnt *et al.*, 1998b), which can be interpreted as an interval of diminished productivity. Decreasing productivity is also suggested by the decrease in the total abundance of nanofossils, and in particular by the low abundance of *Biscutum* and the high abundance of *Watznaueria* (Bergen, 1998).

The White Level was coincident with the last drowning phase of the carbonate platforms and the deposition of deep-water marls over the Southern Provencal Basin (Masse and Fenerci-Masse, 2013a). It is possible that the final demise of carbonate platforms also generated modifications in the paleoceanographic circulation patterns. The observed dinocyst and structured SOM assemblage in Sample 169 may result from the overlap of the final demise of carbonate platforms and the development of a more humid climate.

5.3.3. Niveau Fallot

The Fallot level is sampled in the Southern Provence Basin through the sample MA82 at La Marcouline (Baudin *et al.*, 2008). The relative abundance of continental elements in the structured SOM assemblage of this sample is similar to that of the other analyzed La Marcouline samples. However, relative abundance of pollen grains is the highest of the studied Aptian levels (Fig. 3.17). The increase in the relative abundance of pollen grains (mostly bisaccate pollen grains), decoupled from variations in any other continental constituent, suggest transport sorting. Two main driven mechanism act on sporomorphs sorting; hydraulic transport, which may be associated to an increase of the distance of the source of detrital inputs; and aeolian transport, which may be associated to a strengthening of the wind regime (Traverse, 1988; Tyson, 1995).

Dinoflagellate cyst abundance in this sample is similar to that of other samples in the succession. Dinoflagellate cyst assemblage shows the highest taxonomic richness and evenness values. Paleoproductivity estimated through the P/G ratio reach in this sample its maximum value in the Southern Provence Basin. The conjunction of both the highest diversity and productivity values in one sample is not common; usually dinocysts associations from environments with high productivity are dominated by one or a few species (Regali, 1989). Warm water preferences have been attributed to some fossil peridinioids, so the P/G ratio may partially reflect an increase in temperature (Lentin and Williams, 1980; Arai *et al.*, 1994; Smelror, 1999; Prauss, 2015). The high diversity values of MA82 may be related to the good state of preservation of palynomorphs (Fig. 3.17), which could be associated to a slight decrease in the oxygen level (Baudin *et al.*, 2008) of bottom water masses or in the water-sediment interface.

The negative correlation between the carbonate and TOC content in the La Marcouline samples (Fig. 3.20), suggest that the autochthonous carbonate supply is the main factor controlling the dilution of organic matter throughout the sedimentary sequence (Baudin *et al.*, 2008). So, the high content of TOC in sample MA82 of continental origin (kerogen type III) may be related to a decrease in nannoconus production (Beltran *et al.*, 2007; Baudin *et al.*, 2008). Low marine productivity is also suggested by the low values of $\delta^{13}\text{C}$ (Kuhnt *et al.*, 1998b, 2011). The $\delta^{18}\text{O}$ curve shows at this level a marked negative peak (Fig. 3.20) that may be interpreted as an increase

in temperature or as a decrease in salinity. Because abundance of continental elements in sample MA82 did not show significant variations respect to other samples in the series, temperature is here considered as responsible in the shift of $\delta^{18}\text{O}$.

The particular characteristics of the Falot Level and associated dinocyst and structured SOM assemblages, in the Southern Provence Basin, may result of an increase in temperature (Kuhnt *et al.*, 1998b, 2011) and in the distance to the source of detrital inputs (Fig. 3.17). Nannoconus productivity was reduced during this period (Beltran *et al.*, 2007) and preservation of organic matter slightly enhanced (Baudin *et al.*, 2008). This scenario may be similar to that proposed by Herrle *et al.* (2003), which suggests that a under monsoonal climate system an eccentricity-driven increase in temperature, and the concomitant strengthening of wind speed, increased surface water mixing and thus surface water productivity (Herrle *et al.*, 2003).

5.4. Validity of the paleoenvironmental model on a larger scale

The dinocyst associations keep stable and robust while adding data from the 398D site samples in the dataset. Abundance distributions in the samples from the 398D site are similar to that observed in the Southern Provence Basin, in general terms. Taxa included in cluster TC1-398D+SPB are more abundant in the Early Aptian sample, whereas the abundance of taxa included in cluster TC2-398D+SPB is higher in the Late Aptian sample.

The fact that TC1-398D+SPB taxa are relatively abundant in the Late Aptian from the 398D core site may be related to the differences in the regional geological context between the two studied areas. During the Early Aptian, the Southern Provence Basin was entirely surrounded by carbonate platforms, which resulted in limited exchanges with oceanic water masses. However, the 398D site despite of being near to the Lusitanian carbonate platforms (e.g.Rey, 1979; Masse and Chartrousse, 1997; Burla *et al.*, 2008; Huck *et al.*, 2012), was open to the Atlantic Ocean. The study of both regions allows revealing some similarities and differences between the environments recorded during the Aptian in the Northwestern Tethyan margin and in the western margin of the Iberian Massif, under the influence of the Central Atlantic and the proto-North Atlantic. Carbonate platforms developed in littoral sectors in both regions (e.g. Burla *et al.*, 2008; Huck *et al.*, 2012; Masse and Fenerci-

Masse, 2013a). However, the demise of the carbonate platforms during the Early Aptian followed two different patterns.

In the Provence the physiography of Urgonian-type carbonate platforms changed to a ramp model associated to the *D. weissi* – *D. deshayesi* ammonite zones boundary drowning event. Rudist communities, that were the main carbonate producers until this event, completely disappeared from the region and were first replaced by communities rich in *Palorbitolina*, *Heteraster oblongus* and sponges (Masse and Fenerci-Masse, 2013a). The carbonate platform in the Lusitanian Basin changed similarly from platform to ramp physiography. However, the bypass of siliciclastic-rich sediments and nutrients through the proto-North Atlantic Ocean (Föllmi, 2012) prevented the total demise of the platform (Huck *et al.*, 2014). Oligotrophic rudist communities survived in the southern Lusitanian Basin (Huck *et al.*, 2012) until the upper part of the *R. hambrovi* ammonite sub-zone.

In sample 118-4 of the 398D site, a high proportion of the dinocyst diversity was not considered for the paleoecological analysis, because taxon abundance was lower than 2%, or because they were only present in this sample. Among the excluded taxa, *Subtilisphaera* spp. represents 26% of the assemblage in sample 118-4 and it is responsible of the high paleoproductivity estimated for the sample. The blooming capability of species from the genus *Subtilisphaera* is well known. From the analysis of the distribution of assemblages composed almost exclusively by species from the genus *Subtilisphaera*, Regali (1989) described the *Subtilisphaera* ecozone that is restricted to Early Cretaceous low paleolatitudes (20°N to 20° S) (Jain and Millepied, 1975; Below, 1981; Arai *et al.*, 1994; Lana and Pedrão, 2000; Pedrão and Lana, 2000) revealing the preference of *Subtilisphaera* species for warm waters. Variations in the $\delta^{18}\text{O}$ values of rudist shells have revealed higher temperatures in the early cretaceous Atlantic water masses than in the Tethyan water masses (Steuber *et al.*, 2005). Therefore, climate may be involved in pattern of species distribution, beyond local environmental changes.

5.5 Paleooceanographic and paleogeographic evolution of the Southern Provence Basin during the Aptian

The analysis of the dinocyst and structured SOM assemblages allow us to outline the environmental evolution of the Southern Provence Basin during the Early

and Late Aptian. During the Early Aptian (*Deshayesites deshayesi* ammonites zone) the water exchange between the Southern Provence Basin and the surrounding open marine environments was reduced by the barrier effect of carbonate platforms. Slight environmental variability, temperature and salinity variations, prevented the access of stenotopic open marine taxa to the Southern Provence Basin. Mesotrophic conditions favored a high marine primary productivity. During the OAE 1a, an intensification of monsoonal activity modified the paleoceanographic circulation pattern and led to an increase in temperature and precipitations, resulting in an increase of runoff and marine primary productivity. In the latest Early Albian (*Deshayesites grandis* – *Dufrenoya furcata* transition), the disappearance of the carbonated platforms in the Southern Provence Basin was coeval to a humidity increase that disturbed marine primary production. After the final demise of carbonate platforms, open marine oligotrophic conditions persisted. During the Late Aptian a new episode of intensification of monsoonal climate, coincident with the Falot level (uppermost part of the *Parahoplites melchioris* ammonites zone), may produced the decrease of marine primary productivity and oxygen availability in the water column.

6. Conclusions

The analysis of variations in the dinocyst assemblages allows us to identify two dinocyst associations, reflecting the main environmental changes that affected the Aptian studied series:

- The first dinocyst association is composed of: *Circulodinium distinctum*, *Cribooperidinium orthoceras*, *Odontochitina operculata*, *Ovoidinium diversum* and *Pervosphaeridium* spp. From the analysis of their frequency distribution in the studied series, preference by mesotrophic conditions and slight variations in environmental factors, such as temperature and salinity, are proposed as characterizing these taxa. This association dominates the Early Aptian dinocyst assemblages.
- The second dinocyst association is composed of: *Batiacasphaera* spp., *Cassiculosphaeridia magna*, *Cassiculosphaeridia reticulata*, *Cerbia tabulata*, *Chlamydophorella nyei*, *Dapsilidinium chems*, *Dingodinium albertii*, *Exochosphaeridium* spp., *Kallosphaeridium? ringnesiorum*, *Protoellipsodinium seghire*, *Pterodinium bab*, *Taleisphaera* cf. *hydra* and *Tanyosphaeridium*

isocalamum. From the analysis of their frequency distribution a preference for open marine oligotrophic conditions is proposed for these taxa. This dinocyst association dominates the Late Aptian assemblages.

The consideration of the dinocyst associations distribution together with the results of the structured sedimentary organic matter (SOM) analysis allows us to recognize five stratigraphic set of samples in the Southern Provence Basin that highlight regional and global paleoenvironmental changes.

- The Oceanic Anoxic Event 1a (OAE 1a), named regionally the Goguel Event, has been recognized in the Cassis – La Bédoule succession from the Southern Provence Basin. Samples coeval with the OAE 1a interval, samples 139 to 155C, are dominated by the dinocyst association characteristic of mesotrophic and slightly variable environments. The analysis of the structured SOM reveals an increase in temperature and precipitations. The characteristics of samples coeval with the OAE 1a are interpreted as reflecting the intensification of a monsoonal climate, as proposed by Herrle *et al.* (2003).
- The White level, or Niveau Blanc, is recognized in Sample 169 of the Cassis – La Bédoule succession by a disturbance of marine primary productivity, an increase in the runoff and changes in the paleoceanographic circulation pattern. The concurrence of this level with the last phase of carbonate platform drowning suggests that the observed signal results of the coupling of physiographical and climatic changes.
- The Fallot Level is identified in the upper part of the La Marcoulaine succession of the Southern Provence Basin, in Sample MA82. This level is recognized by a marked increase in the relative abundance of bisaccate pollen grains and in the diversity of the dinocyst assemblage. The particular characteristics of the dinocyst and structured SOM assemblages recorded by the Fallot Level MA82 may be explained by an increase in temperature and in the distance to the source of detrital inputs. Previous studies have proposed a reduction of productivity and an increase of organic matter preservation (Beltran *et al.*, 2007; Baudin *et al.*, 2008). A new event of intensification of a monsoonal climate would explain the organic signature at this level.

The frequency distribution of the dinocyst associations and the structured SOM assemblages allowed us to outline the paleocenographic and paleogeographic

evolution of the Southern Provence Basin during the Aptian. In order to better understand the conditions prior to environmental changes, carbonate platforms demise and oceanic events, and its response to high frequency variations a higher sampling resolution is necessary.

The dinocyst associations identified from the analysis of the Southern Provence Basin keep stable and robust while adding data from the 398D site samples in the dataset. Paleoenvironmental preferences proposed for dinocyst taxa from the analysis of the Southern Provence Basin data are confirmed by coupled analysis with the 398D site data. Dinocyst associations from the 398D site samples reflect the Lusitanian Basin carbonate platforms demise. The high relative abundance of the thermophilic dinocyst *Subtilisphaera* spp. in the dinocyst assemblages, from the 398D site, which is absent in the Southern Provence Basin dinocyst assemblages, reflects the temperature gradient between the Atlantic and the Tethys, suggested from the rudists $\delta^{18}\text{O}$ analysis (Steuber *et al.*, 2005).

The dinocyst environmental preferences and tolerances proposed in the present study based on Aptian data, match precisely with those proposed from the study of Albian dinocysts. This confirmation shows that the methodology used is appropriate and robust. However, is necessary to extend such analyses to many other sections to improve the precision of the paleoenvironmental preferences of fossil dinocysts.

GENERAL CONCLUSIONS AND PERSPECTIVES

The main goal of this thesis was to thoroughly evaluate and to improve the applicability of Cretaceous organic-walled dinoflagellate cysts (dinocyst) for both biostratigraphic and paleoenvironmental interpretations.

Biostratigraphic issues are addressed from the dinocyst of the Côte d'Ivoire – Ghana transform margin ODP hole 959D, a key location in the South Atlantic opening, and critical for understanding of the Cretaceous paleoceanography. A new consensual biostratigraphic scheme is proposed. The differences with previous biostratigraphic studies are explained by inherent properties of the fossil record. The events retained for characterization of stage limits often consider the First Appearance Data (FAD) of species. Biostratigraphic markers are generally rare taxa represented by a low number of specimens in the assemblages (<2% of the occurrences). When different dinocyst based biostratigraphic studies of the same series are compared, the main differences in the position of stage boundaries are due to the low probability of identifying the marker events. In some cases, the miss or discovery of a single cyst can dramatically modify the inferred ages. Although the sampling density and the sample positions influence the placement of biostratigraphic limits, they are less influencing.

The analysis of the ODP hole 959D dinocysts demonstrates the limitations of traditional biostratigraphy dependent of exhaustive sample description and subjected to the potential overprint of paleoenvironmental conditions. A high resolution study of the IODP, ODP and DSDP holes drilled along the South Atlantic margins considering all the information contained in dinocyst assemblages would (1) allow the establishment of an improved correlation scheme, (2) favor the development of dinocysts as paleoenvironmental tracers, and it would also (3) help to propose new paleogeographic and paleoceanographic reconstructions of the South Atlantic increasing our understanding of the complex oceanographic changes associated to the South Atlantic Ocean opening.

The link between paleoenvironmental conditions and dinocyst distribution is obvious but is poorly explored in geological series older than the Pleistocene. This question is addressed through the study of Albian dinocyst distribution along an inshore–offshore transect from the western Iberian Margin, between the Lusitanian Basin and the DSDP hole 398D. The integrative study of biodiversity, structure of dinocyst assemblages and sedimentological information allows discriminating and

defining the dinocyst associations typical of paleoenvironments, and identifying the involved environmental parameters. The partitioning of dinocyst species along the inshore–offshore transect is a clear pattern linking species occurrence with their environmental preferences, or tolerances. The stability and predictability gradient and nutrient availability are the main environmental factors triggering the distribution of cyst-producer dinoflagellates.

The results are tested by extending the spatial and temporal range comparisons to regions within the same climatic belt: the Aptian of the Southern Provence Basin and of the DSDP Hole 398D. The paleoenvironmental interpretation of dinocyst assemblages is consistent and robust within the two studies. The changes in dinocyst taxon associations record local, regional and global events, like the carbonate platform demise, the regional Falot level or the OAE and the long-term sea level rise. The identified taxon-environment relationships are more about ranges of environmental tolerance than to strict affinities. Species are often tolerant to a wide range of environments but are abundant only in their optimal conditions. The presence or absence of a given taxon is not sufficient to determine the paleoenvironmental conditions. Paleoenvironmental information is best reflected by the relative abundance of a dinocyst association within the assemblages. The comparison of dinocyst species associations in sedimentary series from different paleoceanographic domains and different ages confirms the interest of dinocysts as biostratigraphic markers and paleoenvironmental tracers.

The low resolution dinocyst study from the Aptian Southern Provence Basin has showed the potential of dinocyst for recognition and reconstruction of its paleoenvironmental history. A higher resolution study of the series would allow us (1) to describe the “background” conditions of the environment prior to perturbations, (2) to analyze the complete record of paleoenvironmental perturbations, and (3) to recognize paleoenvironmental variations of higher frequency. Extension of similar works to other European basins would surely improve our knowledge about the global and regional paleoenvironmental events during the Cretaceous.

In the current practice of dinocyst biostratigraphy the unit boundaries are defined from the event identification, like the appearance and/or disappearance of index taxa (FAD and/or LAD). The data used in biostratigraphy can be considered as discrete variables, i.e. the useful information is whether a given event is identified or not. So the biostratigraphic information may be considered a propositional variable that

is; a variable which can only take two values, either be “true” or “false”. And the biostratigraphic characterization of the geological stages may be considered through the propositional logic or calculus.

The paleoenvironmental information within dinocyst assemblages is supported by the relative abundance of the common taxa. The most important information for reconstructing the paleoceanographic and/or paleogeographic conditions is the relative frequencies distribution of the dinocysts. The environmental characterization of a particular taxon is founded on its relative frequency distribution within assemblages. The informative unit used for paleoenvironmental characterization and reconstruction is a quantitative continuous variable.

An optimal performance for paleoenvironmental comparison can be achieved from a limited number of tallied dinocysts while the best possible biostratigraphic conclusion requires the screening of many individuals. The formal differences in biostratigraphic and paleoenvironmental information have a direct impact on the working processes. Because the nature and distribution of the biostratigraphic and paleoenvironmental information contained in dinocyst assemblages are different, they must not be analyzed from the same datasets, unless exhaustive quantitative inventory can be produced. However, the qualitative information is useful when aiming at measuring statistical risk on biostratigraphic dating.

Dinocysts and the modeling of paleoclimates

The complexity of the climate systems requires the integration of multiple types of information whether in tomorrow’s weather forecast, in the prediction of the future climate, or in the reconstruction of paleoclimates. The study of paleoclimates has strongly benefited from the increase in the spatiotemporal resolution of the models, and from the integration of several parameters, like atmospheric pCO₂ or cloud cover, enabling the development of more reliable reconstructions. Although much work is to be done, paleoenvironmental reconstructions made from dinocyst should allow a description of the upper water column. Fluxes, stratification and mixing of water masses are major factors of climate regulation. Climate models including a description of the water column would result in more precise reconstructions and even reveal unsuspected climatic patterns. The integration of such information in climate models will solve many questions, nowadays unsolvable, about regional responses to global constraints in the deep time.

CONCLUSIONS GÉNÉRALES ET PERSPECTIVES

L'objectif principal de cette thèse était d'évaluer rigoureusement et d'améliorer l'applicabilité des kystes de dinoflagellés (dinokystes) à paroi organique du Crétacé pour leur utilisation dans les interprétations biostratigraphiques et paléoenvironnementales.

La problématique biostratigraphique est abordée par l'étude des dinokystes du puits ODP 959D situé sur la marge transformant Côte d'Ivoire - Ghana, un emplacement clé dans l'ouverture de l'Atlantique Sud et crucial pour la compréhension de la paléo-océanographie du Crétacé. Un nouveau schéma biostratigraphique consensuel faisant suite aux études biostratigraphiques contradictoires précédentes est proposé. Les incohérences dans les résultats sont expliquées par les effets intrinsèques de l'enregistrement fossile.

En effet, les événements retenus pour caractériser les limites d'étages sont généralement les premières données d'apparition (FAD) des espèces. Les marqueurs biostratigraphiques sont généralement des taxons rares représentés par un faible nombre d'individu dans les assemblages (présence <2%). Lorsque différentes études biostratigraphiques d'une même série sont comparées, les différences dans la position des limites d'étage résultent de la faible probabilité d'observer les événements marqueurs. Or, l'absence ou l'observation d'un unique kyste peut considérablement modifier les âges présumés. Bien que la densité de l'échantillonnage et la position des échantillons aient un impact sur les limites biostratigraphiques, ces facteurs ont une influence moindre.

L'analyse des dinokystes du forage ODP 959D démontre les limites de la biostratigraphie traditionnelle qui dépend de la description exhaustive de l'échantillon, la composition de celui-ci étant par ailleurs assujéti aux conditions paléoenvironnementales. Une prise en compte de l'ensemble des informations contenues dans les assemblages de dinokystes, dans le cadre d'une étude à haute résolution des puits DSDP, ODP et IODP, forés le long des marges de l'Atlantique Sud, (1) permettrait d'établir un schéma de corrélations amélioré, (2) valoriserait les dinokystes comme marqueurs paléoenvironnementaux, et (3) aiderait à proposer de nouvelles reconstructions paléogéographiques et paléocéanographiques en

approfondissant notre compréhension des changements océanographiques complexes associés à l'ouverture de l'Océan Atlantique Sud.

Le lien entre les conditions paléoenvironnementales et la distribution des dinokystes est évident, mais ce lien est insuffisamment exploité dans les séries géologiques pré-Pléistocènes. Cette problématique est abordée à travers l'étude de la distribution des dinokystes à l'Albien, le long d'un transect côte-large de la marge ibérique occidentale, du Bassin Lusitanien au forage DSDP 398D. L'étude intégrée de la biodiversité, de la structure des assemblages, et de la sédimentologie permet de discriminer et de définir des associations de dinokystes caractéristiques de paléoenvironnements, tout en précisant les paramètres environnementaux impliqués. La répartition des espèces le long du transect côte-large concrétisent la relation des espèces avec leurs préférences environnementales et leurs tolérances. Le gradient de stabilité et de prédictibilité, ainsi que la disponibilité des nutriments sont les principaux facteurs environnementaux qui influencent la distribution des espèces planctoniques à l'origine des dinokystes.

Les résultats de la méthodologie développée ci-dessus sont testés en étendant la distribution temporelle et spatiale des comparaisons, dans la même zone climatique, à l'Aptien du Bassin Sud Provençal et du forage DSDP 398D. L'interprétation paléoenvironnementale des assemblages albiens et aptiens est cohérente et robuste. Les changements dans les associations des dinokystes enregistrent des événements locaux, régionaux et globaux, comme la disparition des plateformes carbonatées, le niveau anoxique régional FalLOT, ou l'évènement anoxique océanique (OAE), ainsi que le long processus d'élévation du niveau de la mer. La tolérance aux variations environnementales, plutôt qu'une stricte affinité, semblent mieux expliquer les relations taxon-environnement identifiées. En effet, les espèces sont souvent tolérantes à un large éventail d'environnements, mais leurs abondances maximales sont réservées à leurs conditions optimales. La présence ou l'absence d'un taxon donné ne suffit donc pas à déterminer les conditions paléoenvironnementales. Les informations paléoenvironnementales sont mieux traduites par l'abondance relative d'une association de dinokystes dans les assemblages. La comparaison des associations de taxons d'âges différents dans les séries sédimentaires de différents domaines paléocéanographiques confirme l'intérêt des dinokystes comme marqueurs biostratigraphiques et comme traceurs paléoenvironnementaux.

L'étude à basse résolution de l'Aptien du Bassin Sud Provençal a montré le potentiel des dinokystes pour la reconnaissance et la reconstruction de son histoire. Une étude à haute résolution de la série nous permettrait (1) de retrouver les conditions environnementales qui prévalaient avant les perturbations, (2) d'analyser le registre complet de celles-ci, et (3) d'identifier les variations paléoenvironnementales de fréquence plus élevée. L'extension de travaux similaires à d'autres bassins européens permettrait certainement d'améliorer notre connaissance sur les événements paléoenvironnementaux à l'échelle régionale et mondiale au cours du Crétacé.

Dans la pratique actuelle de la biostratigraphie à partir de l'identification des dinokystes, les limites d'unités sont définies à partir de l'identification d'événements, comme l'apparition et/ou la disparition (FAD, pour First Appearance Data et/ou LAD = Last Appearance Data) de taxons index. Les données utilisées en biostratigraphie peuvent être considérées comme des variables discrètes binaires, i.e. l'information utile est un événement donné soit identifié, soit non identifié. L'information biostratigraphique peut donc être considérée comme une variable propositionnelle qui peut prendre que deux valeurs, "vrai" ou "faux". La caractérisation biostratigraphique des étages géologiques pourrait donc être réalisée à partir d'un simple calcul de logique propositionnelle.

Les informations paléoenvironnementales portées par les assemblages de dinokystes sont révélées par l'abondance relative des taxons fréquents. L'information la plus importante pour reconstruire les conditions paléocéanographiques et/ou paléogéographiques est la distribution des fréquences relatives des dinokystes. La caractérisation environnementale d'un taxon est fondée sur la distribution de ses fréquences relatives dans les assemblages. L'unité d'information utilisée pour la caractérisation et la reconstruction des paléoenvironnements est donc une variable continue quantitative.

Le rendement optimal d'une comparaison paléoenvironnementale peut être obtenu à partir du comptage d'un nombre limité de dinokystes, tandis que la meilleure conclusion biostratigraphique nécessite l'observation des très nombreux spécimens. Les différences formelles dans l'information biostratigraphique et paléoenvironnementale ont un impact direct sur la démarche du travail à effectuer. En raison de la nature et de la distribution différente de l'information biostratigraphique et

paléoenvironnementale contenue dans les assemblages de dinokystes, ils ne doivent pas être analysés à partir des mêmes ensembles de données, à moins qu'un inventaire quantitatif exhaustif puisse être réalisé. Cependant, l'information qualitative est utile lorsque l'on cherche à mesurer le risque statistique d'une datation biostratigraphique.

Les kystes de dinoflagellés et la modélisation des paléoclimats

La complexité du système climatique nécessite l'intégration de plusieurs types d'informations, que ce soit dans les prévisions météo à court terme, dans la prédiction du climat futur, ou dans la reconstruction des paléoclimats. L'étude des paléoclimats a fortement bénéficié de l'augmentation de la résolution spatio-temporelle des modèles et de l'intégration de plusieurs paramètres, comme le $p\text{CO}_2$ atmosphérique ou la couverture nuageuse, permettant le développement de reconstructions plus fiables. Bien que beaucoup de travail reste à faire, les reconstitutions paléoenvironnementales élaborées à partir des dinokystes permettront une description de la colonne d'eau superficielle. Les flux, la stratification et le mélange des masses d'eau sont des facteurs majeurs de la régulation du climat. Les modèles climatiques incluant une description de la colonne d'eau aboutiraient à des reconstructions plus précises et pourraient même révéler des modèles climatiques insoupçonnés. L'intégration de telles informations dans les modèles climatiques résoudrait de nombreuses questions actuellement non résolues pour les durées géologiques, depuis les réponses régionales jusqu'aux contraintes globales.

CONCLUSIONES GENERALES Y PERSPECTIVAS

El principal objetivo de esta tesis es evaluar de forma exhaustiva y mejorar la aplicabilidad de los quistes de dinoflagelados de pared orgánica (dinoquistes) del Cretácico para su uso en estudios bioestratigráficos y paleoambientales.

La dimensión bioestratigráfica se aborda a través del estudio de los dinoquistes del sondeo 959D del ODP (Ocean Drilling Program) en el margen transformante de Costa de Marfil – Ghana, una región clave en la apertura del Océano Atlántico Sur y crucial para la comprensión de la paleoceanografía cretácica. Como resultado del estudio, se propone un nuevo esquema bioestratigráfico consensual. Las propiedades inherentes al registro fósil explican las diferencias con estudios bioestratigráficos previos del mismo sondeo. Los eventos empleados para caracterizar los límites de los pisos geológicos en general consideran la información de la primera aparición en el registro de ciertas especies (First Appearance Data, FAD, en inglés). Los marcadores bioestratigráficos generalmente son taxones “raros” representados por un pequeño número de especímenes en las muestras (<2% de incidencia). Cuando se comparan diferentes estudios bioestratigráficos de una misma serie, las diferencias más importantes en la posición de los límites de los pisos se deben a la baja probabilidad de observar los eventos índice. En algunos casos, la no identificación o el hallazgo de un único dinoquiste pueden modificar de forma considerable las edades deducidas. A pesar de que la densidad de muestreo y la posición de las muestras influyen en la posición de los límites bioestratigráficos establecidos, su efecto es de importancia menor.

El análisis de los dinoquistes del sondeo 959D del ODP muestra las limitaciones de la bioestratigrafía tradicional; dependiente de la descripción exhaustiva de las muestras y potencialmente expuesta a la influencia de las condiciones paleoambientales. Teniendo en cuenta toda la información contenida en las muestras de dinoquistes, un estudio de alta resolución de los sondeos de los programas DSDP, ODP e IODP, de los márgenes del Atlántico Sur; (1) permitiría establecer un esquema de correlación mejorado, (2) ampliaría el desarrollo de los dinoquistes como trazadores ambientales y (3) ayudaría en la propuesta de nuevas reconstrucciones paleogeográficas y paleoclimáticas profundizando nuestro conocimiento sobre los complejos cambios oceanográficos asociados a la apertura del Atlántico Sur.

La relación entre las condiciones paleoambientales y la distribución de los dinoquistes es conocida, pero ha sido poco explorada en series geológicas pre-pliocenas. Esta cuestión se ha abordado a través del estudio de la distribución de dinoquistes durante el Albiense en un transecto costa – océano a lo largo del margen occidental ibérico, entre la Cuenca Lusitánica y el sondeo 398D del DSDP. El estudio integrado de la biodiversidad y la estructura de las muestras de dinoflagelados, junto con el análisis de información sedimentológica permite discriminar y definir las asociaciones de dinoquistes características de los diferentes paleoambientes, identificando de esta forma los parámetros ambientales involucrados. El reparto de las especies de dinoquistes a lo largo del transecto costa – océano muestra un patrón claro que permite asociar la distribución de las especies con sus preferencias ambientales, o con su tolerancia a las variaciones ambientales. El gradiente de estabilidad y predictibilidad ambiental y la disponibilidad de nutrientes son los principales factores que condicionan la distribución de las especies planctónicas que producen dinoquistes.

Los resultados del estudio del Albiense se han evaluado mediante la extensión del rango espacial y temporal de las comparaciones, con regiones dentro del mismo cinturón climático: el Aptiense de la Cuenca Sud Provenzal y del sondeo 398D del DSDP. La interpretación paleoambiental de las asociaciones de dinoquistes albienses y aptienses es consistente y robusta. Los cambios en las asociaciones de taxones de dinoquistes registran eventos locales, regionales y globales, como la desaparición de las plataformas carbonatadas, el evento anóxico regional Fallo o los eventos anóxicos oceánicos (OAE) y el aumento del nivel de mar a largo plazo. Las relaciones “taxón – ambiente” identificadas se refieren fundamentalmente a rangos de tolerancia ambiental y no a afinidades estrictas. Generalmente las especies son tolerantes a un amplio rango de ambientes pero sus máximas abundancias se observan exclusivamente bajo sus condiciones óptimas. La presencia o ausencia de un taxón dado no es suficiente para determinar las condiciones paleoambientales. La información paleoambiental queda expresada de preferencia en la abundancia relativa de las asociaciones de dinoquistes dentro de las muestras. La comparación de las asociaciones de taxones en las series sedimentarias de diferentes dominios paleoceanográficos y de diferentes edades confirma la utilidad de los dinoquistes como marcadores bioestratigráficos y como trazadores paleoambientales.

El estudio de baja resolución del Aptiense de la Cuenca Sud Provenzal muestra el potencial de los dinoquistes para la identificación y reconstrucción de la historia paleoambiental. Un muestreo de mayor resolución permitiría (1) describir las condiciones de “fondo” del ambiente previas a las perturbaciones, (2) analizar el registro completo de las perturbaciones ambientales y (3) reconocer las variaciones ambientales de mayor frecuencia. La extensión de estudios similares a otras cuencas europeas mejorará con certeza nuestro conocimiento sobre los eventos paleoambientales regionales y globales durante el Cretácico.

En la práctica actual de la bioestratigrafía de dinoquistes los límites entre las unidades se definen a través de la identificación de eventos, como la aparición y/o la desaparición de taxones índice (FAD y/o LAD, en inglés). Los datos usados en bioestratigrafía pueden considerarse como variables discretas, es decir, la información útil es si un evento dado es identificado o no. Por tanto, la información bioestratigráfica puede considerarse como una variable proposicional, a saber; una variable que sólo puede ser “cierta” o “falsa”. La caracterización bioestratigráfica de los pisos geológicos podría por tanto considerarse a través de la lógica o cálculo proposicional.

La información paleoambiental de las muestras de dinoquistes está contenida en la abundancia relativa de los taxones frecuentes. La información más importante para reconstruir las condiciones paleoceanográficas o paleogeográficas es la distribución de las frecuencias relativas de los dinoquistes. La caracterización paleoambiental de un taxón se fundamenta en la distribución de su frecuencia relativa en las muestras. La unidad informativa empleada para la caracterización y reconstrucción paleoambiental es una variable cuantitativa continua.

El rendimiento óptimo para las comparaciones ambientales se puede lograr a través del recuento de un número limitado de dinoquistes mientras que la mejor conclusión bioestratigráfica posible exige la observación de muchos especímenes. Las diferencias formales entre la información bioestratigráfica y paleoambiental tienen un impacto directo en el proceso de trabajo. Puesto que la naturaleza y distribución de la información bioestratigráfica y paleoambiental contenida en las muestras de dinoquistes son diferentes, no deben analizarse a través de las mismas bases de datos, a menos que pueda realizarse un inventario cuantitativo minucioso. Sin embargo, la información cualitativa es de gran utilidad para la evaluación de riesgos estadísticos en las dataciones bioestratigráficas.

Los quistes de dinoflagelados y la modelización de paleoclimas

La complejidad del sistema climático exige la integración de múltiples tipos de información ya sea para la predicción meteorológica a corto plazo, para la predicción del clima futuro o para la reconstrucción de paleoclimas. El estudio de la paleoclimatología se ha beneficiado enormemente del aumento de la resolución espacio-temporal de los modelos y de la integración de varios parámetros, como por ejemplo la presión atmosférica de CO₂ o la cobertura nubosa, permitiendo el desarrollo de reconstrucciones más fiables. Aunque hay mucho trabajo por hacer, las reconstrucciones ambientales a partir de la información obtenida de los dinoquistes permitirán la descripción de la parte superficial de la columna de agua. El flujo, estratificación y mezcla de las masas de agua son factores importantes en la regulación del clima. El desarrollo de modelos climáticos que incluya la descripción de la columna de agua propiciaría el desarrollo de reconstrucciones más precisas e incluso podría revelar patrones climáticos impensados. La integración de la información paleoambiental obtenida de los dinoquistes en los modelos climáticos podría resolver numerosas preguntas, irresolubles hoy en día, acerca de las respuestas regionales o de las restricciones globales en el registro del paleoclima.

Bibliography

- Adrain, J.M., Westrop, S.R., Chatterton, B.D.E. and Ramsköld, L. (2000) - Silurian Trilobite Alpha Diversity and the End-Ordovician Mass Extinction. *Paleobiology*, 26 (4): 625–646.
- Alves, T.M., Moita, C., Cunha, T., Ullnaess, M., Myklebust, R., Monteiro, J.H. and Manuppella, G. (2009) - Diachronous evolution of Late Jurassic–Cretaceous continental rifting in the northeast Atlantic (west Iberian margin). *Tectonics*, 28 (4): TC4003.
- Anderson, M.J. (2001) - A new method for non-parametric multivariate analysis of variance. *Austral Ecology*, 26 (1): 32–46.
- Antobreh, A.A., Faleide, J.I., Tsikalas, F. and Planke, S. (2009) - Rift–shear architecture and tectonic development of the Ghana margin deduced from multichannel seismic reflection and potential field data. *Marine and Petroleum Geology*, 26 (3): 345–368.
- Arai, M., Lana, C.C. and Pedrão, E. (1994) - Ecozona *Subtilisphaera* spp.: registro eocretáceo de um importante episódio ecológico do Oceano Atlântico primitivo. *Acta Geológica Leopoldensia*, 17 (39/2): 521–538.
- Archangelsky, S. (1969) - Sobre el paleomicroplancton del Terciario inferior de Río Turbio, Provincia de Santa Cruz. *Ameghiniana*, 5 (10): 406–416.
- Arnaud, H., Arnaud-Vanneau, A., Argot, A. and Carrio, C. (1995) - *Sequence stratigraphy in a carbonate setting, platform to basin section of the Urganian platform (Lower Cretaceous), Vercors Plateau, Glandasse Plateau to Isère Valley, Southeast France*. AAPG, Field Trip Notes, Nice, 124 p.
- Arnaud, H., Arnaud-Vanneau, A., Blanc-Alétru, M.C., Adatte, T., Argot, M., Delanoy, G., Thieuloy, J.-P., Vermeulen, J., Virgone, A., Virlouvét, B. and Wermeille, S. (1998) - Répartition stratigraphique des orbitolinidés de la plate-forme urgonienne subalpine et jurassienne (SE de la France). *Géologie Alpine*, 74: 3–89.
- Arnaud-Vanneau, A. (1980) - Micropaléontologie, paléoécologie et sédimentologie d'une plate-forme carbonatée de la marge passive de la Téthys. *Géologie Alpine*, 11: 874.
- Arnaud-Vanneau, A., Arnaud, H., Charollais, J., Conrad, M.A., Cotillon, P., Ferry, S., Masse, J.-P. and Peybernès, B. (1979) - Paléogéographie des calcaires urgoniens du Sud de la France. *Géobios* (3): 363–383.
- Arthur, M.A. (1979) - North Atlantic Cretaceous black shales; the record at Site 398 and a brief comparison with other occurrences, in Sibuet J.C. and Ryan W.B.F. (eds.), *Initial Reports of the Deep Sea Drilling Project*. U.S. Government Printing Office, Washington, 47 Pt. 2: 719–751.
- Arthur, M.A., Brumsack, H.-J., Jenkyns, H.C. and Schlanger, S.O. (1990) - Stratigraphy, Geochemistry, and Paleoceanography of Organic Carbon-Rich Cretaceous Sequences, in Ginsburg R.N. and Beaudoin B. (eds.), *Cretaceous Resources, Events and Rhythms*. Springer Netherlands, Dordrecht: 75–119.
- Arthur, M.A., Dean, W.E. and Schlanger, S.O. (1985) - Variations in the Global Carbon Cycle During the Cretaceous Related to Climate, Volcanism, and Changes in Atmospheric CO₂, in Sundquist E.T. and Broecker W.S. (eds.), *The Carbon Cycle and Atmospheric CO₂: Natural Variations Archean to Present*. American Geophysical Union: 504–529.
- Aurisano, R.W. (1989) - Upper cretaceous dinoflagellate biostratigraphy of the subsurface Atlantic coastal plain of New Jersey and Delaware, U.S.A. *Palynology*, 13 (1): 143–179.
- Babinot, J.-F., Moullade, M. and Tronchetti, G. (2007) - The upper Bedoulian and lower Gargasian Ostracoda of the Aptian stratotype: Taxonomy and biostratigraphic correlation. *Carnets de Géologie / Notebooks on Geology* (Article 2007/05 (CG2007_A05)): 1–35.

- Baldocchi, D.D., Hincks, B.B. and Meyers, T.P. (1988) - Measuring biosphere-atmosphere exchanges of biologically related gases with micrometeorological methods. *Ecology*, 69 (5): 1331–1340.
- Barron, E.J. (1983) - A warm, equable Cretaceous: The nature of the problem. *Earth-Science Reviews*, 19 (4): 305–338.
- Barron, E.J., Sloan, J.L. and Harrison, C.G.A. (1980) - Potential significance of land—sea distribution and surface albedo variations as a climatic forcing factor; 180 m.y. to the present. *Palaeogeography, Palaeoclimatology, Palaeoecology*, 30: 17–40.
- Basile, C., Mascle, J., Benkheilil, J. and Bouillin, J.-P. (1998) - Geodynamic evolution of the Côte d'Ivoire - Ghana transform margin: an overview of Leg 159 results, in Mascle J., Lohmann G.P. and Moullade M. (eds.), *Proceedings of the Ocean Drilling Program, Scientific Results*. College Station, TX (Ocean Drilling Program), 159: 101–110.
- Batten, D.J. (1996) - Palynofacies and palaeoenvironmental interpretation, in Jansonius J. and McGregor D.C. (eds.), *Palynology: Principles and Applications*. American Association of Stratigraphic Palynologists Foundation, 3 (3): 1011–1064.
- Baudin, F., Moullade, M. and Tronchetti, G. (2008) - Characterisation of the organic matter of upper Bedoulian and lower Gargasian strata in the historical stratotypes (Apt and Cassis-la-Bédoule areas, SE France). *Carnets de Géologie / Notebooks on Geology*, 176 (Letter 2008/01 (CG2008_L01)): 1–9.
- Below, R. (1981) - Dinoflagellaten-Zysten aus dem oberen Hauterive bis unteren Cenoman Süd-West-Marokkos. *Palaeontographica Abteilung B*: 1–145.
- Beltran, C. (2006) - *Variations des paramètres de l'environnement océanique au cours de la sédimentation d'un doublet marne-calcaire. Approches géochimique, minéralogique et micropaléontologique*. Thèse de Doctorat, Université Pierre et Marie Curie - Paris VI, Paris, 252 p.
- Beltran, C., de Rafélis, M., Person, A., Stalport, F. and Renard, M. (2009) - Multiproxy approach for determination of nature and origin of carbonate micro-particles so-called “micarb” in pelagic sediments. *Sedimentary Geology*, 213 (1–2): 64–76.
- Beltran, C., de Rafélis, M., Renard, M., Moullade, M. and Tronchetti, G. (2007) - Environmental changes during marl-limestone formation: evidence from the Gargasian (Middle Aptian) of La Marcouline Quarry (Cassis, SE France). *Carnets de Géologie / Notebooks on Geology* (Article 2007/01 (CG2007_A01)): 1–13.
- Benzécri, J.-P. (1973) - *L'analyse des données. Tome 1: La taxinomie. Tome 2: L'analyse des correspondances*. Dunod, Paris, 619 p.
- Bergen, J.A. (1998) - Calcareous Nannofossils from the lower Aptian historical stratotype at Cassis-La Bédoule (SE France). *Géologie Méditerranéenne*, 25 (3-4): 227–255.
- Berggren, W.A. and van Couvering, J.A. (1978) - Biochronology, in Cohee G.V., Glaessner M.F. and Hedberg H.D. (eds.), *Contributions to the geological time scale*. American Association of Petroleum Geologists, 6: 39–55 (Studies in Geology).
- Berggren, W.A. and Hollister, C.D. (1974) - Paleogeography, Paleobiogeography and the History of Circulation in the Atlantic Ocean, in Hay W.W. (ed.), *Studies in Paleo-Oceanography*. Society of Economic Paleontologists and Mineralogists, 20: 126–186 (Special Publications).
- Berry, J.A. (1992) - Biosphere, Atmosphere, Ocean Interactions: A Plant Physiologist's Perspective, in Falkowski P.G., Woodhead A.D. and Vivirito K. (eds.), *Primary Productivity and Biogeochemical Cycles in the Sea*. Environmental Science Research, 43: 441–454. Springer US. DOI: 10.1007/978-1-4899-0762-2_23.

- Berthou, P.-Y. and Hasenboehler, B. (1982) - Les kystes de dinoflagellés de l'Albien et du Cénomanién de la région de Lisbonne (Portugal). *Cuadernos Geologia Ibérica*, 8: 761–779.
- Berthou, P.Y. and Leereveld, H. (1990) - Stratigraphic implications of palynological studies on Berriasian to Albian deposits from western and southern Portugal. *Review of Palaeobotany and Palynology*, 66 (3): 313–344.
- Berthou, P.-Y. and Schröder, R. (1979) - Découverte d'un niveau à *Simplorbitolina* Ciry et Rat dans l'Albien de Guincho (région de Lisbonne, Portugal). *Comptes Rendus de l'Académie des Sciences*, 288: 591–594.
- Bint, A.N. (1986) - Fossil Ceratiaceae: A restudy and new taxa from the Mid-Cretaceous of the Western Interior, U.S.A. *Palynology*, 10: 135–180.
- Boillot, G., Winterer, E.L., Meyer, A.W., et al. (eds.) (1987) - *Proceedings of the Ocean Drilling Program, 103 Initial Reports*. Ocean Drilling Program, College Station, TX, 103, (Proceedings of the Ocean Drilling Program).
- Boltenhagen, E. (1977) - *Microplancton du Crétacé Supérieur du Gabon*. Centre national de la recherche scientifique, Paris, 150 p. (Cahiers de paléontologie).
- Bonnet, S., de Vernal, A., Gersonde, R. and Lembke-Jene, L. (2012) - Modern distribution of dinocysts from the North Pacific Ocean (37–64°N, 144°E–148°W) in relation to hydrographic conditions, sea-ice and productivity. *Marine Micropaleontology*, 84–85: 87–113.
- Bralower, T.J., Sliter, W.V., Arthur, M.A., Leckie, R.M., Allard, D. and Schlanger, S.O. (1993) - Dysoxic/Anoxic Episodes in the Aptian-Albian (Early Cretaceous), in Pringle Icolm S., Sager W.W., Sliter W.V. and Stein S. (eds.), *The Mesozoic Pacific: Geology, Tectonics, and Volcanism*. American Geophysical Union: 5–37.
- Bréhéret, J.-G. (1988) - Episodes de sédimentation riche en matière organique dans les marnes bleues d'âge aptien et albien de la partie pélagique du bassin vocontien. *Bulletin de la Société géologique de France*, IV (2): 349–356.
- Bréhéret, J.-G. (1995) - *L'Aptien et l'Albien de la fosse vocontienne (des bordures au bassin): évolution de la sédimentation et enseignements sur les événements anoxiques*. Thèse de Doctorat, Université François Rabelais - Tours, 614 p.
- Bréhéret, J.-G. and Delamette, M. (1988) - Séquences de dépôt et couches riches en matière organique (CRMO) dans les marnes bleues aptiennes et albiennes du bassin vocontien, in Ferry S. and Rubino J.-L. (eds.), *Eustatisme et séquences de dépôt dans le Crétacé du Sud-Est de la France*. Association Lyon-Géologie (ALYGE), Université de Lyon I: 74–83 (Livret Guide de l'excursion du Groupe français du Crétacé en fosse vocontienne (25-27 mai 1988)).
- Brinkhuis, H. and Biffi, U. (1993) - Dinoflagellate cyst stratigraphy of the Eocene/Oligocene transition in central Italy. *Marine Micropaleontology*, 22 (1-2): 131–183.
- Brinkhuis, H., Bujak, J., Smit, J., Versteegh, G.J. and Visscher, H. (1998) - Dinoflagellate-based sea surface temperature reconstructions across the Cretaceous–Tertiary boundary. *Palaeogeography, Palaeoclimatology, Palaeoecology*, 141 (1-2): 67–83.
- Brinkhuis, H. and Leereveld, H. (1988) - Dinoflagellate cysts from the Cretaceous/Tertiary boundary sequence of El Kef, Northwest Tunisia. *Review of Palaeobotany and Palynology*, 56 (1): 5–19.
- Brinkhuis, H. and Zachariasse, W.J. (1988) - Dinoflagellate cysts, sea level changes and planktonic foraminifers across the Cretaceous-Tertiary boundary at El Haria, northwest Tunisia. *Marine Micropaleontology*, 13 (2): 153–191.
- Bulinski, K.V. (2007) - Analysis of sample-level properties along a paleoenvironmental gradient: The behavior of evenness as a function of sample size. *Palaeogeography, Palaeoclimatology, Palaeoecology*, 253 (3–4): 490–508.

- Burla, S., Heimhofer, U., Hochuli, P.A., Weissert, H. and Skelton, P. (2008) - Changes in sedimentary patterns of coastal and deep-sea successions from the North Atlantic (Portugal) linked to Early Cretaceous environmental change. *Palaeogeography, Palaeoclimatology, Palaeoecology*, 257 (1–2): 38–57.
- Buzas, M.A. and Gibson, T.G. (1969) - Species diversity: benthonic foraminifera in Western north atlantic. *Science (New York, N.Y.)*, 163 (3862): 72–75, PMID: 17780177.
- Buzas, M.A. and Hayek, L.-A.C. (1996) - Biodiversity Resolution: An Integrated Approach. *Biodiversity Letters*, 3 (2): 40–43.
- Carpenter, L.J., Archer, S.D. and Beale, R. (2012) - Ocean-atmosphere trace gas exchange. *Chemical Society Reviews*, 41 (19): 6473–6506, PMID: 22821066.
- Cavalier-Smith, T. and Chao, E.E. (2004) - Protalveolate phylogeny and systematics and the origins of Sporozoa and dinoflagellates (phylum Myzozoa nom. nov.). *European Journal of Protistology*, 40 (3): 185–212.
- Chamley, H., Debrabant, P., Foulon, J., Giroud d'Argoud, G., Latouche, C., Maillet, N., Maillot, H. and Sommer, F. (1979) - Mineralogy and geochemistry of Cretaceous and Cenozoic Atlantic sediments off the Iberian Peninsula; Site 398, DSDP Leg 47B, in Sibuet J.C. and Ryan W.B.F. (eds.), *Initial Reports of the Deep Sea Drilling Project*. U.S. Government Printing Office, Washington, 47 Pt. 2: 429–449.
- Channell, J.E.T., Erba, E., Nakanishi, M. and Tamaki, K. (1995) - Late Jurassic–Early Cretaceous time scales and oceanic magnetic anomaly block models, in Berggren W.A., Kent D.V., Aubry M.-P. and Hardenbol J. (eds.), *Geochronology, Time Scales and Global Stratigraphic Correlation*. SEPM Special Publications: 51–64.
- Charlson, R.J., Lovelock, J.E., Andreae, M.O. and Warren, S.G. (1987) - Oceanic phytoplankton, atmospheric sulphur, cloud albedo and climate. *Nature*, 326 (6114): 655–661.
- Choffat, P. (1885) - *Recueil de monographies stratigraphiques sur le système crétacique du Portugal. 1ère étude: contrées de Cintra, de Belas et de Lisbonne*. Mem. Com. Serv. Geol., Lisboa, Portugal, 68 p.
- Choffat, P. (1891) - Note sur le Crétacique des environs de Torres Vedras, de Peniche et de Cercal. *Comm. Trab. Geol. Portugal*, II (2): 171–215.
- Choffat, P. (1904) - Le Crétacique dans l'Arrábida et la contrée d'Ericeira. *Com. Serv. Geol. Portugal, Lisboa*, VI (1): 1–55.
- Christopher, R.A. and Goodman, D.K. (1996) - Introduction to biostratigraphy and time scales, in Jansonius J. and McGregor D.C. (eds.), *Palynology: Principles and Applications*. American Associations of Stratigraphic Palynologists Foundation, 2 (3): 463–492.
- Cleal, C.J. (2008) - Palaeofloristics of Middle Pennsylvanian medullosaleans in Variscan Euramerica. *Palaeogeography, Palaeoclimatology, Palaeoecology*, 268 (3–4): 164–180.
- Coccioni, R., Galeotti, S. and Santarelli, A. (1993) - Preliminary palynological analysis of the Maiolica-Scisti a Fucoidi transition (Barremian-Aptian) in the Gorgo a Cerbara section (central Italy). *Paleopelagos*, 3: 195–201.
- Coccioni, A., Nesci, O., Tramontana, M., Wezel, F.C. and Moretti, E. (1987) - Descrizione di un livello-guida "Radiolaritico-bituminoso ittiolitico" alla base delle marne a fucoidi nell'Appennino umbromarchigiano. *Bollettino della Società Geologica Italiana*, 106 (1): 183–192.
- Cornford, C. (1979) - Organic petrography of Lower Cretaceous Shales at DSDP Leg 47B site 398, Vigo Seamount, Eastern North Atlantic, in Sibuet J.C., Ryan W.B.F. and et al. (eds.), *Initial Reports of the Deep Sea Drilling Project*. U.S. Government Printing Office, Washington, 47 Pt. 2: 523–541.

- Corradini, D. (1973) - Non-calcareous microplankton from the Upper Cretaceous of the northern Apennines. *Bollettino della Società Paleontologica Italiana*, 11: 119–97.
- Crouch, E.M. and Brinkhuis, H. (2005) - Environmental change across the Paleocene–Eocene transition from eastern New Zealand: A marine palynological approach. *Marine Micropaleontology*, 56 (3–4): 138–160.
- Dale, B. (1996) - Dinoflagellate cyst ecology: modeling and geological applications, in Jansonius J. and McGregor D.C. (eds.), *Palynology: Principles and Applications*. American Association of Stratigraphic Palynologists Foundation, 3 (3): 1249–1275.
- Dale, A.L. and Dale, B. (2002) - Appendix on statistical methods, in Haslett S. (ed.), *Quaternary Environmental Micropalaeontology*. Arnold, London: 259–286.
- Dale, B. and Fjellså, A. (1994) - Dinoflagellate cysts as paleoproductivity indicators: state of the art, potential, and limits, in Zahn R., Pedersen T.F., Kaminski M.A. and Labeyrie L. (eds.), *Carbon cycling in the glacial ocean: Constraints on the ocean's role in global change*. Springer, Berlin: 521–537.
- Davey, R.J. (1979) - Marine Aptian-Albian palynomorphs from Holes 400A and 402A, IPOD Leg 48, northern Bay of Biscay, in Montadert L., et al. (eds.), *Deep Sea Drilling Project*. Washington, 48: 547–577 (Initial Reports).
- Davey, R.J. and Verdier, J.P. (1971) - An investigation of microplankton assemblages from the Albian of the Paris Basin. *Verhandelingen der Koninklijke Nederlandse Akademie van Wetenschappen, Afdeling Natuurkunde, Eerste Reeks*, 26: 1–58.
- Davey, R.J. and Verdier, J.P. (1973) - An investigation of microplankton assemblages from latest Albian (Vraconian) sediments. *Revista Española de Micropaleontología*, 5: 173–212.
- Davey, R.J. and Verdier, J.P. (1974) - Dinoflagellate cysts from the Aptian type sections at Gargas and La Bédoule, France. *Palaeontology*, 17 (3): 623–653.
- Deroo, G., Herbin, J.P., Roucache, J. and Tissot, B. (1979) - Organic geochemistry of Cretaceous shales from DSDP Site 398, Leg 47B, eastern North Atlantic, in Sibuet J.C., Ryan W.B.F., et al. (eds.), *Initial Reports of the Deep Sea Drilling Project*. U.S. Government Printing Office, Washington, 47 Pt. 2: 513–522.
- Dinis, J.L., Rey, J., Cunha, P.P., Callapez, P. and Pena dos Reis, R. (2008) - Stratigraphy and allogenic controls of the western Portugal Cretaceous: an updated synthesis. *Cretaceous Research*, 29 (5–6): 772–780.
- Dinis, J., Rey, J. and de Graciansky, P.-C. (2002) - Le Bassin lusitanien (Portugal) à l'Aptien supérieur–Albien: organisation séquentielle, proposition de corrélations, évolution. *Comptes Rendus Geoscience*, 334 (10): 757–764.
- Dodge, J.D. (1987) - Dinoflagellate ultrastructure, in Taylor F.J.R. (ed.), *The Biology of Dinoflagellates*. Blackwell Scientific Publications, Oxford: 93–119.
- Dodsworth, P. (1995) - A note of caution concerning the application of quantitative palynological data from oxidized preparations. *Journal of Micropalaeontology*, 14 (1): 6–6.
- Dodsworth, P. (2000) - Trans-Atlantic dinoflagellate cyst stratigraphy across the Cenomanian–Turonian (Cretaceous) Stage boundary. *Journal of Micropalaeontology*, 19 (1): 69–84.
- Dybkjær, K. (2004) - Dinocyst stratigraphy and palynofacies studies used for refining a sequence stratigraphic model—uppermost Oligocene to lower Miocene, Jylland, Denmark. *Review of Palaeobotany and Palynology*, 131 (3–4): 201–249.

- Edwards, L.E. (1992) - Distribution of selected dinoflagellate cysts in modern marine sediments, in Andrieu V.A.S., Head M.J. and Wrenn J.H. (eds.), *Neogene and Quaternary Dinoflagellate Cysts and Acritarchs*. American Association of Stratigraphic Palynologists Foundation, Dallas, TX: 259–288.
- Edwards, L.E., Mudie, P.J. and de Vernal, A. (1991) - Pliocene paleoclimatic reconstruction using dinoflagellate cysts: Comparison of methods. *Quaternary Science Reviews*, 10: 259–274.
- Ellegaard, M., Lewis, J. and Harding, I. (2002) - Cyst–theca relationship, life cycle, and effects of temperature and salinity on the cyst morphology of *Gonyaulax baltica* sp. nov. (dinophyceae) from the Baltic Sea Area 1. *Journal of Phycology*, 38 (4): 775–789.
- Erba, E. (1994) - Nannofossils and superplumes: The Early Aptian “nannoconid crisis.” *Paleoceanography*, 9 (3): 483–501.
- Eshet, Y., Almogi-Labin, A. and Bein, A. (1994) - Dinoflagellate cysts, paleoproductivity and upwelling systems: A Late Cretaceous example from Israel. *Marine Micropaleontology*, 23 (3): 231–240.
- Evitt, W.R. (1985) - *Sporopollenin Dinoflagellate Cysts: Their Morphology and Interpretation*. AASP, Austin, Texas, 333 p.
- Eynaud, F., Turon, J.L., Matthiessen, J., Kissel, C., Peyrouquet, J.P., de Vernal, A. and Henry, M. (2002) - Norwegian sea-surface palaeoenvironments of marine oxygen-isotope stage 3: the paradoxical response of dinoflagellate cysts. *Journal of Quaternary Science*, 17 (4): 349–359.
- Fast, N.M., Kissinger, J.C., Roos, D.S. and Keeling, P.J. (2001) - Nuclear-encoded, plastid-targeted genes suggest a single common origin for apicomplexan and dinoflagellate plastids. *Molecular Biology and Evolution*, 18 (3): 418–426, PMID: 11230543.
- Fauconnier, D. (1979) - *Les Dinoflagellés de l’Albien et du Cénomanién inférieur du bassin de Paris: répartition stratigraphique et relations avec la nature du dépôt*. Thèse de Doctorat, B.R.G.M., 196 p.
- Fensome, R.A., MacRae, G.L. and Williams, G.L. (2008) - DINOFLAJ2, Version 1. *American Association of Stratigraphic Palynologists, Data Series*, no. 1.
- Fensome, R.A., Riding, J.B. and Taylor, F.J.R. (1996) - Dinoflagellates, in Jansonius J. and McGregor D.C. (eds.), *Palynology: Principles and Applications*. American Association of Stratigraphic Palynologists Foundation, 1 (3): 107–169.
- Fensome, R.A., Taylor, F.J.R., Norris, G., Sarjeant, W.A.S., Wharton, D.I. and Williams, G.L. (1993) - *A Classification of Living and Fossil Dinoflagellates*. American Museum of Natural History, 351 p. (Micropaleontology Special Publication; 7).
- Figueroa, R.I. and Bravo, I. (2005) - Sexual reproduction and two different encystment strategies of *Lingulodinium polyedrum* (dinophyceae) in Culture. *Journal of Phycology*, 41 (2): 370–379.
- Figueroa, R.I., Bravo, I. and Garcés, E. (2006) - Multiple routes of sexuality in *Alexandrium taylori* (dinophyceae) in culture. *Journal of Phycology*, 42 (5): 1028–1039.
- Fluteau, F., Ramstein, G. and Besse, J. (1999) - Simulating the evolution of the Asian and African monsoons during the past 30 Myr using an atmospheric general circulation model. *Journal of Geophysical Research: Atmospheres*, 104 (D10): 11995–12018.
- Föllmi, K.B. (2012) - Early Cretaceous life, climate and anoxia. *Cretaceous Research*, 35: 230–257.
- Föllmi, K.B. and Gainon, F. (2008) - Demise of the northern Tethyan Urganian carbonate platform and subsequent transition towards pelagic conditions: The sedimentary record of the Col de la Plaine Morte area, central Switzerland. *Sedimentary Geology*, 205 (3–4): 142–159.

- Föllmi, K.B., Weissert, H., Bisping, M. and Funk, H. (1994) - Phosphogenesis, carbon-isotope stratigraphy, and carbonate-platform evolution along the Lower Cretaceous northern Tethyan margin. *Geological Society of America Bulletin*, 106 (6): 729–746.
- Förster, A., Schouten, S., Baas, M. and Damsté, J.S.S. (2007) - Mid-Cretaceous (Albian–Santonian) sea surface temperature record of the tropical Atlantic Ocean. *Geology*, 35 (10): 919–922.
- Foucher, J.-C. (1979) - Kystes de dinoflagellés et acritarches des craies cénomaniennes du Cap Blanc Nez (Pas-De-Calais): Inventaire et répartition stratigraphique, in 7ème Réunion annuelle des Sciences de la Terre – Lyon.
- Frakes, L.A. (1979) - *Climates throughout geologic time*. Elsevier Scientific Publishing Company, Amsterdam, 310 p.
- Frakes, L.A., Francis, J.E. and Syktus, J.I. (1992) - *Climate modes of the Phanerozoic: the history of the Earth's climate over the last 600 million years*. Cambridge University Press, New York, 286 p.
- Friedrich, O. and Erbacher, J. (2006) - Benthic foraminiferal assemblages from Demerara Rise (ODP Leg 207, western tropical Atlantic): possible evidence for a progressive opening of the Equatorial Atlantic Gateway. *Cretaceous Research*, 27 (3): 377–397.
- Friedrich, O., Norris, R.D. and Erbacher, J. (2012) - Evolution of middle to Late Cretaceous oceans—A 55 m.y. record of Earth's temperature and carbon cycle. *Geology*, 40 (2): 107–110.
- Friedrich, O., Reichelt, K., Herrle, J.O., Lehmann, J., Pross, J. and Hemleben, C. (2003) - Formation of the Late Aptian Niveau Falot black shales in the Vocontian Basin (SE France): evidence from foraminifera, palynomorphs, and stable isotopes. *Marine Micropaleontology*, 49 (1–2): 65–85.
- Galloway, J.M., Tullius, D.N., Evenchick, C.A., Swindles, G.T., Hadlari, T. and Embry, A. (2015) - Early Cretaceous vegetation and climate change at high latitude: Palynological evidence from Isachsen Formation, Arctic Canada. *Cretaceous Research*, 56: 399–420.
- Gili, E., Masse, J.-P. and Skelton, P.W. (1995) - Rudists as gregarious sediment-dwellers, not reef-builders, on Cretaceous carbonate platforms. *Palaeogeography, Palaeoclimatology, Palaeoecology*, 118 (3–4): 245–267.
- Gong, Z., Langereis, C.G. and Mullender, T.A.T. (2008) - The rotation of Iberia during the Aptian and the opening of the Bay of Biscay. *Earth and Planetary Science Letters*, 273 (1–2): 80–93.
- Goodman, D.K. (1987) - Dinoflagellate cysts in ancient and modern sediments., in Taylor F.J.R. (ed.), *The Biology of the Dinoflagellates*. Blackwell, Oxford: 649–722 (Botanical Monographs).
- de Graciansky, P.-C. and Chenet, P.Y. (1979) - Sedimentological study of cores 138 to 56 (upper Hauterivian to middle Cenomanian); an attempt at reconstruction of paleoenvironments, in Sibuet J.C., Ryan W.B.F. et al. (eds.), *Initial Reports of the Deep Sea Drilling Project*. U.S. Government Printing Office, Washington, 47 Pt. 2: 403–418.
- de Graciansky, P.-C., Muller, C., Rehault, J.-P. and Sigal, J. (1978) - Reconstitution de l'évolution des milieux de sédimentation sur la marge continentale ibérique au Crétacé; le flanc sud du haut-fond de Vigo et le forage DSDP-IPOD 398D; problèmes concernant la surface de compensation des carbonates. *Bulletin de la Société géologique de France*, S7-XX (4): 389–399.
- Gradstein, F.M. (1985) - Stratigraphy and the fossil record, in Gradstein F.M., Agterberg F.P., Brower J.C. and Schwarzacher W.S. (eds.), *Quantitative stratigraphy*. Unesco, Paris: 17–39.
- Gradstein, F.M., Ogg, J.G., Schmitz, M.D. and Ogg, M.D. (2012) - *The Geologic Time Scale 2012*. Elsevier, 1176 p.
- Granot, R., Dyment, J. and Gallet, Y. (2012) - Geomagnetic field variability during the Cretaceous Normal Superchron. *Nature Geoscience*, 5 (3): 220–223.

- Gregory, W.A. and Hart, G.F. (1992) - Towards a predictive model for the palynologic response to sea-level changes. *PALAIOS*, 7 (1): 3.
- Guiot, J. (1990) - Methodology of the last climatic cycle reconstruction in France from pollen data. *Palaeogeography, Palaeoclimatology, Palaeoecology*, 80 (1): 49–69.
- Habib, D. (1979) - Sedimentology of palynomorphs and palynodebris in Cretaceous carbonaceous facies south of Vigo Seamount, in Sibuet J.C., Ryan W.B.F., et al. (eds.), *Initial Reports of the Deep Sea Drilling Project*. U.S. Government Printing Office, Washington, 47 Pt. 2: 451–468.
- Habib, D. and Miller, J.A. (1989) - Dinoflagellate species and organic facies evidence of marine transgression and regression in the Atlantic Coastal Plain. *Palaeogeography, Palaeoclimatology, Palaeoecology*, 74 (1-2): 23–47.
- Habib, D., Moshkovitz, S. and Kramer, C. (1992) - Dinoflagellate and calcareous nannofossil response to sea-level change in Cretaceous-Tertiary boundary sections. *Geology*, 20 (2): 165–168.
- Habib, D., Olsson, R.K., Liu, C. and Moskovitz, S. (1996) - High-resolution biostratigraphy of sea-level low, biotic extinction, and chaotic sedimentation at the Cretaceous-Tertiary boundary in Alabama, north of the Chicxulub Crater, in *Special Paper 307: The Cretaceous-Tertiary Event and Other Catastrophes in Earth History*. Geological Society of America, 307: 243–252.
- Hackett, J.D., Yoon, H.S., Li, S., Reyes-Prieto, A., Rümmele, S.E. and Bhattacharya, D. (2007) - Phylogenomic analysis supports the monophyly of cryptophytes and haptophytes and the association of rhizaria with chromalveolates. *Molecular Biology and Evolution*, 24 (8): 1702–1713, PMID: 17488740.
- Hamel, D., Vernal, A. de, Gosselin, M. and Hillaire-Marcel, C. (2002) - Organic-walled microfossils and geochemical tracers: sedimentary indicators of productivity changes in the North Water and northern Baffin Bay during the last centuries. *Deep Sea Research Part II: Topical Studies in Oceanography*, 49 (22–23): 5277–5295.
- Hammer, Ø. and Harper, D.A. (2006) - *Paleontological data analysis*. John Wiley & Sons, 368 p.
- Hammer, Ø., Harper, D.A.T. and Ryan, P.D. (2001) - PAST-Palaeontological statistics. www.uv.es/~pardomv/pe/2001_1/past/pastprog/past.pdf, acessado em, 25 (07): 2009.
- Hansen, J.M. (1977) - Dinoflagellate stratigraphy and echinoid distribution in Upper Maastrichtian and Danian deposits from Denmark. *Bulletin of the Geological Society of Denmark*, 26: 1–26.
- Hansen, J.M. (1979a) - A new dinoflagellate zone at the Maastrichtian/Danian boundary in Denmark. *Danmarks Geologiske Undersøgelse*: 131–140.
- Hansen, J.M. (1979b) - Dinoflagellate zonation around the boundary, in Birkelund T. and Bromley R.G. (eds.), *Cretaceous-Tertiary Boundary Events Symposium: 1. On the Maastrichtian and Danian of Denmark*. University of Copenhagen, Copenhagen.
- Haq, B.U. (2014) - Cretaceous eustasy revisited. *Global and Planetary Change*, 113: 44–58.
- Haq, B.U., Hardenbol, J. and Vail, P.R. (1987) - Chronology of Fluctuating Sea Levels Since the Triassic. *Science*, 235 (4793): 1156–1167, PMID: 17818978.
- Haq, B.U. and Worsley, T.R. (1982) - Biochronology - biological events in time resolution, their potential and limitations, in Odin G.S. (ed.), *Numerical dating in stratigraphy. Part I*. John Wiley & Sons, Ltd., New York: 19–35.
- Harland, R. (1983) - Distribution maps of Recent dinoflagellate cysts in bottom sediments from the North Atlantic Ocean and adjacent seas. *Palaeontology*, 26 (2): 321–387.
- Harper, J.T. and Keeling, P.J. (2003) - Nucleus-encoded, plastid-targeted glyceraldehyde-3-phosphate dehydrogenase (GAPDH) indicates a single origin for Chromalveolate plastids. *Molecular Biology and Evolution*, 20 (10): 1730–1735, PMID: 12885964.

- Harris, A.J. and Tocher, B.A. (2003) - Palaeoenvironmental analysis of Late Cretaceous dinoflagellate cyst assemblages using high-resolution sample correlation from the Western Interior Basin, USA. *Marine Micropaleontology*, 48 (1): 127–148.
- Hasenboehler, B. (1981) - *Étude paléobotanique et palynologique de l'Albien et du Cénomanién du "Bassin Occidental Portugais" au sud de l'accident de Nazaré (province d'Estrémadure, Portugal)*. Thèse de Doctorat, Université Pierre-et-Marie Curie - Paris VI, Paris, 319 p.
- Hay, W., DeConto, R.M., Wold, C.N., Wilson, K.M., Voigt, S., Schulz, M., Rossby Wold, A., Dullo, W.-C., Ronov, A.B., Balukhovskiy, A. and Söding, E. (1999) - Alternative global Cretaceous paleogeography, in Barrera E. and Johnson C.C. (eds.), *Evolution of the Cretaceous Ocean-Climate System.*, 332: 1–47 (Geological Society of America Special Papers).
- Head, M.J. (1996) - Late Cenozoic dinoflagellates from the Royal Society borehole at Ludham, Norfolk, eastern England. *Journal of Paleontology*, 70 (4): 543–570.
- Heimhofer, U., Hochuli, P.-A., Burla, S., Oberli, F., Adatte, T., Dinis, J.L. and Weissert, H. (2012) - Climate and vegetation history of western Portugal inferred from Albian near-shore deposits (Galé Formation, Lusitanian Basin). *Geological Magazine*, 149 (06): 1046–1064.
- Heimhofer, U., Hochuli, P.A., Burla, S. and Weissert, H. (2007) - New records of Early Cretaceous angiosperm pollen from Portuguese coastal deposits: Implications for the timing of the early angiosperm radiation. *Review of Palaeobotany and Palynology*, 144 (1–2): 39–76.
- Heimhofer, U., Hochuli, P.A., Herrle, J.O., Andersen, N. and Weissert, H. (2004) - Absence of major vegetation and palaeoatmospheric pCO₂ changes associated with oceanic anoxic event 1a (Early Aptian, SE France). *Earth and Planetary Science Letters*, 223 (3–4): 303–318.
- Heimhofer, U., Hochuli, P.A., Herrle, J.O. and Weissert, H. (2006) - Contrasting origins of Early Cretaceous black shales in the Vocontian basin: Evidence from palynological and calcareous nanofossil records. *Palaeogeography, Palaeoclimatology, Palaeoecology*, 235 (1–3): 93–109.
- Helenes, J. (1984) - Dinoflagellates from Cretaceous to Early Tertiary Rocks of the Sebastian Vizcaino Basin, Baja California, Mexico.: 89–106.
- Helenes, J. and Somoza, D. (1999) - Palynology and sequence stratigraphy of the Cretaceous of eastern Venezuela. *Cretaceous Research*, 20 (4): 447–463.
- Herrle, J.O., Kössler, P. and Bollmann, J. (2010) - Palaeoceanographic differences of early Late Aptian black shale events in the Vocontian Basin (SE France). *Palaeogeography, Palaeoclimatology, Palaeoecology*, 297 (2): 367–376.
- Herrle, J.O., Pross, J., Friedrich, O., Kößler, P. and Hemleben, C. (2003) - Forcing mechanisms for mid-Cretaceous black shale formation: evidence from the Upper Aptian and Lower Albian of the Vocontian Basin (SE France). *Palaeogeography, Palaeoclimatology, Palaeoecology*, 190: 399–426.
- Hiscott, R.N., Wilson, R.C.L., Gradstein, F.M., Pujalte, V., Garcia-Mondejar, J., Boudreau, R.R. and Wishart, H.A. (1990) - Comparative Stratigraphy and Subsidence History of Mesozoic Rift Basins of North Atlantic (1). *AAPG Bulletin*, 74 (1): 60–76.
- Holland, S.M. (2000) - The Quality of the Fossil Record: A Sequence Stratigraphic Perspective. *Paleobiology*, 26 (4): 148–168.
- Horikx, M., Heimhofer, U., Dinis, J. and Huck, S. (2014) - Integrated stratigraphy of shallow marine Albian strata from the southern Lusitanian Basin of Portugal. *Newsletters on Stratigraphy*, 47 (1): 85–106.
- Huber, B.T., Hodell, D.A. and Hamilton, C.P. (1995) - Middle–Late Cretaceous climate of the southern high latitudes: Stable isotopic evidence for minimal equator-to-pole thermal gradients. *Geological Society of America Bulletin*, 107 (10): 1164–1191.

- Huck, S., Heimhofer, U. and Immenhauser, A. (2012) - Early Aptian algal bloom in a neritic proto–North Atlantic setting: Harbinger of global change related to OAE 1a? *Geological Society of America Bulletin*, 124 (11-12): 1810–1825.
- Huck, S., Heimhofer, U., Immenhauser, A. and Weissert, H. (2013) - Carbon-isotope stratigraphy of Early Cretaceous (Urgonian) shoal-water deposits: Diachronous changes in carbonate-platform production in the north-western Tethys. *Sedimentary Geology*, 290: 157–174.
- Huck, S., Rameil, N., Korbar, T., Heimhofer, U., Wiczeorek, T.D. and Immenhauser, A. (2010) - Latitudinally different responses of Tethyan shoal-water carbonate systems to the Early Aptian oceanic anoxic event (OAE 1a). *Sedimentology*, 57 (7): 1585–1614.
- Huck, S., Stein, M., Immenhauser, A., Skelton, P.W., Christ, N., Föllmi, K.B. and Heimhofer, U. (2014) - Response of proto-North Atlantic carbonate-platform ecosystems to OAE1a-related stressors. *Sedimentary Geology*, 313: 15–31.
- Hultberg, S.U. (1986) - Danian dinoflagellate zonation, the C-T boundary and the stratigraphical position of the fish clay in southern Scandinavia. *Journal of Micropalaeontology*, 5 (1): 37–47.
- Hurlbert, S.H. (1971) - The Nonconcept of Species Diversity: A Critique and Alternative Parameters. *Ecology*, 52 (4): 577–586.
- Imbrie, J. and Imbrie, J.Z. (1980) - Modeling the climatic response to orbital variations. *Science*, 207 (4434): 943–953, PMID: 17830447.
- Imbrie, J. and Kipp, N.G. (1971) - A new micropalaeontological method of quantitative palaeoclimatology: Application to a Late Pleistocene Caribbean core, in Turekian K.K. (ed.), *The Late Cenozoic Glacial Ages*. Yale University Press, New Haven, CT: 71–181.
- Jagoutz, O., Müntener, O., Manatschal, G., Rubatto, D., Péron-Pinvidic, G., Turrin, B.D. and Villa, I.M. (2007) - The rift-to-drift transition in the North Atlantic: A stuttering start of the MORB machine? *Geology*, 35 (12): 1087–1090.
- Jahren, A.H., Arens, N.C., Sarmiento, G., Guerrero, J. and Amundson, R. (2001) - Terrestrial record of methane hydrate dissociation in the Early Cretaceous. *Geology*, 29 (2): 159–162.
- Jain, K.P. and Millepied, P. (1975) - Cretaceous microplankton from Senegal basin, West Africa. Pt II. Systematics and Biostratigraphy. *Geophytology*, 5 (4): 126–171.
- Jan du Chêne, R. (1988) - Étude systématique des kystes de dinoflagellés de la Formation des Madeleines (Danien du Sénégal). *Cahiers de Micropaléontologie*, 2: 147–174.
- Jan du Chêne, R. and Adediran, S.A. (1985) - Late Paleocene to Early Eocene dinoflagellates from Nigeria. *Cahiers de Micropaléontologie*, 3: 5–38.
- Jansa, L.F., Enos, P., Tucholke, B.E., Gradstein, F.M. and Sheridan, R.E. (1979) - Mesozoic-Cenozoic Sedimentary Formations of the North American Basin; Western North Atlantic, in Talwani, H., Hay W. and Ryan W.B.F. (eds.), *Deep Drilling Results in the Atlantic Ocean: Continental Margins and Paleoenvironment*. American Geophysical Union: 275–296 (Maurice Ewing; 3).
- Jansson, I.-M., Mertens, K.N., Head, M.J., de Vernal, A., Londeix, L., Marret, F., Matthiessen, J. and Sangiorgi, F. (2014) - Statistically assessing the correlation between salinity and morphology in cysts produced by the dinoflagellate *Protoceratium reticulatum* from surface sediments of the North Atlantic Ocean, Mediterranean–Marmara–Black Sea region, and Baltic–Kattegat–Skagerrak estuarine system. *Palaeogeography, Palaeoclimatology, Palaeoecology*, 399: 202–213.
- Jaramillo, C.A. and Oboh-Ikuenobe, F.E. (1999) - Sequence stratigraphic interpretations from palynofacies, dinocyst and lithological data of Upper Eocene–Lower Oligocene strata in southern Mississippi and Alabama, U.S. Gulf Coast. *Palaeogeography, Palaeoclimatology, Palaeoecology*, 145 (4): 259–302.

- Jolley, D.W. (1992) - Palynofloral association sequence stratigraphy of the Palaeocene Thanet Beds and equivalent sediments in eastern England. *Review of Palaeobotany and Palynology*, 74 (3–4): 207–237.
- Jones, E.J.W., Cande, S.C. and Spathopoulos, F. (1995) - Evolution of a major oceanographic pathway: the equatorial atlantic. *Geological Society, London, Special Publications*, 90 (1): 199–213.
- Joos, F., Bruno, M., Fink, R., Siegenthaler, U., Stocker, T.F., Le Quéré, C. and Sarmiento, J.L. (1996) - An efficient and accurate representation of complex oceanic and biospheric models of anthropogenic carbon uptake. *Tellus B*, 48 (3): 397–417.
- Kirsch, K.H. (1991) - Dinoflagellaten-Zysten aus der Oberkreide des Helvetikums und Nordultrahelvetikums von Oberbayern. *Müncher Geowiss. Abh., Reihe A, Geol. Palaeontol.*, 22: 1–306.
- Krebs, C.J. (1989) - *Ecological Methodology*. Harper & Row, New York, 678 p.
- Kuhnt, W., Holbourn, A. and Moullade, M. (2011) - Transient global cooling at the onset of early Aptian oceanic anoxic event (OAE) 1a. *Geology*, 39 (4): 323–326.
- Kuhnt, W. and Moullade, M. (2007) - The Gargasian (Middle Aptian) of La Marcoulaine section at Cassis-La Bédoule (SE France): Stable isotope record and orbital cyclicity. *Carnets de Géologie / Notebooks on Geology* (Article 2007/02 (CG2007_A02)): 1–9.
- Kuhnt, W., Moullade, M. and Kaminski, M.A. (1998a) - Upper Cretaceous, K/T boundary, and Paleocene agglutinated foraminifers from Hole 959D (Côte d'Ivoire-Ghana transform margin), in Mascle J., Lohmann G.P. and Moullade M. (eds.), *Proceedings of the Ocean Drilling Program, Scientific Results*. College Station, TX (Ocean Drilling Program), 159: 389–411.
- Kuhnt, W., Moullade, M., Masse, J.-P. and Erlenkeuser, H. (1998b) - Carbon isotope stratigraphy of the lower Aptian historical stratotype at Cassis - La Bédoule (SE France). *Géologie Méditerranéenne*, 25 (3-4): 63–79.
- Kuypers, M.M.M., Lourens, L.J., Rijpstra, W.I.C., Pancost, R.D., Nijenhuis, I.A. and Sinninghe Damsté, J.S. (2004) - Orbital forcing of organic carbon burial in the proto-North Atlantic during oceanic anoxic event 2. *Earth and Planetary Science Letters*, 228 (3–4): 465–482.
- Lana, C.C. and Pedrão, E. (2000) - Um episódio de incursão marinha no Eoaptiano (Eoalagoas) da Bacia de Almada, BA, Brasil. *Revista Universidade de Guarulhos, Geociências*, V (Numero Especial): 89–92.
- Larson, R.L. and Erba, E. (1999) - Onset of the Mid-Cretaceous greenhouse in the Barremian-Aptian: Igneous events and the biological, sedimentary, and geochemical responses. *Paleoceanography*, 14 (6): 663–678.
- Leander, B.S. (2008) - *Alveolates. Alveolata*. <http://tolweb.org/Alveolates/2379/2008.09.16> in The Tree of Life Web Project, <http://tolweb.org/>.
- Lebedeva, N.K. (2010) - Palynofacies in upper cretaceous sediments of northern Siberia. *Stratigraphy and Geological Correlation*, 18 (5): 532–549.
- Lebedeva, N.K. and Nikitenko, B.L. (1999) - Dinoflagellate cysts and microforaminifera of the Lower Cretaceous Yatria River section, Subarctic Ural, NW Siberia (Russia). Biostratigraphy, palaeoenvironmental and palaeogeographic discussion. *Grana*, 38 (2-3): 134–143.
- Leckie, R.M., Bralower, T.J. and Cashman, R. (2002) - Oceanic anoxic events and plankton evolution: Biotic response to tectonic forcing during the mid-Cretaceous. *Paleoceanography*, 17 (3): 13–1.
- De Leeuw, J.W., Versteegh, G.J.M. and Bergen, P.F. van (2006) - Biomacromolecules of algae and plants and their fossil analogues. *Plant Ecology* (182): 209–233.

- Legendre, P. and Legendre, L. (eds.) (1998) - *Developments in Environmental Modelling*. Elsevier, Amsterdam, Second, 20, 853 p. (Numerical Ecology).
- Lentin, J.K. and Williams, G.L. (1980) - Dinoflagellate provincialism with emphasis on Campanian Peridiniaceans. *American Association of Stratigraphic Palynologists, Contribution Series*, 7: 47.
- Lewis, J., Dodge, J.D. and Powell, A.J. (1990) - Quaternary dinoflagellate cysts from the upwelling system offshore Peru, Hole 686B, ODP Leg 112, in E. Suess, R. von Huene and et al. (eds.), *Proceedings of the Ocean Drilling Program, 112 Scientific Reports*. Ocean Drilling Program, 112: 323–328 (Proceedings of the Ocean Drilling Program).
- Limoges, A., de Vernal, A. and Van Nieuwenhove, N. (2014) - Long-term hydrological changes in the northeastern Gulf of Mexico (ODP-625B) during the Holocene and late Pleistocene inferred from organic-walled dinoflagellate cysts. *Palaeogeography, Palaeoclimatology, Palaeoecology*, 414: 178–191.
- Lini, A., Weissert, H. and Erba, E. (1992) - The Valanginian carbon isotope event: a first episode of greenhouse climate conditions during the Cretaceous. *Terra Nova*, 4 (3): 374–384.
- Lister, J.K. and Batten, D.J. (1988) - Stratigraphic and Palaeoenvironmental distribution of Early Cretaceous dinoflagellate cysts in the Hurlands Farm Borehole, West Sussex, England. *Palaeontographica Abteilung B*, 210: 9–89.
- Lorenzen, J., Kuhnt, W., Holbourn, A., Flögel, S., Moullade, M. and Tronchetti, G. (2013) - A new sediment core from the Bedoulian (Lower Aptian) stratotype at Roquefort-La Bédoule, SE France. *Cretaceous Research*, 39: 6–16.
- Machhour, L., Masse, J.P., Oudin, J.L., Lambert, B. and Lapointe, P. (1998) - Petroleum potential of dysaerobic carbonate source rocks in an intra-shelf basin; the Lower Cretaceous of Provence, France. *Petroleum Geoscience*, 4 (2): 139–146.
- Malod, J.A. and Mauffret, A. (1990) - Iberian plate motions during the Mesozoic. *Tectonophysics*, 184 (3–4): 261–278.
- Marret, F., Vernal, A. de, Pedersen, T.F. and McDonald, D. (2001) - Middle Pleistocene to Holocene palynostratigraphy of Ocean Drilling Program Site 887 in the Gulf of Alaska, northeastern North Pacific. *Canadian Journal of Earth Sciences*, 38 (3): 373–386.
- Marret, F. and Zonneveld, K.A.F. (2003) - Atlas of modern organic-walled dinoflagellate cyst distribution. *Review of Palaeobotany and Palynology*, 125 (1–2): 1–200.
- Marshall, K.L. and Batten, D.J. (1988) - Dinoflagellate cyst associations in Cenomanian-Turonian “black shale” sequences of Northern Europe. *Review of Palaeobotany and Palynology*, 54 (1–2): 85–103.
- Masclé, J., Basile, C., Pontoise, B. and Sage, F. (1995) - The Cote D’Ivoire — Ghana Transform Margin: An Example of an Ocean-Continent Transform Boundary, in Banda E., Torné M. and Talwani M. (eds.), *Rifted Ocean-Continent Boundaries*. Springer Netherlands: 327–339, DOI: 10.1007/978-94-011-0043-4_18 (NATO ASI Series; 463).
- Masclé, J. and Blarez, E. (1987) - Evidence for transform margin evolution from the Ivory Coast–Ghana continental margin. *Nature*, 326 (6111): 378–381.
- Masclé, J., Lohmann, G.P., Clift, P.D. and Shipboard Scientific Party (1996) - *Proceedings of the Ocean Drilling Program*. Ocean Drilling Program, College Station, TX, (Initial Reports; 159).
- Masse, J.-P. (1976) - *Les calcaires urgoniens de Provence (Valanginien-Aptien inférieur)*. *Stratigraphie, paléontologie, les paléo-environnements et leur évolution*. Thèse, Université Aix-Marseille, 445 p.

- Masse, J.-P. (1993) - Valanginian to Early Aptian carbonate platforms from Provence, Southeastern France, in Simo T., Scott R.W. and Masse J.-P. (eds.), *Cretaceous Carbonate Platforms*. American Association of Petroleum Geologists, 56: 363–374 (Memoir).
- Masse, J.-P. (1998) - Sédimentologie du stratotype historique de l'Aptien inférieur dans la région de Cassis-La Bédoule (SE France). *Géologie Méditerranéenne*, 25 (3-4): 31–41.
- Masse, J.-P., Borgomano, J. and Maskiry, S.A. (1997) - Stratigraphy and tectonosedimentary evolution of a late Aptian-Albian carbonate margin: the northeastern Jebel Akhdar (Sultanate of Oman). *Sedimentary Geology*, 113 (3–4): 269–280.
- Masse, J.-P., Bouaziz, S., Amon, E.O., Baraboshin, E., Tarkowski, R.A., Bergerat, F., Sandulescu, M., Platel, S.P., Canerot, J., Guiraud, R., Poisson, A., Ziegler, M., Rimmele, G., Charrat, F., and others (2000) - Early Aptian (112-114 Ma), map 13, in Dercourt J., Gateani M., Vrielynck B., Barrier E., Biju-Duval B., Brunet M.F., Cadet J.P., Crasquin S. and Sandulescu M. (eds.), *Atlas Peri-Tethys: palaeoenvironmental maps, Explanatory notes*. Paris: 268.
- Masse, J.-P. and Chartrousse, A. (1997) - Les *Caprina* (Rudistes) de l'Aptien inférieur d'Europe occidentale: systématique, biostratigraphie et paléobiogéographie. *Geobios*, 30 (6): 797–809.
- Masse, J.-P. and Fenerci-Masse, M. (2011) - Drowning discontinuities and stratigraphic correlation in platform carbonates. The late Barremian–early Aptian record of southeast France. *Cretaceous Research*, 32 (6): 659–684.
- Masse, J.-P. and Fenerci-Masse, M. (2013a) - Drowning events, development and demise of carbonate platforms and controlling factors: The Late Barremian–Early Aptian record of Southeast France. *Sedimentary Geology*, 298: 28–52.
- Masse, J.-P. and Fenerci-Masse, M. (2013b) - Stratigraphic updating and correlation of Late Barremian–Early Aptian Urgonian successions and their marly cover, in their type region (Orgon-Apt, SE France). *Cretaceous Research*, 39: 17–28.
- Masse, J.-P. and Fenerci-Masse, M. (2013c) - Bioevents and palaeoenvironmental changes in carbonate platforms: The record of Barremian “Urgonian” limestones of SE France. *Palaeogeography, Palaeoclimatology, Palaeoecology*, 386: 637–651.
- Masse, J.-P. and Machhour, L. (1998) - La matière organique dans la série du stratotype historique de l'Aptien inférieur de Cassis - La Bédoule (SE France). *Géologie Méditerranéenne*, 25 (3-4): 55–62.
- Masse, J.-P. and Philip, J.M. (1986) - L'évolution des rudistes au regard des principaux événements géologiques du Crétacé. *Bulletin du Centre de recherches Elf Exploration-Production* (10): 437–445.
- Masse, J.P. and Rossi, T. (1987) - Le provincialisme sud-caraïbe à l'Aptien inférieur. Sa signification dans le cadre de l'Evolution géodynamique du domaine Caraïbe et de l'Atlantique central. *Cretaceous Research*, 8 (4): 349–363.
- Masure, E. (1984) - L'indice de diversité et les dominances des “communautés” de kystes de Dinoflagellés: marqueurs bathymétriques: forage 398D, croisière 47B. *Bulletin de la Société géologique de France, Paris*, XXVI (1): 93–111.
- Masure, E. (1985) - Les kystes de dinoflagellés de l'Autoroute A 10. *Cretaceous Research*, 6 (3): 199–206.
- Masure, E., Aumar, A.-M. and Vrielynck, B. (2013) - Worldwide palaeogeography of Aptian and Late Albian dinoflagellate cysts: Implications for sea-surface temperature gradients and palaeoclimate, in Lewis J., Marret F. and Bradley L. (eds.), *Biological and Geological Perspectives of Dinoflagellates*. Geological Society, London: 97–125 (The Micropalaeontological Society, Special Publications).

- Masure, E., Rauscher, R., Dejax, J., Schuler, M. and Ferré, B. (1998a) - Cretaceous–Paleocene palynology from the Côte d'Ivoire–Ghana transform margin, Sites 959, 960, 961, and 962, in Mascle J., Lohmann G.P. and Moullade M. (eds.), *Proceedings of the Ocean Drilling Program, Scientific Results*. College Station, TX (Ocean Drilling Program), 159: 253–276.
- Masure, E., Raynaud, J.-F., Pons, D. and de Reneville, P. (1998b) - Palynologie du stratotype historique de l'Aptien inférieur dans la région de Cassis - La Bédoule (SE France). *Géologie Méditerranéenne*, 25 (3-4): 263–287.
- Masure, E., Tea, J. and Yao, R. (1996) - The dinoflagellate *Andalusiella*: emendation of the genus, revision of species, *A. ivoirensis* Masure, Tea and Yao, sp. nov. *Review of Palaeobotany and Palynology*, 91 (1-4): 171–186.
- Masure, E. and Vrielynck, B. (2009) - Late Albian dinoflagellate cyst paleobiogeography as indicator of asymmetric sea surface temperature gradient on both hemispheres with southern high latitudes warmer than northern ones. *Marine Micropaleontology*, 70 (3–4): 120–133.
- Matthiessen, J., Vernal, A., Head, M., Okolodkov, Y., Zonneveld, K. and Harland, R. (2005) - Modern organic-walled dinoflagellate cysts in arctic marine environments and their (paleo-) environmental significance. *Paläontologische Zeitschrift*, 79 (1): 3–51.
- Menegatti, A.P., Weissert, H., Brown, R.S., Tyson, R.V., Farrimond, P., Strasser, A. and Caron, M. (1998) - High-resolution $\delta^{13}\text{C}$ stratigraphy through the Early Aptian "Livello selli" of the Alpine tethys. *Paleoceanography*, 13 (5): 530–545.
- Mertens, K.N., Dale, B., Ellegaard, M., Jansson, I.-M., Godhe, A., Kremp, A. and Louwye, S. (2011) - Process length variation in cysts of the dinoflagellate *Protoceratium reticulatum*, from surface sediments of the Baltic–Kattegat–Skagerrak estuarine system: a regional salinity proxy. *Boreas*, 40 (2): 242–255.
- Mertens, K.N., Verhoeven, K., Verleye, T., Louwye, S., Amorim, A., Ribeiro, S., Deaf, A.S., Harding, I.C., De Schepper, S., González, C., Kodrans-Nsiah, M., De Vernal, A., Henry, M., Radi, T., et al. (2009) - Determining the absolute abundance of dinoflagellate cysts in recent marine sediments: The *Lycopodium* marker-grain method put to the test. *Review of Palaeobotany and Palynology*, 157 (3-4): 238–252.
- Meyers, P.A. and Shaw, T.J. (1996) - Organic matter accumulation, sulfate reduction, and methanogenesis in Pliocene–Pleistocene turbidites on the Iberia Abyssal Plain., in Whitmarsh R.B., Sawyer D.S., Klaus A. and Masson D.G. (eds.), *Proceedings of the Ocean Drilling Program, Scientific Results*. Ocean Drilling Program, College Station, TX, 149: 305–313.
- Monteil, E. and Foucher, J.-C. (1998) - Cretaceous biochrono-stratigraphy, in de Graciansky P.-C., Hardenbol J., Jacquin T. and Vail P. (eds.), *Mesozoic and Cenozoic Sequence Stratigraphy of European Basins.*, 60 (SEPM Special Publication).
- Moreno-Bedmar, J.A., Company, M., Bover-Arnal, T., Salas, R., Delanoy, G., Martínez, R. and Grauges, A. (2009) - Biostratigraphic characterization by means of ammonoids of the lower Aptian Oceanic Anoxic Event (OAE 1a) in the eastern Iberian Chain (Maestrat Basin, eastern Spain). *Cretaceous Research*, 30 (4): 864–872.
- Moullade, M., Granier, B. and Tronchetti, G. (2011) - The Aptian Stage: Back to fundamentals. *Episodes*, 34 (3): 148–156.
- Moullade, M. and Guérin, S. (1982) - Le problème des relations de l'Atlantique Sud et de l'Atlantique Central au Crétacé moyen; nouvelles données microfauniques d'après les forages D.S.D.P. *Bulletin de la Société géologique de France, Paris*, 24 (3): 511–517.
- Moullade, M., Mascle, J., Benkheilil, J., Cousin, M. and Tricart, P. (1993) - Occurrence of marine mid-Cretaceous sediments along the Guinean slope (Equamarge II cruise): their significance for the evolution of the central Atlantic African margin. *Marine Geology*, 110 (1): 63–72.

- Moullade, M. and Tronchetti, G. (2010) - A preliminary quantitative study of Foraminifera within the paleoenvironmental record of the Aptian stratotypes. *Revue de Micropaléontologie*, 53 (3): 193–208.
- Moullade, M., Tronchetti, G. and Bellier, J.-P. (2005) - The Gargasian (Middle Aptian) strata from Cassis-La Bédoule (Lower Aptian historical stratotype, SE France): planktonic and benthic foraminiferal assemblages and biostratigraphy. *Carnets de Géologie / Notebooks on Geology* (Article 2005/02 (CG2005_A02)).
- Moullade, M., Tronchetti, G. and Bellier, J.-P. (2008) - Associations et biostratigraphie des Foraminifères benthiques et planctoniques du Bédoulien sommital et du Gargasien inférieur de La Tuilière-St-Saturnin-lès-Apt (aire stratotypique de l'Aptien, Vaucluse, SE France). *Carnets de Géologie / Notebooks on Geology* (Article 2008/01 (CG2008_A01)).
- Moullade, M., Tronchetti, G., Busnardo, R. and Masse, J.-P. (1998a) - Description lithologique des coupes-types du stratotype historique de l'Aptien inférieur dans la région de Cassis-La Bédoule (SE France). *Géologie Méditerranéenne*, 25 (3-4): 15–29.
- Moullade, M., Tronchetti, G., Granier, B., Bornemann, A., Kuhnt, W. and Lorenzen, J. (2015) - High-resolution integrated stratigraphy of the OAE1a and enclosing strata from core drillings in the Bedoulian stratotype (Roquefort-La Bédoule, SE France). *Cretaceous Research*, 56: 119–140.
- Moullade, M., Tronchetti, G., Kuhnt, W. and Masse, J.-P. (1998b) - Les foraminifères benthiques et planctoniques du stratotype historique de l'Aptien inférieur dans la région de Cassis - La Bédoule (SE France). *Géologie Méditerranéenne*, 25 (3-4): 187–225.
- Moullade, M., Tronchetti, G., Kuhnt, W., Renard, M. and Bellier, J.-P. (2004) - Le Gargasien (Aptien moyen) de Cassis-La Bédoule (stratotype historique de l'Aptien inférieur, SE France): localisation géographique et corrélations stratigraphiques. *Carnets de Géologie / Notebooks on Geology* (CG2004 (L02-fr)): 1–4.
- Moullade, M., Tronchetti, G. and Masse, J.-P. (1998c) - *Le stratotype historique de l'Aptien inférieur (Bédoulien) dans la région de Cassis - La Bédoule (S.E. France)*. *Géologie Méditerranéenne*. Marseille, t. XXV, (n°3-4): 289-298.
- Moullade, M., Watkins, D.K., Oboh-Ikuenobe, F.E., Bellier, J.-P., Masure, E., Holbourn, A.E.L., Erbacher, J., Kuhnt, W., Pletsch, T., Kaminski, M.A., Rauscher, R., Shafik, S., Yepes, O., Dejax, J., et al. (1998d) - Mesozoic biostratigraphic, paleoenvironmental, and paleobiogeographic synthesis, equatorial Atlantic, in Mascle J., Lohmann G.P. and Moullade M. (eds.), *Proceedings of the Ocean Drilling Program, Scientific Results*. College Station, TX (Ocean Drilling Program), 159: 481–490.
- Mudie, P.J. (1992) - Circum-arctic Quaternary and Neogene marine palynofloras: Paleoecology and statistical analysis, in Head M.J. and Wrenn J.H. (eds.), *Neogene and Quaternary Dinoflagellate Cysts and Acritarchs*. American Association of Stratigraphic Palynologists Foundation, Dallas, TX: 347–390.
- Murphy, D.P. and Thomas, D.J. (2013) - The evolution of Late Cretaceous deep-ocean circulation in the Atlantic basins: Neodymium isotope evidence from South Atlantic drill sites for tectonic controls. *Geochemistry, Geophysics, Geosystems*, 14 (12): 5323–5340.
- Nürnberg, D. and Müller, R.D. (1991) - The tectonic evolution of the South Atlantic from Late Jurassic to present. *Tectonophysics*, 191 (1–2): 27–53.
- Oboh-Ikuenobe, F.E., Benson, D.G., Scott, R.W., Holbrook, J.M., Evetts, M.J. and Erbacher, J. (2007) - Re-evaluation of the Albian–Cenomanian boundary in the U.S. Western Interior based on dinoflagellate cysts. *Review of Palaeobotany and Palynology*, 144 (1–2): 77–97.

- Oboh-Ikuenobe, F.E. and Yepes, O. (1997) - Palynofacies analysis of sediments from the Côte d'Ivoire-Ghana transform margin: Preliminary correlation with some regional events in the Equatorial Atlantic. *Palaeogeography, Palaeoclimatology, Palaeoecology*, 129 (3–4): 291–314.
- Oboh-Ikuenobe, F.E., Yepes, O. and Gregg, J.M. (1998) - Palynostratigraphy, palynofacies, and thermal maturation of Cretaceous–Paleocene sediments from the Côte d'Ivoire-Ghana transform margin, in Mascle J., Lohmann G.P. and Moullade M. (eds.), *Proceedings of the Ocean Drilling Program, Scientific Results*. College Station, TX (Ocean Drilling Program), 159: 277–318.
- Patterson, W.P. and Walter, L.M. (1994) - Depletion of ^{13}C in seawater ΣCO_2 on modern carbonate platforms: Significance for the carbon isotopic record of carbonates. *Geology*, 22 (10): 885–888.
- Pearce, M.A., Jarvis, I., Swan, A.R.H., Murphy, A.M., Tocher, B.A. and Edmunds, W.M. (2003) - Integrating palynological and geochemical data in a new approach to palaeoecological studies: Upper Cretaceous of the Banterwick Barn Chalk borehole, Berkshire, UK. *Marine Micropaleontology*, 47 (3–4): 271–306.
- Pearce, M.A., Jarvis, I. and Tocher, B.A. (2009) - The Cenomanian–Turonian boundary event, OAE2 and palaeoenvironmental change in epicontinental seas: new insights from the dinocyst and geochemical records. *Palaeogeography, Palaeoclimatology, Palaeoecology*, 280 (1): 207–234.
- Pedrão, E. and Lana, C.C. (2000) - Ecozona Subtilisphaera e seu registro nas bacias brasileiras. *Revista Universidade de Guarulhos, Geociências*, V (Numero Especial): 81–85.
- Persson, A., Godhe, A. and Karlson, B. (2000) - Dinoflagellate cysts in recent sediments from the West coast of Sweden. *Botanica Marina*, 43 (1): 69–79.
- Peters, S.E. (2001) - The evenness and richness components of taxonomic diversity, in Geological Society of America Annual Meeting – *Abstracts with Programs*. Boulder, CO, 33 (6): 141.
- Peters, S.E. (2003) - *Evenness, Richness and the Cambrian-Paleozoic Faunal Transition in North America: An Assemblage-level Perspective*. PhD, University of Chicago, 279 p.
- Peyrot, D., Barroso-Barcenilla, F., Barrón, E. and Comas-Rengifo, M.J. (2011) - Palaeoenvironmental analysis of Cenomanian–Turonian dinocyst assemblages from the Castilian Platform (Northern-Central Spain). *Cretaceous Research*, 32 (4): 504–526.
- Pfiester, L.A. and Anderson, D.M. (1987) - Dinoflagellate reproduction, in Taylor F.J.R. (ed.), *The Biology of the Dinoflagellates*. Blackwell, Oxford: 611–648 (Botanical Monographs).
- Pielou, E.C. (1969) - *An introduction to mathematical ecology*. Wiley - Interscience, New York, 286 p.
- Pletsch, T., Erbacher, J., Holbourn, A.E.L., Kuhnt, W., Moullade, M., Oboh-Ikuenobede, F.E., Söding, E. and Wagner, T. (2001) - Cretaceous separation of Africa and South America: the view from the West African margin (ODP Leg 159). *Journal of South American Earth Sciences*, 14 (2): 147–174.
- Pospelova, V., de Vernal, A. and Pedersen, T.F. (2008) - Distribution of dinoflagellate cysts in surface sediments from the northeastern Pacific Ocean (43–25°N) in relation to sea-surface temperature, salinity, productivity and coastal upwelling. *Marine Micropaleontology*, 68 (1–2): 21–48.
- Poulsen, C.J., Barron, E.J., Arthur, M.A. and Peterson, W.H. (2001) - Response of the Mid-Cretaceous global oceanic circulation to tectonic and CO₂ forcings. *Paleoceanography*, 16 (6): 576–592.
- Powell, A.J. (1992) - *A Stratigraphic Index of Dinoflagellate Cysts*. Chapman and Hall, London, 290 p.
- Powell, A.J., Lewis, J. and Dodge, J.D. (1992) - The palynological expressions of post-Palaeogene upwelling: a review, in Summerhayes C.P., Prell W.L. and Emeis K.C. (eds.), *The Geological Society, London*, 64: 215–226 (Special Publications).

- Prauss, M.L. (2012a) - The Cenomanian/Turonian Boundary event (CTBE) at Tarfaya, Morocco: Palaeoecological aspects as reflected by marine palynology. *Cretaceous Research*, 34: 233–256.
- Prauss, M.L. (2012b) - The Cenomanian/Turonian Boundary Event (CTBE) at Tarfaya, Morocco, northwest Africa: Eccentricity controlled water column stratification as major factor for total organic carbon (TOC) accumulation: Evidence from marine palynology. *Cretaceous Research*, 37: 246–260.
- Prauss, M.L. (2015) - Marine palynology of the Oceanic Anoxic Event 3 (OAE3, Coniacian – Santonian) at Tarfaya, Morocco, NW Africa – transition from preservation to production controlled accumulation of marine organic carbon. *Cretaceous Research*, 53: 19–37.
- Price, G.D. (1999) - The evidence and implications of polar ice during the Mesozoic. *Earth-Science Reviews*, 48 (3): 183–210.
- Prince, I.M., Jarvis, I., Pearce, M.A. and Tocher, B.A. (2008) - Dinoflagellate cyst biostratigraphy of the Coniacian–Santonian (Upper Cretaceous): New data from the English Chalk. *Review of Palaeobotany and Palynology*, 150 (1–4): 59–96.
- Prince, I.M., Jarvis, I. and Tocher, B.A. (1999) - High-resolution dinoflagellate cyst biostratigraphy of the Santonian–basal Campanian (Upper Cretaceous): new data from Whitecliff, Isle of Wight, England. *Review of Palaeobotany and Palynology*, 105 (3–4): 143–169.
- Pross, J. and Brinkhuis, H. (2005) - Organic-walled dinoflagellate cysts as paleoenvironmental indicators in the Paleogene; a synopsis of concepts. *Paläontologische Zeitschrift*, 79 (1): 53–59.
- Pross, J. and Schmiedl, G. (2002) - Early Oligocene dinoflagellate cysts from the Upper Rhine Graben (SW Germany): paleoenvironmental and paleoclimatic implications. *Marine Micropaleontology*, 45 (1): 1–24.
- Radi, T. and de Vernal, A. (2004) - Dinocyst distribution in surface sediments from the northeastern Pacific margin (40–60°N) in relation to hydrographic conditions, productivity and upwelling. *Review of Palaeobotany and Palynology*, 128 (1–2): 169–193.
- Ramstein, G., Fluteau, F., Besse, J. and Joussaume, S. (1997) - Effect of orogeny, plate motion and land–sea distribution on Eurasian climate change over the past 30 million years. *Nature*, 386 (6627): 788–795.
- Rasmussen, E.S., Lomholt, S., Andersen, C. and Vejbæk, O.V. (1998) - Aspects of the structural evolution of the Lusitanian Basin in Portugal and the shelf and slope area offshore Portugal. *Tectonophysics*, 300 (1–4): 199–225.
- Raup, D.M. (1975) - Taxonomic diversity estimation using rarefaction. *Paleobiology*, 1 (4): 333–342.
- Raup, D.M. and Crick, R.E. (1979) - Measurement of Faunal Similarity in Paleontology. *Journal of Paleontology*, 53 (5): 1213–1227.
- Reboulet, S., Rawson, P.F., Moreno-Bedmar, J.A., Aguirre-Urreta, M.B., Barragán, R., Bogomolov, Y., Company, M., González-Arreola, C., Stoyanova, V.I., Lukeneder, A., Matrimon, B., Mitta, V., Randrianaly, H., Vašiček, Z., et al. (2011) - Report on the 4th International Meeting of the IUGS Lower Cretaceous Ammonite Working Group, the “Kilian Group” (Dijon, France, 30th August 2010). *Cretaceous Research*, 32 (6): 786–793.
- Regali, M.S.P. (1989) - Primeiros registros da transgressão neoptiana na margem equatorial brasileira, in *Proceedings, 11th Congresso Brasileiro de Paleontologia*. Brazilian Paleontological Society, Curitiba, 1: 275–293.
- Renard, M. and de Rafélis, M. (1998) - Géochimie des éléments traces de la phase carbonatée des calcaires de la coupe du stratotype historique de l’Aptien inférieur dans la région de Cassis - La Bédoule (SE France). *Géologie Méditerranéenne*, 25 (3-4): 43–54.

- Renard, M., de Rafélis, M., Emmanuel, L., Beltran, C., Moullade, M. and Tronchetti, G. (2007) - Fluctuations of sea-water chemistry during Gargasian (Middle Aptian) time. Data from trace-element content (Mg, Sr, Mn, Fe) in hemipelagic carbonates from La Marcouline Quarry (Cassis, SE France). *Carnets de Géologie / Notebooks on Geology* (Letter 2007/02 (CG2007_A03)): 1–28.
- Renard, M., de Rafélis, M., Emmanuel, L., Moullade, M., Masse, J.-P., Kuhnt, W., Bergen, J.A. and Tronchetti, G. (2005) - Early Aptian $\delta^{13}\text{C}$ and manganese anomalies from the historical Cassis-La Bédoule stratotype sections (S.E. France): relationship with a methane hydrate dissociation event and stratigraphic implications. *Carnets de Géologie / Notebooks on Geology* (Article 2005/04 (CG2005_A04)).
- Rey, J. (1972) - *Recherches géologiques sur le Crétacé inférieur de l'Estremadura (Portugal)*. Instituto Geologico e Mineiro, 477 p. (Memorias dos Serviços Geológicos de Portugal; 21).
- Rey, J. (1979) - Le Crétacé inférieur de la marge atlantique portugaise: biostratigraphie, organisation séquentielle, évolution paléogéographique. *Ciencias Terra* (5): 97–120.
- Rey, J. (1992) - Les unités lithostratigraphiques du Crétacé inférieur de la région de Lisbonne. *Comunicações Serv. Geol. Portugal*, 78 (2): 103–124.
- Rey, J., Bilotte, M. and Peybernes, B. (1977) - Analyse biostratigraphique et paléontologique de l'Albien marin d'Estremadura (Portugal). *Géobios*, 10 (3): 369–393.
- Rey, J., Dinis, J.L., Callapez, P. and Cunha, P.P. (2006) - *Da rotura continental à margem passiva: composição e evolução do Cretácico de Portugal*. INETI, 75 p. (Cadernos de Geologia de Portugal).
- Reyment, R.A. (1969) - Ammonite biostratigraphy, continental drift and oscillatory transgressions. *Nature*, 224 (5215): 137–140.
- Ribeiro, C. (1857) - *Reconhecimento geológico e hidrológico dos terrenos das vizinhanças de Lisboa*. Academia Real das Sciencias de Lisboa, Lisboa, 1, (n°1), 153 p.
- Riding, R. (2006) - Cyanobacterial calcification, carbon dioxide concentrating mechanisms, and Proterozoic–Cambrian changes in atmospheric composition. *Geobiology*, 4 (4): 299–316.
- Riding, J.B., Penn, I.E. and Woollam, R. (1985) - Dinoflagellate cysts from the type area of the Bathonian stage (Middle Jurassic; Southwest England). *Review of Palaeobotany and Palynology*, 45 (1–2): 149–169.
- Rochon, A., de Vernal, A., Turon, J.-L., Matthiessen, J. and Head, M.J. (1999) - Distribution of recent dinoflagellate cysts in surface sediments from the North Atlantic Ocean and adjacent seas in relation to sea-surface parameters. *American Association of Stratigraphic Palynologists Contribution Series*, 35: 1–146.
- Ropolo, P., Conte, G., Gonnet, R., Masse, J.-P. and Moullade, M. (1998) - Les faunes d'Ammonites du Barrémien supérieur / Aptien inférieur (Bédoulien) dans la région stratotypique de Cassis - La Bédoule (SE France): état des connaissances et propositions pour une zonation par Ammonites du Bédoulien-type. *Géologie Méditerranéenne*, 25 (3-4): 167–175.
- Ropolo, P., Conte, G., Moullade, M., Tronchetti, G. and Gonnet, R. (2008) - The Douvilleiceratidae (Ammonoidea) of the Aptian stratotype region at Cassis - La Bédoule (SE France). *Carnets de Géologie / Notebooks on Geology* (Memoir 2008/03): 60.
- Ropolo, P., Moullade, M., Gonnet, R., Conte, G. and Tronchetti, G. (2006) - The Deshayesitidae Stoyanov, 1949 (Ammonoidea) of the Aptian historical stratotype region at Cassis-La Bédoule (SE France). *Carnet de Géologie*, 1: 46.

- Ross, D.J. and Skelton, P.W. (1993) - Rudist Formations of the Cretaceous: A Palaeoecological, Sedimentological and Stratigraphical Review, in Wright V.P. (ed.), *Sedimentology Review*. Blackwell Publishing Ltd., Oxford, 1: 73–91.
- Saint-Marc, P. and N'Da, V. (1997) - Biostratigraphie et paléoenvironnements des dépôts crétacés au large d'Abidjan (Golfe de Guinée). *Cretaceous Research*, 18 (4): 545–565.
- Sanders, H.L. (1968) - Marine Benthic Diversity: A Comparative Study. *The American Naturalist*, 102 (925): 243–282.
- Saporta, G. (1990) - *Probabilités, analyse des données et statistique*. Editions Technip, Première édition, 496 p.
- Schiøler, P., Brinkhuis, H., Roncaglia, L. and Wilson, G.J. (1997) - Dinoflagellate biostratigraphy and sequence stratigraphy of the Type Maastrichtian (Upper Cretaceous), ENCI Quarry, The Netherlands. *Marine Micropaleontology*, 31 (1–2): 65–95.
- Schlanger and Jenkyns, H. (1976) - Cretaceous Oceanic Anoxic Events: Causes and Consequences. *Geologie en Mijnbouw*, 55 (3-4).
- Scholle, P.A. and Arthur, M.A. (1980) - Carbon Isotope Fluctuations in Cretaceous Pelagic Limestones: Potential Stratigraphic and Petroleum Exploration Tool. *AAPG Bulletin*, 64 (1): 67–87.
- Schrank, E. (1987) - Paleozoic and Mesozoic palynomorphs from northeast Africa (Egypt and Sudan) with special reference to Late Cretaceous pollen and dinoflagellates. *Berliner Geowissenschaftliche Abhandlungen A*, 75 (1): 249–310.
- Scott, R.W. (1970) - Paleoecology and Paleontology of the Lower Cretaceous Kiowa Formation, Kansas, in The Paleontological Institute, The University of Kansas, Kansas, 52 (1): 94 (The University of Kansas Paleontological Contributions).
- Seifert, H. (1963) - Beiträge zur Geologie der Serra da Arrábida in Portugal. *Geologisches Jahrbuch*, 81: 277–344.
- Shafik, S., Watkins, D.K. and Shin, I.C. (1998) - Calcareous nannofossil Paleogene biostratigraphy, Côte d'Ivoire-Ghana marginal ridge, eastern equatorial Atlantic, in Mascle J., Lohmann G.P. and Moullade M. (eds.), *Proceedings of the Ocean Drilling Program, Scientific Results*. College Station, TX (Ocean Drilling Program), 159: 413–431.
- Shipboard Scientific Party (1979) - Site 398, in Sibuet J.C., Ryan W.B.F., et al. (eds.), *Initial Reports of the Deep Sea Drilling Project*. Government Printing Office, Washington, 47: 25–233.
- Shipboard Scientific Party (1996) - Site 959, in Mascle J., Lohmann G.P., Clift P.D., et al. (eds.), *Proceedings of the Ocean Drilling Program, Initial Reports*. College Station, TX (Ocean Drilling Program), 159: 65–150.
- Sibuet, J.-C., Ryan, W.B.F., et al. (1979) - *Initial Reports of the Deep Sea Drilling Project*. U.S. Government Printing Office, Washington, 47 Pt. 2, 787 p. (Initial Reports of the Deep Sea Drilling Project).
- Sigal, J. (1979) - Chronostratigraphy and ecostratigraphy of Cretaceous formations recovered on DSDP Leg 47B, Site 398, in Sibuet J.C., Ryan W.B.F., et al. (eds.), *Initial Reports of the Deep Sea Drilling Project*. U.S. Government Printing Office, Washington, 47 Pt. 2: 287–326.
- Simoneit, S.T. and Mazurek, M.A. (1979) - Lipid geochemistry of Cretaceous sediments from Vigo Seamount, DSDP/IODP Leg 47B, in Sibuet J.C., Ryan W.B.F., et al., (eds.), *Initial Reports of the Deep Sea Drilling Project*. U.S. Government Printing Office, Washington, 47 Pt. 2: 565–570.
- Simpson, E.H. (1949) - Measurement of Diversity. *Nature*, 163 (4148): 688.
- Skelton, P.W. and Gili, E. (2011) - Rudists and carbonate platforms in the Aptian: a case study on biotic interactions with ocean chemistry and climate. *Sedimentology*, 59 (1): 81–117.

- Slimani, H., Louwye, S. and Toufiq, A. (2010) - Dinoflagellate cysts from the Cretaceous–Paleogene boundary at Ouled Haddou, southeastern Rif, Morocco: biostratigraphy, paleoenvironments and paleobiogeography. *Palynology*, 34 (1): 90–124.
- Sluijs, A., Pross, J. and Brinkhuis, H. (2005) - From greenhouse to icehouse; organic-walled dinoflagellate cysts as paleoenvironmental indicators in the Paleogene. *Earth-Science Reviews*, 68 (3): 281–315.
- Smelror, M. (1999) - Pliocene - Pleistocene and redeposited dinoflagellate cysts from the western Svalbard margin (Site 986): biostratigraphy, paleoenvironments, and sediment provenance, in Raymo M.E., Jansen E., Blum P. and Herbert T.D. (eds.), *Proceedings of the Ocean Drilling Program, Scientific Results*. Ocean Drilling Program, College Station, TX, 162: 83–97.
- Smelror, M. and Leereveld, H. (1989) - Dinoflagellate and acritarch assemblages from the Late Bathonian to early Oxfordian of Montagne Crussol, Rhône valley, southern France. *Palynology*, 13 (1): 121–141.
- Soares, D.M., Alves, T.M. and Terrinha, P. (2012) - The breakup sequence and associated lithospheric breakup surface: Their significance in the context of rifted continental margins (West Iberia and Newfoundland margins, North Atlantic). *Earth and Planetary Science Letters*, 355–356: 311–326.
- Solignac, S., de Vernal, A. and Hillaire-Marcel, C. (2004) - Holocene sea-surface conditions in the North Atlantic—contrasted trends and regimes in the western and eastern sectors (Labrador Sea vs. Iceland Basin). *Quaternary Science Reviews*, 23 (3–4): 319–334.
- Soncini, M.-J. (1990) - *Palynologie des phosphates des Oulad Abdoun (Maroc). Biostratigraphie et environnements de la phosphatogenèse dans le cadre de la crise Crétacé — Tertiaire*. Thèse de doctorat, Université Louis Pasteur, Strasbourg, 243 p.
- Soncini, M.-J. and Rauscher, R. (1988) - Associations de dinokystes du Maastrichtien-Paléocène phosphaté au Maroc. *Bulletin du Centre de recherches Elf Exploration-Production*, 12: 427–450.
- Stein, M., Westermann, S., Adatte, T., Matera, V., Fleitmann, D., Spangenberg, J.E. and Föllmi, K.B. (2012) - Late Barremian–Early Aptian palaeoenvironmental change: The Cassis-La Bédoule section, southeast France. *Cretaceous Research*, 37: 209–222.
- Steuber, T. (2002) - Plate tectonic control on the evolution of Cretaceous platform- carbonate production. *Geology*, 30 (3): 259–262.
- Steuber, T., Rauch, M., Masse, J.-P., Graaf, J. and Malkoč, M. (2005) - Low-latitude seasonality of Cretaceous temperatures in warm and cold episodes. *Nature*, 437 (7063): 1341–1344.
- Stover, L.E. and Evitt, W.R. (1978) - *Analyses of Pre-Pleistocene organic-walled dinoflagellates*. Stanford University Publications, Stanford, California, 300 p.
- Taugourdeau-Lantz, J., Azéma, C., Hasenboehler, B., Masure, E. and Moron, J.M. (1984) - Évolution des domaines continentaux et marins de la marge portugaise (Leg 47B, site 398D) au cours du Crétacé: essai d'interprétation par l'analyse palynologique comparée. *Bulletin de la Société géologique de France, Paris*, XXIV (3): 447–459.
- Taylor, F.J.R. (1987) - General group characteristics; special features of interest; short history of dinoflagellate study, in Taylor F.J.R. (ed.), *The Biology of Dinoflagellates*. Blackwell Scientific Publications, Oxford: 1–23.
- Taylor, F.J.R. and Pollinger, U. (1987) - Ecology of dinoflagellates, in Taylor F.J.R. (ed.), *The Biology of Dinoflagellates*. Blackwell Scientific Publications, Oxford: 399–529.
- Tiraboschi, D., Erba, E. and Jenkyns, H.C. (2009) - Origin of rhythmic Albian black shales (Piobbico core, central Italy): Calcareous nannofossil quantitative and statistical analyses and paleoceanographic reconstructions. *Paleoceanography*, 24 (2): PA2222.

- Traverse, A. (1988) - *Paleopalynology*. Unwing Hyman, Boston, 600 p.
- Traverse, A. (2007) - *Paleopalynology*. Springer Netherlands, Dordrecht, 28, (Topics in Geobiology).
- Tucholke, B.E., Sibuet, J.-C., Klaus, A., et al. (eds.) (2004) - *Proceedings of the Ocean Drilling Program, 210 Initial Reports*. Ocean Drilling Project, College Station, TX, 210, (Initial Reports).
- Tyson, R.V. (1995) - *Sedimentary Organic Matter*. Chapman and Hall, London, 615 p.
- Upchurch, G.R., Kiehl, J., Shields, C., Scherer, J. and Scotese, C. (2015) - Latitudinal temperature gradients and high-latitude temperatures during the latest Cretaceous: Congruence of geologic data and climate models. *Geology*, 43 (8): 683–686.
- Vellekoop, J., Smit, J., van de Schootbrugge, B., Weijers, J.W.H., Galeotti, S., Sinninghe Damsté, J.S. and Brinkhuis, H. (2015) - Palynological evidence for prolonged cooling along the Tunisian continental shelf following the K–Pg boundary impact. *Palaeogeography, Palaeoclimatology, Palaeoecology*, 426: 216–228.
- Verdier, J.P. (1975) - Les kystes de Dinoflagellés de la section de Wissant et leur distribution stratigraphique du Crétacé moyen. *Revue de Micropaléontologie*, 17 (4): 191–197.
- de Vernal, A., Eynaud, F., Henry, M., Hillaire-Marcel, C., Londeix, L., Mangin, S., Matthiessen, J., Marret, F., Radi, T., Rochon, A., Solignac, S. and Turon, J.-L. (2005) - Reconstruction of sea-surface conditions at middle to high latitudes of the Northern Hemisphere during the Last Glacial Maximum (LGM) based on dinoflagellate cyst assemblages. *Quaternary Science Reviews*, 24 (7–9): 897–924.
- de Vernal, A., Guiot, J. and Turon, J.-L. (1993) - Late and Postglacial Paleoenvironments of the Gulf of St. Lawrence: Marine and Terrestrial Palynological Evidence. *Géographie physique et Quaternaire*, 47 (2): 167–180.
- de Vernal, A. and Mudie, P.J. (1989) - Pliocene and Pleistocene palynostratigraphy at ODP Sites 646 and 647, eastern and southern Labrador Sea, in Srivastava S.P., Arthur M.A., Clement B., et al. (eds.), *Proceedings of the Ocean Drilling Program*. Ocean Drilling Program, College Station, TX: 401–422 (Scientific Results; 105).
- de Vernal, A., Turon, J.-L. and Guiot, J. (1994) - Dinoflagellate cyst distribution in high-latitude marine environments and quantitative reconstruction of sea-surface salinity, temperature, and seasonality. *Canadian Journal of Earth Sciences*, 31 (1): 48–62.
- Versteegh, G.J.M. (1994) - Recognition of cyclic and non-cyclic environmental changes in the Mediterranean Pliocene: a palynological approach. *Marine Micropaleontology*, 23 (2): 147–183.
- Versteegh, G.J.M., Blokker, P., Bogus, K.A., Harding, I.C., Lewis, J., Oltmanns, S., Rochon, A. and Zonneveld, K.A.F. (2012) - Infra red spectroscopy, flash pyrolysis, thermally assisted hydrolysis and methylation (THM) in the presence of tetramethylammonium hydroxide (TMAH) of cultured and sediment-derived *Lingulodinium polyedrum* (Dinoflagellata) cyst walls. *Organic Geochemistry*, 43: 92–102.
- Versteegh, G.J.M., Blokker, P., Marshall, C. and Pross, J. (2007) - Macromolecular composition of the dinoflagellate cyst *Thalassiphora pelagica* (Oligocene, SW Germany). *Organic Geochemistry*, 38 (10): 1643–1656.
- Versteegh, G.J.M. and Zonneveld, K.A.F. (2002) - Use of selective degradation to separate preservation from productivity. *Geology*, 30 (7): 615–618.
- Vilas, L., Masse, J.P. and Arias, C. (1995) - *Orbitolina* episodes in carbonate platform evolution: the early Aptian model from SE Spain. *Palaeogeography, Palaeoclimatology, Palaeoecology*, 119 (1–2): 35–45.

- Wagner, T. and Pletsch, T. (1999) - Tectono-sedimentary controls on Cretaceous black shale deposition along the opening Equatorial Atlantic Gateway (ODP Leg 159), in Cameron N.R., Bate R.H. and Clure V.S. (eds.), *The Oil and Gas Habitats of the South Atlantic*. Geological Society, London, 153: 241–265 (Special Publications).
- Wall, D., Dale, B., Lohmann, G.P. and Smith, W.K. (1977) - The environmental and climatic distribution of dinoflagellate cysts in modern marine sediments from regions in the North and South Atlantic Oceans and adjacent seas. *Marine Micropaleontology*, 2: 121–200.
- Wang, G. and Eltahir, E.A.B. (2000) - Modeling the Biosphere–Atmosphere System: The Impact of the Subgrid Variability in Rainfall Interception. *Journal of Climate*, 13 (16): 2887–2899.
- Watkins, D.K., Shafik, S. and Shin, I.C. (1998) - Calcareous nannofossils from the Cretaceous of the Deep Ivorian Basin, in Mascle J., Lohmann G.P. and Moullade M. (eds.), *Proceedings of the Ocean Drilling Program, Scientific Results*. College Station, TX (Ocean Drilling Program), 159: 319–333.
- Wegener, A.L. (1915) - *Die Entstehung der Kontinente und Ozeane*. Friedrich Vieweg & Sohn (ed.) Braunschweig, Germany, 1st, 23, 94 p.
- Weissert, H., Lini, A., Föllmi, K.B. and Kuhn, O. (1998) - Correlation of Early Cretaceous carbon isotope stratigraphy and platform drowning events: a possible link? *Palaeogeography, Palaeoclimatology, Palaeoecology*, 137 (3–4): 189–203.
- Westermann, S., Stein, M., Matera, V., Fiet, N., Fleitmann, D., Adatte, T. and Föllmi, K.B. (2013) - Rapid changes in the redox conditions of the western Tethys Ocean during the early Aptian oceanic anoxic event. *Geochimica et Cosmochimica Acta*, 121: 467–486.
- Williams, G.L., Brinkhuis, H., Pearce, M.A., Fensome, R.A. and Weegink, J.W. (2004) - Southern Ocean and global dinoflagellate cyst events compared: index events for the Late Cretaceous–Neogene, in Exon N.F., Kennett J.P. and Malone M.J. (eds.), *Proceedings of the Ocean Drilling Program, Scientific Results*. Ocean Drilling Program, College Station, TX, 189: 1–98.
- Williams, G.L. and Bujak, J.P. (1985) - Mesozoic and Cenozoic dinoflagellates, in Bolli H.M., Saunders J.B. and Perch-Nielsen K. (eds.), *Plankton Stratigraphy*. Cambridge University Press, Cambridge: 847–964.
- Willumsen, P.S. (2000) - Late Cretaceous to early Paleocene palynological changes in midlatitude Southern Hemisphere, New Zealand. *GFF (Geologiska Föreningens i Stockholm Förhandlingar)*, 122: 180–181.
- Willumsen, P.S. (2004) - Two new species of the dinoflagellate cyst genus *Carpatella* Grigorovich 1969 from the Cretaceous / Tertiary transition in New Zealand. *Journal of Micropalaeontology*, 23: 119–125.
- Willumsen, P.S. (2006) - *Palynodinium minus* sp. nov., a new dinoflagellate cyst from the Cretaceous–Paleogene transition in New Zealand; its significance and palaeoecology. *Cretaceous Research*, 27 (6): 954–963.
- Wilpshaar, M. and Leereveld, H. (1994) - Palaeoenvironmental change in the Early Cretaceous Vocontian Basin (SE France) reflected by dinoflagellate cysts. *Review of Palaeobotany and Palynology*, 84 (1–2): 121–128.
- Wilson, G.J. (1967) - Some new species of Lower Tertiary dinoflagellates from McMurdo Sound, Antarctica. *New Zealand Journal of Botany*, 5: 57–83.
- Wilson, P.A. and Norris, R.D. (2001) - Warm tropical ocean surface and global anoxia during the mid-Cretaceous period. *Nature*, 412 (6845): 425–429.

- Zimmerman, H.B., Boersma, A. and McCoy, F.W. (1987) - Carbonaceous sediments and palaeoenvironment of the Cretaceous South Atlantic Ocean. *Geological Society, London, Special Publications*, 26 (1): 271–286.
- Zonneveld, K.A.F., Marret, F., Versteegh, G.J.M., Bogus, K., Bonnet, S., Bouimetarhan, I., Crouch, E., de Vernal, A., Elshanawany, R., Edwards, L., Esper, O., Forke, S., Grøsfjeld, K., Henry, M., et al. (2013) - Atlas of modern dinoflagellate cyst distribution based on 2405 data points. *Review of Palaeobotany and Palynology*, 191: 1–197.
- Zonneveld, K.A.F. and Susek, E. (2007) - Effects of temperature, light and salinity on cyst production and morphology of *Tuberculodinium vancampoae* (the resting cyst of *Pyrophacus steinii*). *Review of Palaeobotany and Palynology*, 145 (1–2): 77–88.
- Zonneveld, K.A.F., Versteegh, G. and Kodrans-Nsiah, M. (2008) - Preservation and organic chemistry of Late Cenozoic organic-walled dinoflagellate cysts: A review. *Marine Micropaleontology*, 68 (1–2): 179–197.

Figure list

Figure 1. Paleogeographic evolution during the Cretaceous.6

Figure 2. Synoptic history of Cretaceous carbonate platform development.8

Figure 3. Geographic distribution of sections containing the OAE1a and major igneous provinces actives during the Cretaceous 10

Figure 4. Phylogenetic tree including dinoflagellates. 11

Figure 5. Synoptic dinoflagellate life cycle involving sexual reproduction and cyst formation.. 13

Figure 6. Main dinocyst morphological attributes. 14

Figure 1.1. Location map of the 959D ODP site22

Figure 1.2. Paleogeographic evolution of the South Atlantic Ocean.23

Figure 1.3. Schematic representation of the regional evolution of the Côte d'Ivoire – Ghana transform margin 24

Figure 1.4. Lithology and lithological units in the 959D site26

Figure 1.5. Stratigraphic distribution of selected dinocyst taxa in the 959D site.....28

Figure 1.6. Main dinocyst events in 959D site samples.29

Figure 1.7. Summary of organic matter assemblage characteristics and relative abundance distribution of selected dinocyst from 959D site assemblages.32

Figure 2.1. Paleogeographical position of Albian studied sites after Masse *et al.*, 2000. 1) Lusitanian Basin, 2) 398D DSDP Hole.....46

Figure 2.2. Synthetic column of the Galé Formation (modified from Rey *et al.*, 2006).48

Figure 2.3. Location of Lusitanian Basin studied sections49

Figure 2.4. Simplified lithological log and correlation of the 398D hole with the outcrops of the Lusitanian Basin.52

Figure 2.5. Crossplot of Taxonomic Richness, E(S₃₀), and Evenness values from Lusitanian Basin and 398D DSDP site samples.57

Figure 2.6. Lusitanian Basin and 398D site taxonomic richness merged by time intervals57

Figure 2.7. Lusitanian Basin and 398D site sample Evenness merged by time intervals.....58

Figure 2.8. UPGMA R-mode cluster analysis of Lusitanian Basin and 398D data.	59
Figure 2.9. UPGMA Q-mode cluster analysis of Lusitanian Basin and 398D data.	59
Figure 2.10. Taxa clusters abundance along the Lusitanian Basin and the 398D hole..	63
Figure 2.11. Plotting of taxon and sample clusters together in the scatter diagram of CA from Lusitanian Basin and 398D site data.....	64
Figure 2.12. Plotting the clusters of samples from the Lusitanian Basin and the 398D site together with their sedimentological and paleontological properties in the CA scattergram	65
Figure 2.13. UPGMA R-mode cluster from Lusitanian Basin data	66
Figure 2.14. UPGMA Q-mode cluster from Lusitanian Basin data	66
Figure 2.15. Lusitanian Basin taxon clusters abundance in the Lusitanian Basin outcrops.....	69
Figure 2.17. Plotting of the clusters of samples from the Lusitanian Basin together with their sedimentological and paleontological properties in the CA scattergram.....	70
Figure 2.17. Scatter diagram of Correspondence Analysis for the Lusitanian outcrops data	70
Figure 2.18. UPGMA R-mode cluster from 398D hole data.....	71
Figure 2.19. UPGMA Q-mode cluster from Hole 398D data.	74
Figure 2.20. Taxa clusters abundance distribution along the 398D site.....	74
Figure 2.21. Scatter diagram of Correspondence analysis from 398D site data and cluster analysis	75
Figure 2.22. Plotting of the clusters of samples from the 398D site together with the main lithonological characteristics of samples plotting in the area	76
Figure 2.23. Plotting the clusters of samples from the analysis of the whole dataset together with those from the Lusitanian Basin alone in the CA scattergram from the whole dataset.....	79
Figure 2.24. Morphological differences between the four species of the genus <i>Oligosphaeridium</i> here considered..	89
Figure 2.25. Distribution of species from the genus <i>Oligosphaeridium</i> along the inshore – offshore studied transect.....	90
Figure 2.26. Morphological differences between the three considered species of the genus <i>Odontochitina</i>	91

Figure 2.27. Distribution of species from the genus <i>Odontochitina</i> along the inshore – offshore studied transect.	91
Figure 2.28. Distribution of the dinocyst associations recognized in function of their environmental preferences.	92
Figure 2.29. Maps of dinocyst associations distribution related to the depositional environments during the Middle Albian to the Vraconian (uppermost Upper Albian) in the western Iberian margin.....	95
Figure 3.1. Aptian palaeogeographic reconstruction with location of the studied sections....	103
Figure 3.2. Location of the studied outcrops from the Southern Provence Basin.....	104
Figure 3.3. Composite section from Gare de Cassis section, La Marcouline Quarry, and Camping Section at Roquefort – La Bédoule from the South Provence Basin, and its biostratigraphical correlation with the 398D DSDP site.....	108
Figure 3.4. Values of diversity metrics and estimation of paleoproductivity from the Cassis – La Bédoule studied samples.....	114
Figure 3.5. Values of diversity metrics and estimation of paleoproductivity in studied samples from the 398D	115
Figure 3.6. Crossplot of Taxonomic Richness and Evenness values Cassis – La Bédoule and La Marcouline successions and 398D DSDP hole samples.....	115
Figure 3.7. Seriation of paleoproductivity values estimated for the Cassis – La Bédoule and La Marcouline successions and for the 398D hole samples.....	116
Figure 3.8. UPGMA R-mode cluster analysis of Southern Provence Basin data.	116
Figure 3.9. UPGMA Q-mode cluster analysis of Southern Provence Basin data.....	117
Figure 3.10. Temporal changes in dinocyst associations in the Southern Provence Basin...	119
Figure 3.11. Plotting the clusters of taxa from the Southern Provence Basin samples together with the sedimentological properties of the studied samples in the scatter diagram from the Correspondence Analysis.....	120
Figure 3.12. Plotting of taxon and sample clusters together in the scatter diagram of CA from the Southern Provence Basin data	120
Figure 3.13. UPGMA R-mode cluster analysis of Southern Provence Basin and 398D hole data.	122
Figure 3.14. UPGMA Q-mode cluster analysis of Southern Provence Basin and 398D data	124

Figure 3.15. Temporal changes in dinocyst associations in the 398D samples	125
Figure 3.16. Plotting of taxon and sample clusters together in the scatter diagram of CA from Southern Provence Basin and 398D data.	126
Figure 3.17. Properties of the structured sedimentary organic matter during the Aptian of the Southern Provence Basin.	127
Figure 3.18. Properties of the structured sedimentary organic matter during the Aptian of the 398D site.	128
Figure 3.19. Diversity values and paleoproductivity from Cassis – La Bédoule and La Marcouline samples merged by interval.....	130
Figure 3.20. Synthesis of published data in the Early – Late Aptian studied interval from the South Provence Basin.	133
Figure 3.21. Comparison of the distribution of dinocysts associations, with the distribution of benthic and planktonic foraminifera associations along the Cassis – La Bédoule and the La Marcouline successions.	136

Table list

Table 1.1. ODP Hole 959D Sample list.....	25
Table 1.2. Comparison of sampling density, stage boundaries position, “gaps” and “errors”.....	35
Table 1.3. Frequency distribution of the dinocyst considered as biostratigraphical markers. ..	36
Table 2.1. Taxa included in TC1-LB+398D, 53 samples contained taxa included in this cluster.	60
Table 2.2. Taxa included in TC2-LB+398D, 58 samples contained taxa included in this cluster.	61
Table 2.3. Taxa included in TC3-LB+398D, 45 samples contained taxa included in this cluster.	62
Table 2.4. Taxa included in TC1-LB, 40 samples contained taxa included in this cluster.....	67
Table 2.5. Taxa included in TC2-LB, 39 samples contained taxa included in this cluster.....	67
Table 2.6. Taxa included in TC3-LB, 32 samples contained taxa included in this cluster.....	68
Table 2.7. Taxa included in TC3-398D, 20 samples contained taxa included in this cluster....	72
Table 2.8. Taxa included in TC4-398D, 16 samples contained taxa included in this cluster....	73
Table 2.9. Taxa included in TC6-398D, 17 samples contained taxa included in this cluster....	73
Table 3.1. Structured sedimentary organic matter categories.....	113
Table 3.2. Taxa included in TC1-SPB.	117
Table 3.3. Taxa included in TC2-SPB.	118
Table 3.4. Other taxa occurring with relative abundances over 2% in more than two samples.....	118
Table 3.5. Taxa included in TC1- 398D+SPB.	123
Table 3.6. Taxa included in TC2- 398D+SPB.	123
Table 3.7. Other taxa occurring with relative abundances over 2% in more than two samples.....	123

PLATES

Plate 1..... 195

Plate 2..... 197

Plate 3..... 199

Plate 4..... 201

Plate 5..... 203

Plate 1

Photomicrographs of dinoflagellate cysts from the ODP Hole 959D. All the specimens are at the same scale, scale bar = 50 μm .

- 1-2** *Unipontidinium grande*, sample 64R01 (92-95 cm); 1015.6 mbsf, lame 5. **1** External dorsal view, **2** Internal ventral view.
- 3** *Phelodinium magnificum*, sample 60R04 (58-61cm); 981.18 mbsf, lame 2, EF: 40J. Middle focus.
- 4** *Dinogymnium* sp., sample 62R01 (76-80cm); 996.16 mbsf, lame 2, EF: 26L4. Middle focus.
- 5** *Palaeohystrichophora cheit*, 62R01 (76-80cm); 996.16 mbsf, lame 2, EF: 43U1. Middle focus.
- 6** *Palaeohystrichophora infusorioides*, sample 67R02 (57-61 cm); 1045.4 mbsf, lame 2. External left lateral view.
- 7** *Spinidinium* sp., sample 57R04 (114-117 cm); 952.74 mbsf, lame 1, EF: 40X1. External ventral view.
- 8** *Trithyrodinium* sp., sample 62R01 (76-80cm); 996.16 mbsf, lame 2, EF: 33Y3. External dorsal view.
- 9, 12-14** *Turbiosphaera* sp.
- 9** sample 51R04 (8-11 cm); 893.78 mbsf, lame 1, EF: 48W. Middle focus.
- 12-13** sample 53R06 (18-20 cm); 914.97 mbsf, lame 2. **12** External right lateral view. **13** Internal left lateral view.
- 14** sample 55R03 (83-85 cm); 930.39 mbsf, lame 1. External left lateral view.
- 10** *Trichodinium castaneum*, sample 60R04 (58-61cm); 981.18 mbsf, lame 1, EF: 39M1. External right lateral view.
- 11** *Xenascus gochtii*, sample 67R02 (57-61 cm); 1045.4 mbsf, lame 2. External dorsal view.

Plate 1

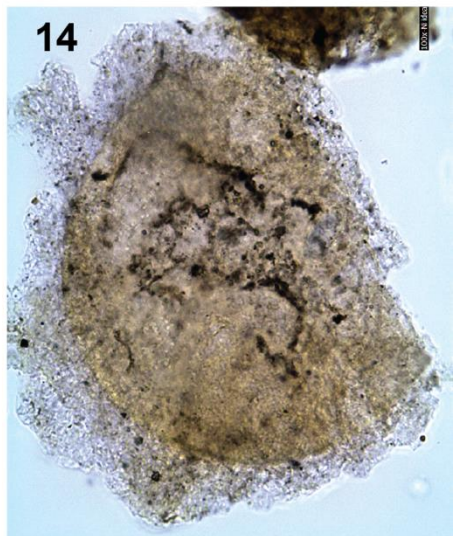
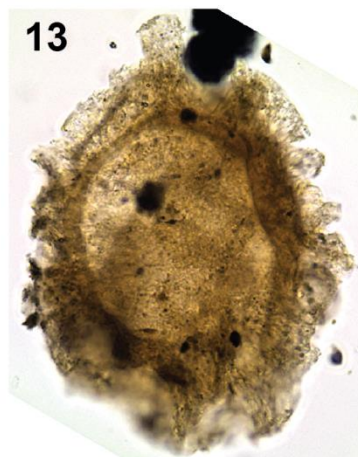
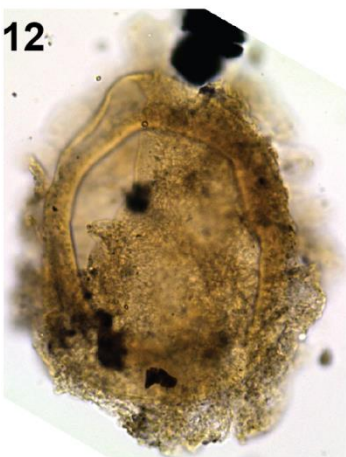
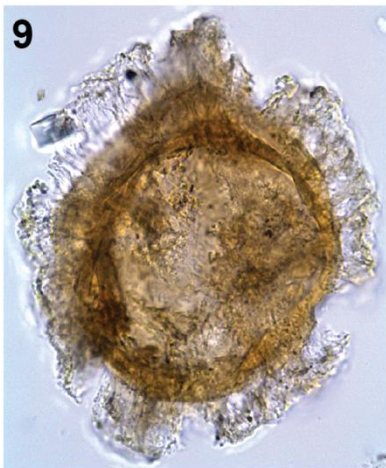
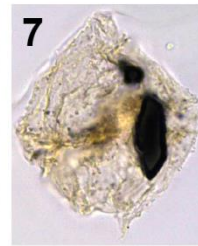
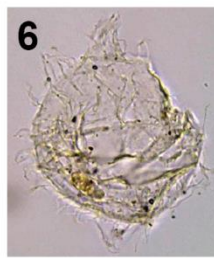
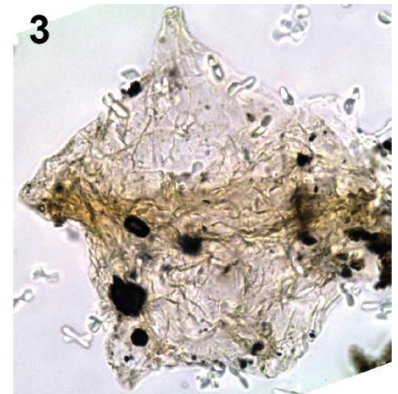
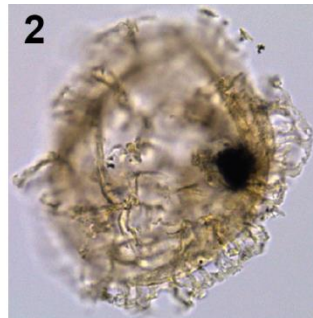


Plate 2

Photomicrographs of dinoflagellate cysts from the ODP Hole 959D. All the specimens are at the same scale, scale bar = 50 μm .

- 1** *Adnatosphaeridium multispinosum*. Sample 44R06 (60-62 cm); 828.7 mbsf, lame 1, EF: 55M. Middle focus.
- 2** *Areoligera* sp. Sample 52R03 (10-13 cm); 901.91 mbsf, lame 2. External dorsal view.
- 3, 6** *Impagidinium celineae*. Sample 48R03 (65-68 cm); 864.25, lame 1.
 - 3** EF: 33W4, external dorso-lateral left view. Note that the operculum (Type P, 3') is within the body cyst.
 - 6** EF: 38P4. External lateral right view.
- 4-5** *Carpatella cornuta*, sample 52R03 (10-13 cm); 901.91 mbsf, lame 1. **4** External dorsal view. **5** Internal ventral view.
- 7** *Cerodinium diebelii*, sample 47R01 (35-37 cm); 851.25 mbsf, lame 1, EF: 46F3. External dorsal view.
- 8-9** *Palaeocystodinium lidiae*.
 - 8** Sample 56R04 (60-62 cm); 942.5 mbsf. External dorsal view.
 - 9** Sample 57R04 (114-117 cm); 952.74 mbsf, lame 1.
- 10** *Andalusiella ivoirensis*. Sample 57R04 (114-117 cm); 952.74 mbsf, lame 2, EF: 28W2. External left lateral view

Plate 2

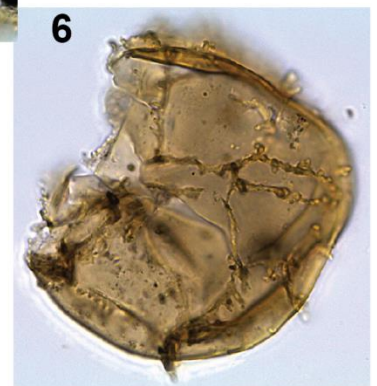
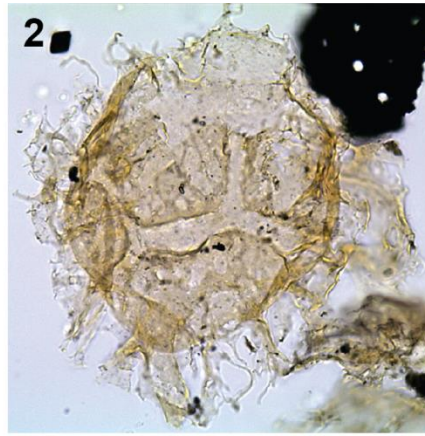
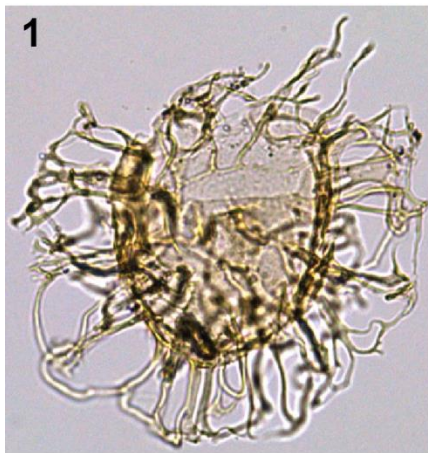


Plate 3

Photomicrographs of Aptian dinoflagellate cysts from the Southern Provence Basin and from the DSDP Hole 398D. All the specimens are at the same scale, scale bar = 50 μm .

All the illustrated taxa, except *Oligosphaeridium complex* and *Subtilisphaera* sp., are included in TC1-SPB and TC1-398D-SBP. *O. complex*, present in all the studied samples, and *Subtilisphaera* sp., only present in one of the studied samples, are not considered for the cluster analyses.

- 1 *Cribopteridinium orthoceras*. Sample 150 (M30729); 93.8 m, lame B, EF: 60N24. Internal dorsal view.
- 2 *Pervosphaeridium* sp. Sample MA 10; 3.6m, lame 1, EF: 55K. External right lateral view.
- 3 *Ovoidinium diversum*. Sample 155C; 99m, lame 1, EF: 51P. External ventral view.
- 4-5 *Circulodinium distinctum*.
 - 4 Sample 146 (M30728); 89m, EF: 33S. Apical view.
 - 5 Sample 155C; 99m, lame 1, EF: 42V. External ventral view.
- 6, 9 *Odontochitina operculata*. Sample MA 10; 3.6m, lame 1.
 - 6 EF: 42S. Operculum.
 - 9 EF: 45V1. External ventral view.
- 7 *Oligosphaeridium complex*. Sample MA15; 6.6 m, lame 1, EF: 44V.
- 8 *Subtilisphaera* sp. Sample 398D_118-4 (113-115 cm); 1549.63 mbsf, lame A, EF: 55P3. External ventral view.

Plate 3

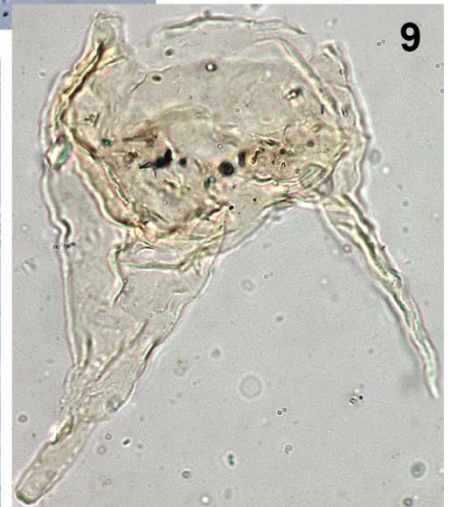
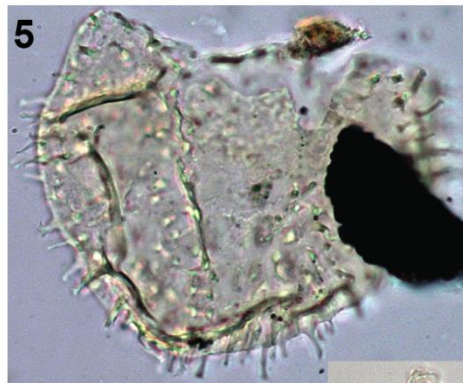
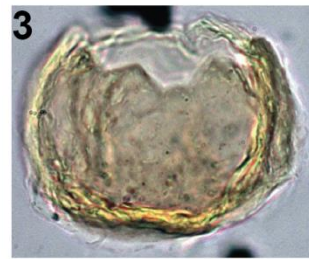
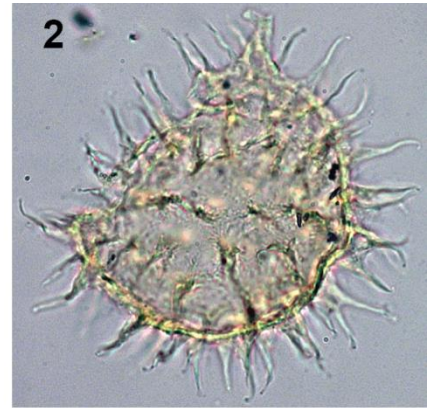


Plate 4

Photomicrographs of Aptian dinoflagellate cysts from the Southern Provence Basin and from the DSDP Hole 398D. All the specimens are at the same scale, scale bar = 50 μm .

All the taxa illustrated, except the three *Spiniferites*, are included in TC2-SPB and TC2-398D-SPB. *Spiniferites*, present in all the studied samples, is not considered for the cluster analysis.

- 1** *Cerbia tabulata*. Sample MA15; 6.6 m, lame 1, EF: 41N, external dorsal view.
- 2-3** *Kallosphaeridium? ringnesiorum*.
 - 2** Sample 398D_111-5 (110 cm); 1484.6 mbsf, lame 2, EF: 46F4. External dorsal view.
 - 3** Sample 398D_118-4 (113-115 cm); 1549.63 mbsf, lame A, EF: 54L3. Internal dorsal view.
- 4-5** *Dingodinium albertii*.
 - 4** Sample MA65; 34.3 m, lame 2, EF: 44U1. Middle focus.
 - 5** Sample MA34; 17 m, lame 1, EF: 46G3. Middle focus.
- 6-7** *Pterodinium* sp. Sample 398D_111-5 (110 cm); 1484.6 mbsf.
 - 6** Lame 2, EF:58T.
 - 7** Lame A, EF: 53G1. Internal ventral-antapical view.
- 8-9** *Pterodinium bab*. Sample MA24; 10.92m, EF: 46R, apical view. Note in illustration 8 the presence of perforations and cavations in the septa. In illustration 9 some granule are visible.
- 10-12** *Spiniferites* sp.
 - 10** Sample 139 (M30727); 80m, EF: 46K. External ventral view.
 - 11** Sample MA82; 42.8 m, EF: 44V4. External ventral view.
 - 12** Sample MA65; 34.3 m, lame 2, EF: 38V. Internal dorsal view.

Plate 4

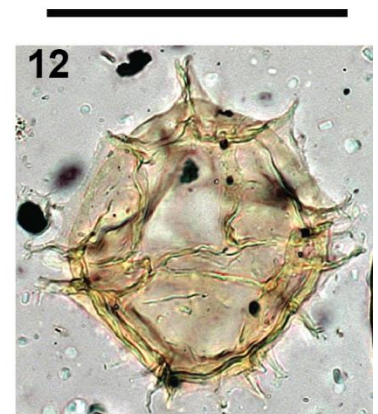
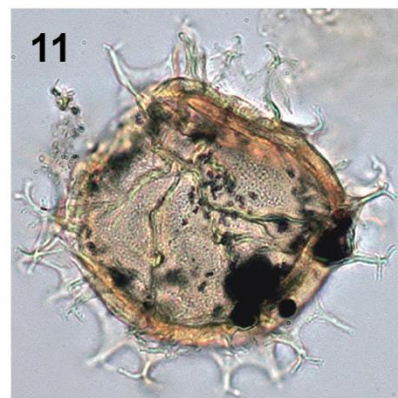
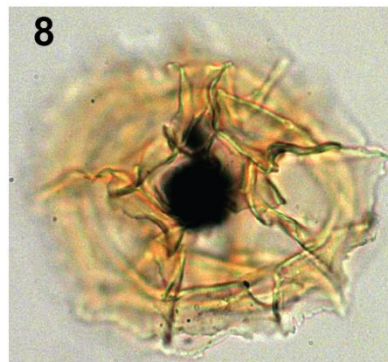
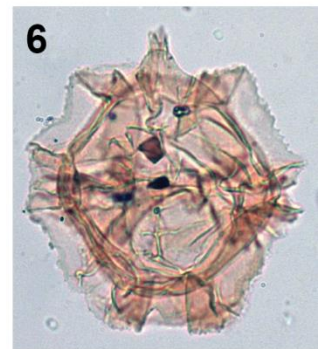
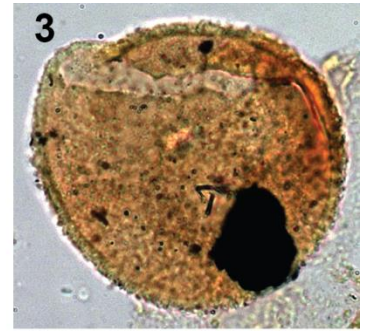
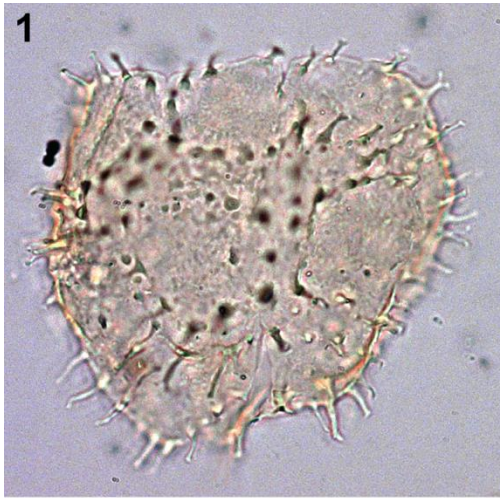


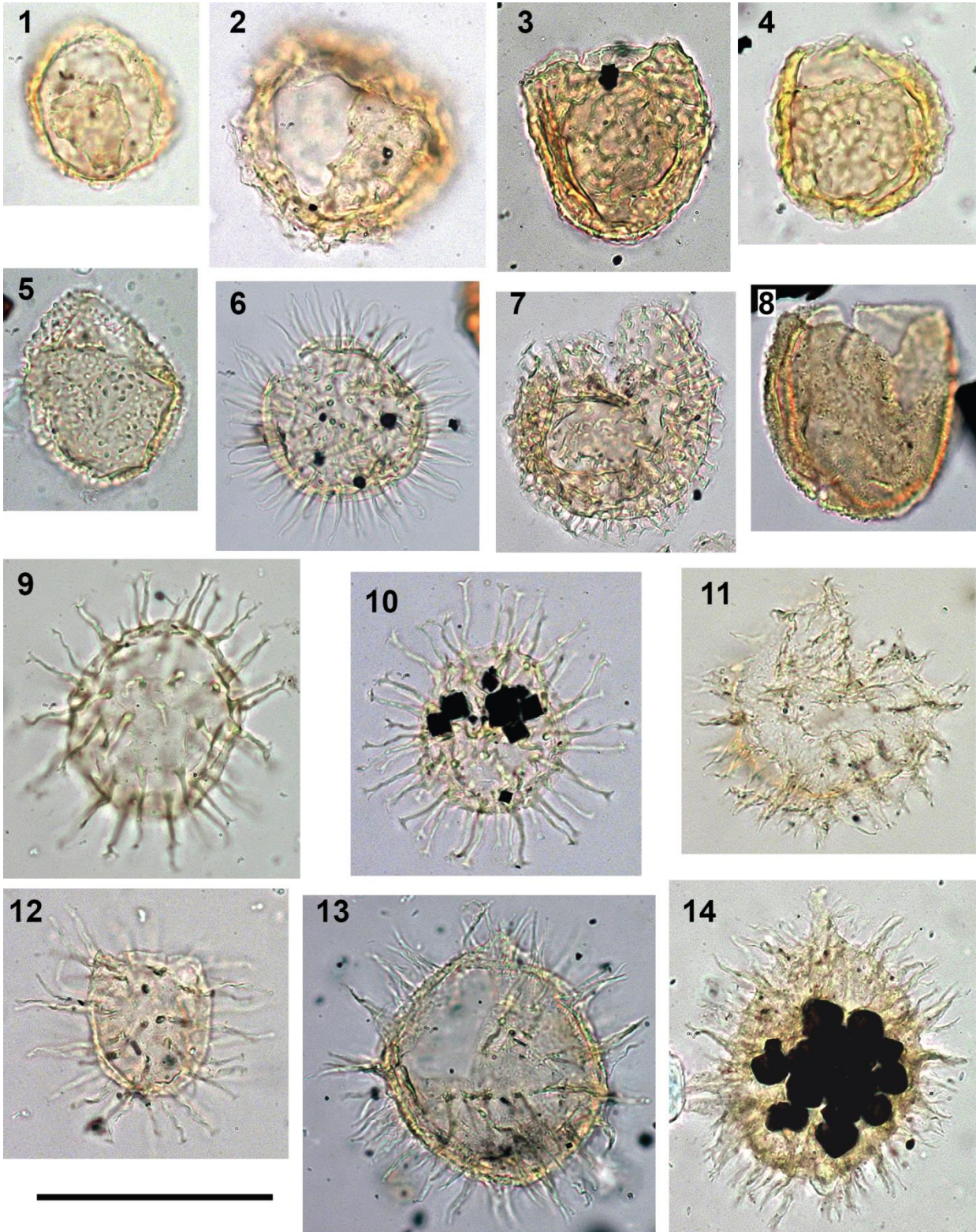
Plate 5

Photomicrographs of Aptian dinoflagellate cysts from the Southern Provence Basin and from the DSDP Hole 398D. All the specimens are at the same scale, scale bar = 50 μm .

All the taxa illustrated are included in TC2-SPB and TC2-398D-SPB.

- 1-2** *Cassiculosphaeridia magna*.
- 1** Sample MA15; 6.6 m, lame 1, EF: 41T. Middle focus, the operculum (Type tA) is within the body cyst.
- 2** Sample MA24; 10.92m, EF: 61N2. Apical view.
- 3-4** *Cassiculosphaeridia reticulata*.
- 3** Sample MA65; 34.3 m, lame 2, EF: 45V4. External ventral view.
- 4** Sample MA34; 17 m, lame 1, EF: 46G3. External dorso-lateral right view.
- 5** *Protoellipsodinium seghire*. Sample MA15; 6.6 m, lame 1, EF: 41X2. External dorso-lateral left view.
- 6** *Dapsilidinium chems*. Sample MA 10; 3.6m, lame 1, EF: 50O. Middle focus.
- 7** *Chlamydothorella nyei*. Sample MA82; 42.8 m, EF: 51Y3. Middle focus.
- 8** *Batiacasphaera* sp. Sample 155C; 99m, lame 1, EF: 48V. External ventro-lateral left view.
- 9** *Taleisphaera cf hydra*. Sample MA 10; 3.6m, lame 1, EF: 37P. Internal dorsal view.
- 10** *Kiokansium unituberculatum*. Sample MA24; 10.92m, EF: 43O2. Middle focus.
- 11** *Exochosphaeridium arnace*. Sample MA15; 6.6 m, lame 1, EF: 32N1. External left lateral view.
- 12** *Tanyosphaeridium isocalamum*. Sample MA15; 6.6 m, lame 1, EF: 33N. External ventro-lateral right view.
- 13** *Exochosphaeridium muelleri*. Sample 155C; 99m, lame 1, EF: 45S2. External dorso-lateral right view.
- 14** *Exochosphaeridium phragmites*. Sample MA48; 25.5 m, lame 2, EF: 32G1. External dorsal view.

Plate 5



APPENDIX

APPENDIX A - Taxa List.....	207
APPENDIX B - Dinocyst stratigraphic distribution	221
APPENDIX C - Correspondence Analysis scatter diagrams	240
APPENDIX D - Structured Sedimentary Organic Matter data	248
APPENDIX E - Foraminifera UPGMA cluster results	249

APPENDIX A - Taxa List

Alphabetical listing of dinoflagellate cyst occurring in samples from the ODP Hole 959D, the Albian outcrops from the Lusitanian Basin, the Aptian and Albian from the DSDP Hole 398D and the Aptian (Bedoulian and Gargasian *p.p.*) from the Southern Provence Basin. Taxa illustrated are followed by plate and figure references in parentheses. The taxonomy and authorship of dinocysts follows Fensome *et al.* (2008).

The use of a genus name followed by “spp.”, as for example *Achomosphaera* spp., is herein used to indicate that several species from the genus *Achomosphaera*, but not necessarily all *Achomosphaera* species, are considered.

Order GONYAULACALES

Genus ACHOMOSPHAERA Evitt, 1963

Achomosphaera crassipellis (Deflandre and Cookson, 1955) Stover and Evitt, 1978

Achomosphaera ramulifera (Deflandre, 1937) Evitt, 1963

Achomosphaera ramulifera subsp. *gabonensis* (Boltenhagen, 1977) Lentin and Williams, 1981

Achomosphaera spp.

Genus ADNATOSPHAERIDIUM Williams and Downie, 1966. Emendation: Stancliffe and Sarjeant, 1990

Adnatosphaeridium multispinosum Williams and Downie, 1966 (Plate 2, Fig. 1)

Adnatosphaeridium tutulosum (Cookson and Eisenack, 1960) Morgan, 1980

Genus AMPHOROSPHAERIDIUM Davey, 1969

Amphorosphaeridium spp.

Genus APTEA Eisenack, 1958. Last emendation: Dörhöfer and Davies, 1980

Aptea polymorpha Eisenack, 1958. Emendation: Dörhöfer and Davies, 1980

Aptea spp.

Genus APTEODINIUM Eisenack, 1958. Last emendation: Lucas-Clark, 1987

Apteodinium deflandrei (Clarke and Verdier, 1967) Lucas-Clark, 1987. Emendation: Lucas-Clark, 1987

Apteodinium fallax (Morgenroth, 1968) Stover and Evitt, 1978

Apteodinium sp. H1 in Hasenboehler, 1981 as *Apteodinium* sp. 1 (pl. 23, fig 8)

Genus AREOLIGERA Lejeune-Carpentier, 1938. Emendation: Williams and Downie, 1966

Areoligera gippingensis Jolley, 1992

Areoligera medusettiformis Wetzel, 1933

Areoligera volata Drugg, 1967

Areoligera spp. (Plate 2, Fig. 2)

Genus ATOPODINIUM Drugg, 1978. Emendation: Masure, 1991

Atopodinium haromense Thomas and Cox, 1988

Atopodinium perforatum (Clarke and Verdier, 1967) Masure, 1991. Last emendation: Masure, 1988 as *Maghrebinia perforata*

Atopodinium spp.

Genus BATICASPHAERA Drugg, 1970. Last emendation: Dörhöfer and Davies, 1980

Batiacasphaera macrogranulata Morgan, 1975

Batiacasphaera (cf *Batiacasphaera*)

Batiacasphaera spp. (Plate 5, Fig. 8)

Genus CALIGODINIUM Drugg, 1970. Emendation: Manum and Williams, 1995

Caligodinium aceras (Manum and Cookson, 1964) Lentin and Williams, 1973

Genus CALLAIOSPHAERIDIUM Davey and Williams, 1966. Last emendation: Below, 1981

Callaiosphaeridium asymmetricum (Deflandre and Courteville, 1939) Davey and Williams, 1966. Emendation: Clarke and Verdier, 1967 as *Hexasphaera asymmetrica*

Callaiosphaeridium spp.

Genus CANNINGIA Cookson and Eisenack, 1960. Last emendation: Helby, 1987

Canningia reticulata Cookson and Eisenack, 1960. Last emendation: Helby, 1987

cf. *Canningia reticulata* Cookson and Eisenack, 1960. Last emendation: Helby, 1987

Canningia? rotundata Cookson and Eisenack, 1961

Canningia torulosa Davey and Verdier, 1973

Canningia spp.

Genus CANNINGINOPSIS

Canninginopsis? Sp. Cookson and Eisenack, 1962. Emendation: Marshall, 1990

Genus CARPATELLA Grigorovich, 1969. Last emendation: Damassa, 1988

Carpatela cornuta Grigorovich, 1969. Last emendation: Damassa, 1988 (Plate 2, Fig. 4-5)

Genus CARPODINIUM Cookson and Eisenack, 1962. Emendation: Leffingwell and Morgan, 1977

Carpodinium granulatum Cookson and Eisenack, 1962. Emendation: Leffingwell and Morgan, 1977

Genus CASSICULOSPHAERIDIA Davey, 1969

Cassiculosphaeridia magna Davey, 1974. Emendation: Harding, 1990 (Plate 5, Fig. 1-2)

Cassiculosphaeridia reticulata, Davey, 1969 (Plate 5, Fig. 3-4)

Cassiculosphaeridia spp.

Genus CAUVERIDINIUM Khowaja-Ateequzaman and Jain, 1990

Cauveridinium membraniphorum (Cookson and Eisenack, 1962) Masure in Fauconnier and Masure, 2004

Genus CERBIA Below, 1981

Cerbia tabulata (Davey and Verdier, 1974) Below, 1981 (Plate 4, Fig. 1)

Genus CHLAMYDOPHORELLA Cookson and Eisenack, 1958. Emendation: Duxbury, 1983

Chlamydophorella discreta Clarke and Verdier, 1967

Chlamydophorella nyei Cookson and Eisenack, 1958 (Plate 5, Fig. 7)

Chlamydophorella spp.

Genus CHYTROEISPHAERIDIA (Sarjeant, 1962) Downie and Sarjeant, 1965. Last emendation: Davey, 1979

Chytroeisphaeridia spp.

Genus CIRCULODINIUM Alberti, 1961

Circulodinium? *brevispinosum* (Pocock, 1962) Jansonius, 1986. Emendation: Brideaux, 1977 as *Tenua brevispinosa*

Circulodinium colliveri (Cookson and Eisenack, 1960) Helby, 1987

Circulodinium distinctum (Deflandre and Cookson, 1955) Jansonius, 1986 (Plate 3, Fig. 4-5)

Circulodinium spp.

Genus CLEISTOSPHAERIDIUM Davey et al., 1966. Emendation: Eaton et al., 2001

Cleistosphaeridium spp.

Genus CODONIELLA Cookson and Eisenack, 1961. Emendation: Davey, 1979.

Substitute name for *Codonia* Cookson and Eisenack, 1960 (an illegitimate name)

Codoniella campanulata (Cookson and Eisenack, 1960) Downie and Sarjeant, 1965.

Emendation: Davey, 1979

Codoniella psygma Davey, 1979

Genus COMETODINIUM Deflandre and Courteville, 1939. Emendation: Monteil, 1991

Cometodinium whitei (Deflandre and Courteville, 1939) Stover and Evitt, 1978. Emendation: Monteil, 1991

Cometodinium spp.

Cometodinium (cf. *Cometodinium*)

Cometodinium spp.

Genus CORDOSPHAERIDIUM Eisenack, 1963. Last emendation: He Chengquan, 1991

Cordosphaeridium spp.

Genus CORONIFERA Cookson and Eisenack, 1958. Last emendation: Mao Shaozhi and Norris, 1988

Coronifera albertii Millioud, 1969

Coronifera oceanica Cookson and Eisenack, 1958. Emendation: May, 1980

Coronifera spp.

Genus CRIBROPERIDINIUM Neale and Sarjeant, 1962. Last emendation: Helenes, 1984

Cribroperidinium boreas (Davey, 1974) Helenes, 1984

Cribroperidinium? *edwardsii* (Cookson and Eisenack, 1958) Davey, 1969

Cribroperidinium intricatum Davey, 1969

Cribroperidinium orthoceras (Eisenack, 1958) Davey, 1969. Emendation: Sarjeant, 1985 (Plate 3, Fig. 1)

Cribroperidinium tensiftense Below, 1981

Criboperidinium sp. H1 in Hasenboehler, 1981 as *Criboperidinium* sp. 1 (pl. 24, fig 4)
Criboperidinium spp.

Genus CTENIDODINIUM Deflandre, 1939. Last emendation: Benson, 1985
Ctenidodinium elegantulum Milliod, 1969. Emendation: Below, 1981

Genus CYCLONEPHELIUM Deflandre and Cookson, 1955. Last emendation: Dörhöfer and Davies, 1980

Cyclonephelium compactum Deflandre and Cookson, 1955

Cyclonephelium sp cf. *Cyclonephelium compactum* Deflandre and Cookson, 1955. In Hasenboehler, 1981 (pl. 18, fig 14)

Cyclonephelium inconspicuum Duxbury, 1983

Cyclonephelium sp. H1 in Hasenboehler, 1981 as *Cyclonephelium* sp. 1 (pl. 18, fig 14)

Cyclonephelium sp. H2 in Hasenboehler, 1981 as *Cyclonephelium* sp. 2 (pl. 18, fig 13)

Cyclonephelium vannophorum, Davey, 1969.

Genus DAMASSADINIUM Fensome et al., 1993. Substitute name for *Danea* Morgenroth, 1968 (an illegitimate name). Emendation: Drugg, 1970 for *Danea*

Damassadinium californicum (Drugg, 1967) Fensome et al., 1993

Damassadinium chibane (Below, 1981) Fensome et al., 1993

Damassadinium cf. *Damassadinium chibane* (Below, 1981) Fensome et al., 1993

Damassadinium sp.

Genus DAPSILIDINIUM Bujak et al., 1980

Dapsilidinium chems (Below, 1982) Lentin and Williams, 1985 (Plate 5, Fig. 6)

Dapsilidinium duma (Below, 1982) Lentin and Williams, 1985

Dapsilidinium laminaspinosum (Davey and Williams, 1966) Lentin and Williams, 1981

Dapsilidinium? *pumilum* (Davey and Williams, 1966) Lentin and Williams, 1981

Dapsilidinium warrenii (Habib, 1976) Lentin and Williams, 1981

Dapsilidinium spp.

Genus DINGODINIUM Cookson and Eisenack, 1958. Last emendation: Stover and Helby, 1987

Dingodinium albertii Sarjeant, 1966. Taxonomic senior synonym: *Dingodinium cerviculum*

Cookson and Eisenack, 1958. Last emendation: Khowaja-Ateequzaman et al., 1990 (Plate 4, Fig. 4-5)

Genus DINOPTERYGIUM Deflandre, 1935. Emendation: Stover and Evitt, 1978

Dinopterygium cladoides, Deflandre, 1935

Genus DIPHYES Cookson, 1965 nomen conservandum propositum. Last emendation: Goodman and Witmer, 1985

Diphyes spp.

Genus DISSILIODINIUM Drugg, 1978. Last emendation: Feist-Burkhardt and Monteil, 2001

Dissiliodinium globulus Drugg, 1978

Genus DOWNIESPHAERIDIUM Islam, 1993. Emendation: Masure in Fauconnier and Masure, 2004

Downiesphaeridium armatum (Deflandre, 1937) Islam, 1993. Emendation: Davey, 1969, as *Cleistosphaeridium armatum*

Genus ELLIPSODINIUM Clarke and Verdier, 1967

Ellipsodinium rugulosum Clarke and Verdier, 1967

Genus ELLIPSOIDICTYUM Klement, 1960

Ellipsoidictyum sagena (Duxbury, 1980) Below, 1982. Emendation: Harding, 1990

Genus ENDOCERATIUM Vozzhennikova, 1965

Endoceratium dettmanniae (Cookson and Hughes, 1964) Stover and Evitt, 1978. Emendation: Harding and Hughes, 1990

Genus EOCLADOPYXIS Morgenroth, 1966. Emendation: Stover and Evitt, 1978

Eocladopyxis peniculata Morgenroth, 1966. Emendation: McLean, 1976

Genus EXOCHOSPHAERIDIUM Davey et al., 1966. Emendation: Helenes, 2000

Exochosphaeridium arnace Davey and Verdier, 1973 (Plate 5, Fig. 11)

Exochosphaeridium bifidum (Clarke and Verdier, 1967) Clarke et al., 1968. Emendation: Davey, 1969

Exochosphaeridium muelleri Yun Hyesu, 1981 (Plate 5, Fig. 13)

Exochosphaeridium phragmites Davey et al., 1966 (Plate 5, Fig. 14)

Exochosphaeridium spp. In SPB and 398D apt groups *E. muelleri* and *E. phragmites*

Exochosphaeridium spp.

Genus FIBROCYSTA Stover and Evitt, 1978

Fibrocysta sp.

Genus FLORENTINIA Davey and Verdier, 1973. Emendation: Duxbury, 1980

Florentinia buspina (Davey and Verdier, 1976) Duxbury, 1980

Florentinia clavigera (Deflandre, 1937) Davey and Verdier, 1973. Emendation: Davey and Verdier, 1976

Florentinia cooksoniae (Singh, 1971) Duxbury, 1980. Emendation: Duxbury, 1980

Florentinia ferox (Deflandre, 1937) Duxbury, 1980

Florentinia laciniata Davey and Verdier, 1973.

Florentinia mantellii (Davey and Williams, 1966) Davey and Verdier, 1973

Florentinia radiculata (Davey and Williams, 1966) Davey and Verdier, 1973. Emendation: Davey and Verdier, 1976

Florentinia stellata (Maier, 1959) Below, 1982

Florentinia sp. H1 in Hasenboehler, 1981 as *Florentinia* sp. 1 (pl. 25, fig 5, 6)

Florentinia spp.

Genus GARDODINIUM Alberti, 1961. Emendation: Harding, 1996

Gardodinium eisenackii Alberti, 1961.

Genus GLAPHYROCYSTA Stover and Evitt, 1978

Glaphyrocysta spp.

Genus GONYAULACYSTA Deflandre, 1964. Last emendation: Helenes and Lucas-Clark, 1997

Gonyaulacysta spp.

Genus HAFNIASPHAERA Hansen, 1977

Hafniasphaera fluens Hansen, 1977. As *Spiniferites fluens* in Oboh et al. (1998).

Hafniasphaera hyalospinosa Hansen, 1977

Hafniasphaera septata (Cookson and Eisenack, 1967) Hansen, 1977. Emendation: McLean, 1971

Genus HAPSOCYSTA Davey, 1979

Hapsocysta peridictya (Eisenack and Cookson, 1960) Davey, 1979. Emendation: Davey, 1979

Genus HETEROSPHAERIDIUM Cookson and Eisenack, 1968. Emendation: Yun Hyesu, 1981

Heterosphaeridium heteracanthum (Deflandre and Cookson, 1955) Eisenack and Kjellström, 1972

Genus HYSTRICHODINIUM Deflandre, 1935. Last emendation: Clarke and Verdier, 1967

Hystrichodinium furcatum Alberti, 1961 / *ramoides* Alberti, 1961

Hystrichodinium pulchrum Deflandre, 1935.

Hystrichodinium sp.

Hystrichodinium spp.

Hystrichodinium voigtii (Alberti, 1961) Davey, 1974, emendation: Sarjeant, 1966.

Genus HYSTRICHOSPHAERIDIUM Deflandre, 1937. Emendation: Davey and Williams, 1966

Hystrichosphaeridium recurvatum (White, 1842) Lejeune-Carpentier, 1940

Hystrichosphaeridium spp.

Genus HYSTRICHOSPHAERINA Alberti, 1961. Emendation: Stancliffe and Sarjeant, 1990

Hystrichosphaerina scindewolfii Alberti, 1961

Hystrichosphaerina spp.

Genus HYSTRICHOSTROGYLON Agelopoulos, 1964. Emendation: Stover and Evitt, 1978

Hystrichostrogylon spp.

Genus IMPAGIDINIUM Stover and Evitt, 1978

Impagidinium celineae Jan du Chêne, 1988 (Plate 2, Fig. 3,6)

Impagidinium verrucosum (Brideaux and McIntyre, 1975) Stover and Evitt, 1978

Impagidinium spp.

Genus IMPLETOSPHAERIDIUM Morgenroth, 1966. Emendation: Islam, 1993

Impletosphaeridium sp.

Genus KALLOSPHAERIDIUM de Coninck, 1969. Emendation: Jan du Chêne et al., 1985
Kallosphaeridium coninckii (Burger, 1980) Burger, 1980
Kallosphaeridium? helbyi Lentin and Williams, 1989. As cf. *Canningia minor* in Masure 1984
Kallosphaeridium? ringnesiorum (Manum and Cookson, 1964) Helby, 1987 (Plate 4, Fig. 2-3)
Kallosphaeridium spp.

Genus KENLEYIA Cookson and Eisenack, 1965
Kenleyia spp.

Genus KIOKANSIUM Stover and Evitt, 1978. Emendation: Duxbury, 1983
Kiokansium polypes (Cookson and Eisenack, 1962) Below, 1982. Emendation: Duxbury, 1983.
 Taxonomic senior synonym (at specific rank): *Hystrichosphaeridium* (as *Kiokansium*)
unituberculatum, by implication in Duxbury (1983, p.49)
Kiokansium unituberculatum (Tasch in Tasch et al., 1964) Stover and Evitt, 1978 (Plate 5, Fig. 10)
Kiokansium sp. H1 in Hasenboehler, 1981 as *Bacchidinium* sp. H1 (pl. 24, fig 5 to 8)
Kiokansium spp.

Genus KLEITHRIASPHAERIDIUM Davey, 1974. Emendation: Torricelli, 2001
Kleithriasphaeridium eoinodes (Eisenack, 1958a, p.402, pl.27, figs.3-4) Davey, 1974, p.58.
 Emendation: Sarjeant, 1985
Kleithriasphaeridium readei (Davey and Williams, 1966) Davey and Verdier, 1976.
 Emendation: Davey and Verdier, 1976 OU *corrugatum* Davey, 1974
Kleithriasphaeridium? sarmentum (Davey, 1979) Below, 1982.
Kleithriasphaeridium tubulosum (Cookson and Eisenack, 1969) Stover and Evitt, 1978.
Kleithriasphaeridium spp.

Genus LEPTODINIUM Klement, 1960. Last emendation: Sarjeant, 1982
Leptodinium spp.

Genus LITOSPHAERIDIUM Davey and Williams, 1966. Last emendation: Lucas-Clark, 1984
Litosphaeridium arundum (Eisenack and Cookson, 1960) Davey, 1979. Emendation: Lucas-Clark, 1984.
Litosphaeridium conispinum Davey and Verdier, 1973. Emendation: Lucas-Clark, 1984.
Litosphaeridium siphoniphorum (Cookson and Eisenack, 1958) Davey and Williams, 1966.
 Emendation: Lucas-Clark, 1984.

Genus MEIOUROGONYAULAX Sarjeant, 1966
Meiourogonyaulax psora Davey and Verdier, 1974.
Meiourogonyaulax stoverii Millioud, 1969
Meiourogonyaulax sp.

Genus MICRODINIUM Cookson and Eisenack, 1960. Last emendation: Slimani, 1994
Microdinium opacum Brideaux, 1971
Microdinium ornatum Cookson and Eisenack, 1960
Microdinium spp.

Genus MUDERONGIA Cookson and Eisenack, 1958. Emendation: Monteil, 1991
Muderongia tetracantha (Gocht, 1957) Alberti, 1961. Emendation: Monteil, 1991

Genus NEXOSISPINUM Davey, 1979
Nexosispinum hesperus Davey, 1979. Emendation: Torricelli, 2000
Nexosispinum sp.

Genus OCCISUCYSTA Gitmez, 1970. Emendation: Jan du Chêne et al., 1986
Occisucysta spp.

Genus ODONTOCHITINA Deflandre, 1937. Last emendations: Núñez-Betelu and Hills, 1998

Odontochitina ancala, Bint, 1986.

Odontochitina costata, Alberti, 1961, emendation: Clarke and Verdier, 1967.

Odontochitina inflata according to Hasenboehler, 1981 (pl 19, fig 9; pl 20, fig 3 to 8 and 11).

Corresponds to *O. ancala* and *O. rakhodes*

Odontochitina operculata (Wetzel, 1933) Deflandre and Cookson, 1955 (Plate 3, Fig. 6,9)

Odontochitina rhakodes Bint, 1986.

Odontochitina spp.

Genus OLIGOSPHAERIDIUM Davey and Williams, 1966. Emendation: Davey, 1982

Oligosphaeridium abaculum Davey, 1979

Oligosphaeridium albertense (Pocock, 1962) Davey and Williams, 1969

Oligosphaeridium? *asterigerum* (Gocht, 1959) Davey and Williams, 1969

Oligosphaeridium? cf. *asterigerum*, *Oligosphaeridium?* *asterigerum* (Gocht, 1959) Davey and Williams, 1969

Oligosphaeridium complex (White, 1842) Davey and Williams, 1966.

Oligosphaeridium complex subsp. *brevispinum* Jain, 1977 (Plate 3, Fig. 7)

Oligosphaeridium diliculum Davey, 1982

Oligosphaeridium dividuum Williams, 1978

Oligosphaeridium pulcherrimum, (Deflandre and Cookson, 1955) Davey and Williams, 1966.

Oligosphaeridium totum, Brideaux, 1971.

Oligosphaeridium vasiformum (Neale and Sarjeant, 1962) Davey and Williams, 1966

Oligosphaeridium spp.

Genus OPERCULODINIUM Wall, 1967. Emendation: Matsuoka et al., 1997

Operculodinium spp.

Genus PAREODINIA Deflandre, 1947d. Last emendation Below, 1990

Pareodinia ceratophora Deflandre, 1947. Emendation Gocht, 1970.

Genus PERISSEIASPHAERIDIUM Davey and Williams, 1966

Perisseiasphaeridium pannosum Davey and Williams, 1966

Genus PERVOSPHAERIDIUM Yun Hyesu, 1981

Pervosphaeridium cenomaniense, (Norvick, 1976) Below, 1982.

Pervosphaeridium truncatum (Davey, 1969) Below, 1982: Last emendation: Harker and Sarjeant in Harker et al., 1990.

Pervosphaeridium spp. (Plate 3, Fig. 2)

Genus PROTOELLIPSODINIUM Davey and Verdier, 1971

Protoellipsodinium corollum, according to Hasenboehler (1981) in Masure, 1984 (name not validly published: no description).

Protoellipsodinium seghire Below, 1981 (Plate 5, Fig. 5)

Protoellipsodinium touile subsp. *touile* Below, 1981

Genus PSALIGONYAULAX Sarjeant, 1966b. Emendation: Sarjeant, 1982

Psaligonyaulax deflandrei Sarjeant, 1966. Emendation: Sarjeant, 1982.

Genus PSEDUOCERATIUM (Gocht, 1957) emendation Helby, 1987

Pseudoceratium anaphrissum (Sarjeant, 1966) Bint, 1986. Last emendation: Harding, 1990.

Pseudoceratium eisenackii (Davey, 1969) Bint, 1986.

Pseudoceratium securigerum (Davey and Verdier, 1974) Bint, 1986. As *Cyclonephelium* sp. 3 in Hasenboehler, 1981 (pl. 19, fig 1 and 2)

Pseudoceratium spp. SPB AND 398D

Genus PTERODINIUM Eisenack, 1958. Last emendation Sarjeant, 1985

Pterodinium bab Below, 1981 (Plate 4, Fig. 8-9)

Pterodinium cingulatum, (Wetzel, 1933) Below, 1981.

Pterodinium cf. *cornutum*, *Pterodinium?* *cornutum* Cookson and Eisenack, 1962

Pterodinium spp. (Plate 4, Fig. 6-7)

Genus RHYNCHODINIOPSIS Deflandre, 1935. Last emendation Jan du Chêne et al., 1985

Rhynchodiniopsis spp.

Genus ROTTNESTIA Cookson and Eisenack, 1961

Rottnestia borussica (Eisenack, 1954) Cookson and Eisenack, 1961

Genus SENONIASPHAERA Clarke and Verdier, 1967

Senoniasphaera spp.

Genus SEPISPINULA Islam, 1993

Sepispinula? *huguoniotii* (Valensi, 1955) Islam, 1993.

Sepispinula spp.

Genus SPINIFERITES Mantell, 1850. Emendation Sarjeant, 1970

Spiniferites bejui Masure et al., 1998

Spiniferites cf. *bejui*, *Spiniferites bejui* Masure et al., 1998

Spiniferites G after Masure et al., 1998

Spiniferites multibrevis (Davey and Williams, 1966) Below, 1982.

Spiniferites ramosus (Ehrenberg, 1838) Mantell, 1854.

Spiniferites ramosus subsp. *cingulatus* He Chengquan, 1991.

Spiniferites ramosus subsp. *gracilis* (Davey and Williams, 1966) Lentin and Williams, 1973.

Spiniferites ramosus subsp. *granomembranaceus* (Davey and Williams, 1966) Lentin and Williams, 1973.

Spiniferites ramosus subsp. *granosus* (Davey and Williams, 1966) Lentin and Williams, 1973.

Spiniferites ramosus subsp. *reticulatus* (Davey and Williams, 1966) Lentin and Williams, 1973.

Spiniferites spp. (Plate 4, Fig. 10-12)

Genus STANFORDELLA Helenes and Lucas-Clark, 1997

Stanfordella fastigiata (Duxbury, 1977) Helenes and Lucas-Clark, 1997. Emendation Helenes and Lucas-Clark, 1997

Genus STIPHROSPHAERIDIUM Davey, 1982

Stiphrosphaeridium anthophorum, (Cookson and Eisenack, 1958) Lentin and Williams, 1985.

Genus SURCULOSPHAERIDIUM Davey et al., 1966. Emendation Davey, 1982 - however see Stancliffe and Sarjeant (1990)

Surculosphaeridium sp. H 1 in Hasenboehler, 1981 as *Surculosphaeridium* sp. 1 (pl. 22 fig 2 - 3)

Genus SYSTEMATOPHORA Klement, 1960. Last emendation Riding and Helby, 2001

Systematophora cretacea Davey, 1979

Systematophora granulosa Jain, 1977

Systematophora cf. *silybum*, *Systematophora silybum* Davey, 1979

Systematophora sp.

Genus TALEISPHAERA Duxbury, 1979. Emendation Massee, 1986

Taleisphaera cf. *hydra*, *Taleisphaera hydra* Duxbury, 1979. Emendation Harding, 1986 (Plate 5, Fig. 9)

Taleisphaera sp.

Genus TANYOSPHAERIDIUM Davey and Williams, 1966

Tanyosphaeridium variecalamum, Davey and Williams, 1966

Tanyosphaeridium isocalamum (Deflandre and Cookson, 1955) Davey and Williams, 1969 (Plate 5, Fig. 12)

Tanyosphaeridium spp.

Genus TECATODINIUM Wall, 1967. Emendation Head, 1994

Tectatodinium spp.

Genus TEHAMADINIUM Jan du Chêne et al., 1986

Tehamadinium coummia, (Below, 1981) Jan du Chêne et al., 1986. Emendation: Jan du Chêne et al., 1986.

Tehamadinium spp. SPB and 398D

Genus TENUA Eisenack, 1958. Last emendation: Sarjeant, 1985

Tenua hystrix Eisenack, 1958. Emendation Sarjeant, 1985

Tenua spp.

Genus TRICHODINIUM Eisenack and Cookson, 1960. Emendation Clarke and Verdier, 1967

Trichodinium castaneum Deflandre, 1935 (Plate 1, Fig. 10)

Trichodinium sp. H1 in Hasenboehler, 1981 as *Trichodinium* sp. 1 (pl. 26, fig 7 to 10)

Genus TURBIOSPHAERA Archangelsky, 1969

Turbiosphaera spp. (Plate 1, Fig. 9, 12-14)

Genus UNIPONTIDIUM Wrenn, 1988

Unipontidium grande (Davey, 1975) Wrenn, 1988 (Plate 1, Fig. 1-2)

Genus WALLODINIUM Loeblich Jr. and Loeblich III, 1968. Emendation Riding, 1994

Walloodium krutzschii (Alberti, 1961) Habib, 1972.

Walloodium luna (Cookson and Eisenack, 1960) Lentin and Williams, 1973

Walloodium sp.

Genus WREVITTIA Helenes and Lucas-Clark, 1997

Wrevittia cassidata (Eisenack and Cookson, 1960) Helenes and Lucas-Clark, 1997. Last emendation Helenes and Lucas-Clark, 1997

Wrevittia helicoidea (Eisenack and Cookson, 1960) Helenes and Lucas-Clark, 1997. Last emendation Helenes and Lucas-Clark, 1997

Wrevittia sp.

Genus XENASCUS Cookson and Eisenack, 1969. Last emendation Stover and Helby, 1987

Xenascus ceratioides, (Deflandre, 1937) Lentin and Williams, 1973.

Xenascus gochtii (Corradini, 1973) Stover and Evitt, 1978 (Plate 1, Fig. 11)

Xenascus sp.

Genus XENICODINIUM Klement, 1960

Xenicodinium sp.

Genus XIPHOPHORIDIUM Sarjeant, 1966b

Xiphophoridium alatum, (Cookson and Eisenack, 1962) Sarjeant, 1966. Emendation Sarjeant, 1966

Order PYTOCHODISCALES

Genus ALISOGYMNIIUM Lentin and Vozzhennikova, 1990

Alisogymnium sp.

Genus DINOGYMNIUM Evitt et al., 1967. Emendation: Lentin and Vozzhennikova, 1990

Dinogymnium undulosum Cookson and Eisenack, 1970

Dinogymnium vozzhennikovae Lentin and Williams, 1973. Emendation: Lentin and Vozzhennikova, 1990

Dinogymnium sp. (Plate 1, Fig. 4)

Order PERIDINIALES

Genus ALTERBIDIINIUM Lentin and Williams, 1985. Substitute name for *Albertia* Vozzhennikova, 1967 (an illegitimate name) and *Alterbia* Lentin and Williams, 1976 (an illegitimate name). Emendation: Khowaja-Ateequzzaman et al., 1991
Alterbidinium spp.

Genus ANDALUSIELLA Riegel, 1974. Last emendation: Masure et al., 1996

Andalusiella inflata (Rauscher and Doubinger, 1982) Lentin and Williams, 1985

Andalusiella ivoirensis Masure et al., 1996 (Plate 2, Fig. 10)

Andalusiella mauthei subsp. *Punctata* (Jain and Millepied, 1973) Masure et al., 1996.

Emendation: Masure et al., 1996

Andalusiella polymorpha (Malloy, 1972) Lentin and Williams, 1977

Andalusiella romboides (Boltenhagen, 1977) Lentin and Williams, 1980. Emendation: Masure et al., 1996

Andalusiella spp.

Genus CANGXIANELLA Xu Jinli et al., 1997

Cangxianella elongata (Jiabo, 1978) Xu Jinli et al., 1997

Genus CEPADINIUM Duxbury, 1983

Cepadinium cf. *Cepadinium ventriosum* (Alberti, 1959) Lentin and Williams, 1989

Genus CERODINIUM Vozzhennikova, 1963. Emendation: Lentin and Williams, 1987

Cerodinium boloniense (Riegel, 1974) Lentin and Williams, 1989. Emendation: Riegel and Sarjeant, 1982 as *Phelodinium boloniense*

Cerodinium diebelii (Alberti, 1959) Lentin and Williams, 1987 (Plate 2, Fig. 7)

Cerodinium granulostriatum (Jain and Millepied, 1973) Lentin and Williams, 1987

Cerodinium leptodermum (Vozzhennikova, 1963) Lentin and Williams, 1987

Cerodinium spp.

Genus CHICHAOUADINIUM Below, 1981

Chichaouadinium vestitum (Brideaux, 1971) Bujak and Davies, 1983

Chichaouadinium arabicum Below, 1981

Chichaouadinium spp.

Genus DEFLANDREA Eisenack, 1938b. Last emendation: Lentin and Williams, 1976

Deflandrea? sp.

Genus EPELIDOSPHAERIDIA Davey, 1969

Epelidosphaeridia spinosa Cookson and Hughes, 1964

Genus EURYDINIUM Stover and Evitt, 1978

Eurydinium euthemum (Davey and Verdier, 1971) Stover and Evitt, 1978

Genus HEXAGONIFERA Cookson and Eisenack, 1961. Last emendation: Stover and Evitt, 1978

Hexagonifera spp.

Genus ISABELIDINIUM

Isabelidinium acuminatum, (Cookson and Eisenack, 1958) Stover and Evitt, 1978.

Isabelidinium? *globosum* (Davey, 1970) Lentin and Williams, 1977.

Genus LEBERIDOCYSTA Stover and Evitt, 1978

Leberidocysta chlamydata, (Cookson and Eisenack, 1962) Stover and Evitt, 1978, emendations: Fechner, 1985, and Marheinecke, 1992.

Genus OVOIDINIUM Davey, 1970. Last emendation: Duxbury, 1983

Ovoidinium diversum Davey, 1979 (Plate 3, Fig. 3)

Ovoidinium scabrosum (Cookson and Hughes, 1964) Davey, 1970.

Ovoidinium verrucosum (Cookson and Hughes, 1964) Davey, 1970

Ovoidinium sp. Present in the Albian data from the Lusitanian basin refers to *Ovoidinium tenue* in Hasenboehler, 1981 (pl. 26, fig. 12 to 16)

Ovoidinium spp.

Genus PALAEOCYSTODINIUM Alberti, 1961

Palaeocystodinium australinum (Cookson, 1965) Lentin and Williams, 1976. Emendation: Malloy, 1972

Palaeocystodinium bulliforme Ioannides, 1986

Palaeocystodinium? deflandrei Gruas-Cavagnetto, 1968

Palaeocystodinium golzowense Alberti, 1961

Palaeocystodinium granulatum (Wilson, 1967) Lentin and Williams, 1976

Palaeocystodinium lidiae (Górka, 1963) Davey, 1969. Emendation: Davey, 1969 (Plate 2, Fig. 8-9)

Palaeocystodinium stockmansii Boltenhagen, 1977

Palaeocystodinium sp. H1, according to Hasenboehler, 1981 (pl. 22, fig 8).

Palaeocystodinium spp.

Genus PALAEOHYSTRICHOPHORA Deflandre, 1935. Emendation Deflandre and Cookson, 1955

Palaeohystrichophora cheit (Below, 1981) Mahmoud, 1998 (Plate 1, Fig. 5)

Palaeohystrichophora infusorioides, Deflandre, 1935 (Plate 1, Fig. 6)

Palaeohystrichophora cf. *Infusorioides*, *Palaeohystrichophora infusorioides*, Deflandre, 1935.

Palaeohystrichophora spp.

Genus PALAEOPERIDINIUM Deflandre, 1934. Emendation Evitt et al., 1998

Palaeoperidinium cretaceum, (Pocock, 1962) Lentin and Williams, 1976, emendations: Harding, 1990 and Evitt et al., 1998.

Palaeoperidinium pyrophorum, (Ehrenberg, 1838) Sarjeant, 1967, emendations: Sarjeant, 1967; Gocht and Netzel, 1976; Evitt et al., 1998..

Palaeoperidinium spp.

Genus PHELODINIUM Stover and Evitt, 1978. Emendation: Mao Shaozhi and Norris, 1988

Phelodinium magnificum (Stanley, 1965) Stover and Evitt, 1978 (Plate 1, Fig. 3)

Phelodinium sp.

Genus PIERCEITES Habib and Drugg, 1987

Pierceites spp.

Genus SENEGALINIUM Jain and Millepied, 1973. Emendation Stover and Evitt, 1978

Senegalinium bicavatum Jain and Millepied, 1973

Senegalinium laevigatum (Malloy, 1972) Bujak and Davies, 1983

Senegalinium sp.

Genus SPINIDINIUM Cookson and Eisenack, 1962. Last emendation Quattrocchio and Sarjeant, 2003

Spinidinium spp. (Plate 1, Fig. 7)

Genus SUBTILISPHAERA Jain and Millepied, 1973. Emendation Lentin and Williams, 1976

Subtilisphaera balcattensis (Cookson and Eisenack, 1969) Lentin and Williams, 1976.

Subtilisphaera? pirnaensis (Alberti, 1959) Jain and Millepied, 1973.

Subtilisphaera cf. *Subtilisphaera senegalensis* Jain and Millepied, 1973.

Subtilisphaera terrula (Davey, 1974) Lentin and Williams, 1976. Emendation: Harding, 1986.

Subtilisphaera spp. (Plate 3, Fig. 8)

Genus TRITHYRODINIUM Drugg, 1967. Last emendation: Marheinecke, 1992

Trithyrodinium sp. (Plate 1, Fig. 8)

Order uncertain

Genus PROLIXOSPHAERIDIUM Davey et al., 1966. Emendation: Davey, 1969

Prolixosphaeridium capitatum, (Cookson and Eisenack, 1960) Singh, 1971.

Prolixosphaeridium conulum, Davey, 1969.

Prolixosphaeridium deirense Davey et al., 1966. Emendation: Harding, 1990

Prolixosphaeridium parvispinum, (Deflandre, 1937) Davey et al., 1969.

Prolixosphaeridium sp H1 in Hasenboehler, 1981 as *Prolixosphaeridium* sp. 1 (pl. 19, fig 10).

Prolixosphaeridium spp. SPB and 398D apt alb

APPENDIX B - Dinocyst stratigraphic distribution

B.1. Dinocyst relative abundance distribution in the ODP Hole 959 D samples.

Core, Section, cm	Depth (mbsf)	Stage / Age	
44R06, 060-062	828.7	Thanetian	<i>Xenascus gochtii</i>
45R01, 034-039	831.94		<i>Cyclonephelium vannophorum</i>
46R02, 018-023	842.48	Danian	<i>Spiniferites</i> G.
47R01, 035-037	851.25		<i>Oligosphaeridium</i> spp.
48R03, 065-068	864.25	Maastrichtian	<i>Canninginopsis</i> ? sp.
49R04, 133-137	876.03		<i>Oligosphaeridium</i> complex
50R05, 098-101	886.88	Campanian	<i>Palaeohystrichophora cheit</i>
51R04, 008-011	893.78		<i>Spiniferites bejui</i>
52R03, 010-013	901.91	Unknown	<i>Palaeohystrichophora infusorioides</i>
53R06, 018-020	914.97		<i>Cyclonephelium</i> ? <i>hirsute</i>
54R02, 097-099	920.57	Santonian	<i>Hystriochodinium furcatum / ramoides</i>
55R03, 083-085	930.39		<i>Palaeohystrichophora</i> sp.
56R04, 060-062	942.5	Coniacian	<i>Dinogymnium undulosum</i>
57R04, 114-117	952.74		<i>Oligosphaeridium</i> complex subsp. <i>brevispinum</i>
58R03, 093-096	960.3		<i>Hystriochodinium</i> spp.
59R05, 039-044	972.89		<i>Phelodinium</i> sp.
60R01, 056-059	976.66		<i>Phelodinium magnificum</i>
60R04, 058-061	981.18		<i>Andalusiella mauthei</i> subsp. <i>punctata</i>
62R01, 076-080	996.16		<i>Palaeocystodinium deflandrei</i>
63R05, 091-093	1011.91		<i>Dinogymnium vozzhennikovae</i>
64R01, 092-095	1015.62		<i>Cometodinium</i> spp.
66R03, 0440-043	1037.1		<i>Unipontidinium grande</i>
67R02, 057-061	1045.37		<i>Odontochitina costata</i>
			<i>Andalusiella romboides</i>
			<i>Andalusiella polymorpha</i>
			<i>Palaeocystodinium granulatum</i>
			<i>Oligosphaeridium pulcherrimum</i>
			<i>Trichodinium castaneum</i>
			<i>Trithyrodinium</i> spp.
			<i>Odontochitina</i> spp.
			<i>Xenascus</i> sp.
			<i>Senegalinium laevigatum</i>
			<i>Deflandrea</i> ? sp.
			<i>Andalusiella ivoiensis</i>
			<i>Dapsilidinium</i> spp.
			<i>Spinidinium</i> spp.
			<i>Hystriochodinium pulchrum</i>
			<i>Palaeocystodinium</i> spp.

B.1. Dinocyst relative abundance distribution in the ODP Hole 959 D samples (continued).

Core, Section, cm	Depth (mbsf)	Stage / Age
44R06, 060-062	828.7	Thanetian
45R01, 034-039	831.94	
46R02, 018-023	842.48	Danian
47R01, 035-037	851.25	
48R03, 065-068	864.25	Maastrichtian
49R04, 133-137	876.03	
50R05, 098-101	886.88	Campanian
51R04, 008-011	893.78	
52R03, 010-013	901.91	Unknwon
53R06, 018-020	914.97	
54R02, 097-099	920.57	Santonian
55R03, 083-085	930.39	
56R04, 060-062	942.5	Coniacian
57R04, 114-117	952.74	
58R03, 093-096	960.3	
59R05, 039-044	972.89	
60R01, 056-059	976.66	
60R04, 058-061	981.18	
62R01, 076-080	996.16	
63R05, 091-093	1011.91	
64R01, 092-095	1015.62	
66R03, 040-043	1037.1	
67R02, 057-061	1045.37	
		<i>Peridinioidie various</i>
		<i>Cerodinium granulostriatum</i>
		<i>Exochosphaeridium</i> spp.
		<i>Batiacasphaera</i> spp.
		<i>Cribooperidinium</i> sp.
		<i>Spiniferites</i> spp.
		<i>Alisogymnium</i> spp.
		<i>Circulodinium</i> spp.
		<i>Kallosphaeridium coninckii</i>
		<i>Florentinia</i> spp.
		<i>Operculodinium</i> spp.
		<i>Cerodinium</i> spp.
		<i>Palaeocystodinium lidiae</i>
		<i>Areoligera</i> spp.
		<i>Kallosphaeridium</i> spp.
		<i>Palaeocystodinium golzowense</i>
		<i>Achomosphaera</i> spp.
		<i>Tectatodinium</i> spp.
		<i>Turbiosphaera</i> spp.
		<i>Tanyosphaeridium</i> spp.
		<i>Carpatella cornuta</i>
		<i>Andalusiella</i> spp.
		<i>Cerodinium leptodermum</i>
		<i>Kenleyia</i> spp.
		<i>Canningia?? like</i>
		<i>Achomosphaera ramulifera</i> subsp. <i>gabonensis</i>
		<i>Andalusiella inflata</i>
		<i>Cerodinium diebelii</i>
		<i>Hafniasphaera hyalospinosa</i>
		<i>Areoligera volata</i>
		<i>Senoniasphaera</i> spp.
		<i>Glaphyrocysta</i> spp.
		<i>Damassadinium californicum</i>
		<i>Impagidinium</i> spp.
		<i>Hystriochostrogylon</i> spp.
		<i>Palaeocystodinium australinum / gabonensis</i>
		<i>Cerodinium elongatum</i>

B.1. Dinocyst relative abundance distribution in the ODP Hole 959 D samples (continued).

Core, Section, cm	Depth (mbsf)	Stage / Age	
44R06, 060-062	828.7	Thanetian	<i>Palaeocystodinium stockmansii</i>
45R01, 034-039	831.94		0
46R02, 018-023	842.48	Danian	<i>Cerodinium boloniense</i>
47R01, 035-037	851.25		0
48R03, 065-068	864.25	Danian	<i>Alterbidinium</i> spp.
49R04, 133-137	876.03		0
50R05, 098-101	886.88	Danian	<i>Impagidinium celineae</i>
51R04, 008-011	893.78		0
52R03, 010-013	901.91	Danian	<i>Damassadinium</i> spp.
53R06, 018-020	914.97		0
54R02, 097-099	920.57	Maastrichtian	<i>Florentinia mantelii</i>
55R03, 083-085	930.39		0
56R04, 060-062	942.5	Maastrichtian	<i>Cordosphaeridium</i> spp.
57R04, 114-117	952.74		0
58R03, 093-096	960.3	Maastrichtian	<i>Florentinia buspina</i>
59R05, 039-044	972.89		0
60R01, 056-059	976.66	Campanian	<i>Rottnestia</i> spp.
60R04, 058-061	981.18		0
62R01, 076-080	996.16	Campanian	<i>Florentinia clavigera</i>
63R05, 091-093	1011.91		0
64R01, 092-095	1015.62	Unknown	<i>Palaeocystodinium bulliformum</i>
66R03, 0440-043	1037.1		0
67R02, 057-061	1045.37	Coniacian	<i>Hafniasphaera septata</i>
			0
			<i>Diphyes</i> spp.
			<i>Spiniferites</i> cf. <i>benjui</i>
			<i>Senegalinium bicavatatum</i>
			<i>Florentinia ferox</i>
			<i>Amphorosphaeridium</i> spp.
			<i>Adnatosphaeridium multispinosum</i>
			<i>Fibrocysta</i> sp.
			<i>Apteodinium</i> spp.
			<i>Exochosphaeridium bifidum</i>
			<i>Perisseiasphaeridium pannosum</i>
			<i>Areoligera medusettiformis</i>
			<i>Areoligera gippingensis</i>

B.2. Dinocyst relative abundance distribution in the São Julião - Falcão - Magoito outcrop samples (continued). Data from Hasenboehler (1981) and the associated census counts.

Sample	Height (m)	Stage / Age	<i>Odontochitina ancala</i> / <i>O. rakhodes</i>	<i>Cyclonephelium sph3</i>	<i>Oligosphaeridium vasiformum</i>	<i>Oligosphaeridium sp 2</i>	<i>Cyclonephelium compactum</i>	<i>Oligosphaeridium irregulare</i>	<i>Cometodinium whitei</i>	<i>Palaeoperidinium cretaceum</i>	<i>Chichauadinium vestitum</i>	<i>Pervosphaeridium truncatum</i>	<i>Subtilisphaera ?pirnaensis</i>	<i>Kallosphaeridium ?ringnesiorum</i>	<i>Subtilisphaera balcattensis</i>	<i>Subtilisphaera "ventriosa"</i>	<i>Microdinium opacum</i>	<i>Cyclonephelium vannophorum</i>	<i>Xiphophoridium alatum</i>	<i>Hystrichodinium pulchrum</i>	<i>Dinopterygium cladoides</i>	<i>Canningia torulosa</i>	<i>Florentinia sph1</i>	<i>Eurydinium euthemum</i>	<i>Oligosphaeridium pulcherrimum</i>	<i>Cribroperidinium intricatum</i>	<i>Xenascus ceratioides</i>	<i>Coronifera oceanica</i>	<i>Palaeohystrichophora cf. infusorioides</i>	<i>Cribroperidinium sp H1</i>	<i>Microdinium ornatum</i>	<i>Exochosphaeridium bifidum</i>	<i>Epelidosphaeridia spinosa</i>					
FM 83	128,3	Middle Albian	3,0	0,0	0,0	0,0	0,0	0,0	0,0	0,0	0,0	0,0	0,0	0,0	0,0	0,0	0,0	0,0	0,0	0,0	0,0	0,0	0,0	0,0	0,0	0,0	0,0	0,0	0,0	0,0	0,0	0,0	0,0	0,0	0,0	0,0		
VS 15	122,8	Late Albian	25,0	0,0	0,0	0,2	0,2	0,0	0,0	0,2	0,0	0,2	0,0	0,0	0,0	0,0	0,0	46,0	1,5	1,5	0,0	1,0	0,0	0,0	0,0	0,0	0,0	0,0	1,5	0,0	25,0	0,0	0,2	0,2	0,0			
VS 7-3	110,7	Vraconian	17,0	0,0	0,0	0,0	0,0	0,2	0,0	0,2	0,0	0,5	0,0	0,2	0,0	0,0	0,0	1,5	1,5	0,0	1,0	0,0	0,0	0,0	0,2	3,0	0,0	0,2	51,0	3,5	0,0	0,0	0,0	0,0				
VS 4	107,4		10,5	0,0	0,0	0,0	0,0	0,2	1,5	0,2	1,5	0,2	0,0	0,0	0,0	0,0	0,0	2,5	1,6	10,5	1,5	0,0	0,0	0,0	0,0	0,8	5,0	0,2	0,0	55,0	10,5	0,0	0,0	0,0	0,0			
FM 56	89,9		1,5	0,0	0,0	0,0	0,0	1,5	1,5	0,0	0,0	0,0	0,0	0,0	0,0	0,0	1,5	0,0	1,5	0,0	1,5	0,0	1,5	0,0	0,0	0,0	0,0	0,0	20,0	0,0	0,0	0,0	0,0	0,0	0,0			
FM 28-29	45,8		5,0	0,0	0,0	10,5	0,0	0,0	0,0	0,0	0,0	0,0	0,0	0,0	0,0	0,0	0,0	0,0	5,5	0,0	6,0	0,0	0,0	0,0	10,5	0,0	10,5	0,0	0,0	0,0	0,0	0,0	0,0	0,0	0,0	0,0		
FM 26	44,3		20,0	0,0	0,0	1,5	1,5	1,5	1,5	7,5	0,0	0,0	1,5	0,0	0,0	0,0	1,5	0,0	0,0	0,0	0,0	0,0	0,0	0,0	0,0	0,0	0,0	0,0	0,0	0,0	0,0	0,0	0,0	0,0	0,0	0,0	0,0	
FM 22	39,0		56,0	0,0	0,0	3,5	1,5	10,5	0,0	1,5	0,0	1,5	0,0	1,5	1,5	1,5	0,0	0,0	1,5	1,5	0,0	1,5	0,0	0,0	3,5	1,5	0,0	1,5	0,0	0,0	0,0	0,0	0,0	0,0	0,0	0,0	0,0	0,0
FM 16	28,0		2,0	3,5	0,2	0,0	1,5	0,2	0,2	0,0	7,1	0,2	0,2	0,0	0,0	1,0	2,5	5,0	0,0	5,0	0,0	5,0	0,0	0,2	0,0	0,0	0,0	0,0	0,0	0,0	0,0	0,0	0,0	0,0	0,0	0,0	0,0	
FM 12	22,9		23,0	0,0	0,0	0,0	3,5	10,5	3,5	0,0	0,0	3,5	0,0	0,0	0,0	1,5	2,5	10,0	1,5	10,5	0,0	0,0	0,0	0,0	0,0	0,0	0,0	0,0	0,0	0,0	0,0	0,0	0,0	0,0	0,0	0,0	0,0	0,0
FM 6c	15,1		60,0	0,0	0,0	0,0	0,0	0,0	0,0	0,0	0,0	0,0	0,0	0,0	0,0	0,0	0,0	0,0	2,5	0,0	0,0	0,0	0,0	0,0	0,0	0,0	0,0	0,0	0,0	0,0	0,0	0,0	0,0	0,0	0,0	0,0	0,0	
FM 2	10,3		55,0	0,0	0,0	0,0	0,0	1,5	0,9	1,5	0,0	1,5	0,0	0,0	0,0	0,0	0,0	1,5	0,0	0,0	0,0	0,0	0,0	0,0	0,0	0,0	0,0	0,0	0,0	0,0	0,0	0,0	0,0	0,0	0,0	0,0	0,0	
SI 12	7,5		0,5	0,0	0,0	0,0	3,5	0,9	0,9	0,0	0,0	0,0	0,0	0,0	0,0	0,0	0,0	0,0	0,0	0,0	0,0	0,0	0,0	0,0	0,0	0,0	0,0	0,0	0,0	0,0	0,0	0,0	0,0	0,0	0,0	0,0	0,0	
SI 11s	6,0		0,3	0,0	0,0	0,0	0,0	0,0	0,0	0,0	0,0	0,0	0,0	0,0	0,0	0,0	0,0	0,0	0,0	0,0	0,0	0,0	0,0	0,0	0,0	0,0	0,0	0,0	0,0	0,0	0,0	0,0	0,0	0,0	0,0	0,0	0,0	
SI 11b	5,5		7,5	0,0	0,0	0,0	0,0	0,0	0,0	3,5	0,0	0,0	0,0	0,0	0,0	0,0	0,0	0,0	0,0	0,0	0,0	0,0	0,0	0,0	0,0	0,0	0,0	0,0	0,0	0,0	0,0	0,0	0,0	0,0	0,0	0,0	0,0	
SI 10	2,2		4,0	0,0	0,0	0,9	10,5	3,5	0,0	4,0	0,0	1,5	0,0	0,0	0,0	0,0	5,5	0,0	0,0	0,0	0,0	0,0	0,0	0,0	0,0	0,0	0,0	0,0	0,0	0,0	0,0	0,0	0,0	0,0	0,0	0,0	0,0	
SI 9	0,0		1,5	0,0	0,0	0,0	0,9	0,9	0,9	43,0	0,0	0,0	0,0	0,0	0,0	0,0	0,0	0,0	0,0	0,0	0,0	0,0	0,0	0,0	0,0	0,0	0,0	0,0	0,0	0,0	0,0	0,0	0,0	0,0	0,0	0,0	0,0	

B.3. Dinocyst relative abundance distribution in the Magoito Aguda – Azenhas do Mar outcrop samples. Data from Hasenboehler (1981) and the associated census counts.

Sample	Height (m)	Stage/Age	
AZ 32-1	180,2	Late Albian	
AZ 28-1	169,7		
MA 32-1	95,3		
MA 30-2	82,9		
MA 27-3	78,7		
MA 27-1	73,6		
MA 26-3	71,3		
MA 23-3	63,2		
MA 19-19	56,1		
MA 19-1	47,0		
MA 17	42,0		
MA 16	40,1		
MA 10-3	33,1		Vraco.
MA 6-4	19,7		
MA 4mill	8,0		
MA 2-1	0,0		
		<i>Prolixosphaeridium capitatum</i>	
		<i>Subtilisphaera ?pirnaensis</i>	
		<i>Subtilisphaera senegalensis</i>	
		<i>Kallosphaeridium ?ringnesiorum</i>	
		<i>Xenascus ceratioides</i>	
		<i>Odontochitina operculata</i>	
		<i>Ovoidinium sp.</i>	
		<i>Subtilisphaera "ventriosa"</i>	
		<i>Circulodinium colliveri</i>	
		<i>Stiphrosphaeridium anthophorum</i>	
		<i>Xiphophoridium alatum</i>	
		<i>Cometodinium whitei</i>	
		<i>Florentinia radiculata</i>	
		<i>Cyclonephelium spH3</i>	
		<i>Florentinia laciniata</i>	
		<i>Callaiosphaeridium asymmetricum</i>	
		<i>Hystrichodinium pulchrum</i>	
		<i>Gardodinium eisenackii</i>	
		<i>Oligosphaeridium pulcherrimum</i>	
		<i>Spiniferites multibrevis</i>	
		<i>Isabelidinium acuminatum</i>	
		<i>Dapsilidinium laminaspinosum</i>	
		<i>Canningia torulosa</i>	
		<i>Microdinium opacum</i>	
		<i>Carpodinium granulatum</i>	
		<i>Trichodinium castanea</i>	
		<i>Odontochitina inflata</i>	
		<i>Dinopterygium cladoides</i>	
		<i>Cribrerodinium intricatum</i>	
		<i>Cribrerodinium ?edwardsii</i>	
		<i>Oligosphaeridium totum</i>	

B.3. Dinocyst relative abundance distribution in the Magoito Aguda – Azenhas do Mar outcrop samples (continued). Data from Hasenboehler (1981) and the associated census counts.

Sample	Height (m)	Stage/Age	<i>Pervosphaeridium truncatum</i>	<i>Spiniferites ramosus</i>	<i>Chichouadinium vestitum</i>	<i>Palaeoperidinium cretaceum</i>	<i>Oligosphaeridium albertense</i>	<i>Exochosphaeridium phragmites</i>	<i>Cyclonephelium vannophorum</i>	<i>Circulodinium distinctum</i>	<i>Subtilisphaera terrula</i>	<i>Florentinia cooksoniae</i>	<i>Cyclonephelium compactum</i>	<i>Protoellipsodinium corollum</i>	<i>Psaligonyaulax deflandrei</i>	<i>Hystrichodinium voigtii</i>	<i>Trichodinium sp H1</i>	<i>Subtilisphaera spp.</i>	<i>Palaeohystrichophora cf. infusorioides</i>
AZ 32-1	180,2	Vraco.	0	0	0	0	1,5	0	7,5	3,5	0	3,5	3,5	36	0	0	0	0	2
AZ 28-1	169,7	Late Albian	0	0	0	0	0	1,5	26	0	0	0	3,5	33	0	0	0	1,5	4,5
MA 32-1	95,3		0	10,5	0	8	0	0	0	3,5	1,5	3,5	0	0	0	0	1,5	0	0
MA 30-2	82,9		0,2	0	74	1	0,2	0,2	0	0	10,5	0	0	15	0	0	0	0	0
MA 27-3	78,7		0,2	0,2	13	0	22,5	0,2	7,5	3,5	0,2	0,2	3,5	40	0	0,2	0	0	0
MA 27-1	73,6		1,5	1,5	4	0	10,5	0	2,5	10,5	1,5	0	0	32	0	0	0	0	0
MA 26-3	71,3		1,5	0,2	74	1,5	3,5	0,2	2,5	3,5	1,5	0	10,5	6	0,2	0	0	0	0
MA 23-3	63,2		0	0	0	0	0	0	0	0	0	0	0	0	0	0	0	0	0
MA 19-19	56,1		0	0	16	7,5	0	0	0	0	0	1,5	0	0	0	0	0	0	0
MA 19-1	47,0		0,2	0	75	0	1,5	0,2	0	1,5	0,2	0	3,5	3	0	0	0	0	0
MA 17	42,0		0	0	15	0	3,5	0,2	0	0,2	1,5	0	0	36	0	0	0	0	0
MA 16	40,1		0,2	3,5	0	15	0	0,2	1,5	0,2	0,2	1,5	3,5	0	0	0	0	0	0
MA 10-3	33,1		3,5	0	0	14	1,5	0	20	0	0	0	3,5	4	0	0	0	0	0
MA 6-4	19,7		0	0,2	1,5	66	0,2	0	2,5	0,2	0	1,5	1,5	4	0	0	0	0	0
MA 4mill	8,0		0,2	10,5	1,5	1	10,5	0,2	2,5	3,5	3,5	0,2	0	0	0	0	0	0	0
MA 2-1	0,0		0,2	0,2	2,5	0	0,2	3,5	2,5	0,2	0,2	0	0	11	0	0	0	0	0

B.4. Dinocyst relative abundance distribution in the Guincho outcrop samples. Data from Hasenboehler (1981) and the associated census counts.

G 2a	G 3b base	G 13b	G 17c	G 29	G 32sup	G 35	G 37a	Sample
0,0	2,2	27,1	37,5	71,6	82,1	91,3	92,4	Height (m)
Middle Albian				Late Albian				Stage / Age
0	2,5	0	0	0	0	0	0	<i>Surculosphaeridium sp 1</i>
0	1,5	0	0	0	0	0	0	<i>Prolixosphaeridium capitatum</i>
0	0,9	0	0	0	0	0	0	<i>Cyclonephelium sp2</i>
0	0,9	0	0	0	0	0	0	<i>Cyclonephelium sp1</i>
0	0,9	0	0	0	0	0	0	<i>Subtilisphaera ?pirmaensis</i>
0	7	0	0	0	0	0	0	<i>Bacchidinium sp 1</i>
0	0,9	0	0	0	0	0	0	<i>Palaeocystodinium sp 1</i>
0	0,9	0	0	0	0	0	0	<i>Callaiosphaeridium asymmetricum</i>
0	5	4	17,5	16	3	0	0	<i>Cribroperidinium ?edwardsii</i>
67	7,5	4	0	17,5	28	12	0	<i>Palaeoperidinium cretaceum</i>
0	18	5	0	0	0	4	0	<i>Ovoidinium sp</i>
30,1	3,5	0	22	10,5	10,5	3,5	0	<i>Spiniferites ramosus</i>
10	20	64	33	21	24	24	45	<i>Trichodinium castaneum</i>
0	0,9	0	0	0	0	4	0	<i>Protoellipsodinium corollum</i>
0	3,5	3,5	0	0	0,2	3,5	0	<i>Circulodinium distinctum</i>
0	1,5	0	0	1,5	0	3,5	0	<i>Subtilisphaera "ventriosa"</i>
0	1	4	0	0	6	0	6	<i>Dinopterygium cladoides</i>
0	10,5	0	22	10,5	1,5	3,5	0	<i>Cyclonephelium compactum</i>
0	3,5	0	0	0	0,2	3,5	0	<i>Cometodinium whitei</i>
0	0,9	0	0	0	1,5	3,5	0	<i>Carpodinium granulum</i>
0	0,9	0,9	0	0	0,2	22,5	3,5	<i>Subtilisphaera terrula</i>
0	0,9	0	0	1,5	0,2	0	1,5	<i>Exochosphaeridium phragmites</i>
0	0	3,5	0	0	1,5	1,5	0	<i>Gardodinium eisenackii</i>
0	1,5	0	0	0	6	0	5	<i>Xiphophoridium alatum</i>
0	0,9	0	0	0	0,2	0	10,5	<i>Spiniferites multibrevis</i>
0	0	0	0	0,2	1,5	0	0	<i>Oligosphaeridium totum</i>
0	0	0	0	5	1,5	0	0	<i>Cribroperidinium intricatum</i>
0	0	0	0	2,5	1,5	0	0	<i>Odontochitina operculata</i>
0	0,2	0	0	6,5	1,5	0,2	1,5	<i>Odontochitina ancala/O. rakhodes</i>
0	0,9	0	0	0	1,5	10,5	3,5	<i>Oligosphaeridium albertense</i>
0	10	0	0	0	2,5	7	5,5	<i>Cyclonephelium vannophorum</i>
0	0	0	0	0	3,5	0	0	<i>Florentinia cooksoniae</i>
0	0	0	0	0	3,5	0	0	<i>Isabelidinium acuminatum</i>
0	0	0	0	3,5	3,5	3,5	0	<i>Coronifera oceanica</i>
0	0	0	0	2	0	0	2	<i>Hystrichodinium pulchrum</i>
0	0	0	0	0	3,5	0	1,5	<i>Pervosphaeridium truncatum</i>
0	0	0	0	0	1,5	5	1,5	<i>Circulodinium colliveri</i>
0	0	0	0	0	0	3,5	1,5	<i>Oligosphaeridium pulcherrimum</i>

B.5. Dinocyst relative abundance distribution in the Ponta do Sal outcrop samples. Data from Hasenboehler (1981) and the associated census counts.

PSalm	PS 3sup	PS 5-1	PS 8	Sample
0,0	7,1	8,5	16,6	Height (m)
Late Albian		Vracon.		Stage / Age
3	0	0	0	<i>Subtilisphaera terrula</i>
5	0	0	0	<i>Palaeoperidinium cretaceum</i>
0	1,5	0	0	<i>Cribooperidinium ?edwardsii</i>
0	3,5	0	0	<i>Oligosphaeridium albertense</i>
0	8	0	0	<i>Cribooperidinium intricatum</i>
0	0,2	0	0	<i>Isabelidium? globosum</i>
0	1,75	0	0	<i>Ovoidinium tenue</i>
0	2,5	0	0	<i>Dinopterygium cladoides</i>
1,5	3,5	10,5	0	<i>Oligosphaeridium totum</i>
0	1,75	7,5	0	<i>Xiphophoridium alatum</i>
1,5	1,5	2,5	2,5	<i>Protoellipsoidinium corollum</i>
0	0,2	3,5	0	<i>Cometodinium whitei</i>
0	0,2	3,5	0	<i>Stiphrosphaeridium anthophorum</i>
45	0	45	4	<i>Trichodinium castaneum</i>
0	0	13	0	<i>Odontochitina inflata</i>
0	0	10,5	0	<i>Carpodinium granulatum</i>
0	2,5	0	2,5	<i>Cyclonephelium vannophorum</i>
0	0	1,5	0	<i>Dapsilidinium laminaspinosum</i>
0	0	1,5	0	<i>Circulodinium distinctum</i>
0	0	10,5	0	<i>Eurydinium euthemum</i>
0	0,2	1,5	3,5	<i>Spiniferites ramosus</i>
0	0,2	3,5	3,5	<i>Pervosphaeridium truncatum</i>
0	1,5	0	10,5	<i>Oligosphaeridium pulcherrimum</i>
0	75	0	35	<i>Chichaouadinium vestitum</i>
0	0	5	21,5	<i>Palaeohystrichophora cf. infusorioides</i>
0	0	0	0,2	<i>Circulodinium colliveri</i>

B.6. Dinocyst relative abundance distribution in the Baforeira Rana outcrop samples. Data from Hasenboehler (1981) and the associated census counts.

Br 1b	Br 1f	Br 2b	Br 8d	Br 23	Sample
0,0	2,5	10,8	54,0	82,7	Height (m)
Mid. Alb.		Late	Vraconian		Stage / Age
5	0	0	0	0	<i>Ovoidinium</i> sp.
1,5	0	0	0	0	<i>Subtilisphaera balcattensis</i>
1,5	0	0	1,5	0	<i>Gardodinium eisenackii</i>
1,5	0	0	1,5	0	<i>Florentinia laciniata</i>
10,5	0	10,5	10,5	0	<i>Subtilisphaera terrula</i>
0	50	0	2,5	0	<i>Palaeoperidinium cretaceum</i>
1,5	0	0	0	3,5	<i>Carpodinium granulatum</i>
10,5	0	10,5	0	1,5	<i>Oligosphaeridium albertense</i>
1,5	0	0	0	1,5	<i>Cribroperidinium ?edwardsii</i>
1,5	0	0	0	1,5	<i>Coronifera oceanica</i>
1,5	0	0	0	0,2	<i>Circulodinium ?brevispinosum</i>
3	0	12,5	17	16	<i>Dinopterygium cladoides</i>
33	0	71	4	3	<i>Trichodinium castaneum</i>
7	0	6	35	13	<i>Odontochitina ancala/O. rakhodes</i>
1,5	0	0	16	3	<i>Xiphophoridium alatum</i>
10,5	0	0	1,5	0,2	<i>Spiniferites ramosus</i>
0,1	0	0	3	6,5	<i>Circulodinium distinctum</i>
3,5	0	0	1,5	1,5	<i>Pervosphaeridium truncatum</i>
1,5	0	0	1,5	1,5	<i>Exochosphaeridium phragmites</i>
1,5	0	0	10,5	0,2	<i>Cometodinium whitei</i>
0	50	0	0	3	<i>Chichaouadinium vestitum</i>
0	0	0	1,5	0	<i>Florentinia cooksoniae</i>
0	0	0	1,5	0	<i>Callaiosphaeridium asymmetricum</i>
0	0	0	1,5	0	<i>Kallosphaeridium ?ringnesiorum</i>
0	0	0	3,5	3,5	<i>Chlamydothorella discreta</i>
0	0	0	1,5	3,5	<i>Circulodinium colliveri</i>
0	0	0	2,5	13	<i>Protoellipsodinium corollum</i>
0	0	0	3,5	10,5	<i>Cyclonephelium vannophorum</i>
0	0	0	0	0,2	<i>Microdinium ornatum</i>
0	0	0	0	0,2	<i>Epelidosphaeridia spinosa</i>
0	0	0	0	10,5	<i>Cribroperidinium intricatum</i>
0	0	0	0	10	<i>Palaeohystrichophora cf. infusorioides</i>
0	0	0	0	3,5	<i>Oligosphaeridium totum</i>
0	0	0	0	0,2	<i>Spiniferites multibrevis</i>

B.7. Dinocyst relative abundance distribution in the DSDP Hole 398D Albian samples (continued). Data from Masure (1984) and the associated census counts.

<i>Spiniferites ramosus</i> subsp. <i>granomembraneus</i>	0,7	0,0	0,0	0,0	0,0	0,0	0,0	0,0	0,0	0,0	0,0	0,0	
<i>Pterosphaeridium perforatum</i>	1,5	0,0	0,0	0,0	0,0	0,0	0,0	0,0	0,0	0,0	0,0	0,0	
<i>Xenascus ceratioides</i>	2,8	0,0	0,0	0,0	0,0	0,0	0,0	0,0	0,0	0,0	0,0	0,0	
<i>Palaeohystrichophora infusorioides</i>	0,7	1,7	3,5	0,0	0,0	0,0	0,0	0,0	0,0	0,0	0,0	0,0	
<i>Epelidosphaeridia spinosa</i>	0,0	1,7	0,0	0,0	0,0	0,0	0,0	0,0	0,0	0,0	0,0	0,0	
<i>Hapsocysta peridictya</i>	0,0	1,7	0,0	0,0	0,0	0,0	0,0	0,0	0,0	0,0	0,0	0,0	
<i>Pterodinium cf. cornutum</i>	0,0	0,0	2,7	0,0	0,0	0,0	0,0	0,0	0,0	0,0	0,0	0,0	
<i>Litosphaeridium siphoniphorum</i>	2,1	0,0	0,9	0,0	5,5	0,0	0,0	0,0	0,0	0,0	0,0	0,0	
<i>Batiacasphaera</i> spp.	0,0	0,0	0,9	0,0	0,0	0,0	0,0	0,0	0,0	0,0	0,0	0,0	
<i>Gonyaulacysta</i> spp.	0,0	0,0	0,9	0,0	0,0	0,0	0,0	0,0	0,0	0,0	0,0	0,0	
<i>Leptodinium</i> spp.	0,0	0,0	2,7	0,0	0,0	0,0	0,0	0,0	0,0	0,0	0,0	0,0	
<i>Palaeohystrichophora cf. infusorioides</i>	0,0	1,7	1,8	0,0	0,0	0,0	3,0	0,0	0,0	0,0	0,0	0,0	
<i>Paucilobimorpha extrema</i>	0,7	0,0	0,0	0,0	0,0	0,0	0,6	0,0	2,6	0,0	0,0	0,0	
<i>Oligosphaeridium totum</i>	1,5	0,0	1,8	0,0	0,0	0,0	0,0	0,0	0,0	0,0	0,0	0,0	
<i>Oligosphaeridium</i> spp.	0,0	0,0	0,9	0,0	0,0	0,0	0,0	0,0	2,6	0,0	0,0	0,0	
<i>Codoniella campanulata</i>	0,0	0,0	0,0	0,0	0,0	0,0	0,6	0,0	0,0	0,0	0,0	0,0	
<i>Exochosphaeridium bifidum</i>	0,0	0,0	0,0	0,0	0,0	0,0	1,8	0,0	0,0	0,0	0,0	0,0	
<i>Prolixosphaeridium corolum</i>	0,0	0,0	0,0	0,0	0,0	0,0	1,2	0,0	0,0	0,0	0,0	0,0	
<i>Endoceratium dettmanniae</i>	0,0	0,0	0,0	0,0	0,0	0,0	4,1	0,0	0,0	0,0	0,0	0,0	
<i>Oligosphaeridium anthophorum</i>	1,5	1,7	0,0	0,0	0,0	0,0	0,6	0,0	0,0	0,0	2,0	0,0	
cf. <i>Canningia reticulata</i>	16,9	0,0	0,0	0,0	0,0	0,0	0,0	0,0	0,0	0,0	0,0	0,0	
<i>Pervosphaeridium truncatum</i>	0,7	0,0	0,9	0,0	2,7	0,0	0,0	0,0	0,0	0,0	0,0	0,0	
<i>Cyclonephelium vannophorum</i>	14,8	0,0	0,0	0,0	0,0	0,0	1,8	0,0	0,0	0,0	0,0	0,0	
<i>Lithosphaeridium conispinum</i>	0,0	0,0	0,0	0,0	5,5	0,0	4,7	18,2	0,0	0,0	0,0	0,0	
<i>Odontochitina costata</i>	0,0	0,0	2,7	0,0	2,7	0,0	1,2	0,0	0,0	0,0	0,0	2,3	
<i>Sepispinuloa hugouniotii</i>	0,7	1,7	0,0	0,0	0,0	0,0	0,0	5,1	17,6	0,0	0,0	2,3	
<i>Psalygonyaulax deflandrei</i>	0,0	0,0	0,0	0,0	0,0	0,0	0,6	0,0	0,0	0,0	2,0	0,0	
<i>Pervosphaeridium cenomaniense</i>	1,5	0,0	2,7	0,0	5,5	0,0	7,7	0,0	0,0	0,0	2,0	13,6	
<i>Spiniferites ramosus</i> subsp. <i>granosus</i>	0,7	3,4	1,8	0,0	0,0	0,0	0,0	0,0	2,6	0,0	0,0	0,0	
<i>Subtilisphaera</i> spp.	0,0	5,8	0,0	0,0	0,0	0,0	0,0	0,0	2,6	0,0	0,0	0,0	
<i>Trichodinium</i> spp.	0,0	0,0	0,9	0,0	0,0	0,0	0,0	10,0	0,0	5,9	0,0	0,0	
<i>Protoellipsodinium corollum</i>	12,7	0,0	1,6	0,0	2,7	0,0	7,7	0,0	2,6	0,0	3,9	0,0	
<i>Xipophoridium alatum</i>	1,5	0,0	0,0	0,0	8,2	0,0	4,7	0,0	0,0	0,0	0,0	0,0	
<i>Meiourugonyaulax psora</i>	0,0	0,0	0,0	0,0	0,0	0,0	0,0	0,0	0,0	0,0	2,0	0,0	
<i>Odontochitina</i> spp.	0,0	0,0	2,7	0,0	0,0	0,0	0,0	0,0	2,6	0,0	0,0	0,0	
<i>Dapsilidinium pumilum</i>	0,0	0,9	0,0	0,0	0,0	0,0	1,2	0,0	2,6	0,0	3,9	2,3	
<i>Florentinia radiculata</i>	0,7	0,0	0,9	0,0	2,7	0,0	2,4	0,0	0,0	0,0	0,0	0,0	
<i>Ovoidinium scabrosum</i>	7,7	0,0	0,9	0,0	0,0	0,0	0,0	0,0	0,0	0,0	3,9	0,0	
<i>Oligosphaeridium pulcherrimum</i>	0,0	0,0	0,0	0,0	2,7	0,0	0,6	0,0	0,0	0,0	0,0	2,3	
<i>Cyclonephelium</i> spp.	0,0	0,0	0,9	0,0	0,0	0,0	0,0	0,0	0,0	0,0	0,0	0,0	
<i>Apteodinium deflandrei</i>	0,7	0,0	0,9	0,0	0,0	0,0	0,0	18,2	0,0	0,0	3,9	0,0	
<i>Pterodinium cingulatum</i>	0,0	6,8	8,0	5,0	0,0	1,0	0,0	10,0	5,1	11,8	0,0	10,0	
<i>Achomosphaera ramulifera</i>	2,1	6,8	0,9	0,0	5,5	0,0	1,2	0,0	0,0	0,0	0,0	0,0	
<i>Canningia</i> spp.	0,0	0,0	0,9	5,0	0,0	0,0	0,0	0,0	2,5	0,0	0,0	0,0	
<i>Spiniferites ramosus</i>	5,6	3,4	28,3	0,0	8,2	0,0	11,2	10,0	7,7	11,8	2,0	6,8	
<i>Downiesphaeridium armatum</i>	0,7	0,0	0,0	0,0	0,0	0,0	0,0	0,0	0,0	0,0	0,0	0,0	
<i>Cribroperidinium intricatum</i>	0,0	0,0	0,0	0,0	2,7	0,0	0,0	0,0	0,0	5,9	0,0	2,3	
<i>Gonyaulacysta cassidata</i>	0,0	0,0	0,0	0,0	8,2	0,0	0,0	0,0	0,0	5,9	0,0	0,0	
<i>Heterosphaeridium heteracanthum</i>	0,0	0,0	0,0	0,0	5,5	0,0	0,0	0,0	0,0	0,0	0,0	0,0	
<i>Odontochitina ancala/O. rakhodes</i>	0,0	0,0	0,0	0,0	5,5	0,0	0,0	0,0	0,0	11,8	0,0	0,0	
<i>Florentinia</i> spp.	0,0	1,7	1,8	0,0	0,0	0,0	0,0	0,0	0,0	0,0	2,0	0,0	
<i>Coronifera oceanica</i>	0,7	0,0	0,0	0,0	5,5	0,0	0,0	0,0	0,0	0,0	0,0	0,0	
<i>Pseudoceratium eisenackii</i>	0,0	0,0	0,0	0,0	0,0	0,0	0,6	0,0	0,0	0,0	9,8	0,0	
<i>Tehamadinium coummia</i>	0,0	0,0	0,0	0,0	0,0	0,0	0,0	0,0	0,0	0,0	0,0	0,0	
<i>Gardodinium eisenackii</i>	0,0	0,0	0,0	0,0	0,0	0,0	3,6	0,0	0,0	0,0	0,0	0,0	
<i>Spiniferites multibrevis</i>	2,1	0,0	0,0	0,0	2,7	0,0	0,6	0,0	0,0	0,0	7,8	0,0	
<i>Tanyosphaeridium variecalum</i>	0,0	0,0	0,0	0,0	0,0	0,0	1,2	0,0	2,6	0,0	2,0	0,0	
<i>Oligosphaeridium complex</i>	1,5	5,8	3,5	0,0	0,0	0,0	1,2	10,0	0,0	0,0	3,9	2,3	
<i>Odontochitina operculata</i>	1,5	0,0	0,0	0,0	2,7	0,0	0,6	0,0	0,0	0,0	2,0	13,6	
<i>Cyclonephelium compactum</i>	0,0	1,7	0,0	0,0	2,7	0,0	0,0	0,0	5,1	0,0	2,0	4,5	
<i>Circulodinium colliveri</i>	1,5	0,0	0,0	0,0	13,5	0,0	5,3	0,0	0,0	0,0	0,0	16,0	
		Vraconian					Late Albian						
Depth (mbsf)	966,8	966,85	978,29	985	1002,5	1013,4	1031,7	1070,2	1075	1079,8	1082,7	1089,9	
Sample	58-2,8cm	58-2,84-86cm	59-3,125-130cm	60-2,0cm	62-1,10cm	63-1,137-139cm	65-1,68cm	69-1,115-117cm	69-4,114cm	70-1,129-131cm	70-3,70cm	71-2,36cm	

B.8. Dinocyst relative abundance distribution in the DSDP Hole 398D Aptian samples.

Sample	118-4, 113-115cm	111-5, 110cm
Depth (mbsf)	1549,65	1484,6
<i>cf. Damassadinium</i>	0,00	0,47
<i>Trichodinium</i> spp.	0,00	1,88
<i>Tenua</i> ? spp.	0,00	0,47
<i>Tanyosphaeridium</i> spp.	0,34	0,47
<i>Hystrichodinium</i> spp.	0,68	0,94
<i>Canningia</i> spp.	0,34	0,47
<i>Exochosphaeridium</i> spp.	0,68	0,47
<i>Wrevittia - Stanfordella</i>	4,74	0,47
<i>Pterodinium</i> spp.	7,48	66,67
<i>Prolixosphaeridium</i> spp.	0,34	0,94
<i>Dapsilidinium</i> spp.	0,68	0,97
<i>Oligosphaeridium</i> complex	3,40	1,88
<i>Odontochitina operculata</i>	6,46	1,41
<i>Cribooperidium orthoceras</i>	2,72	7,51
<i>Meiourogonyaulax</i> spp.	0,68	0,94
<i>Spiniferites</i> spp.	13,95	5,16
<i>Subtilisphaera</i> spp.	25,51	2,35
<i>Kallosphaeridium ringnesiorum</i>	5,78	0,47
<i>Kiokansium unituberculatum</i>	2,72	4,23
<i>Aptea</i> spp.	0,68	1,88
<i>Ovoidinium diversum</i>	5,44	0,00
<i>Pervosphaeridium</i> spp.	0,34	0,00
<i>Palaeoperidium</i> spp.	1,36	0,00
<i>Cyclonephelium</i> spp.	0,34	0,00
<i>Taleisphaera</i> spp.	1,02	0,00
<i>Chlamydophorella</i> spp.	0,34	0,00
<i>Cassiculosphaeridia magna</i>	4,76	0,00
<i>Atopodinium</i> spp.	0,68	0,00
<i>Nexospinum</i> ? spp.	0,34	0,00
<i>Circulodinium</i> spp.	1,70	0,00
<i>Tehamadinium</i> spp.	0,34	0,00
<i>Batiacasphaera</i> spp.	3,06	0,00
<i>Dingodinium alberti</i>	2,72	0,00

B.9. Dinocyst relative abundance distribution in the Southern Provence Basin samples.

Sample	Height (m)	<i>Xenascus</i> spp.	<i>Rhynchodiniopsis</i> spp.	<i>Sepispinula</i> spp.	cf. <i>Protoellipsodinium</i>	<i>Chlamydotheca discreta</i>	<i>Cribrerodinium orthoceras</i>	<i>Oligosphaeridium</i> sp.	<i>Ctenidodinium elegantulum</i>	<i>Kiokansium</i> spp.	<i>Aptea anaphrysa</i>	cf. <i>Subtilisphaera</i>	<i>Hystrichodinium pulchrum</i>	<i>Pseudoceratium securigerum</i>	<i>Pseudoceratium</i> spp.	<i>Aptea securigera</i>	<i>Chihaouadinium arabicum</i>	<i>Taleisphaera</i> spp.	<i>Ovoidinium diversum</i>	<i>Oligosphaeridium diliculum</i>	<i>Meiourogonyaulax</i> spp.	<i>Kleithrasphaeridium eionodes</i>	<i>Aptea</i> spp.	<i>Pterodinium</i> spp.	<i>Oligosphaeridium</i> cf. <i>asterigerum</i>	<i>Chlamydotheca</i> spp.	<i>Coronifera oceanica</i>	<i>Kleithrasphaeridium</i> spp.	<i>Tenua</i> spp.	
MA82	42.8	0	0	0	0	0	0	0	0	0	0	0	0	0	0	0	0	0	0	0	0	0	0	0	0	0	0	0	0	0
MA65	34.3	0	0	0	0	0	0	0	0	0	0	0	0	0	0	0	0	0	0.93	0	0	0	0.31	1.61	0	0	0	0	0.62	0
MA48	25.5	0	0	0	0	0	0	0	0	0	0	0	0	0	0	0	0	0	0	0	0	0	0	0	0	0	0	0.97	0	0
MA34	17	0	0	0	0	0	0	0	0	0	0	0	0	0	0	0	0	0.3	0.3	0	0	0	0	0	0	0	0	0	0	1.49
MA24	10.92	0	0	0	0	0	0	0	0	0.98	0	0	0	0	0	0	0	0	0	0	0	0	0.66	0	0	0	0	0	0.33	0.66
MA15	6.6	0	0	0	0	0	0	0.33	0	0	0	0	1.33	0	0	0	0	0	0	0	0	0	0	0	0	0	0	0	0	0
MA10	3.6	0	0	0	0	0	0	0	0	0	0	0	0	0	0	0	0	0.26	0	1.66	0.33	0	0	0	0	0	0	0	0	0
M.30732 - 169	117.45	0	0	0	0	0	0	0	0.66	0	0	0	0	0	0	0	0	0	0	1.99	0.33	0.33	1	0	0	0	0	0	1	0
155C	9.9	0	0	0	0	0	0	0	0.57	0	0	0	0	0	0	0	0	0	0	1.99	0.33	0.33	1.7	0	0	0	0	0	0	0
M.30729 - 150	93.8	0	0	0	0	0.31	3.41	0	0	0	0	0	0	0	0	0	0	0	0	8.46	0.31	0	0.31	0.31	0	0	0	0.94	0	0
M.30728 - 146	89	0	0	0	0	12.4	12.5	2.19	0	0	0	0	0	0	0	0	0	0	0	6.19	0	0	0	0.31	0	0	0	0.31	0.31	0
M30727-139	80	0	0	0.27	0.53	0.27	0	0	1.86	0	0	0	0.53	0	0	0	0	0	0	1.06	0.27	0	1.33	1.86	0.8	2.93	1.86	2.13	0.27	0
M.30726 - 122	58.1	0.31	29.5	0	0	0	3.68	1.23	0	0.92	0	0	0	0	0	0	0	0	3.37	0	0.92	0	0.61	0	0	0	0	0	0.92	0

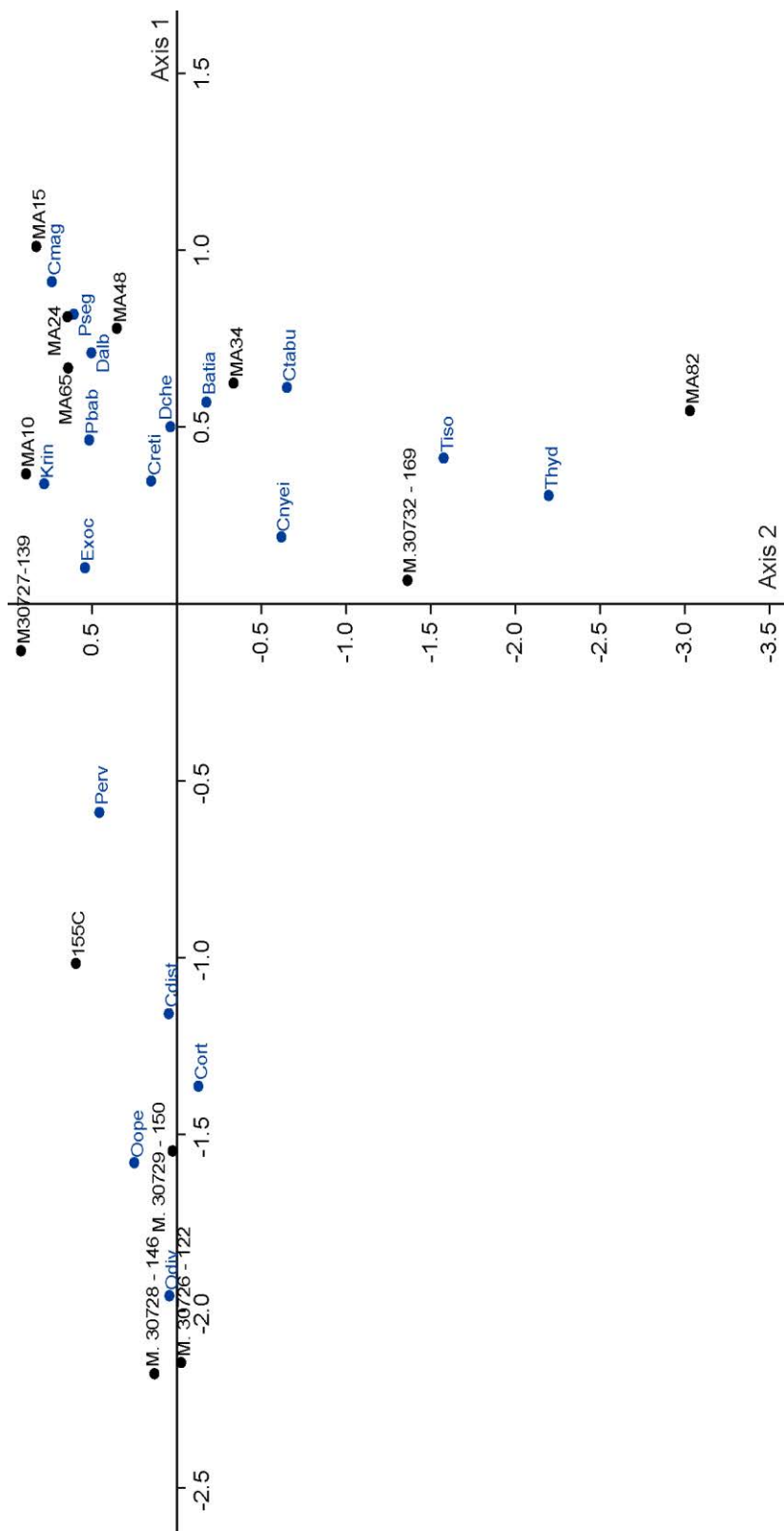
B.9. Dinocyst relative abundance distribution in the Southern Provence Basin samples (continued).

Sample	Height (m)	<i>Tanyosphaeridium</i> spp.	<i>Achomosphaera</i> spp.	<i>Circulodinium distinctum</i>	<i>Odontochitina operculata</i>	<i>Meiourogonyaulax sagena</i>	<i>Hystrichosphaerina</i> spp.	<i>Hystrichosphaeridium recurvatum</i>	<i>Spiniferites</i> spp.	<i>Florentinia lacinata</i>	<i>Kallosphaeridium</i> spp.	<i>Prolixosphaeridium parvispinum</i>	<i>Oligosphaeridium complex</i>	<i>Exochosphaeridium</i> spp.	<i>Protoellipsoidinium</i> spp.	<i>Dapsilidinium warrenii</i>	<i>Taleisphaera cf. hydra</i>	<i>Dingodinium albertii</i>	<i>Callaiosphaeridium asymmetricum</i>	<i>Cassiculosphaeridia reticulata</i>	<i>Wrevittia helicoidea</i>	<i>Pervosphaeridium</i> spp.	<i>Florentinia</i> spp.	<i>Cassiculosphaeridia magna</i>	<i>Cometodinium</i> spp.	<i>Tehamadinium</i> spp.	<i>Chlamydothorea nyei</i>	<i>Hystrichosphaerina scindewolfii</i>	<i>Exochosphaeridium amace</i>		
MA82	42.8	0	0.32	0.32	0.96	0	0	0	27.01	0	0	0	16.4	0.64	0.64	1.29	2.89	0	0.32	0.32	0.32	0.64	2.25	0	0	0	1.29	2.57	0	0	
MA65	34.3	0	0.31	0.31	0.62	0	0	0	29.19	0	0.62	0	6.52	0.62	0	0.62	0	5.28	0	0	1.86	0.31	0	0.62	0	0	7.14	2.8	0	0	
MA48	25.5	0.97	0	0.65	1.62	0	0	0	30.74	0	0	0	2.91	0.32	0	0.97	0	11.3	0.32	0.97	0	0	0.65	0.32	0.65	0.97	4.21	0	0	0	
MA34	17	0	0.6	0.3	1.49	0	0	0	18.81	0	0	0	17.6	0	0	0	0	8.96	0.3	5.37	0	0.6	0.6	0	0.6	0.3	8.06	0	0	0	
MA24	10.92	0.98	0.98	0.33	0.66	0	0	0	36.07	0	0.33	0	3.61	1.64	0	0	0	12.8	0.33	1.97	0	0	0.33	1.97	1.31	0	0	0	0	0	
MA15	6.6	0.33	1.33	0	0.33	0	0	0	23.59	0	0.66	0	6.64	0.33	0	0	0	29.6	0.33	0.33	0	0.66	0.66	1.99	0	0	0	0	0.33	0.33	
MA10	3.6	0.26	0.78	1.56	0.78	0.52	0.26	0.78	15.36	0.26	0.52	0.26	1.56	0	0.78	0.78	0	36.2	0	2.34	0	2.86	1.04	1.82	1.04	0.78	0	0	0	0	
M.30732-169	117.45	0	2.99	13.62	1	0	0	0.33	30.23	0	0	0	10.6	1.33	0	1	4.32	0	0.66	3.32	0	0.57	0.85	0.28	0.28	1.42	0	0	0	0	
155C	99	0	0	29.26	3.69	0	0	0	24.15	0	1.14	0	6.25	0	1.14	0	0	0	2.27	1.42	0	0.57	0.85	0.28	0.28	1.42	0	0	0	0	
M.30729-150	93.8	0	0.31	21	3.76	0	0	0	15.99	0	0	0	8.15	0	0.31	0.63	0	0.94	0	0.31	0	2.19	0.63	0.94	0	0.31	16.9	0	0	0	
M.30728-146	89	0.31	0.62	32.2	10.2	0	0	0	9.91	0	0	0	6.81	0.31	0	0.93	0.62	0.93	0.31	1.55	0	0	0	0	0	0	0	0	0	0	
M30727-139	80	0.53	0.27	16.49	1.86	0	0	0	28.99	0	0	0	11.4	0.27	0	0.53	0	0.8	1.06	3.72	0.27	1.33	0.53	0	0.27	0.27	0.27	0	0	0	
M.30726-122	58.1	0	0.92	50.31	0.61	0	0	0	2.15	0	0.31	0	2.45	0.31	0	0	0	0	0	0	0	0	0	0	0	0	0	0	0	0	0

C.1. Aram - *Achomosphaera ramulifera*; Adef - *Apteodinium deflandrei*; Cace - *Caligodinium aceras*; Casy - *Calliosphaeridium asymmetricum*; Cnret - *Canningia reticulata*; Cgra - *Carpodinium granulatum*; Csret - *Cassiculosphaeridia reticulata*; Ccol - *Circulodinium colliveri*; Cdist - *Circulodinium distinctum*; Cves - *Chichaouadinium vestitum*; Chdis - *Chlamydophorella discreta*; Cwit - *Cometodinium withei*; Coce - *Coronifera oceanica*; Cedw - *Cribooperidinium? edwardsii*; Ccom - *Cyclonephelium compactum*; Cvan - *Cyclonephelium vannophorum*; Dchi - *Damassadinium chibane*; Dlam - *Dapsilidinium laminaspinosum*; Dcla - *Dinopteridium cladoides*; Ephr - *Exochosphaeridium phragmites*; Fcoo - *Florentinia cooksoniae*; Fman - *Florentinia mantellii*; Frad - *Florentinia radiculata*; Geis - *Gardodinium eisenackii*; Hpul - *Hystrichodinium pulchrum*; Iver - *Impagidinium verrucosum*; Krin - *Kallosphaeridium? ringnesiorum*; Ktub - *Kleithriasphaeridium tubulosum*; Kio - *Kiokansium* sp.; Lcon - *Litosphaeridium conispinum*; Mopa - *Microdinium opacum*; OancRak - *Odontochitina ancala/O. rhakodes*; Oope - *Odontochitina operculata*; Oalb - *Oligosphaeridium albertense*; Ocom - *Oligosphaeridium complex*; Opul - *Oligosphaeridium pulcherrimum*; Otot - *Oligosphaeridium totum*; Ovo - *Ovoidinium* sp.; Pcret - *Palaeoperidinium cretaceum*; Pcen - *Pervosphaeridium cenomaniense*; Pcor - *Protoellipsodinium corollum*; Peis - *Pseudoceratium eisenackii*; Pcin - *Pterodinium cingulatum*; Shug - *Sepispinula? huguoniotii*; Smul - *Spiniferites multibrevis*; Sram - *Spiniferites ramosus*; SrGra - *Spiniferites ramosus* subsp. *granosus*; Surc - *Surculosphaeridium* sp.; Tvar - *Tanyosphaeridium variecalamum*; Thys - *Tenua hystrix*; Tcas - *Trichodinium castaneum* and Wcas - *Wrevittia cassidata*

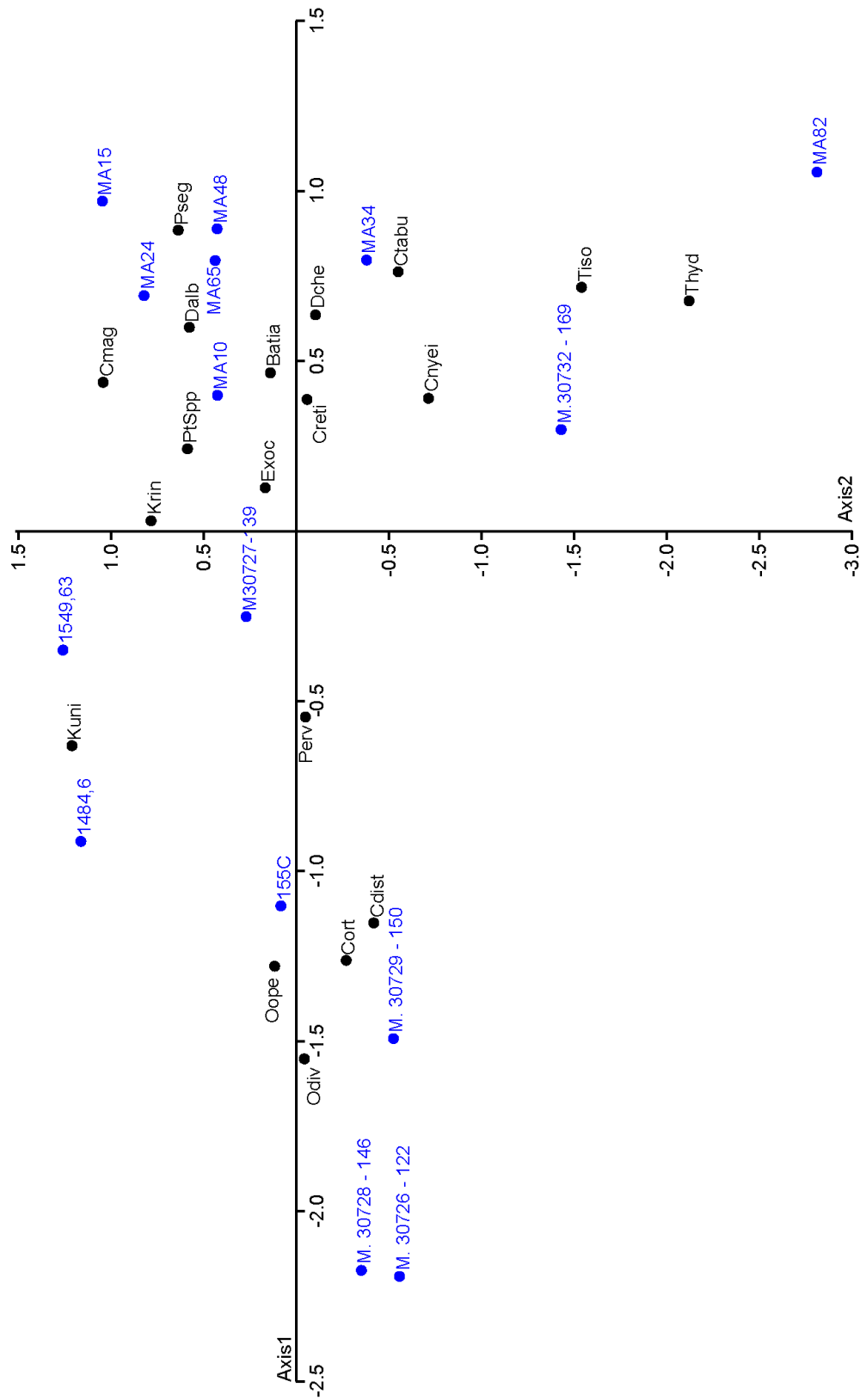
C.3. Aram - *Achomosphaera ramulifera*; Adef - *Apteodinium deflandrei*; Cace - *Caligodinium aceras*; Cnret - *Canningia reticulata*; Csret - *Cassiculosphaeridia reticulata*; Cves - *Chichaouadinium vestitum*; Chdis - *Chlamydothorea discreta*; Ccol - *Circulodinium colliveri*; Cdist - *Circulodinium distinctum*; Cwit - *Cometodinium withei*; Coce - *Coronifera oceanica*; Cedw - *Cribooperidinium? edwardsii*; Ccom - *Cyclonephelium compactum*; Cvan - *Cyclonephelium vannophorum*; Dchi - *Damassadinium chibane*; Dlam - *Dapsilidinium laminaspinosum*; Dcla - *Dinopteridium cladoides*; Ephr - *Exochosphaeridium phragmites*; Fman - *Florentinia mantellii*; Frad - *Florentinia radiculata*; Geis - *Gardodinium eisenackii*; Hpul - *Hystrichodinium pulchrum*; Iver - *Impagidinium verrucosum*; Krin - *Kallosphaeridium? ringnesiorum*; Ktub - *Kleithriasphaeridium tubulosum*; Lcon - *Litosphaeridium conispinum*; OancRak - *Odontochitina ancala/O. rhakodes*; Oope - *Odontochitina operculata*; Oalb - *Oligosphaeridium albertense*; Ocom - *Oligosphaeridium complex*; Pcre - *Palaeoperidinium cretaceum*; Pcen - *Pervosphaeridium cenomaniense*; Pcor - *Protoellipsodinium corollum*; Peis - *Pseudoceratium eisenackii*; Pcin - *Pterodinium cingulatum*; Shug - *Sepispinula? huguonotii*; Smul - *Spiniferites multibrevis*; Sram - *Spiniferites ramosus*; SrGra - *Spiniferites ramosus* subsp. *Granosus*; Tvar - *Tanyosphaeridium variecalamum*; Thys - *Tenua hystrix*; Tcas - *Trichodinium castaneum* and Wcas - *Wrevittia cassidata*

C.4. Scatter diagram resulting from the correspondence analysis of the Southern Provence Basin data.



C.4. Batia - *Batiacasphaera* spp.; Cmag - *Cassiculosphaeridia magna*; Creti - *Cassiculosphaeridia reticulata*; Ctabu - *Cerbia tabulata*; Cnyei - *Chlamydochorella nyei*; Cdist - *Circulodinium distinctum*; Corth - *Cribroperidinium orthoceras*; Dche - *Dapsilodinium chems*; Dalb - *Dingodinium albertii*; Exoc - *Exochosphaeridium* spp.; Krin - *Kallosphaeridium ringnesiorum*; Oope - *Odontochitina operculata*; Odiv - *Ovoidinium diversum*; Perv - *Pervosphaeridium* spp.; Pseg - *Protoellipsodinium seghire* subsp. *seghire*; Pbab - *Pterodinium bab*; Thyd - *Taleisphaera* cf.

C.5. Scatter diagram resulting from the correspondence analysis of the Southern Provence Basin and Aptian 398D data.



C.5. Batia - *Batiacasphaera* spp.; Cmag - *Cassiculosphaeridia magna*; Creti - *Cassiculosphaeridia reticulata*; Ctabu - *Cerbia tabulata*; Cnye - *Chlamydocphorella nyei*; Cdist - *Circulodinium distinctum*; Cort - *Cribrerodinium orthoceras*; Dche - *Dapsilodinium chems*; Dalb - *Dingodinium albertii*; Exoc - *Exochosphaeridium* spp.; Krin - *Kallosphaeridium ringnesiorum*; Kuni - *Kiokansium unituberculatum*; Oope - *Odontochitina operculata*; Odiv - *Ovoidinium diversum*; Pev - *Pervosphaeridium* spp.; Pseg - *Protoellipsoidinium seghire* subsp. *seghire*; Pbab -

APPENDIX D - Structured Sedimentary Organic Matter data

D.1. Relative abundance of the considered Structured SOM categories in the Southern Provence Basin samples

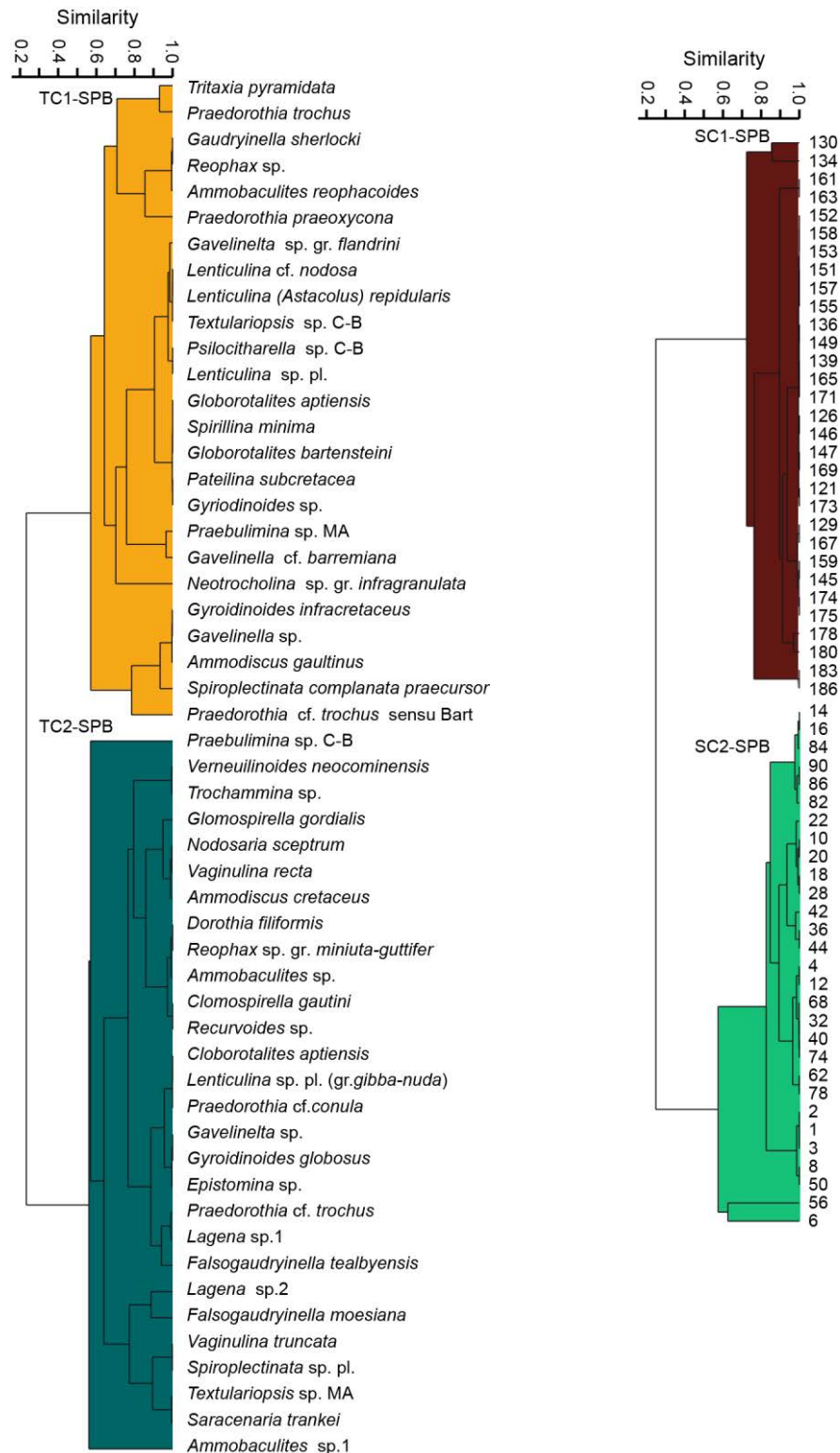
Sample	Height (m)	Foraminifera test Linning	Dinocyst	Acritarch	Other algae	Pollen	Spores	Pseudoamorphous sporomorphs	Pseudoamorphous dinocysts	Equidimensional (O- Eq)	Lath (O-La)	Wood tracheid with pits (Wp)	Cuticle (Cu)	Membranes (Mb) transp	Pseudoamorphous phytoclasts	Fungal remains
MA82	42,8	3,56	16,15	0,30	0,00	10,52	11,11	0,00	6,52	23,56	12,30	1,63	2,07	8,30	3,56	0,44
MA65	34,3	3,78	5,41	0,00	0,00	1,08	5,23	0,00	7,75	36,04	17,30	1,98	0,00	19,28	1,98	0,18
MA48	25,5	1,15	22,33	3,24	0,00	1,91	4,20	0,00	12,98	15,84	12,79	3,44	0,38	12,21	9,35	0,19
MA34	17	1,66	16,76	0,00	2,58	1,84	3,31	0,00	12,34	21,18	16,76	2,58	0,00	10,68	10,13	0,00
MA24	10,92	1,34	15,60	0,67	0,00	2,68	5,70	0,00	9,06	26,34	15,94	3,36	0,00	11,91	7,21	0,17
MA15	6,6	0,97	25,34	0,19	0,00	0,77	3,09	0,00	11,03	33,08	11,99	1,93	0,00	6,77	4,84	0,00
MA10	3,6	3,38	25,52	0,19	0,00	2,63	11,26	0,00	8,82	20,83	12,01	1,88	0,00	9,01	3,94	0,56
M.30732 - 169	117,45	1,73	2,70	0,00	0,00	3,08	2,89	0,00	3,47	38,73	30,44	2,12	0,00	8,48	6,36	0,00
155C	99	12,70	23,79	0,00	0,00	2,22	2,22	0,00	13,10	15,73	7,26	0,60	0,20	15,12	3,63	3,43
M. 30729 - 150	93,8	1,72	14,50	0,00	0,00	1,15	3,05	0,00	7,63	24,62	20,23	0,76	0,00	17,94	5,92	2,48
M. 30728 - 146	89	0,20	18,24	0,20	0,00	0,59	0,98	0,00	10,59	28,63	22,75	0,59	0,00	9,02	4,71	3,53
M. 30727 - 139	80	3,99	7,44	0,00	0,00	0,54	1,81	0,00	5,26	32,30	23,23	1,09	0,36	10,53	9,80	3,63
M. 30726 - 122	58,1	0,00	5,54	0,00	0,00	2,18	0,59	0,00	8,32	42,97	20,79	0,20	0,20	8,12	11,09	0,00

D.1. Relative abundance of the considered Structured SOM categories in the Aptian samples from the DSDP Hole 398D

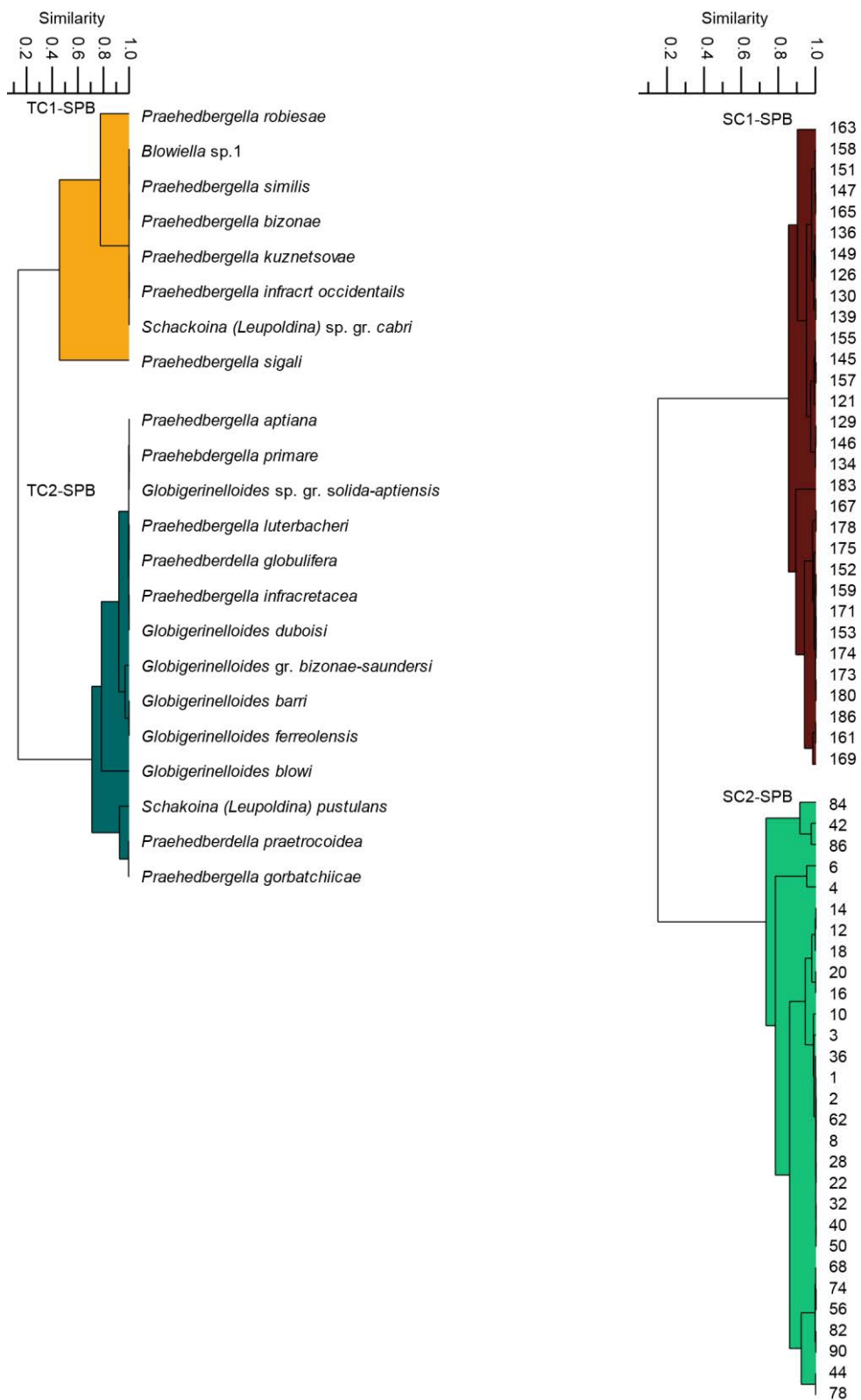
Sample	Depth (mbsf)	Foraminifera test Linning	Dinocyst	Acritarch	Other algae	Pollen	Spores	Pseudoamorphous sporomorphs	Pseudoamorphous dinocysts	Equidimensional (O-Eq)	Lath (O-La)	Wood tracheid with pits (Wp)	Cuticle (Cu)	Membranes (Mb) transp	Pseudoamorphous phytoclasts	Fungal remains
111-5	1484,6	0,00	1,27	0,00	0,00	3,99	0,91	0,54	0,00	28,44	12,14	0,72	0,00	27,72	24,28	0,00
118-4	1549,63	0,00	5,28	0,00	0,00	21,53	4,11	0,98	0,00	13,89	5,68	0,59	0,00	37,57	10,37	0,00
119-5	1559,74	1,10	1,10	0,00	0,00	4,77	3,67	3,85	0,00	18,90	10,64	0,37	0,18	26,24	28,81	0,37
121-3	1575,7	0,75	0,00	0,00	0,00	32,58	7,53	16,76	0,00	9,23	5,27	0,56	0,00	21,66	5,65	0,00
127-5, 80	1636,3	0,39	0,00	0,00	0,00	5,62	5,23	7,56	0,00	32,95	8,14	0,19	0,00	25,39	14,53	0,00
127-5, 118-128	1636,68	0,39	0,00	0,00	0,00	0,78	4,47	0,39	0,00	20,62	13,04	0,58	0,00	33,66	26,07	0,00
127-5, 127-129	1636,77	0,54	0,00	0,00	0,00	3,98	7,23	0,36	0,00	24,05	11,21	0,54	0,00	16,46	35,44	0,18

APPENDIX E - Foraminifera UPGMA cluster results

E.1. UPGMA cluster analyses of Southern Provence Basin benthic foraminifera data, using Raup-Crick coefficient as similarity measure. Taxa associated by the R-mode in a cluster usually appear together in samples. Samples clustered in the Q-mode share similar taxon assemblages. Data from Moullade *et al.* (1998b, 2005).



E.1. UPGMA cluster analyses of Southern Provence Basin planktonic foraminifera data, using Raup-Crick coefficient as similarity measure. Taxa associated by the R-mode in a cluster usually appear together in samples. Samples clustered in the Q-mode share similar taxon assemblages. Data from Moullade *et al.* (1998b, 2005).



ABSTRACT

Awareness of the vulnerability of modern society to possible changes in the global climate has stirred up the interest of the scientific community to better understand the mechanisms and feedbacks regulating the climate system. The Cretaceous period is considered a good example for the study of the Earth under “greenhouse” climate conditions and thus a good analog for future global climate evolution. Modern dinoflagellate cysts (dinocysts) are very efficient in reconstruction of oceanic fluctuations, and fossil dinocysts have great values for biostratigraphy. The thesis evaluates the performance of Cretaceous dinocyst as biostratigraphic markers, and develops an appropriate methodology, grounded on biodiversity and multivariate analysis to improve paleoenvironmental reconstructions.

In the first chapter, dinocysts are used to recognize the Upper Cretaceous and Paleocene stage boundaries in the ODP Hole 959D, drilled on the Côte d’Ivoire – Ghana transform margin. The comparison of the results with two previous evidences uncertainties in time interval delimitation. Conflicts are mostly due to low frequencies of biostratigraphic dinocyst markers.

The second chapter analyzes the dinocyst distribution along an inshore to offshore transect on the western Iberian Margin during the Albian. Contrasting the dinocyst occurrence data with the sedimentological and paleontological data allow identifying dinocyst associations with common preferences and tolerances to environmental conditions. The main factors contributing to the dinocyst distribution are the stability and predictability gradient and the nutrient availability. Paleooceanographic and paleogeographic evolution of the western Iberian margin during the Albian are clearly recorded in the spatiotemporal occurrence patterns of dinocyst associations.

The third chapter compares Aptian dinocyst distribution from two different oceanic domains, Central Atlantic and northwestern Tethyan. It is used to test the methodology and the hypothesized paleoenvironmental preferences of dinocyst issued from analysis of the Albian data. The recognized paleoenvironmental preferences and tolerances of the Aptian dinocysts precisely match those proposed for the Albian species. The distribution and evolution of Aptian dinocyst associations reflect the evolution of carbonate platforms of both the Southern Provence Basin and the western Iberian margin. The combination of dinocyst and sedimentary organic matter (SOM) allows the identification of regional and global oceanic changes, like the demise of carbonate platforms, the Oceanic Anoxic Event 1a (OAE 1a) or the regional anoxic event Fallot level.

Keywords: Dinoflagellate cysts, biostratigraphy, multivariate analysis, paleoenvironment, Cretaceous, western Iberian Margin, Southern Provence Basin